

Modulation of cerebral β -amyloidosis by myeloid cells

Dissertation

zur Erlangung des Grades eines
Doktors der Naturwissenschaften

der Mathematisch-Naturwissenschaftlichen Fakultät
und
der Medizinischen Fakultät
der Eberhard-Karls-Universität Tübingen

vorgelegt

von

Karoline Degenhardt
aus Berlin, Deutschland

März - 2018

Tag der mündlichen Prüfung: 19-09-2018

Dekan der Math.-Nat. Fakultät: Prof. Dr. W. Rosenstiel
Dekan der Medizinischen Fakultät: Prof. Dr. I. B. Autenrieth

1. Berichterstatter: Dr. Jonas Neher
2. Berichterstatter: Prof. Philipp Kahle
3. Berichterstatter: Prof. Josef Priller

Prüfungskommission:
Dr. Jonas Neher
Prof. Philipp Kahle
Prof. Olga Garaschuk
Prof. Rudolf Martini

Erklärung:

Ich erkläre, dass ich die zur Promotion eingereichte Arbeit mit dem Titel:

“Modulation of cerebral β -amyloidosis by myeloid cells”

selbständig verfasst, nur die angegebenen Quellen und Hilfsmittel benutzt und wörtlich oder inhaltlich übernommene Stellen als solche gekennzeichnet habe. Ich versichere an Eides statt, dass diese Angaben wahr sind und dass ich nichts verschwiegen habe. Mir ist bekannt, dass die falsche Abgabe einer Versicherung an Eides statt mit Freiheitsstrafe bis zu drei Jahren oder mit Geldstrafe bestraft wird.

Tübingen, den

.....

Unterschrift /Signature

Für meine liebe Familie.

Danksagung

In den vergangenen vier Jahren habe ich am Hertie-Institut für klinische Hirnforschung an meiner Promotion gearbeitet. Während dieser Zeit bekam ich jederzeit Unterstützung von Arbeitskollegen, Freunden und Verwandten, denen ich hiermit meinen Dank aussprechen möchte. Der größte Dank gebührt Dr. Jonas Neher, der mir fortwährend mit seinem umfangreichen Wissen und vielen Ideen zur Seite stand. Ich möchte mich ebenfalls bei Prof. Mathias Jucker für die Möglichkeit bedanken, meine Doktorarbeit in seiner Arbeitsgruppe durchzuführen aber auch für seine volle Unterstützung meiner promotionsrelevanten Projekte. Des Weiteren bin ich über die wertvollen Diskussionen mit Frau Prof. Garaschuk und Herrn Prof. Heneka als Mitglieder meines Advisory Boards sehr dankbar.

Ein ebenso großes Dankeschön für das kreative und sehr anregende Arbeitsumfeld geht an alle Kollegen, mit denen ich im Verlauf meiner Promotion am Hertie-Institut sowie am Deutschen Zentrum für Neurodegenerative Erkrankungen zusammenarbeiten durfte. Hierbei möchte ich mich besonders bei allen Mitgliedern und ehemaligen Mitgliedern unserer Arbeitsgruppe: Ann-Christin Wendeln, Sarah Fritschi, Angelos Skodras, Jessica Wagner, Anika Bühler, Ulrike Obermüller, Katleen Wild, Maren Lösch, Bernadette Graus, Timo Eninger, Stephan Käser, Sonia Mazzitelli, Simone Eberle, Ruth Dröge, Rawaa Al-Shaana, Nathalie Beschorner, Melanie Barth, Mehtap Bacioglu, Lisa Häsler, Juliane Schelle, Jörg Odenthal, Jay Rasmussen, Carina Leibssle, Bettina Wegenast-Braun, Marius Lambert und Anja Apel für Ihre wissenschaftliche aber auch freundschaftliche Unterstützung bedanken. Ein besonderern Dank möchte ich dabei Andrea Bosch aussprechen, die mich sehr freundschaftlich im Labor willkommen heißen und mich in viele wissenschaftliche Techniken eingeführt hat. Des Weiteren möchte ich mich bei Eva David für ihre zuverlässige Betreuung unserer Labormäuse und die gute Kooperation bedanken.

Ich möchte mich ebenso bei unseren Kollaborationspartnern in Frankfurt, Göttingen, Bonn und Liverpool für die freundliche und erfolgreiche Zusammenarbeit bedanken.

Ein großer Dank geht an meine Eltern Annett und Frank Degenhardt sowie an meinen Bruder Klemens Degenhardt. Ihr mich habt mich in meiner Ausbildung von Anfang an unterstützt und wart auf jedem noch so schweren Weg immer an meiner Seite. Vielen Dank an Oma und Opa für die liebevolle Unterstützung mit Paketen und Telefonaten aus der Heimat.

Zuletzt möchte ich mich bei meinen Sportfreunden im Tübinger Schwimmverein und des Post-SV Tübingen für die vielen gemeinsamen Trainingsstunden und Erfolge bedanken, mit euch haben viele anstrengende Tage einen entspannten Abschluss gefunden.

Table of Contents

| | |
|---|------------|
| 1. Summary | 7 |
| 2. Preface | 10 |
| 3. Synopsis | 11 |
| 3.1 Alzheimer's disease | 11 |
| 3.1.1 An overview on 110 years of Alzheimer's disease research | 11 |
| 3.1.2 Pathophysiology of Alzheimer's disease – APP processing | 12 |
| 3.1.3 Genetic susceptibility to Alzheimer's disease | 13 |
| 3.1.4 Genetic risk factors for LOAD | 14 |
| 3.1.5 Microglia – mediators of the innate immune response in AD | 19 |
| 3.2 Environmental factors as regulator for myeloid cell function | 23 |
| 3.2.1 Microglia targeting approaches | 23 |
| 3.2.2 Monocytes – co-workers of microglia? | 25 |
| 3.2.3 Environment determines macrophage function in the brain | 28 |
| 3.3. Modification of CNS pathology by molecular reprogramming of the innate immune response | 30 |
| 3.3.1 Systemic inflammation as trigger for neurological disease | 30 |
| 3.3.2 The concept of innate immune memory | 32 |
| 3.3.3 Epigenetic reprogramming induces immune memory in macrophages | 34 |
| 3.3.4 The molecular basis of immune memory in macrophages | 37 |
| 3.3.5 Innate immune memory in the brain shapes neurological disease hallmarks | 39 |
| 3.4 Genetic modification of the microglial phagocytic capacity during AD | 46 |
| 3.4.1 A β clearance mechanisms in the CNS | 46 |
| 3.4.2 MFG-E8-mediated phagocytosis | 48 |
| 3.4.3 Lack of MFG-E8 does not affect microglia-mediated A β phagocytosis | 50 |
| 3.5 Conclusions | 53 |
| 3.6 References | 55 |
| 4. Publications | 77 |
| 4.1 Description of personal contribution | 77 |
| 4.2 Replacement of brain-resident myeloid-cells does not alter cerebral amyloid-β deposition in mouse models of Alzheimer's disease | 79 |
| 4.3 Innate immune memory in the brain shapes neurological disease hallmarks | 87 |
| 4.4 Lack of MFG-E8 reduces pathology in mouse models of cerebral β-amyloidosis | 123 |
| 5. Appendix | 149 |
| 5.1 Abbreviations | 149 |
| 5.2 Curriculum Vitae | 152 |
| 5.2.1 Personal Data | 152 |
| 5.2.2 Education and Academic Degrees | 152 |
| 5.3 Bibliography | 153 |
| 5.4 Conference Proceedings | 154 |

1. Summary

Alzheimer's disease (AD) is an age-related neurodegenerative disorder and the most common form of dementia. Thereby, the abnormal deposition of the amyloid- β (A β) peptide into plaques is considered to be the primary neuropathological insult in AD. For a small proportion of all AD cases it is well known that rare genetic mutations are causative for very early A β deposition (familial Alzheimer's disease). However, the vast majority of all AD cases manifest at later ages (late-onset Alzheimer's disease (LOAD)) and are most likely caused by an interplay of multiple genetic variants and the environment.

During the last ten years, genome-wide association studies revealed several risk loci that increase the susceptibility for LOAD, and interestingly, many of these genetic variants were found to be associated with innate immune functions of which the resident tissue macrophages of the brain – the microglia – are prime regulators.

In general, the innate immune response mediated by the resident tissue macrophages is considered protective as it induces the production of inflammatory modulators and enables phagocytosis and killing of pathogens to prevent further tissue damage. However in the AD brain, the progressive accumulation of A β deposits leads to a chronic exposure of microglia to A β aggregates and induces an excessive neuro-inflammatory response that is thought to promote disease progression.

Interestingly, microglia display a highly plastic phenotype and studies from peripheral tissue macrophages reported that a variety of environmental stimuli can determine but also reprogram their functional phenotype. To this end, this thesis summarizes three different approaches, which aimed to understand but also modulate the myeloid cell immune function during AD with regard to their effects on the pathology of cerebral β -amyloidosis.

To begin with, we examined whether peripheral monocytes, which were previously shown to adopt a microglia-like phenotype in the healthy brain, can replace dysfunctional microglia in brains of two different mouse models of cerebral β -amyloidosis and may then restrict A β accumulation. For this purpose, we depleted microglia in APPPS1 and APP23 transgenic (tg) mice that expressed the herpes simplex virus thymidine kinase (HSVTK) under the myeloid-cell specific *CD11b* promoter; the application of the thymidine kinase substrate ganciclovir (GCV), which is converted into a cytotoxic product, then induced microglial death. After a two-week ganciclovir treatment, application was discontinued from two weeks up to six months to allow the peripheral monocytes to repopulate the brain. Interestingly, during the first weeks of repopulation the number of infiltrated monocytes were twice the number of resident microglia in control mice, but the engrafted monocytes failed to cluster around A β plaques.

Consequently, we did not observe alterations in plaque pathology. Also, a pro-longed incubation for up to six months did not change A β load. However, long-term monocyte engraftment for five months induced in pre-depositing APP23 mice enabled the infiltrated monocytes to behave most similar to resident microglia: they began clustering around A β depositions, the cell number was virtually equal to control mice and plaque-associated monocytes were TREM2-positive. However, these cells also failed to alter A β plaque load.

This work indicates that the tissue environment in the brain dominates over myeloid cell origin and thus reprograms myeloid cells to match the resident microglia population, however without prevention of A β pathology.

Recent studies provide evidence that cells of the innate immune system can, similar to the adaptive immune cells, acquire immunological memory. In particular, a distinct set of primary immune stimuli can either enhance or suppress a subsequent immune response, which is referred to as “training” and “tolerance”, respectively. In a second study, we tested the applicability of the immune memory concept to microglia and examined if the induction of innate immune memory can induce long-lasting changes in the brain’s immune response and thereby alter pathology of neurological diseases. To this end, we injected two different doses of the endotoxin lipopolysaccharide (LPS) into pre-depositing APP23 mice. Whereas a single LPS injection was identified to induce acute training effects, consecutive injections for four days induced tolerance effects in microglia. Accordingly, in the brain, we acutely measured initially enhanced concentrations of inflammatory cytokines which decreased with further LPS injections.

When we examined the long-lasting effects of the induced immune memory on A β pathology and cortical ischemia at the later time points, the initial training stimulus increased while the tolerance stimulus reduced pathology, which was reflected by changes in A β plaque load and neuronal damage, respectively.

Immune memory in macrophages was previously shown to be mediated by epigenetic changes in enhancer regions that either stimulate or prevent gene transcription. In accordance, we performed chromatin immunoprecipitation sequencing for histone modifications in isolated microglia to determine changes in their enhancer landscape. Notably, we identified the active enhancer repertoire for hypoxia-inducible factor 1 α (HIF-1 α), a key modulator for macrophage inflammatory responses, to be enriched in microglia after the induction of trained immune memory (1xLPS). In contrast, pathways related to phagocytic functions showed an increase in active enhancers in the 4xLPS treatment group. Importantly, these epigenetic alterations were reflected by expression changes in the respective genes in the isolated microglia population. By

this study, we provide first evidence for long-lasting innate immune memory in the brain that can shape neurological disease outcome and is driven by epigenetic modifications of the microglial enhancer landscape.

In a last study, we focused on the microglial phagocytic capacity as an important factor for the modulation of A β plaque pathology, as *in vitro* experiments have reported that microglia can bind to, and engulf A β fibrils. However, so far, *in vivo* studies have not convincingly confirmed these results. Therefore, we investigated the role of the soluble milk fat globule-epidermal growth-factor 8 (MFG-E8) protein, that was recently hypothesized to mediate A β phagocytosis in AD pathology. To test the *in vivo* function of MFG-E8, we crossed mice expressing a functional knockout variant of *Mfge8* (*Mfge8*^{-/-}) with the APPPS1 and APP23 tg mouse models of cerebral β -amyloidosis.

In contrast to previous reports, our results indicated that the depletion of MFG-E8 has no impact on A β uptake by microglia or subsequent A β degradation processes. However, contrary to our expectations, MFG-E8 deficiency reduced A β plaque load and A β levels in both mouse models without affecting amyloid precursor protein (APP) processing.

When we immunohistochemically analyzed MFG-E8 distribution in the brain we observed a strong accumulation of MFG-E8 with congophilic A β deposits and co-staining of MFG-E8 with A β even showed a partial co-localization of both proteins at the sites of A β plaques. While the mechanism of these effects requires further studies, our results suggests that a direct interaction between MFG-E8 and A β promotes amyloid aggregation.

Taken together, these studies examined different ways of modulating the microglial immune response during AD pathology. Interestingly, the replacement of dysfunctional microglia by peripheral monocytes in the diseased brain did not modify A β deposition although the infiltrated monocytes adopted features of plaque-associated microglia. However, when we applied the concept of innate immune memory to the brain through the remodeling of the innate immune response by epigenetic reprogramming of the microglial enhancer repertoire, we identified a promising approach to modify A β pathology. Especially the induction of a microglial tolerance state had beneficial long-term effects on the pathology of cerebral β -amyloidosis while training aggravated disease outcome. These results provide, for the first time, evidence that long-lasting modulation of the innate immune reaction may occur due to immunological priming – a mechanism that introduces new targets for dampening A β pathology in Alzheimer's disease.

However, in contrast, a direct modification of microglial A β phagocytosis through the knockout of *Mfge8* is most likely not sufficient to modulate microglia function in AD.

2. Preface

In summer 2013 when I started my PhD my grandfather was sent to hospital because he was diagnosed with lung cancer. The clinicians could successfully remove the tumor and in theory he was cured. However, the surgery, and also the following weeks where he was confined to his bed, weakened his physiological constitution. During the next months, he got several lung infections and soon every physical activity became arduous. Finally, his cognitive abilities progressively declined. In the beginning, he failed to follow conversations, then he preferred to talk about his childhood and currently he sees faces in trees, against which he wants to fight. My grandfather became demented; but was it just co-incidence that he started to develop dementia or was it a side effect of his former illness? There is emerging evidence that systemic inflammation can aggravate the state of a neurological disease by inducing an exaggerated inflammatory environment in the brain and thus promote disease onset or speed up disease progression (Dunn et al., 2005). Therefore, the modulation of the innate immune system to induce an appropriate inflammatory immune response is regarded as a potential therapeutic target for neurological diseases. For that reason, this work will focus on the role of the innate immune system in Alzheimer's disease, the most common form of dementia (Holtzman et al., 2011).

3. Synopsis

3.1 Alzheimer's disease

3.1.1 An overview on 110 years of Alzheimer's disease research

Alzheimer's disease is a chronic and progressive neurodegenerative disease that, in 90-95 percent of the cases, affects people above 65 years of age (Harman, 2006). Patients develop cognitive dysfunctions, behavioral disturbances and in end stages also difficulties with performing activities of daily living. Notably, this disease was first described in the 51-year-old woman Auguste D. In 1901, she was presented to the physician Alois Alzheimer with changes in her personality such as impaired memory, disorientation or erratic behavior (Maurer et al., 1997). After her death in 1906, Alzheimer did a histological examination of her brain and found an analogous pathology as described in the context of senile dementia: a massive neuron loss, the presence of "small miliary foci" (later called senile plaques) of a "peculiar material in the cortex" (identified as amyloid- β) and clumps and condensations of intracellular fibrils he referred to "neurofibrillary degeneration" (Alzheimer, 1907; Maurer et al., 1997). However, when Alzheimer presented his findings at a congress in Tübingen, the audience paid no attention to this first description of a case of "pre-senile dementia". It was four years later, when his mentor Emil Kraepelin introduced the eponym „Alzheimer's disease" (AD) for the very first time to distinguish the atypical form of pre-senile dementia from the more common senile variant (Kraepelin, 1910). However, for the next decades, AD was regarded as a particularly serious form of senile dementia that played only a minor role as a neurological disorder (Hodges, 2006). But in the 1960s, when life expectancy started to rise and more elderly people were affected by the senile form of dementia, clinical delineation of dementia sub-forms and correlation between the abundance of pathology and cognitive decline unified the young onset Alzheimer's disease and the common elderly dementia (Blessed et al., 1968; Roth et al., 1966). Finally, it was Katzmann in 1976 who commented on the concern that AD is not only a rare disease of younger patients, but also affects the ageing population. He suggested to consistently use the term Alzheimer's disease for the pre-senile but also the common senile form of dementia, as both diseases share the same pathology (Katzman, 1976).

Soon after, first attempts were made to understand the mechanisms of the disease that led to the discovery of the two major proteins involved in the pathological lesions, which were already described many years ago: the amyloid- β (A β) peptide forming the extracellular amyloid plaques (Glennner and Wong, 1984b; 1984a; Masters et al., 1985b) and microtubule-associated protein tau (MAPT) as component of the intracellular filamentous lesions (Kosik et al., 1986). Furthermore, amyloid precursor protein (APP) was identified as the precursor protein

for A β (Kang et al., 1987; Masters et al., 1985a) and finally first studies could assign genetically heritable mutations to the pre-senile form of AD (Goate et al., 1991; Sherrington et al., 1995).

Today, 46.8 million people worldwide are affected by AD and an estimation for 2030 predicts 74.7 million people living with AD (Prince et al., 2015). As anticipated, AD has developed into a major public health challenge and is one of the most economically burdensome diseases in the world. According to a Forbes ranking in 2015, the global costs for dementia care are 818 billion US dollars annually, corresponding to the 18th largest economy in the world and exceeding the market values of Apple or Google (Wimo et al., 2017). The fears that arose 50 years ago came true, however the consequent effort that was made to understand the disease has so far been insufficient to develop a therapy for the devastating disease. Very recently, the first approved AD immunotherapeutic drug, the A β antibody Solanezumab failed to slow down cognitive decline in people with mild AD (Eli Lilly Press Release, 2016). Thus, only therapeutics that alleviate the symptoms of AD, such as acetylcholinesterase inhibitors or glutamatergic receptor inhibitors – both boosting neurotransmission and thus compensating for neuron – loss are available (Fleischhacker et al., 1986; Jorm, 1986; McGleenon et al., 1999; van Marum, 2009). Therefore, even more than 110 years after the first case description of a patient with “pre-senile dementia” by Alois Alzheimer in Tübingen (Alzheimer, 1906; 1907), it is of utmost importance to study the pathogenesis of AD to identify molecular targets or pathways that may one day facilitate a pharmacological therapy for AD.

3.1.2 Pathophysiology of Alzheimer’s disease – APP processing

The principal proteinaceous component of amyloid plaques in AD are aggregates of the A β peptide (Gorevic et al., 1986; Masters et al., 1985b; Selkoe et al., 1986). A β is a small carboxy-terminal fragment of the amyloid precursor protein (APP) with its size varying between 36 and 43 amino acids (Goldgaber et al., 1987; Kang et al., 1987; Robakis et al., 1987; Tanzi et al., 1987). APP is a transmembrane protein with a large amino-terminal extracellular domain and a small carboxy-terminal cytoplasmic domain (Dyrks et al., 1988; Weidemann et al., 1989). It is expressed in several isoforms with APP₆₉₅, APP₇₅₁ and APP₇₇₀ being the most abundantly expressed isoforms (Selkoe et al., 1988). In the brain, APP₆₉₅ is amply produced in neurons (Kang and Müller-Hill, 1990; Rohan de Silva et al., 1997), however after a relatively brief half-life of around 45-60 min, APP is metabolized very rapidly (Weidemann et al., 1989).

APP is processed via at least two proteolytic cleavage pathways involving three different secretases. APP cleavage can occur either via the non-amyloidogenic pathway, that includes alpha-secretase-mediated ectodomain shedding of APP within the A β sequence and thus precluding the formation of A β , or via the amyloidogenic pathway resulting in the release

of the A β peptide (Zhang et al., 2011). The first critical step in liberating A β during amyloidogenic processing of APP is the amino-terminal cleavage by the beta-site APP cleaving enzyme (BACE1 or β -secretase) that cleaves APP into the soluble APP- β ectodomain-fragment, which is released into the extracellular space, and a membrane-bound 99 amino acid carboxy-terminal fragment (CTF- β) (Seubert et al., 1993). CTF- β is further cleaved by a multi-subunit protease complex, the γ -secretase, that consists of the two transmembrane proteins (amongst other components), presenilin 1 (PS1) and presenilin 2 (PS2), that provide the catalytic core of the secretase (De Strooper et al., 1998; Wolfe et al., 1999). The stepwise processing of the CTF- β fragment by γ -secretase at several cleavage sites in the carboxy-terminal end of the A β sequence results in the production of A β species with varying lengths ranging between 36 and 43 amino acids, with A β ₄₀ and A β ₄₂ being the most abundant cleavage products (Selkoe, 2001; Takami et al., 2009). However, the longer A β ₄₂ is considered the more pathogenic form as it is more prone to aggregate (Jarrett et al., 1993).

3.1.3 Genetic susceptibility to Alzheimer's disease

As Alzheimer indicated 110 years ago, there exist two different forms of AD that can be distinguished by their age of onset. The rare pre-senile form of AD (familial Alzheimer's disease (FAD)) and the very common form of late-onset AD (LOAD). Genetic studies from families, which are affected by the pre-senile form of AD, identified dominantly inherited mutations in the *APP*, presenilin 1 (*PSEN1*) and presenilin2 (*PSEN2*) genes, which could be either linked to an increase in total A β concentrations or to an elevation of the A β ₄₂/A β ₄₀ ratio (Citron et al., 1992; Shen and Kelleher, 2007; Szaruga et al., 2017).

For AD up to date, 52 mutations in the *APP* gene are known (Alzforum, 2017a), from which most cluster around the γ -secretase cleavage site (Weggen and Behr, 2012). However, the well-known "Swedish double mutation", that is commonly used to generate transgenic mouse models of AD, is adjacent to the β -secretase-cleavage site and promotes APP β -site cleavage by BACE1 (Haass et al., 1995; Mullan et al., 1992).

For *PSEN1* and 2 more than 250 mutations are described (Alzforum, 2017b) and all have been shown to consistently increase the relative amounts of the more aggregation prone A β ₄₂ in relation to A β ₄₀ (Weggen and Behr, 2012).

A recent study identified a mechanism showing that mutations in *APP* and *PSEN1/2* cause a less stable enzyme-substrate interaction between γ -secretase and CTF- β resulting in the generation of longer more amyloidogenic A β species due to less sequential cleavage of A β (Szaruga et al., 2017). Consequently, in FAD, the majority of the identified mutations in *APP* or *PSEN1/2* alter proteolytic processing of APP and thus suggest that the abnormal elevation

of A β ₄₂ relative to A β ₄₀ is critical for AD pathogenesis. On that basis, the early pathogenic protein accumulation of A β into extracellular plaques observed in FAD was postulated to be causative for AD and thus, the “amyloid cascade hypothesis” became the most accepted model for AD pathogenesis and formed the basis for many therapeutic treatment approaches (Beyreuther and Masters, 1991; Hardy and Higgins, 1992; Hardy and Allsop, 1991; Selkoe, 1991).

However, for LOAD, the disease origin is less well understood as no causative familial mutations have been identified. Although a variety of studies identified several different risk factors from observational and experimental analyses such as diabetes (Leibson et al., 1997), cerebrovascular diseases (Lefrère et al., 1990), hypertension (Davies), smoking or physical inactivity (Davies), evidence is still lacking for a definitive cause of LOAD. Thus for a long time, ageing was assumed to be the only causative risk factor for LOAD, which was corroborated by a study speculating that if life would be twice as long, everyone would develop AD (Research1995). In addition, a study demonstrated that ageing increases the expression of inflammation-related genes, a process named “inflammaging” (Cribbs et al., 2012). As brain inflammation is a hallmark of AD, a predisposition to inflammatory processes may contribute to AD with ageing.

Interestingly in 2004, a twin study indicated that 50 percent of the risk for LOAD may be due to genetic factors (Pedersen et al., 2004), which were confirmed by subsequent studies to be crucial for LOAD (Lambert et al., 2010; 2009; 2013). Today, it is accepted that the interplay between the accumulation of age-related malfunctions, environmental factors and a pre-disposing genetic background most likely triggers pathology in LOAD and thus suggests to consider LOAD as a multifactorial disease (Borenstein et al., 2006).

3.1.4 Genetic risk factors for LOAD

Population-based association studies and genetic linkage analysis led to the identification of the first genetic risk loci for LOAD, the apolipoprotein (*APOE*) E4 allele which encodes the apolipoprotein E4 isoform (ApoE4) (Blacker et al., 1997; Saunders et al., 1993). Until today, *APOE*-E4 is the most prominent and strongest risk allele associated with LOAD (Corder et al., 1993). The *APOE* gene is polymorphic with three major alleles (E2, E3, E4), of which the *APOE*-E3 allele is the most common one (79%) (Ghebranious et al., 2005). Physiologically, the protein is involved in cholesterol transport and lipid metabolism and is produced primarily in the liver, but has also been found in the kidneys, spleen and brain (Mahley, 1988). Whereas the *APOE*-

E2 allele is considered to be protective against LOAD (Corder et al., 1994), carriers of two copies of the *APOE*-E4 allele have an eightfold increased risk for AD (Corder et al., 1993).

Follow up studies in humans and mice investigated the functional impact of the ApoE4 lipoprotein on AD and found that it can bind to A β and influence its aggregation as well as impair its metabolism (Castellano et al., 2011; Kim et al., 2009). This can occur by competing with A β for the low-density lipoprotein receptor-related protein 1 (LRP1), which is known to initiate endocytosis of A β by astrocytes (Verghese et al., 2013). Additionally, ApoE4 disrupts LRP1-mediated efflux of soluble A β across the BBB through the redirection of ApoE4-bound A β to a very-low-density-lipoprotein receptor (VLDLR) that is slower at internalizing A β at the BBB (Deane et al., 2008).

During the last decade, novel techniques such as genome wide association studies (GWAS), whole genome sequencing and gene-expression network analysis emerged that enabled the screening for many more gene networks and genetic variants, which are associated with LOAD. These data support LOAD as a disease with polygenic contributions in which the identified common disease susceptibility loci have small effects on AD risk (Escott-Price et al., 2015). A set of these identified genes such as clusterin (*CLU*), ATP-binding cassette transporter 7 (*ABCA7*) or sortilin related receptor 1 (*SORL1*) are involved in lipid metabolism as shown for *APOE*, and thus support the importance of this pathway in conferring AD risk (Harold et al., 2009; Hollingworth et al., 2011; Lambert et al., 2009; 2013).

Another important role was attributed to functions of the innate immune system, which represents the first line of immune defense in the brain. Thereby the immune response is conducted by microglia, which are immune cells of the myeloid lineage and the brain resident tissue-macrophages (Prinz and Priller, 2014). Once activated, microglia can produce a set of neurotoxic molecules to trigger an inflammatory response, but also possess the capability to engulf pathogens through phagocytosis (a more detailed overview on the microglial immune response can be found in section 3.1.5). Numerous of the identified genetic variants associated to the innate immune system are either directly expressed by glial cells or are part of the innate immune response, for example: triggering receptor expressed on myeloid cells 2 (*TREM2*), complement receptor 1 (*CR1*), myocyte enhancer factor 2c (*MEF2C*), and inositol polyphosphate-5-phosphatase D (*INPP5D*) (Fig. 1) (Gjoneska et al., 2015; Guerreiro et al., 2013; Hollingworth et al., 2011; Jonsson et al., 2013; Lambert et al., 2013; Naj et al., 2011). However, the investigation on the functional impact of the identified risk genes on LOAD has only recently started and thus our understanding remains limited.

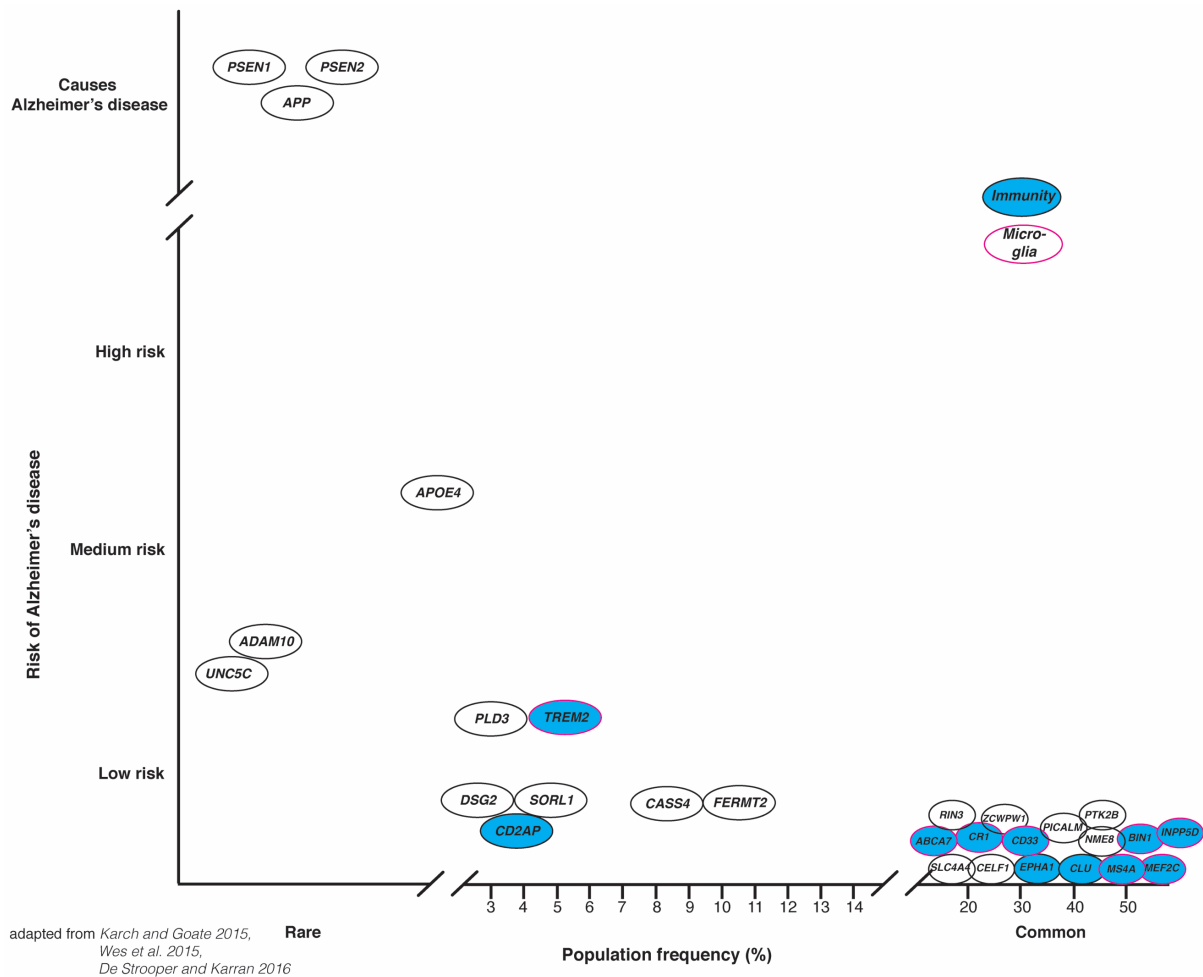


Figure 1: Genetic risk factors for Alzheimer's disease. Apart from rare mutations in the *APP*, *PSEN1* and *PSEN2* genes, which cause familial Alzheimer's disease, genetic analysis methods have identified a set of common genomic variants that show smaller effects on AD risk. Although, a variety of the genes encode proteins that can be related to functions of the innate immune system (highlighted in blue) and are expressed in microglia (encircled in red), the ascription of alterations in the biological functions to all detected variants is still on-going.

The most controversially discussed risk factor is *TREM2*. Rare coding variants identified in the gene locus such as the arginine to histidine amino acid substitution (R47H) significantly increase the risk for LOAD by two- to threefold (Guerreiro et al., 2013; Jonsson et al., 2013). *TREM2* is a V-type immunoglobulin domain that is highly expressed by microglia and is suggested to play a role in phagocytosis (Hickman and Houry, 2014). *TREM2* expression is not restricted to the brain and can also be found on peripheral tissue macrophages like osteoclasts (Cella et al., 2003; Humphrey et al., 2006; Paloneva et al., 2003) or alveolar macrophages (Ulrich et al., 2017; Wu et al., 2015). The exact ligands that activate *TREM2* signaling are not known but are assumed to include phospholipids, bacterial products or cell debris (De Strooper and Karran, 2016). After activation, *TREM2* associates with its signaling partners, DAP12 (DNAX-activation protein 12/TYROBP) and DAP10 (Peng et al., 2010), leading to the initiation of signaling cascades, which promote the anti-inflammatory functions

of the immune system such as phagocytosis (Takahashi et al., 2005), the suppression of pro-inflammatory cytokines and chemokines (Bouchon et al., 2001; Mazaheri et al., 2017), but also cell survival (Wang et al., 2015) and proliferation (Otero et al., 2012). Moreover, TREM2 activation can interfere with toll-like receptors (TLRs)-induced cytokine production by macrophages to restrain macrophage activation and thus negatively regulate the inflammatory response (Hamerman et al., 2006; Turnbull et al., 2006).

The linkage between TREM2 and AD is not entirely clear. It remains to be elucidated whether genetic variants of *TREM2* that are associated with LOAD increase or impair TREM2 function. Remarkably, loss of function mutations in *TREM2*, which cause the severe neurological disorder Nasu Hakola disease, were also found to increase the risk for AD (Guerreiro et al., 2013; Song et al., 2017). This supports a similar impairment of TREM2 function in AD. Conversely, other mutations (D87N and T96K), which are potentially associated with LOAD, increase TREM2 activity (Guerreiro et al., 2013; Song et al., 2017). Thus, it seems that an overall disruption of TREM2 homeostasis by several different genetic variants may be responsible for the increased risk of LOAD.

For this reason, the modulation of AD pathology by TREM2 has now started to be extensively studied in mouse models in which TREM2 levels were found to be increased in plaque-associated myeloid cells (Frank et al., 2008; Melchior et al., 2010) and seem to be important for plaque-associated myeloid-cell accumulation (also known as microgliosis) as TREM2 deficiency decreased the number of cells that surround A β plaques (Jay et al., 2015; Wang et al., 2015; 2016). A reduction of microgliosis has also been observed in human post-mortem brain sections from R47H variant carriers (Yuan et al., 2016). Additionally, gene expression analysis revealed that knocking out *Trem2* in mouse models for AD results in a decrease in inflammation-related genes associated with microglial activation in response to A β (Ulrich et al., 2014; Wang et al., 2015). Furthermore, TREM2 deficiency was reported to suppress the induction of microglial phagocytic pathways and to impair A β phagocytosis by myeloid cells (Jay et al., 2017; Keren-Shaul et al., 2017). However, the effect of TREM2 deficiency on A β burden is very conflicting and different studies either reported decreased A β deposition at early diseases stages but conversely exacerbated plaque pathology at later stages (Jay et al., 2017) or aggravated pathology restricted to certain brain regions (Wang et al., 2015). Ultimately, these results suggest opposing roles for TREM2 at different stages of the disease and consequently further studies are required to decipher its definite role in the regulation of the inflammatory immune response during AD.

Other genetic variants associated with the immune system were identified in the locus encoding complement receptor 1 protein (*CR1*) (Lambert et al., 2009). CR1 is a glycoprotein and a component of the complement response that can adhere to particles that are opsonized with complement factors C1q or iC3b to initiate phagocytosis. *CR1* is predominantly expressed in the periphery, but was also identified in cultured human microglia (Walker et al., 1995). CR1 is also an important regulator of the converting process of the central complement component C3 to the active C3b and iC3b complement factors (Krych-Goldberg and Atkinson, 2001; van Beek et al., 2003). It was shown that *CR1* expression on erythrocytes is involved in the peripheral clearance of iC3b-opsonized A β from human blood, suggesting that alterations in CR1 structure or expression due to genetic polymorphisms could influence A β clearance (Rogers et al., 2006). Studies also reported a positive correlation between mRNA expression of the rs6656401 *CR1* variant and A β plaque burden (Chibnik et al., 2011; Zhang et al., 2010). However, no further study could confirm a correlation of the identified genetic variants in the *CR1* locus and AD pathology so far (Fonseca et al., 2016).

Even though the functional association of these genes is still under investigation, the understanding for the innate immune response as an important factor driving AD pathology impressively increased during the last 20 years and was further reinforced by the identification of several genetic variants expressed in genes of the innate immune system reported in landmark studies by Lambert et al. in 2009 and 2010 (Fig. 2) (Lambert et al., 2009; 2010).

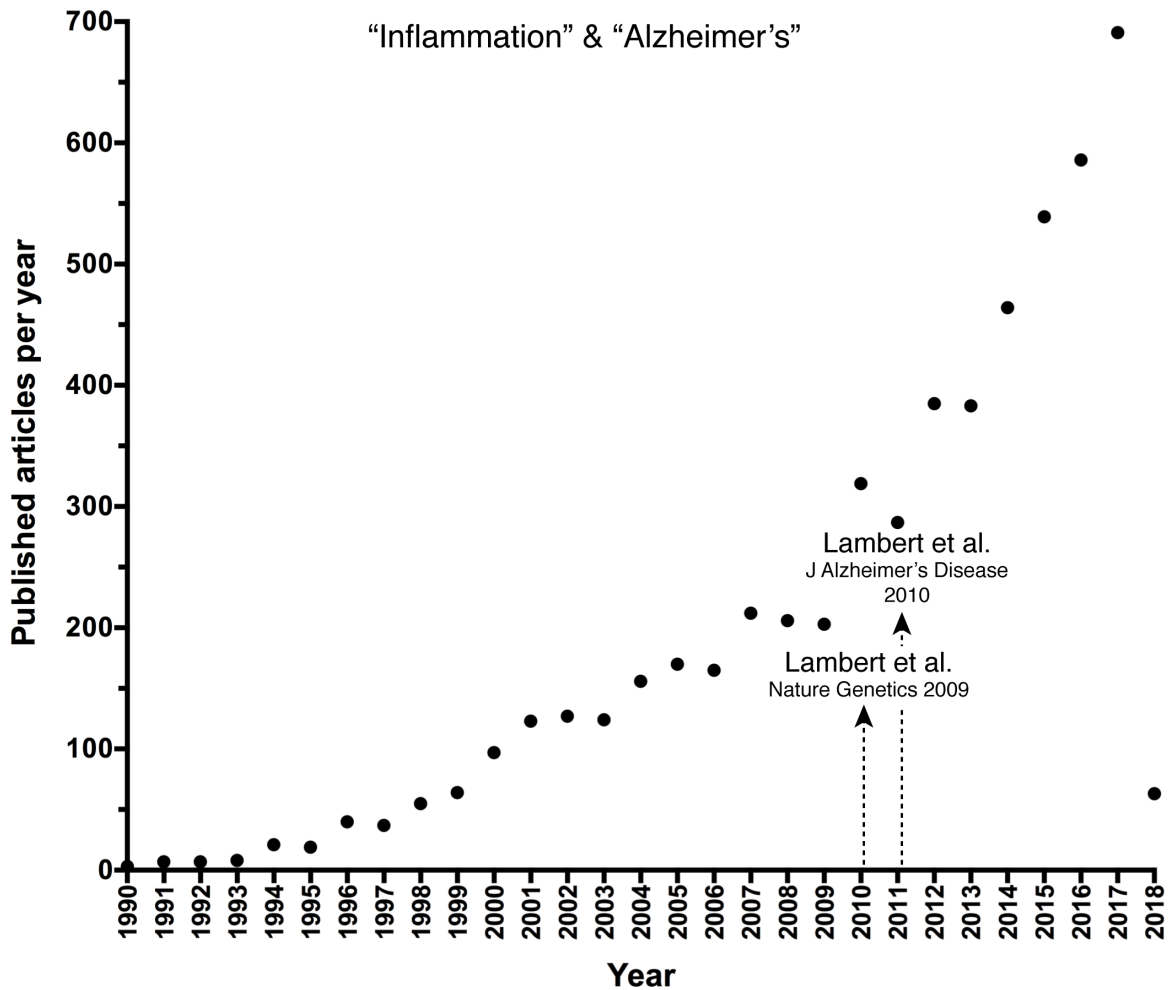


Figure 2: Evolution of the importance for inflammation in Alzheimer’s disease. During the last 20 years, research on the contribution of inflammatory processes to the etiology of Alzheimer’s disease grew exponentially and was further reinforced by the identification of several genetic variants in immune-related genes by Lambert et al. in 2009 and 2010 (Lambert et al., 2009; 2010). The numbers of published papers per year for the term “Inflammation” and “Alzheimer’s” were assessed on PubMed Central (26.01.2018).

3.1.5 Microglia – mediators of the innate immune response in AD

The identification of several risk genes that contribute to innate immune responses in the central nervous system (CNS) or are directly encoded by microglia, support the long-standing hypothesis that alterations in the innate immune system contribute to the pathology of AD (Heneka et al., 2015b; Meyer-Luehmann and Prinz, 2015; Ransohoff and Khoury, 2015). As the resident immune cells in the CNS, microglia play an essential role in brain immune responses.

Microglia, as a new cell entity, were first described in 1919 by the Spanish neuroscientist Pío del Río Hortega. Through the invention of a new staining method based on silver carbonate he was able to visualize the finest morphological details of different brain cells

and classified the formerly named “third element” cells into two new cell types: microglia and oligodendrocytes (Rezaie and Hanisch, 2014). However, the functional designation of these cells was inconclusive for a long period. Today, it is well known that microglia are the tissue resident immune cells and the fundamental effectors and regulators of the innate immune response in the brain. They account for 5-12 percent of the cells in the CNS (Lawson et al., 1990). Fate mapping analysis in mice revealed that these cells arise from primitive myeloid progenitors of the yolk sac during embryonic development (Ginhoux et al., 2010). In particular, before embryonic day 10.5 (E10.5), primitive macrophages exit the yolk sac and invade the neuroepithelium where they start to differentiate, expand and colonize the whole CNS. Through the closure of the blood brain barrier (BBB) around day E13.5 (Ben-Zvi et al., 2014), the CNS is uncoupled from the periphery resulting in a restricted environment that excludes the invasion of any peripheral blood-derived monocytes into the healthy brain (Ajami et al., 2011; Ginhoux and Jung, 2014; Hagan and Ben-Zvi, 2015). Based on the segregation of the CNS from the peripheral macrophage cell pool, it is suggested that microglia maintenance is mediated by self-renewal via local proliferation that resembles peripheral tissue-resident macrophages in the steady-state (Ajami et al., 2007; Hashimoto et al., 2013). However, in contrast to other short-lived peripheral tissue macrophages, microglia were initially assumed to be extremely long-lived cells with a turnover rate of 0.05 percent (Lawson et al., 1992), implicating that microglia are almost never renewed. However, a recent study revisited the longevity of microglia and found a ten times higher turnover rate in mice that estimates the self-renewal of the brain’s microglial population every 95 days and questions the view of microglia as a long-lived population (Askew et al., 2017; Tay et al., 2017). A similar study with human microglia reported an average lifespan for these cells of around four years with an annual turnover rate of 28 percent implicating multiple cycles of microglial renewal throughout life (Réu et al., 2017). Conversely, a recently published study, in which single microglia were imaged *in vivo* for up to 15 months, calculated an average lifetime of adult mouse microglia of 22 months proving the longevity of these cells (Füger et al., 2017).

This relative longevity of microglia makes these cells vulnerable to environmental insults or monogenic disorders. Noteworthy, mutations in the gene for colony stimulating factor 1 receptor (*CSF1R*), a key regulator of myeloid lineage cells, which controls proliferation, differentiation and survival of macrophages (Patel and Player, 2009), causes hereditary diffuse leukoencephalopathy with spheroids (HDLS) (Rademakers et al., 2011), a disease of the CNS with a variety of neurological symptoms such as dementia, depression or seizures (Axelsson et al., 1984; Wider et al., 2009).

Under steady-state conditions, microglia execute several functions. They actively scan their microenvironment for any tissue disturbances and support neuronal function and survival by synapse maintenance and elimination via phagocytosis (Kettenmann et al., 2013; Paolicelli et al., 2011; Tremblay et al., 2010). They are further involved in the remodeling of neuronal circuits and the release of different trophic factors (Parkhurst et al., 2013; Schafer et al., 2012). However, a major part of the microglial role in the brain is the initiation of an immune response. Upon sensing of pathogen invasion, tissue damage, toxic proteins or apoptotic cells by pattern recognition receptors (PRRs), microglia become activated to undergo morphological remodeling. They begin extending their processes towards the lesion and subsequently migrate to the site of the injury where they finally mediate the immune response. This includes the production of pro- or anti-inflammatory cytokines, chemokines and other neurotoxic factors, but also the induction of phagocytic pathways to engulf the invaded pathogens or other toxic material (Ransohoff and Perry, 2009). During acute inflammatory events, the microglial immune response supports the resolution of the pathological alterations with immediate benefit to the environment. However, long-lasting pathological events, can induce a microglia-mediated non-resolving inflammatory milieu that in turn drives microglia into a persistent dysfunctionality with a detrimental outcome for pathology (Heneka et al., 2015a).

In particular, during AD the recognition of A β by microglia is mediated by a repertoire of cell-surface innate immune receptors and receptor complexes consisting of scavenger- or toll-like receptors (TLRs) (Liu et al., 2005; Paresce et al., 1996; Stewart et al., 2010). Receptor ligation triggers the initiation of the microglial innate immune response with the production and secretion of pro-inflammatory modulators such as the cytokines IL-1 β , IL-6 or tumor necrosis factor alpha (TNF- α), reactive oxygen species or nitrogen monoxide (Mogi et al., 1994; Morimoto et al., 2011). However, the enduring production and deposition of A β during AD leads to a sustained exposure of microglia to A β and thus to a chronic activation of the cells with a permanent production of inflammatory cytokines which can in turn for example upregulate BACE1 enzymatic activity for enhanced A β production and, subsequently, stimulate a positive feedback loop that may induce microglial dysfunction (Sastre et al., 2003). Furthermore, it has been reported that the persistent exposure to A β or other pro-inflammatory molecules impairs A β internalization by microglia (Heneka et al., 2013; Krabbe et al., 2013). Thus, AD reflects a chronic pathological event that modulates the microglial immune response in a detrimental fashion, contributing to disease progression rather than supporting the resolution of inflammation.

However, several studies on macrophages suggest different experimental approaches to alter the macrophage phenotype. In this context, it was reported that the phenotype of already differentiated macrophages can be re-programmed by alterations in the local tissue environment (Lavin et al., 2014). Moreover, it was also shown that an appropriate immune stimulus to macrophages can induce epigenetic changes in these cells that shape the immune response upon future immune challenges (Saeed et al., 2014). Finally, the genetic depletion of proteins involved in the mediation of the myeloid immune response was utilized to modify the phenotype of microglia and concomitantly alleviate cerebral β -amyloidosis and cognitive dysfunction in AD mouse models (Berg et al., 2012; Heneka et al., 2013; Yamamoto et al., 2007). Altogether, these concepts present promising methods to modify the microglial immune response in AD and will be comprehensively addressed in relation to the findings of my doctoral project in the following sections.

3.2 Environmental factors as regulator for myeloid cell function

In reference to:

Replacement of brain-resident myeloid cells does not alter cerebral amyloid- β deposition in mouse models of Alzheimer's disease

Nicholas H. Varvel*, Stefan A. Grathwohl*, Karoline Degenhardt, Claudia Resch, Andrea Bosch, Mathias Jucker and Jonas J. Neher

The Journal of Experimental Medicine 2015 Vol. 212, No. 11, 1803-1809,
doi:10.1084/jem.20150478

3.2.1 Microglia targeting approaches

The best methods to study microglial function are genetic modification strategies, which enable labeling, alteration of gene expression and depletion of microglia. However, although microglia are a myeloid cell population that is developmentally and functionally distinguishable from other tissue macrophages such as peripheral monocytes, the specific targeting of microglia to study their biological function *in vivo* is difficult (Hoeffel and Ginhoux, 2015; Lavin et al., 2014). While some putative microglia-specific genes such as *P2ry12* or *Hexb*, *Sall1* have been identified (Butovsky et al., 2014; Hickman et al., 2013; Koso et al., 2016), both microglia and monocytes share a wide range of receptors.

The *in vivo* visualization of cells by fluorescent protein expression in mice is a commonly used method to analyze cell development, morphology or transcription of specific genes (Chudakov et al., 2010). In the brain, the replacement of one allele of the *Cx3cr1* gene, encoding the fractalkine receptor (CX3CR1), with complementary DNA encoding fluorescent proteins (for example: green fluorescence protein (GFP)) (*Cx3cr1^{+GFP}*), is the most widely used technique to investigate the function of microglia (Jung et al., 2000). However, *Cx3cr1* is also expressed by other peripheral mononuclear phagocytes and circulating monocytes (Geissmann et al., 2003; Jung et al., 2000). Therefore, *Cx3cr1^{+GFP}* mouse models would only allow for selected targeting and visualization of the CX3CR1-positive immune cells and not specifically microglia. This makes it challenging to specifically mark one of these populations, especially for the controversial debate under which conditions peripheral monocytes can invade into the CNS.

However, the insertion of a sequence encoding a Cre recombinase fused to a mutant estrogen-binding domain (Cre/ER system) into a microglia-specific gene allows an inducible

activation of the Cre recombinase to induce site-specific recombination of loxP-sites flanked (floxed) genes upon administration of tamoxifen (Feil et al., 2009; Hayashi and McMahon, 2002; Yona et al., 2013). In terms of microglia visualization, mice carrying the Cre/ER system under the macrophage-specific promoters *Cx3cr1* (Goldmann et al., 2013), *CD11c* (Town et al., 2008) or *LysM* (Dighe et al., 1995), can be crossed to reporter mouse lines such as *Rosa26* (*R26-yfp*) in which yellow fluorescent protein (YFP) reporter gene activity is induced after tamoxifen induced recombinase activation to excise a floxed STOP element preceding the reporter gene (Goldmann et al., 2013; Wieghofer et al., 2015). Consequently, this technique allows for the specific visualization of the long-lived microglia in *Cx3cr1^{CreER}:R26-yfp* animals, because after tamoxifen-induced recombination the short-lived peripheral monocytes are replaced by bone-marrow-derived progenitor cells, which experienced no tamoxifen-induced recombinase activity. Thus, a complete microglia-specific labeling was reported to be achieved around four weeks after tamoxifen administration (Goldmann et al., 2013; Parkhurst et al., 2013).

Additionally, these mouse lines can be used to conditionally delete floxed genes to study their impact on microglia function. In order to assess the effect of the microglial mediated inflammatory immune response on CNS homeostasis for example, the inducible site-specific recombinase technique was used for the dissection of microglia-specific pathways or single genes such as the “transforming growth factor (TGF)- β -activated kinase 1” (*Tak1*), which is a kinase known to be involved in the upstream signaling of NF- κ B-mediated microglial immune response (Sato et al., 2005). The genetic deletion of *Tak1* showed that this kinase acts as a key regulator of microglia-mediated CNS inflammation, as the inflammatory response was mitigated in autoimmune demyelination as well as after acute LPS stimulation in conditional *Tak1* knockout mice (Goldmann et al., 2013; Wendeln et al., 2018) These results underline the unfavorable role of microglia when executing their inflammatory response, both in models of multiple sclerosis and AD.

Another approach to study the role of microglia in brain pathology is to delete the total microglia pool. This can be achieved through the insertion of the herpes simplex virus thymidine kinase (*HSVTK*) gene under the *CD11b* promoter. HSVTK is a “suicide kinase” that phosphorylates the antiviral nucleotide analog ganciclovir (GCV), a synthetic analog of 2'-deoxy-guanosine. Instead of 2'-deoxy-guanosine triphosphate, phosphorylated GCV is incorporated into the DNA leading to strand breaks, which induce apoptosis in CD11b-positive cells (Wieghofer et al., 2015). To restrict *HSVTK* (TK⁺) expression to the brain, TK⁺ mice can either be lethally irradiated and reconstituted with wildtype bone marrow or GCV can be

applied exclusively to the brain by a surgically implanted osmotic pump (Grathwohl et al., 2009; Heppner et al., 2005; Varvel et al., 2012). In the latter case, intracerebroventricular (i.c.v.) administration of GCV ablates up to 90 percent of the microglia within two weeks. The few remaining microglia show a hyper-ramified phenotype (Varvel et al., 2012). This approach was used to investigate whether microglia are necessary for the formation and maintenance of A β plaques. However, after two and also four weeks of nearly complete absence of microglia no effect on A β formation, number and morphology of neurons or dystrophic neurites were observed (Grathwohl et al., 2009). In principle, this argues against a significant contribution of microglia to AD pathology; however, the period of microglial absence may have been too short to reveal any significant effects.

Interestingly, studies suggest that infiltrating monocytes are the principle cells that mediate A β plaque-associated gliosis and that its elimination cause a reduction in pathology as well as decreased neuroinflammation (Jay et al., 2015). These results posit that, not microglia but infiltrating monocytes are involved in the inflammatory milieu that emerges in the brain regions where A β deposition occurs.

3.2.2 Monocytes – co-workers of microglia?

In the healthy brain the blood brain barrier (BBB) shields the brain from the invasion and differentiation of circulating monocytes into brain macrophages (Geissmann et al., 2010; Obermeier et al., 2013). However, engraftment of monocytes into the microglia-populated brain during inflammation is controversially discussed and could be promoted by damage of the BBB due to age-induced cerebrovascular dysfunctions or during cerebrovascular changes in AD pathology (Bell and Zlokovic, 2009; Minogue et al., 2014; Pimentel-Coelho and Rivest, 2012).

Peripheral circulating blood monocytes express several receptors, which are used for classification into different subsets. In mice, there exists the pro-inflammatory (classical) cell population (CX3CR1^{low}, CCR2^{pos}, Ly6C^{high}) that is recruited to inflamed tissue where it differentiates into a monocyte-derived macrophage population to mediate an inflammatory response, and an anti-inflammatory (non-classical) cell population (CX3CR1^{high}, CCR2^{neg}, Ly6C^{low}) representing the patrolling monocytes of the blood (Auffray et al., 2009). The patrolling monocytes are the longer-lived cells with a half-life of around two days, whereas the immune response-mediating CX3CR1^{low}, CCR2^{pos}, Ly6C^{high} cells are short-lived, having a half-life of about 20 hours (Yona et al., 2013). In humans, the presence of CD14⁺, CD16⁻ cell surface receptors corresponds to the pro-inflammatory (classical) monocyte subpopulation, which has a relatively short circulation life span in the blood of one day, but can be recruited to sites of infection. In contrast, cells expressing higher levels of CD16 (CD14^{low}, CD16⁺) have a

longer circulation life span of about seven days and represent the patrolling (non-classical) monocytes of the vasculature (Passlick et al., 1989; Patel et al., 2017).

Peripheral monocytes can be targeted by antibodies, liposomes or cell transfer and thus display an attractive option for therapeutic manipulation (Biber et al., 2016). For example, the induction of experimental autoimmune encephalomyelitis (EAE), a murine model for the inflammatory aspects of multiple sclerosis, initiates the production of the monocyte chemoattractant protein 1 (MCP-1 or CCL2) in the CNS which is the ligand for C-C chemokine receptor type 2 (CCR2) expressed on the surface of monocytes (Dogan et al., 2008). Increased levels of CCL2 were shown to affect BBB integrity and to attract the reactive CX3CR1^{low}, CCR2^{pos}, Ly6C^{high} monocyte population to transmigrate into the brain where they contribute to the severity of autoimmunity (Izikson et al., 2000; Mildner et al., 2009; Saederup et al., 2010; Stamatovic et al., 2005). In line with this, depletion of CX3CR1^{low}, CCR2^{pos}, Ly6C^{high} monocytes by application of liposomes containing dichloromethylene diphosphonate induced a significant alleviation of the symptoms of experimental autoimmune encephalomyelitis (EAE) (Brosnan et al., 1981; Huitinga et al., 1990).

In AD, however, it remains to be clarified whether a CCL-CCR2-dependent infiltration of monocytes occurs and whether this would affect disease outcome. Studies have shown that CCL2 concentrations are increased in AD and may be released by microglia and astrocytes in response to A β deposition (Khoury et al., 2003; Naert and Rivest, 2013; Smits et al., 2002; Vukic et al., 2009). This in turn, would induce monocyte extravasation from the blood into the brain (Fiala et al., 1998). Interestingly, the genetic deletion of *Ccr2* reduced plaque-associated cells and increased A β deposition as well as intracellular forms of A β (Khoury et al., 2007; Naert and Rivest, 2011). These studies hypothesize that recruitment of peripheral monocytes upon CCL attraction into the brain play a critical role for the etiology of AD. However, none of these studies could clearly prove that the aggravation of A β pathology was due to a failure of the CCL-CCR2-mediated infiltration of peripheral monocytes or caused by secondary effects of *Ccr2* deletion, because of the lack of a specific marker that enables discrimination between invaded monocytes and the resident microglia.

For that reason, studies made usage of bone marrow irradiation to first eliminate bone marrow (BM)-derived monocytes, which were then replaced by GFP-labelled bone marrow cells in mouse models of AD. These studies showed a massive infiltration of GFP-positive cells into the brain where they associated to A β depositions and modulated plaque pathology (Mildner et al., 2007; Simard et al., 2006; Stalder et al., 2005). However, total-body irradiation was shown to cause artificial damage of the BBB that promotes and thereby obscures the

relative contribution of the infiltration of peripheral monocytes (Mildner et al., 2007). This can be circumvented by shielding the head of animals during irradiation, which remarkably resulted in a lack of GFP-positive monocytes in the brain (Mildner et al., 2011). Similar results were seen in a parabiosis study in which the blood circulation of CD45.2⁺ 5xFAD mice was joined with congenic CD45.1⁺ mice. Analogous to head-shielded mice, the brain of 5xFAD was free of BM-derived CD45.1⁺ monocytes (Wang et al., 2016).

Another approach to study a possible monocyte infiltration after a potential microglia loss or dysfunctionality in disease, is the HSVTK-dependent ablation of microglia in the adult brain. Therefore, mice that expressed the CD11b-HSVTK (TK⁺) construct were crossed to mice which carried the gene for red fluorescent protein (RFP) under the *Ccr2* promoter (*Ccr2*^{+Rfp}). Microglia ablation was induced by two weeks of GCV treatment that was shown to deplete >90 percent of all brain myeloid cells (Grathwohl et al., 2009; Varvel et al., 2012). To examine cell repopulation of the brain, the mice were housed for another two weeks until an infiltration of cells positive for the cell surface marker CD45 and RFP-labeled CCR2 was observed. These cells entered the brain from small blood vessels confirming their peripheral and hematopoietic origin. Of note, the CCR2-RFP-positive cells were distributed across the brain as observed for the resident microglia in control mice, however their number was highly enriched and morphological differences like enlarged cell soma and shorter, asymmetrically orientated processes were detected (Varvel et al., 2012). Remarkably, the number of the invaded CCR2-RFP-positive cells remained stable over a 27-week observation period with a similar rate of proliferation as observed in microglia. Furthermore, the engrafted myeloid cells took over essential surveillance functions such as covering of the neuropil by their processes or the migration towards experimentally induced neuronal damage indicating that under certain conditions monocytes can replace dysfunctional microglia and adopt their phenotype. These results were further supported by a study in which infiltration of peripheral myeloid cells after GCV application was tracked by performing isochronic parabiosis with mice expressing enhanced green fluorescent protein (*GFP*) under the ubiquitously expressed actin promoter (*Act.GFP*). In the TK⁺ mice, where microglia were depleted, a substantial number of GFP-positive cells were found in the brain two weeks after GCV discontinuation (Prokop et al., 2015).

Contrary to the HSVTK model, another study found that after microglial depletion using pharmacological inhibition of colony stimulating factor 1 receptor (CSF1R) signaling that is mandatory for microglial survival, the repopulating cells that rapidly infiltrated the brain resembled microglia in morphology and cell number (Elmore et al., 2014). However, these cells

were assumed to originate from a resident microglia progenitor pool through self-renewal rather than being replaced by infiltrating monocytes, as no CCR2-RFP-positive cells could be detected (Elmore et al., 2014). The reported controversies for the origin of the repopulating cells could be due to the different approaches that were used to deplete the initial microglia pool. It is possible that pharmacological CSF1R inhibition leads to a small subset of surviving cells, which could be responsible for the rapid self-renewing of phenotypically similar microglia.

In summary, under special conditions such as a compromised BBB or pharmacological microglia ablation the brain becomes repopulated by cells that have the ability to adopt a microglial phenotype.

3.2.3 Environment determines macrophage function in the brain

Based on the findings from Varvel et al. that, upon microglia depletion, invading myeloid cells were capable of maintaining tissue homeostasis in a similar way as microglia do (Varvel et al., 2012), we wanted to examine whether the replacement of dysfunctional microglia by myeloid cells in mouse models of cerebral β -amyloidosis alters amyloid deposition and could thus be of therapeutic value as already implicated in a mouse model of Rett syndrome (Derecki et al., 2012). To this end, CD11b-HSVTK (TK⁺) mice were crossed to two mouse models of AD, namely APPPS1 mice which contain human transgenes for mutated APP and PSEN1 with early A β deposition and APP23 mice which overexpress mutated human APP with late A β deposition (Radde et al., 2006; Sturchler-Pierrat et al., 1997). Remarkably, in TK⁺-APPPS1 mice, which were analyzed two weeks after discontinuation of GCV treatment to deplete the endogenous microglia pool, the infiltrated cells did not cluster around congophilic plaques as observed in TK⁻ control mice. In fact, all cells displayed a homogenous phenotype with shorter processes and enlarged cell bodies in accordance with what was described by Varvel et al. in wildtype animals (Varvel et al., 2012). Interestingly, the lack of clustering around A β deposits induced no changes in A β load. Also, extended ageing time points (up to six months) after GCV treatment in the APP23 mouse line did not change plaque pathology. However, after this long-term brain engraftment, some of the myeloid cells in the TK⁺ mice were found to cluster around A β plaques. Furthermore, the initial myeloid cell number in TK⁺ mice that was determined two weeks after discontinuation of GCV application was approximately doubled in comparison to TK⁻ mice, but was virtually equal to cell number of age matched TK⁻ controls after long-term cell engraftment (Varvel et al., 2015).

Finally, we tested whether the replacement of microglia before amyloid deposition in APP23 mice might be more beneficial in terms of the pathology of cerebral β -amyloidosis. Therefore, GCV treatment was started before A β plaque deposition allowing the myeloid cells

to repopulate the brain before onset of A β deposition. Surprisingly, five months after treatment, when A β plaque pathology was present, myeloid cells of TK⁺ mice behaved similar to microglia of TK⁻ mice. Cells clustered tightly around plaques and those in plaque-free areas reflected a more microglia-like morphology, with smaller cell bodies and a ramified appearance. Of note, no changes in plaque pathology became apparent. Furthermore, similar to microglia, the engrafted plaque-associated cells in the long-term repopulated brain were positive for TREM2, whereas myeloid cells that were analyzed shortly after repopulation were TREM2-negative (Varvel et al., 2015). Thus, it can be concluded, that *Trem2* expression seems to be influenced by the local environment and is not strictly cell-specific regulated.

In line with our findings that monocytes that engraft in the brain become microglia-like and adopt essential microglial functions, a study from Lavin et al. could show that bone marrow-derived macrophages that arise from transplanted bone marrow after lethal irradiation replace the ablated tissue resident macrophages and establish a new but tissue-specific identity (Lavin et al., 2014). Additionally, differentiated peritoneal macrophages, which were isolated and transferred into the alveolar cavity, showed downregulation of peritoneal-specific markers and a parallel upregulation of lung-macrophage specific genes. Overall, in the engrafted peritoneal derived macrophages, 70 percent of genes that were differentially expressed in peritoneal macrophages compared lung macrophages were switched to resemble lung macrophages indicating that the new environment can reprogram the genetic identity of macrophages (Lavin et al., 2014). Another study showed that isolated microglia, which were only cultured with IL-34, an essential factor for microglia development (Greter et al., 2012; Wang et al., 2012), expressed a completely different gene set than observed *in vivo* (Gosselin et al., 2014).

According to our findings that the AD brain micro-environment shapes monocyte and microglial function independent of cell origin, these studies additionally suggest that the environmental-induced identities and functions of tissue resident macrophages are regulated through the induction of tissue-specific regulatory elements of the transcriptional process that modify the enhancer landscapes of the macrophages genes (Lavin et al., 2014).

However, apart from signals of the micro-environment, systemic alterations during lifetime might also be able to influence the genomic profile of tissue resident macrophages and could therefore be a potential tool to manipulate these cells.

3.3. Modification of CNS pathology by molecular reprogramming of the innate immune response

In reference to:

Innate immune memory in the brain shapes neurological disease hallmarks

Ann-Christin Wendeln*, Karoline Degenhardt*, Lalit Kaurani, Michael Gertig, Thomas Ulas, Gaurav Jain, Jessica Wagner, Lisa M. Häsler, Katleen Wild, Angelos Skodras, Thomas Blank, Ori Staszewski, Moumita Datta, Tonatiuh Pena Centeno, Vincenzo Capece, Md. Rezaul Islam, Cemil Kerimoglu, Matthias Staufenbiehl, Joachim L. Schultze, Marc Beyer, Marco Prinz, Mathias Jucker, André Fischer, and Jonas J. Neher

Accepted in Nature 23.02.2018

3.3.1 Systemic inflammation as trigger for neurological disease

The CNS is considered an immune-privileged region as the BBB shields the brain from the periphery. However, communication between the periphery and the CNS clearly exists, since several peripheral diseases, for example viral infections or sepsis, induce the development of a sickness behavior. Sickness behavior describes behavioral changes of the affected individuals such as the loss of appetite, lethargy or hyperalgesia, which are accompanied by metabolic changes going along with an altered body temperature, increased somnolence and loss of body weight, to facilitate the organisms combating of a disease (Hart, 1988). Also, an experimentally-induced acute systemic infection by infusion of recombinant cytokines or injections of bacterial cell wall components such as the endotoxin lipopolysaccharide (LPS) was reported to induce sickness behavior (Brydon et al., 2008; Dantzer, 2001; Harrison et al., 2009).

During systemic infection, inflammatory modulators which are produced by the resident immune cells as a local inflammatory response to the infection are transmitted to the brain along different humoral and nerve routes without compromising of the BBB (Kent et al., 1992; Konsman et al., 2002). In turn, microglia, as the resident immune effector cells in the brain, become rapidly activated and induce a robust non-specific but systemic response to the infection including the above-mentioned behavioral and metabolic alterations (Dantzer, 2001). The duration of sickness behavior upon an acute systemic infection is tightly regulated by the production of anti-inflammatory modulators like IL-10, TGF- β or glucocorticoids in the brain to dampen the immune response in the periphery but also in the CNS to avoid detrimental effects for the brain (Bogdan et al., 1992; Rivest, 2009).

Apart, from acute systemic infections that induce a strong release of inflammatory mediators, the presence of subclinical but sustained endotoxemia experimentally induced by LPS administration was reported to positively correlate with peripheral pathologies such as insulin resistance, atherosclerosis or chronic kidney disease mediated by an upregulation of the inflammatory immune response (Mehta et al., 2010; Terawaki et al., 2010; Wiesner et al., 2010).

Interestingly, an enhanced expression of inflammatory cytokines was also seen in brains of animal models of neurodegenerative diseases, a state that is suggested to prime or pre-activate microglia to become more susceptible to phenotype switching following further immune challenges (Betmouni et al., 1996; Cunningham et al., 2002; Depino et al., 2003; Perry et al., 2002; 2007; Sly et al., 2001; Walsh et al., 2001). Moreover, increased levels of the pro-inflammatory IL-6 cytokine, but decreased levels for the anti-inflammatory IL-10 cytokine were reported in the brain of aged mice, implying that ageing causes an inflammatory environment as already described by the term “inflammaging” (Cribbs et al., 2012; Ye and Johnson, 1999; 2001). Remarkably, studies showed that a systemic immune stimulus, when administered to aged mice or during chronic neuroinflammation, induced an exaggerated inflammatory response with enhanced production of pro-inflammatory cytokines, but also increased acute neurodegeneration (Cunningham et al., 2005; Godbout et al., 2005).

With respect to AD as a chronic neurodegenerative disease, an acute systemic immune challenge temporarily increased the production of cytokines such as IL-1 β , TNF- α and IL-6, A β ₄₀ levels and tau hyperphosphorylation in transgenic mouse models of AD (Lee et al., 2002; Sly et al., 2001). Intriguingly, the exposure to a chronic but localized inflammation exacerbated and accelerated neuroinflammation as well as A β pathology in APP/PS1 mice (Kyrkanides et al., 2011).

Additionally, several human studies reported similar trends. Thus, people that were affected by chronic periodontitis or type 2 diabetes were reported to have a higher risk to be affected of AD (Kamer et al., 2008; Rojas-Gutierrez et al., 2017; Sparks Stein et al., 2012). Accordingly, patients with mild to severe AD, which suffered from severe infections, show an accelerated cognitive decline (Holmes et al., 2011; 2009). Furthermore, a recent study examined the relationship between systemic inflammation in midlife and neurodegeneration. Interestingly, this longitudinal study could associate heightened inflammatory markers in the blood during midlife with lower brain volumes and reduced episodic memory 24 years later (Walker et al., 2017). Additional evidence for the influence of systemic inflammation on neurological disease outcome comes from a retrospective study that examined patients with

incident dementia, in which it was observed that preceding infections episodes increased the likelihood for a later dementia diagnosis (Dunn et al., 2005). Consequently, these observations suggest that systemic infections may not only exacerbate ongoing neurological diseases, but also promote their onset.

However independently of the exacerbation or promotion of a neurological disease, the occurrence of systemic inflammatory events of different severity and duration during or before chronic neurodegenerative diseases cause an exaggerated immune response of the CNS. As microglia are exclusively sensitive to disturbances in the brain, it is assumed that “microglial priming” through the mentioned preceding inflammatory events is the principle process inducing an exaggerated secondary immune response towards emerging neurological diseases (Perry et al., 2007). Accordingly, microglial priming implicates that the innate immune system possesses the capability – following the adaptive immune system – to elicit an exaggerated immune reaction in response to subsequent inflammatory insults.

3.3.2 The concept of innate immune memory

Systemic infections within a host initiate an immune response that is mediated by the innate immune system – an evolutionarily old defense strategy and the first line of protection against invading pathogens. This form of immunity is found in all classes of plant and animal life as well as in fungi and other multicellular eukaryotes (Janeway et al., 2001) and is triggered by the sensing of pathogen-derived molecules (pathogen-associated molecular patterns (PAMPs)) or endogenous danger signals (damage-associated molecular patterns (DAMPs)) by pattern recognition receptors (PRRs), which initiate the synthesis of inflammatory cytokines and chemokines by macrophages and other immune cells (C A Janeway, 1989). Upon the generation of an inflammatory milieu to restrict spreading of the infection, tissue- resident macrophages engulf the pathogenic substance through phagocytosis and recruit monocytes and other leucocytes as well as lymphocytes from the blood to rapidly resolve the inflammation. Collectively, the innate immune response presents a first, relatively unspecific, line of host defense that is, in the later stages of an infection, supported by the adaptive immune system, which triggers a very specific but delayed immune reaction (Alberts et al., 2002).

It was long believed that only the adaptive immune system is able to create an immunological memory after exposure to a pathogenic stimulus, which leads to an enhanced response in case of a second encounter with the same pathogen (Janeway et al., 2001). First evidence for immunological memory of the innate immune system was provided by studies in plants and invertebrates, which lack the adaptive immune system. In plants, the phenomenon of “systemic acquired resistance” (SAR) describes the heightened immune response towards

reinfection by a primary pathogen (Durrant and Dong, 2004; Kachroo and Robin, 2013). Invertebrate animals also exhibit a similar form of immune memory; for example, after the first exposure to the tapeworm *Schistocephalus solidus*, the copepod crustacean is protected against a reinfection with the same pathogen through a more efficient and specific immune response (Kurtz and Franz, 2003). These results point towards a special form of immunity that is gained after the first contact with pathogens and intensifies the second immune response; an effect that was recently denoted as “trained immunity” (Netea et al., 2011).

Furthermore, studies in mice, which showed that the animals were protected against a lethal infection after the initial exposure and priming with microbial ligands of PRRs such as β -glucan, the peptidoglycan component muramyl dipeptide or flagellin, introduced the principle of trained immunity to vertebrates (Di Luzio and Williams, 1978; Krahenbuhl et al., 1981; Muñoz et al., 2010; Zhang et al., 2014). Moreover, compelling evidence for trained immunity was provided by studies conducted in mice that lacked the thymus, the essential organ for T-cell maturation. In these mice, vaccination with tuberculosis bacillus Calmette Guérin (BCG) protected, in a T-cell-independent fashion, against reinfection with *Candida albicans* or *Schistosoma mansoni* (Tribouley et al., 1978; van 't Wout et al., 1992). Importantly, there is also evidence for innate immune memory from vaccination studies in humans, in which immunization with live but attenuated vaccines such as the BCG or the measles virus turned out to be protective against non-targeted diseases (Benn et al., 2013).

Interestingly, studies in which macrophages were challenged with LPS to examine their potential for acquiring memory, it could be shown that macrophages became more or less responsive as a result of the initial differential stimulation paradigms with LPS (Foster et al., 2007). These findings expand the capability of innate immune memory from a priming or training effect to a “tolerizing” effect mediated by chronic exposure to LPS. LPS-induced tolerance is considered an immune paralysis state characterized by a hypoinflammatory profile that can be induced by severe sepsis or experimentally mimicked by continuous or high-dose endotoxin challenges possibly as result of receptor desensitization or an imbalance in the production of inflammatory mediators (Medvedev et al., 2000; van der Poll and Opal, 2008). Accordingly, cultured monocytes, which were exposed for 24 hours to LPS to induce immune-tolerance, showed a decreased production of pro-inflammatory cytokines such as TNF- α or IL-6 upon a secondary immune stimulation (Saeed et al., 2014).

However, it is of importance to distinguish between immune memory and acute immunological processes as both include immune cell activation. Whereas immune cell activation or differentiation in the context of immunological processes occurs as a direct and

acute function of pathogen sensing or changes in the environment, mechanistic studies suggest that alterations in macrophage function due to training or tolerizing immune challenges through primary pathogen contact are mediated by epigenetic reprogramming that results in *persistent* changes in chromatin marks, which modify the cell-mediated immune response upon further stimuli subsequent to the initial insult (Netea et al., 2016).

So far, persistence of microbial ligand-induced immune memory *in vitro*, in short-lived monocytes or macrophages, was studied only for a limited time period from one to five days (Ifrim et al., 2014; Ostuni et al., 2013; Saeed et al., 2014). However recently, long-lived epithelial stem cells were also attributed to innate immune memory, as a preceding immune stimulus resulted in a more rapid wound healing 180 days after the primary immune stimulus (Naik et al., 2017). In line, vaccination studies with BCG in healthy volunteers showed an enhanced release of cytokines from blood monocytes for up to three months (Kleinnijenhuis et al., 2012), indicating the possibility of a longer-lasting acquirement of trained immunity that must take place at the level of progenitor cells, as circulating monocytes have a suggested half-life in circulation of about one day (Yona et al., 2013).

3.3.3 Epigenetic reprogramming induces immune memory in macrophages

The DNA of a cell is arranged around histone cores and further structured in nucleosomes, which are the primary components of chromatin. Besides other functions, the chromatin complex is required to tightly pack DNA but also to control gene expression. Epigenetic modification of specific regions in histones, for example by methylation or acetylation of certain amino acid residues, can induce changes in the local chromatin structure allowing enhanced or repressed transcription of genes. In particular, post-translational methylation of the lysine (K) residue 4 and acetylation of K27 at histone 3 (H3) were shown to define active enhancer sites, which are positively associated with gene transcription of nearby genes (Fig. 3C). In contrary, histones that bear H3K9 and H3K27 trimethylation (me₃) mark a closed chromatin conformation that does not allow gene transcription (Ivashkiv, 2013). Additionally, trimethylation of H3K4 (H3K4me₃) and acetylation of H3K27 (H3K27ac) are reliable marks for active promoter regions where the RNA polymerase II protein complex can easily bind to the DNA to catalyze transcription (Fig. 3D).

Enhancer regions belong to cis-regulatory elements that contain DNA-binding sites for transcription factors that, upon binding, can increase the likelihood for transcription of a particular gene. Structurally, active enhancer regions are devoid of nucleosomes and the DNA is easily accessible for transcription factors. Thereby, the DNA-binding sites are flanked by histones characterized through the above mentioned H3K4me₁ or H3K27ac modifications.

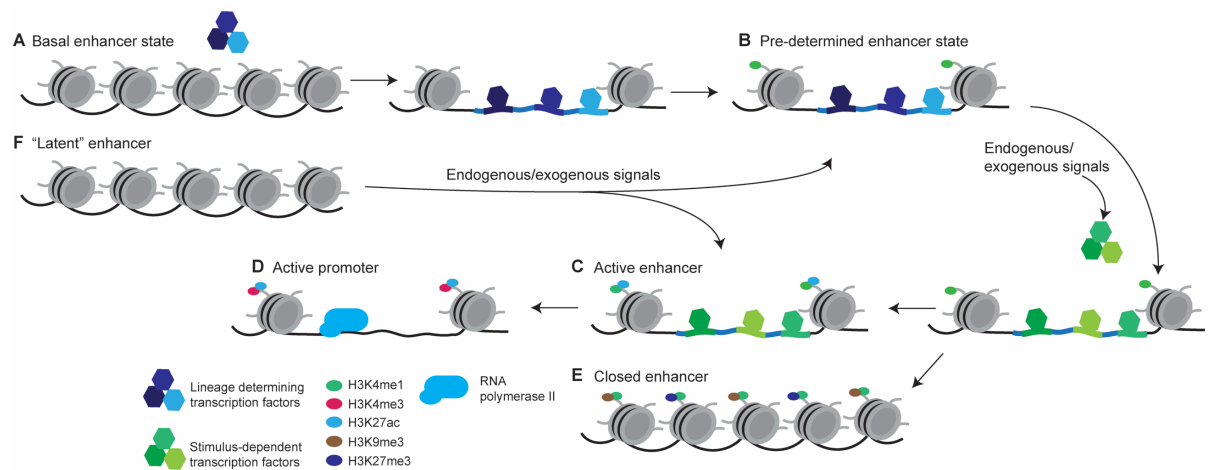


Figure 3: Epigenetic changes in the chromatin landscape of macrophages can occur in response to endogenous but also exogenous signals. (A) During macrophage development, lineage determining transcription factors bind to enhancer regions of genes that are essential for cell maturation and (B) induce the acquisition of histone 3 (H3) lysine residue 4 (K4) monomethylation (me1) (H3K4me1), the main epigenetic signature for potentially active enhancers (pre-determined enhancer state). Upon further endogenous or exogenous signals H3K4me1 labeled enhancer become activated (C) through the recruitment of stimulus-dependent transcription factors that initiate H3K27 acetylation (ac). (D) Active enhancers support the transcription of the required genes by promoting gene transcription via RNA polymerase II at interacting promotor sites. (E) Rather than activating enhancers, recruitment of stimulus-dependent transcription factors can also induce a suppressed enhancer configuration by trimethylation of the H3K9 and H3K27 residues. (F) Developmentally unmarked “latent” enhancer regions can become marked via stimulus-dependent transcription factors to induce gene transcription.

During the process of cell maturation, the binding of lineage determining transcription factors (LDTFs) to nucleosomes enables the recruitment of enzymes for H3K4 methylation, shifting the marked enhancer regions into a pre-determined poised, active (which is further characterized by additional H3K27ac marks (Creyghton et al., 2010; Rada-Iglesias et al., 2011)) or repressive state, (Fig. 3A,B (shown is an exemplary representation of a poised enhancer)) (Heinz et al., 2010; Ostuni et al., 2013). Studies in primary macrophages have shown that PU.1 acts as a master LDTF that determines cell specificity of the macrophage lineage (Barozzi et al., 2014; Ghisletti et al., 2010; Heinz et al., 2010).

Upon further macrophage stimulation, due to environmental changes for example, stimulus-responsive transcription factors, such as NF- κ B, AP-1 or STAT family members, are recruited to pre-marked enhancer and promoter regions within the genome. These proteins act, similar to LDTFs, as co-activators for enzymes such as the histone acetyltransferase to enable histone acetylation (H3K27ac) in enhancer regions of genes whose enhanced transcription is required (Fig. 3C, D) (Barozzi et al., 2014; Ghisletti et al., 2010; Heinz et al., 2010; Ramirez-Carrozzi et al., 2009; 2006; Smale and Natoli, 2014; Smale et al., 2014). On a molecular basis, it was shown that histone acetylation leads to the addition of negative charges to the positive

lysine residue, which in turn further reduces the interaction between DNA and histones leading to improved accessibility of the DNA for other co-regulatory proteins required for the transcriptional process (Creighton et al., 2010; Smale et al., 2014).

In addition to LDTFs pre-marked enhancer regions, *in vitro* experiments defined “latent” enhancer regions in macrophages, which are epigenetically unmarked and inactivated regulatory elements, but can be directly activated in response to distinct environmental stimuli and gain H3K4 monomethylation as well as H3K27 acetylation (Fig. 3F) (Kaikkonen et al., 2013; Ostuni et al., 2013). Notably, histone modifications in such “latent” enhancer regions, which were acquired upon LPS or cytokine stimulation, were shown to have different stability (Fig. 4A/B). Whereas H3K27ac was lost quickly after the cessation of the stimulation, H3K4me1 was maintained leading to a poised enhancer state with an enhanced epigenetic status (Fig. 4C). However, upon subsequent re-stimulation histone acetylation was re-established, enhanced and in turn induced a faster and stronger induction of genes adjacent to these enhancer regions (Fig. 4D) indicating the presence of a short-term transcriptional memory (Ostuni et al., 2013).

Interestingly, the identified “latent” enhancer in that study accounted for 15% of all LPS-induced activated enhancer and were assigned closer than LDTF-pre-determined enhancer to nearby induced genes, suggesting an important role for “latent” enhancer during the LPS-mediated cellular response (Ostuni et al., 2013). Consequently, it can be assumed that the unveiling of “latent” enhancers resembles the *in vivo* situation, in which the response of differentiated tissue macrophages towards microenvironment-specific signals may be mediated by the activation of “latent” enhancers as regulators for the induction of an individual environment-specific enhancer repertoire (Gosselin et al., 2014; Lavin et al., 2014).

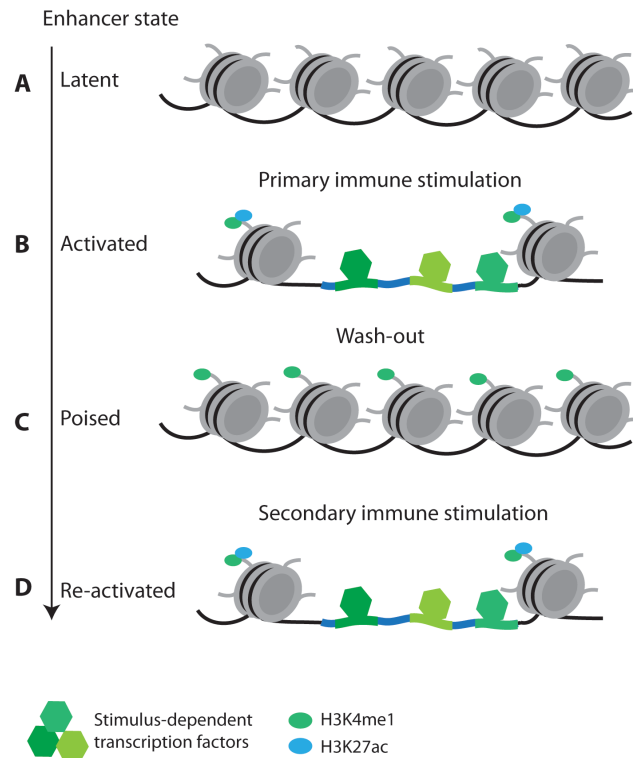


Figure 4: A model for the temporary acquisition of histone modifications for latent enhancer. (A, B) During macrophage stimulation the binding of stimulus-dependent transcriptions factors, to “latent” enhancer regions enables the deposition of H3K4me1 and H3K27ac marks to shift these enhancers into an active state. (C) After cessation of the of the primary stimulus, bound transcription factors and H3K27ac marks are lost, whereas H3K4me1 modifications are retained (so-called poised enhancers). (D) Upon a secondary immune stimulation, “re-activated” enhancer regions can more quickly re-acquire H3K27ac marks, leading to stronger and faster activation of the corresponding gene transcription.

3.3.4 The molecular basis of immune memory in macrophages

Emerging data support that apart from a direct influence on innate immune signaling pathways upon acute macrophage activation, changes in metabolic pathways play critical roles in the induction of the immune response as well (Ganeshan and Chawla, 2014). Macrophages acutely activated by LPS were reported to shift their energy metabolism from oxidative phosphorylation to the faster adenosine trisphosphate (ATP) supply via the glycolytic pathway in the cytosol. The sudden metabolic switch from oxidative phosphorylation to glycolysis increases the mitochondrial membrane potential due to the electron transport chain across the mitochondrial membrane being disrupted (Tannahill et al., 2013). Additionally, acute activation of macrophages was shown to interfere with the citric acid cycle to enable a sufficient supply of the intermediate product succinate. Oxidized succinate (fumarate), in combination with an increased mitochondrial membrane potential, is required for the enhanced production of

reactive oxygen species (ROS) by reverse electron transport (RET), which in turn alters activity of the transcription factor (TF), hypoxia-inducible factor-1 α (HIF-1 α) (Mills et al., 2016).

HIF-1 α is known to drive gene expression of the pro-inflammatory cytokine IL-1 β (Jha et al., 2015; Mills et al., 2016; Tannahill et al., 2013). Concurrently, accumulation of fumarate decreases the expression of the anti-inflammatory cytokine IL-10 (Mills et al., 2016).

To pursue the role of cellular metabolism during epigenetic macrophage reprogramming, further *in vitro* studies were performed, in which isolated human or murine monocytes were stimulated with a training or tolerizing immune stimulus and incubated for up to seven days until a secondary immune stimulus was administered to induce immune memory (Cheng et al., 2014; Saeed et al., 2014). Remarkably, the applied inflammatory stimuli largely altered cellular metabolism pathways acutely, but also after the prolonged incubation period. Specifically, β -glucan stimulation of monocytes, which induced trained immunity, increased glucose consumption, lactate production and the ratio of nicotinamide adenine dinucleotide (NAD(+)) to its reduced form (NADH) representing a shift to aerobic glycolysis energy metabolism upon restimulation of the cells. These alterations indicate that changes in the cellular metabolism are crucial for the induction of trained immune memory (Cheng et al., 2014). Moreover, the glycolysis favored-ATP production induced by training was reported to be dependent on the activation of the dectin-1/Akt/mammalian target of rapamycin (mTOR)/hypoxia-inducible factor-1 α (HIF-1 α) (Akt/mTOR/HIF-1 α)-pathway (Cheng et al., 2014).

So far, it is not completely clear why metabolic circuits are drastically affected during the epigenetic formation of immune memory. It is suggested, that metabolic intermediates of the respective up- or down-regulated metabolic pathways are co-factors for the regulation of histone modifications which, in turn, suppress or activate phenotype-associated genes (Bénil et al., 2014; Donohoe and Bultman, 2012; Gut and Verdin, 2013; Saeed et al., 2014).

Apart from alterations in the cellular metabolism during the induction of training or immune tolerance, further signaling pathways were shown to be differentially modified. The cyclic adenosine monophosphate (cAMP)-dependent signaling pathway, which is important for the cell communication, was also identified as a crucial regulator of trained immunity in macrophages (Saeed et al., 2014). Additionally, it was found that immune training of monocytes induced phosphorylation of the activating transcription factor 7 (ATF7) which, in turn, reduces the repressive histone mark H3K9me2 in regions where genes of the immunological network are located (Yoshida et al., 2015). In contrast, LPS-induced tolerance increases levels of repressive histone modifications in promoter regions of the inflammatory cytokines IL-1 β and

TNF- α , which inhibits the transcription of these genes upon subsequent pathogen stimulation (Gazzar et al., 2009).

While there is convincing evidence for innate immune memory in macrophages from *in vitro* studies, none of the studies has examined the consequences of epigenetic remodeling of the innate immune response in macrophages on a subsequent pathology *in vivo* and only a few experiments investigated the microglial potential of immune memory (Holtman et al., 2015). For that reason, we applied the model of trained- and tolerance-induced immune memory to a mouse model of cerebral β -amyloidosis to investigate the effects of immune memory on the reflected neurological disease hallmarks of AD pathology.

3.3.5 Innate immune memory in the brain shapes neurological disease hallmarks

Most of the studies on training and tolerance-induced epigenetic remodeling of the chromatin landscape during the establishment of innate immune memory have been done in peripheral macrophages or blood-derived monocytes (Cheng et al., 2014; Saeed et al., 2014). For microglia, the resident tissue macrophages of the brain, it is generally accepted that these cells can adopt altered phenotypes upon different pathogenic stimuli (Norden and Godbout, 2013; Perry and Holmes, 2014; Raj et al., 2014). However, the often-described microglial priming is only a functional definition as few studies have investigated the transcriptional profile that is induced by different priming stimuli. Moreover, priming is normally observed during acute inflammatory processes and could therefore not reveal microglial immune memory (Combrinck et al., 2002; Cunningham et al., 2005). Therefore, we were interested if LPS-induced inflammation in the periphery – a well-established method to prompt a microglial response in the brain – can evoke a training or tolerance immune memory effect in microglia, similar to what was reported for monocyte-derived macrophages (Saeed et al., 2014).

In our study, we could show that low dose LPS (500 μ g/kg bodyweight) injected intraperitoneally (i.p.) on four consecutive days in young adult mice induced acute alterations in brain cytokines, reminiscent of immune training and tolerance (Fig. 5A). Thus, after a small cytokine response following the first LPS injection, the second LPS injection induced a drastic increase in brain cytokine levels (such as IL-1 β , IL-6 or TNF- α) indicating a training effect induced by the first LPS injection. However, the third and fourth LPS injections abolished cytokine production and thus implied a tolerant immune state in the brain.

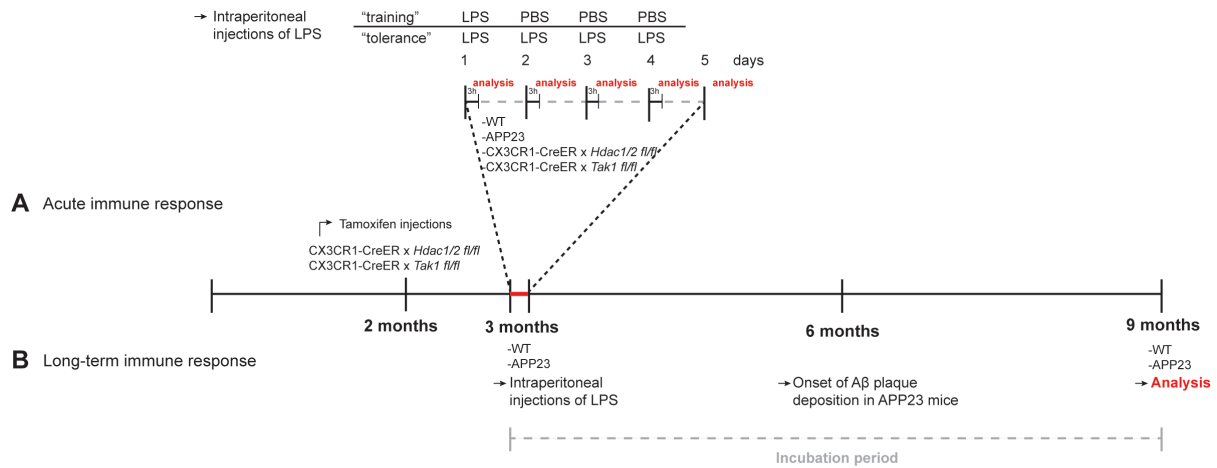


Figure 5: Experimental design to induce immune memory in microglia. (A) To study the acute effects of different doses of peripherally applied LPS in the brain and to identify microglia as mediators of the immune response, wildtype, APP23 and CX3CR-CreER x *Hdac1/2*^{fl/fl} as well as CX3CR-CreER x *Tak1*^{fl/fl} mice, which received prior tamoxifen treatment to induce *Hdac1/2* and *Tak1* depletion, were treated at three months of age with different immune challenges (1xLPS, 2xLPS, 3xLPS, 4xLPS), and analyzed 3h after the injections. Thereby, a single LPS injection was identified to induce training effects whereas four consecutive LPS injections induced immune tolerance. (B) In a second experiment, the long-term effects of LPS treatment on immune memory and the consequences for the pathology of cerebral β -amyloidosis in the APP23 mouse model were investigated. After six months of incubation, the mice were anesthetized and analyzed for their immune profile and A β pathology as well as for potential changes in the microglial epigenetic signature of histones and in expression levels of corresponding genes.

To examine whether the observed memory effects were microglia-specific, we used the CX3CR1-CreER (Cre) mouse line that was crossed to mice carrying either the loxP flanked genes: “transforming growth factor (TGF)- β -activated kinase 1” (*Tak1*) or “histone deacetylases-1 and -2” (*Hdac1/2*). TAK1 and *Hdac1/2* are major regulators of transcriptional processes, macrophage inflammatory responses and the epigenetic chromatin architecture (Goldmann et al., 2013; Kannan et al., 2013; Sato et al., 2005; Shakespear et al., 2011). In these mice, tamoxifen induced Cre recombinase expression results in efficient target gene inactivation. After an incubation period of four weeks following tamoxifen application, the loxP flanked (floxed; fl) genes: *Tak1* and *Hdac1/2* are efficiently ablated in the stable microglia population but present in the short-lived and continuously replenished peripheral monocytes (Fig. 5A) (Goldmann et al., 2013). Consequently, LPS injections into the CX3CR1-CreER x *Tak1*^{fl/fl} and CX3CR1-CreER x *Hdac1/2*^{fl/fl} mice did not alter the peripheral immune response but restricted the amplification of brain cytokines. Thus, we could confirm that the alterations in brain cytokine levels after the LPS-induced inflammatory state were mediated predominantly by microglia. Based on these observations, a single peripheral LPS stimulus (1xLPS) was

identified to elicit a training effect whereas prolonged (four days, 4xLPS) peripheral LPS administration induced immune tolerance in microglia.

After identification of these two different stimulation paradigms, we tested whether the induced immune training and tolerance state in microglia can lead to long-term alterations in the brain and thereupon modulate the pathology of neurological diseases. Therefore, we peripherally injected three-month-old APP23 mice, which develop cerebral β -amyloidosis and microgliosis from six months of age (Sturchler-Pierrat et al., 1997), as well as wildtype littermate controls and analyzed pathology at an age of nine months (Fig. 5B). Notably, our two different microglial stimulation paradigms (1xLPS vs. 4xLPS) significantly influenced A β pathology in APP23 mice. Thus, a training stimulus resulted in an increased cortical A β plaque load compared to PBS-treated control APP23 mice. In contrary, the induction of tolerance by consecutive injections of LPS for four days, decreased A β plaque load significantly. In line with these observations, the cytokine production in the brain, but not in the periphery, was influenced at that stage of the disease. Immune tolerance suppressed IL-1 β production whereas training blocked IL-10 production.

When we tested the immune memory function of microglia in a second mouse model of neuropathology, in particular, after the induction of a focal cortical ischemia one month after peripheral LPS treatment, we observed also differences in the acute microglial immune response. Remarkably, the release of inflammatory cytokines with suppression of IL-10 by 1xLPS and IL-1 β by 4xLPS, but enhancement of IL-1 β by 1xLPS was similar to what we observed in the APP23 mice with A β pathology. Moreover seven days after the ischemic insult, 4xLPS treatment reduced the volume of neuronal damage and microglia activation indicating that the induced immune tolerance can modify stroke pathology through long-term modulation of the brain's immune response.

In a third approach, we tested whether immune stimuli other than LPS elicit a similar immune memory effect in the brain. Therefore, we peripherally injected individual cytokines at different concentrations and analyzed mice four weeks later after the administration of an acute secondary immune stimulus. In line with the previous results, the measured brain cytokines reflected comparable training and tolerance effects that were undetectable in the periphery.

In vitro studies established that immune memory in monocytes can be induced by epigenetic reprogramming of the enhancer landscape, which leads to changes in the transcription of assigned genes involved in the innate immune response (Ivashkiv, 2013; Saeed et al., 2014). To test whether our peripheral immune challenges could induce alterations in the

microglial enhancer repertoire *in vivo*, we analyzed the epigenetic landscape of the microglia isolated from the differentially treated APP23 or wildtype mice by the examination of H3K4me1 and H3K27ac histone marks, which define active enhancers states (Kaikkonen et al., 2013; Ostuni et al., 2013).

To begin with, we analyzed the profile of H3K4me1 histone modifications, which should be persistently established in response to the initial stimulus, that is i.p. LPS stimulation (compare Fig. 3/4). As expected, H3K4me1 histone marks were established both in wildtype and APP23 mice after primary immune stimulation. However, H3K4me1 levels were differentially regulated among wildtype and APP23 mice that received either the training or tolerant immune stimulus and showed diverse pathway enrichment patterns. In particular, H3K4me1 levels that were increased by a single LPS treatment compared to the 4xLPS treatment in wildtype mice were almost exclusively enriched for the “thyroid hormone signaling pathway”. Strikingly, that pathway includes an enhancer for HIF-1 α , which is known to be a key modulator of pro-inflammatory gene expression (Cheng et al., 2012; Tannahill et al., 2013). Likewise, detected upregulations in H3K4me1 histone modifications in microglia from APP23 mice with 1xLPS compared to 4xLPS treatment were found to be enriched for the “HIF-1 signaling pathway”.

Interestingly, the tolerant immune challenge (4xLPS) in APP23 but also wildtype mice induced the largest number of differentially expressed H3K4me1 levels and showed enrichment in pathways related to phagocytosis (for example: “Ras-related protein 1 (Rap1) signaling pathway” or “Endocytosis” pathway). Importantly, neither wildtype nor APP23 microglia from mice that received no priming stimulus displayed any pathway enrichment in relation to the differentially regulated H3K4me1 state underlining the induction of distinct molecular signaling pathways upon varying primary immune stimuli.

As a second marker for enhancer activation, we analyzed the differential regulation of the H3K27ac histone modification among our wildtype and APP23 treatment groups. Here, we could detect a high number of differentially activated enhancers among the APP23 groups that was rather low in the wildtype groups pointing towards the requirement of an (secondary) acute stimulus to induce changes in the H3K27 acetylation pattern (Ostuni et al., 2013).

In line with the reported HIF-1 α -dependent induced trained immunity in monocytes (Cheng et al., 2014) and the observed increase in H3K4me1 levels enriched for the “HIF-1 signaling pathway”, increased H3K27ac levels in APP23 mice that received a single LPS injection showed highest enrichment for the same pathway in microglia compared to APP23 control mice.

Again, in line with the H3K4me1 signature, the identified active H3K27ac enhancers in the group of APP23 mice that received the immune tolerance stimulus (4xLPS) were enriched for the “Rap1 signaling pathway” in comparison to APP23 control animals without LPS stimulation. Interestingly, the “Rap1 signaling pathway” induces the activation of the $\alpha_M\beta_2$ integrin receptor on macrophages (complement receptor 3) and thereby enhances phagocytosis of C3bi-opsonized targets (Caron et al., 2000).

Moreover, when we compared the 1xLPS treatment to the 4xLPS treatment in APP23 mice, it became apparent, that a set of inflammation-related pathways such as the “Toll-like receptor signaling pathway” or the “Chemokine signaling pathway” were enriched by the highly increased H3K27ac levels observed in the 1xLPS group supporting the induction two epigenetically differentially regulated signatures by 1xLPS or 4xLPS.

Interestingly, acute brain pathology alone was also sufficient to induce a small number of differentially regulated H3K27ac levels in untreated APP23 mice compared to the wildtype group, which could be related to the “thyroid hormone signaling pathway” as well as the “mTOR signaling pathway”.

Remarkably, microglial mRNA sequencing and subsequent gene expression analysis by weighted gene correlation network analysis (WGCNA) to cluster genes into certain modules revealed significant correlations between the epigenetically induced alterations in H3K27ac levels of enhancer regions and the direction of change in the expression of their nearest genes. For example, increased gene expression in the red module that included the “HIF-1 signaling pathway” correlated positively with the 1xLPS-treated APP23 animals, in which we detected an enrichment in microglial H3K27ac levels for the “HIF-1 signaling pathway”. Furthermore, single genes within that module such as *Hif1a* or *Inpp5d* were significantly upregulated in the 1xLPS-treated APP23 group, but downregulated with 4xLPS.

HIF-1 α has been shown to play an essential role in the regulation of pro-inflammatory signal molecules, but also in the expression of glycolytic enzymes in inflammatory-stimulated macrophages (Cheng et al., 2014; Cramer et al., 2003). In that context, it was interesting to note, that the green module, which was enriched for pathways involved in glycolysis, showed a positive correlation with the 1xLPS APP23 group. Simultaneously, there was also an upregulation of genes included in that module in APP23 versus wildtype control animals, which was further increased by 1xLPS and decreased by 4xLPS treatment in APP23 animals.

Energy generation via glycolysis results in faster energy supply, but also in mitochondrial hyperpolarization and lactate production, which has been reported to be dependent on HIF-1 α signaling (Cheng et al., 2014; Mills et al., 2016). Accordingly, the

measured mitochondrial membrane potential in our 1xLPS-treated APP23 animals was strongly increased and correlated well with lactate production compared to the untreated and 4xLPS APP23 group. Furthermore when we immuno-stained brain sections for HIF-1 α , we could detect increased HIF-1 α protein levels in plaque-associated microglia (which are the cells mostly affected by A β -pathology), which were even more upregulated in the 1xLPS-treated APP23 mice. This finding of differentially regulated HIF-1 α signaling and the subsequent metabolic switch to glycolysis in response to A β -pathology suggests an important function of HIF-1 α signaling in AD, which can be further enhanced by immune training or alleviated by immune tolerance induced in microglia. Interestingly, the *ApoE* gene, whose E4 allele is described as major risk factor for LOAD (Corder et al., 1993), can be found in the same module (red) as *Hif1a* and thus strengthens the assumption of HIF-1 α being a modulator of AD pathology.

In contrast to the previous modules, the grey module, which was enriched in pathways related to phagocytosis such as the “Rap1 signaling pathway”, showed a positive correlation with wildtype control animals but not with APP23 control animals. In line, there was a downregulation of genes assigned to that module in the control and 1xLPS APP23 groups. However, the 4xLPS-treated APP23 group showed similar levels of gene expression as wildtype controls. Accordingly, when we measured microglial phagocytosis by the determination of A β levels in isolated microglia in APP23 animals we saw an increase in the A β content after 4xLPS administration compared to the APP23 control and 1xLPS-treated groups, which may be responsible for the decrease in cortical A β deposition observed in the 4xLPS APP23 treatment group and provides further functional evidence for the detected changes in the microglial gene expression analysis.

Interestingly, the brown module comprised genes that were recently described to distinguish different microglial phenotypes due to their activation state (Keren-Shaul et al., 2017). These genes characterizing homeostatic but also “disease-associated microglia” were significantly upregulated after a single but also repeated LPS stimulation in wildtype as well as APP23 microglia implicating once more a change in the microglial phenotype due to inflammatory stimuli.

Taken together, our *in vivo* study provides first evidence for a long-lasting innate immune memory function in a tissue-resident macrophage population, which is sufficient to alter the pathology of neurological diseases in response to the induction of a trained or tolerant microglial phenotype. Importantly, we show that the training or tolerance induced remodeling of the microglial immune response occurs due to epigenetic changes in their enhancer

landscape. Although we observed a significant impact of primary immune stimulation on secondary pathology, the epigenetic changes were rather small in magnitude. However, data obtained by immunohistochemical staining for HIF-1 α , a transcription factor that was differentially regulated by our training or tolerance immune stimulus, suggest that the observed alterations in epigenetic reprogramming and gene expression are mainly mediated by plaque-associated microglia, which represent the minority of microglia at the examined stage of pathology. Thus, for further studies, it would be of great interest to discriminate the microglia population into different subgroups based on their localization in the brain in order to examine the epigenetic profile of plaque-associated and non-plaque associated microglia individually.

Furthermore, our two different LPS stimulation paradigms identified a differential regulation of the “mTOR signaling pathway” and the transcription factor HIF-1 α , which was strongest APP23 mice. Interestingly, the “mTOR signaling pathway” as well as HIF-1 α are known to play a role in AD and interact via the Akt/mTOR/HIF-1 α pathway (Cheng et al., 2014; Ulland et al., 2017; Wang et al., 2014). Since 4xLPS treatment suppressed, but 1xLPS treatment enhanced HIF-1 α signaling, which occurred in parallel with alleviated or aggravated A β deposition, we suggest that epigenetic activation of mTOR and the subsequent regulation of HIF-1 α might induce alterations in AD pathology.

Even if we provide evidence for an immune memory effect in microglia after the induction of systemic inflammation that had detrimental or beneficial consequences for brain pathology, it would be misleading to predict preceding peripheral infections as trigger for changes in the microglial immune function. Thus, future studies are required to investigate the effect of further peripheral pathological conditions on neurological diseases, but also on other developmentally distinct macrophage populations as well as to determine the exact duration of innate immune memory.

3.4 Genetic modification of the microglial phagocytic capacity during AD

In reference to:

Lack of MFG-E8 reduces pathology in mouse models of cerebral β -amyloidosis

Karoline Degenhardt*, Jessica Wagner*, Konstantina Kapolou, Domenico Del Turco, Thomas Deller, Mathias Jucker, Jonas J. Neher

Manuscript in preparation

3.4.1 A β clearance mechanisms in the CNS

Based on the “amyloid cascade hypothesis”, research suggests that impaired clearance mechanisms for soluble or fibrillar A β structures contribute to the induction of LOAD (Mawuenyega et al., 2010). Under physiological conditions there exist several pathways for A β clearance and degradation, which maintain a balanced A β metabolism. Importantly, A β transport across the BBB – a process named transcytosis – represents a major systemic clearance route from the brain to the plasma (Bell et al., 2006; Deane et al., 2009; 2004; Shibata et al., 2000; Storck et al., 2016). Thereby A β_{40} is rapidly cleared by direct binding to the soluble lipoprotein receptor-related protein 1 (sLRP1), which is localized in capillaries at the abluminal side of the cerebral endothelium (Bell et al., 2006; Deane et al., 2004; Shibata et al., 2000). In addition, studies have shown that extracellular chaperons such as ApoE, or ApoJ (clusterin) can also stimulate A β clearance from the CNS most likely through binding to LRP receptors (DeMattos et al., 2004). Especially, A β_{42} binding to ApoJ enhances efflux across the BBB, whereas A β_{40} /ApoE3 complex formation delays efflux rate (Bell et al., 2006).

Furthermore, A β from the interstitial fluid (ISF) in the brain can be cleared via bulk flow into the cerebrospinal fluid (CSF) sink, which comprises the ventricles and subarachnoid space (Abbott, 2004). In turn, A β in the circulation of CSF can either be absorbed through arachnoid villi to cross the blood-cerebrospinal fluid barrier (BCSFB) into the blood (Silverberg et al., 2003), or cleared along the perivascular lymphatic drainage pathway, which has recently been identified as predominant outflow pathway (Carare et al., 2008; Iliff et al., 2012; Ma et al., 2017; Tarasoff-Conway et al., 2015; Weller et al., 2008). However, A β that is transported along the perivascular drainage route is hypothesized to become entrapped in the perivascular basement membranes and impair perivascular clearance as seen in cerebral amyloid angiopathy (CAA) (Hawkes et al., 2011; 2014).

Consistently, the A β clearance rate measured in CSF of human AD patients (>60 years) was reduced by ~30 percent compared to healthy individuals and reflects a clear defect in A β clearance that occurs during AD (Mawuenyega et al., 2010).

Besides the absorption of A β into the peripheral circulation, A β uptake by the resident glial cells is another important mechanism for A β clearance. A β degrading enzymes such as insulin degrading enzyme (IDE), neprilysin or different matrix-metalloproteinases (MMPs), represent a group of proteases, which cleave A β into smaller fragments in the brain (Miners et al., 2008). These proteases are mainly produced by glial cells and get released into the extracellular space via exosomes where they degrade monomeric but also fibrillar A β species (Saido and Leissring, 2012). Moreover, neprilysin can also degrade intracellular A β (Tarasoff-Conway et al., 2015).

Furthermore, microglia may also directly internalize and degrade A β . *In vitro*, soluble A β , for example, is engulfed via fluid phase pinocytosis, while uptake of A β fibrils is mediated by receptor-mediated endocytosis (Chung, 1999; Mandrekar et al., 2009). Thereby, microglia use pattern recognition receptors (PRRs) to sense exogenous pathogen-associated molecular patterns (PAMPs) including misfolded and aggregated A β (Lucin and Wyss-Coray, 2009). In particular, scavenger receptors of class A, a subgroup of PRRs, were shown to be involved in the uptake of A β by primary murine microglia (Chung et al., 2001; Paresce et al., 1996). Conversely, scavenger receptors of class B such as CD36 only produce chemokines for further microglia recruitment upon A β binding (Coraci et al., 2002). Another group of PRRs are toll-like-receptors (TLRs), which are also able to bind to A β and induce engulfment. In particular, TLR2 and 4 in conjunction with the co-receptor CD14 were shown to induce phagocytosis of monomeric as well as fibrillar A β (Liu et al., 2005; Reed-Geaghan et al., 2009; Tahara et al., 2006). Accordingly, knockout of *Tlr2* in APP/PS1 mice increased levels of A β ₄₂ (Richard et al., 2008).

Furthermore, the complement system, another pathogen defending mechanism of the innate immune system, is involved in the uptake of A β by microglia. Thus, the deficiency of complement 3 (C3) factor, but also the absence of the respective microglial membrane attack complex receptor (Mac-1/C3-receptor/CD11b) reduced A β uptake *in vivo* (Fu et al., 2012). However, these experiments were done in wildtype mice that received injections of fluorescently labeled fibrillar A β preparations into the brain and, also, many of the aforementioned studies, which presented microglial uptake of A β , were conducted under *in vitro* conditions and could not always be confirmed *in vivo*. Alarmingly, recent studies showed that microglia that were cultured *in vitro* have reduced expression of microglia-specific genes

(Gosselin et al., 2017) and, even more important, the addition of serum to microglia cultures increases their intrinsic phagocytic capacity (Bohlen et al., 2017). Thus, it is conceivable that the capability of microglia to phagocytose A β *in vivo* is very limited. Studies from Grathwohl et al., Spangenberg et al. and Dagher et al., which showed that depletion of microglia does not impair plaque deposition and A β levels, underline the possibility that microglia are unable to efficiently phagocytose A β (Dagher et al., 2015; Grathwohl et al., 2009; Spangenberg et al., 2016). However, *in vivo* studies, in which single A β plaques were continuously tracked by two-photon imaging, reported decreasing plaque sizes when amyloid plaques were surrounded by a growing number of microglia (Bolmont et al., 2008). Furthermore, enlarged plaques after diphtheria toxin-induced microglia depletion indicate that microglia can regulate plaque size (Zhao et al., 2017).

These results would suggest that microglia are indeed able to phagocytose A β . However, as already discussed in the previous sections, several environmental factors such as the modification of the innate immune system or a developing pathology can influence the microglial gene expression profile and thereby determine cell functionality. Accordingly, the exposure of microglia to A β , was reported to induce a downregulation of microglial A β phagocytosis receptors and consequently impair microglial A β phagocytosis (Hickman et al., 2008; Krabbe et al., 2013). Following these findings and to gain further insight into the *in vivo* phagocytic capacity of microglia during AD pathology, I will focus on “milk fat globule-epidermal growth-factor 8” (MFG-E8), a protein that was recently identified to be involved in the phagocytosis of A β (Boddaert et al., 2010).

3.4.2 MFG-E8-mediated phagocytosis

Milk fat globule-epidermal growth-factor 8 (MFG-E8) is a bivalent-binding, secretory glycoprotein, which was initially identified as a mammary epithelial cell surface protein (Stubbs et al., 1990). In mice, the protein consists of an amino-terminal signal peptide, which is required for its secretion into the extracellular space, two epidermal growth-factor homologous regions (E1, E2) and two carboxy-terminal discoidin regions homologous to coagulation factor-V/VIII (C1, C2) (Fig. 6) (Wang, 2014). MFG-E8 is present in two isoforms, with the shorter isoform being more abundant but lacking a proline/threonine-rich domain between E2 and C1. MFG-E8 has been implicated in wound healing, autoimmune disease and cancer. However, the major function of the protein is the recognition of apoptotic cells or molecular debris in order to initiate its uptake by phagocytes in many different tissues (Hanayama et al., 2002; 2004). Thus, MFG-E8 acts as an opsonin to mark dead or dying cells for phagocytosis. Thereby, the carboxy-terminal end of C2 of MFG-E8 has a high binding activity to phosphatidylserine (PS) (Oshima

et al., 2002). PS is exposed by apoptotic cells and acts as an “eat me” signal that can be bound by MFG-E8 but also other opsonins (Hanayama et al., 2002; Li et al., 2012). Upon binding of MFG-E8 to apoptotic cells, an arginyl-glycyl-aspartic acid (RGD)-motif in the E2 domain facilitates phagocytic engulfment via the ligation to the vitronectin receptor ($\alpha_v\beta_3$, $\alpha_v\beta_5$ integrin dimer) expressed on the cell surface of the tissue macrophages. Upon MFG-E8 recognition, the $\alpha_v\beta_3$, $\alpha_v\beta_5$ integrin induces the CrkII-DOCK180-dependent Rac1 signaling pathway to transform the macrophage into a phagocyte (Akakura et al., 2004; Albert et al., 2000).

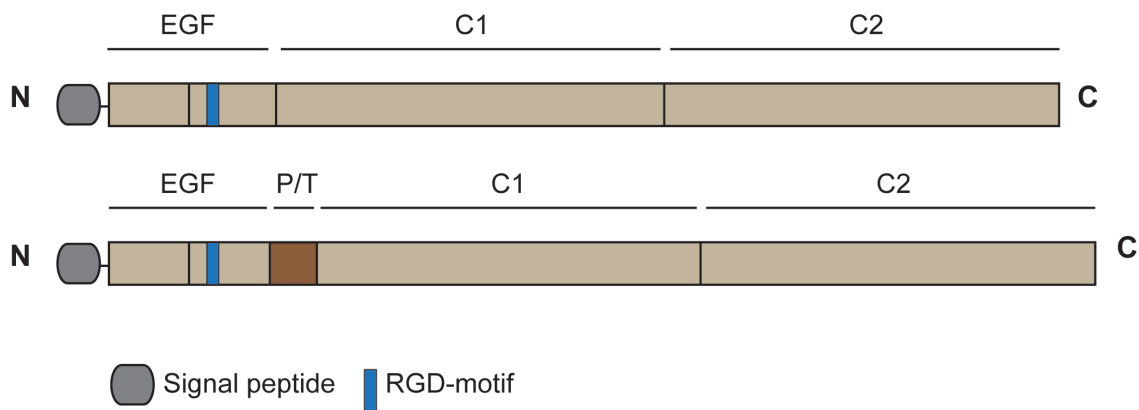


Figure 6: Murine MFG-E8 protein structure. MFG-E8 consists of two amino-terminal EGF-like domains (EGF) and two carboxy-terminal discoidin-like domains (C1, C2). In addition, the amino-terminal part harbors a signal peptide, which is required for secretion of the protein. In mice, the more abundant, shorter isoform of MFG-E8 lacks a proline/threonine-enriched domain, which is located between the EGF and C1 domain in the long isoform. The cell adhesion RGD-motif, which enables the recognition by macrophages via the $\alpha_v\beta_3/5$ integrin dimer, is positioned in the second EGF domain. N: amino-terminal, C: carboxy-terminal, EGF: epidermal growth-factor homologous regions, C1/C2: discoidin regions, P/T: proline/threonine-enriched domain, RGD: arginyl-glycyl-aspartic acid.

In the brain, the majority of MFG-E8 was shown to be expressed and secreted by astrocytes and microglia in order to induce the phagocytosis of apoptotic cells or PS-exposing stressed neurons (Boddaert et al., 2010; Fricker et al., 2012; Fuller and Van Eldik, 2008; Kawabe et al., 2018; Spittau et al., 2014). Strikingly, one *in vitro* study showed that addition of synthetic A β to a mixed neuronal/glial culture induced release of MFG-E8, which in turn, mediated engulfment of A β by microglia. Interestingly, this study reported a strong accumulation of MFG-E8 around synthetic A β preparations before internalization (Kawabe et al., 2018). This interaction of MFG-E8 and A β was further confirmed by the surface plasmon resonance technique, which identified a dose-dependent increase in the interaction of the recombinant proteins A β and MFG-E8 (Boddaert et al., 2010). In accordance, the

pharmacological neutralization or genetic deletion of MFG-E8 suppressed phagocytosis of synthetic A β in murine and human peripheral macrophages indicating an essential contribution of MFG-E8 on macrophage-mediated phagocytosis of A β (Boddaert et al., 2010). Furthermore, it was reported that mRNA as well as protein levels of MFG-E8 in brains of human AD patients and Tg2576 mice were altered in comparison to healthy individuals and wildtype mice (Boddaert et al., 2010; Fuller and Van Eldik, 2008). Remarkably, MFG-E8 levels were dramatically decreased with AD. Nevertheless, MFG-E8 was detectable in brains of AD patients where it was mainly found in plaque-free regions indicating that in regions with high A β levels the protein may be depleted due to its requirement for A β phagocytosis (Boddaert et al., 2010). However, whether MFG-E8 is indispensable for the microglial-mediated removal of A β during AD pathology *in vivo* is unknown, but was addressed in a study presented in the following.

3.4.3 Lack of MFG-E8 does not affect microglia-mediated A β phagocytosis

To examine how deficiency of MFG-E8 affects microglial phagocytosis and the pathology of cerebral β -amyloidosis, we crossed *Mfge8*^{-/-} mice to the APPPS1 tg mouse line (Radde et al., 2006; Silvestre et al., 2005). We used the resulting APPPS1 x *Mfge8*^{-/-} mouse line, which shows rapid amyloid deposition starting at six weeks of age, to investigate possible alterations in microglial function as well as A β pathology (Radde et al., 2006).

To begin with, we quantified the number of cortical and plaque-associated microglia in APPPS1 x *Mfge8*^{+/+} and APPPS1 x *Mfge8*^{-/-} mice at two and four months of age. The number of microglia was indistinguishable between the two different genotypes, but showed the pathology-induced increase in microgliosis between the two and four-month-old examined age groups.

When we next analyzed the *in vivo* phagocytic capacity of microglia for A β in these mice, we observed that deficiency of MFG-E8, in contrast to what was reported for peripheral macrophages (Boddaert et al., 2010), had no influence on microglial phagocytosis of A β as assessed by Methoxy-X04 labeled detection of A β in primary isolated microglia by fluorescence activated cell sorting and direct A β measurements in isolated microglia. Using these methods, we neither observed differences in A β phagocytosis at early disease stages (two months of age) nor during more advanced A β pathology (four months of age). Accordingly, activation of the phagolysosomal compartments, quantified by immunohistochemical staining for CD68, within microglia was unchanged between APPPS1 x *Mfge8*^{+/+} and APPPS1 x *Mfge8*^{-/-} mice.

However interestingly, the microglial production of different inflammatory cytokines such as TNF- α or IL-10 was attenuated in four-month-old APPPS1 x *Mfge8*^{-/-} mice, nonetheless indicating that the lack of MFG-E8 influences the inflammatory profile emerging during AD pathology, but possibly by a mechanism different from A β phagocytosis. We therefore quantified A β plaque pathology in cortical regions of two- and four-month-old APPPS1 x *Mfge8*^{+/+} and APPPS1 x *Mfge8*^{-/-} mice. Unexpectedly, we observed a significant reduction in A β deposits in APPPS1 x *Mfge8*^{-/-} mice at two months of age. Correspondingly, total A β levels assessed by ELISA and Western blot were significantly decreased whereas as the A β _{42/40} ratio was only slightly affected. However, at four months of age the reduction in A β pathology in APPPS1 x *Mfge8*^{-/-} mice was lost. Thus, the decline we observed in the cytokine levels in four-month-old APPPS1 x *Mfge8*^{-/-} primary microglia may be a consequence of the reduced plaque load at earlier time points, as A β deposition is thought to be causative for the inflammatory response.

To confirm the reduction in A β pathology in the absence of MFG-E8, we generated APP23 x *Mfge8*^{-/-} mice, which were analyzed at nine and twelve months of age. In line with the APPPS1 x *Mfge8*^{-/-} mice, we detected a decrease in A β levels as well as in the cortical A β plaque load in the younger APP23 x *Mfge8*^{-/-} mice, whereas in twelve-month-old mice, which show robust A β pathology, A β plaque load was indistinguishable from the APP23 x *Mfge8*^{+/+} group.

When we investigated the brain levels of MFG-E8 in relation to ageing in wildtype but also in mouse models of AD pathology (APPPS1 and APP23) we observed an age-dependent increase in MFG-E8 levels that was also reported earlier (Fuller and Van Eldik, 2008). However, A β pathology also altered MFG-E8 levels, which started to dramatically rise with the onset of A β plaque deposition. Remarkably, immunohistochemical staining of brain sections identified MFG-E8 accumulating in close vicinity to A β deposits and electron microscopy revealed that MFG-E8 was associated to A β fibrils. These results support on one hand a recently published study showing a strong accumulation of MFG-E8 around freshly prepared A β *in vitro*, but are in contrast with the described functional consequences of the A β -MFG-E8 co-localization, as accumulation of MFG-E8 around A β *in vitro* was suggested to regulate A β uptake, which we were unable to confirm (Kawabe et al., 2018).

Intriguingly, studies in humans identified a 50-amino acid long amyloidogenic fragment named medin in the C2 domain of human MFG-E8 (Häggqvist et al., 1999). Medin forms vascular amyloid deposits in the medial layer of arteries in 97 percent of the human population >50 years (Häggqvist et al., 1999). However, so far there exists no evidence for a pathological

outcome of these deposits. As human and mouse MFG-E8 share 64 percent of their amino acid sequence, it is conceivable that medin exists also in mice.

Of note, in the *Mfge8*^{-/-} mouse model used in our study, the C2 domain that contains the medin sequence, is truncated and thus *Mfge8*^{-/-} mice potentially lack medin. Furthermore, medin was shown to promote the aggregation of Serum amyloid A (AA) into fibrils – another amyloid depositing in the vasculature – by a potential cross-seeding mechanism (Larsson et al., 2011). Accordingly, we hypothesize that the decrease in A β pathology we observed in the APP tg mice deficient for MFG-E8 may be due to an effect of MFG-E8 on the A β fibril formation process that promotes initial A β aggregation, but is delayed in the absence of MFG-E8. This hypothesis is reinforced by the observation of a reduced number of small-sized, but not medium or large-sized A β plaques in brains of APPPS1 x *Mfge8*^{-/-} mice.

Ultimately, this study showed that, *in vivo*, MFG-E8 is not required for microglial phagocytosis of A β in mouse models of cerebral β -amyloidosis. However, we identified MFG-E8 to be strongly associated with aggregated A β and hypothesize that MFG-E8 promotes the initial process of A β fibrillization as absence of MFG-E8 decreased A β pathology in APP tg mice.

3.5 Conclusions

In this work, we investigated three different strategies to modulate the pathology of cerebral β -amyloidosis through manipulating the innate immune system in the CNS, which is represented by microglia.

Our initial approach to deplete dysfunctional microglia and to replace them with infiltrating monocytes failed to improve $A\beta$ pathology, but confirmed that a new microenvironment can induce fundamental changes in the function of engrafted or infiltrated macrophage populations. This knowledge will help to further understand the high plasticity of myeloid cells during the pathogenesis of AD, which is accompanied by many different disease states and molecular changes in the brain.

Remarkably, in a second study, which examined the modulation of the microglial innate immune response, we provide first evidence for experimentally induced immune training and tolerance in microglia and confirm the presence of innate immune memory in tissue-resident macrophages *in vivo*. Moreover, we identified epigenetic reprogramming to cause changes in the microglial immune response by affecting the expression profile of different immune-related genes, which subsequently resulted in alterations of the pathology of cerebral β -amyloidosis. Strikingly, we identified the transcription factor HIF-1 α to be simultaneously to the observed changes in $A\beta$ deposition upregulated by immune training and suppressed by tolerance. Thus, we suggest HIF-1 α activation as an important modulator of AD, whose inhibition might have beneficial effects for pathology.

Since genetic data have placed inflammatory processes at the center of the etiology of LOAD, it would be of great interest to investigate further downstream events of the $A\beta$ cascade such as neuronal loss, synaptic dysfunction and finally also cognitive behavior after induction of innate immune memory in microglia. Furthermore, having shown that epigenetic and functional changes of microglial can last for at least six months, pro-longed experiments could help to examine whether epigenetic remodeling of the microglial immune response could last for the whole life of microglia or might even be inherited after cell division.

Recent studies have revealed the transcriptome of certain microglial subsets by single cell sequencing approaches and identified differential phenotypes in response to their parenchymal environment (Keren-Shaul et al., 2017). The discrimination into these microglial subpopulations after the induction of immune memory in microglia would provide further information about the effects of epigenetic reprogramming in distinct categories of microglia. This would finally allow for the application of customized stimuli in order to effectively shape the immune memory function of different microglia populations.

Finally, when we investigated whether microglial phagocytosis of A β – an important function of the microglial immune response – is dependent on MFG-E8, we unexpectedly revealed a prominent co-localization between MFG-E8 and aggregated A β as well as a reduction of cerebral β -amyloidosis upon MFG-E8 deletion, but no obvious alterations in the microglial phenotype. These results suggest that MFG-E8 is dispensable for microglial phagocytosis. However, the presence of median amyloid, as a fragment of MFG-E8 has lead us to the hypothesis that MFG-E8 may be involved in the formation of A β fibrils and thus contribute to the progression of AD.

The here presented results highlight microglia and their innate immune response as an essential factor in the pathogenesis of AD. However, importantly, we could show that a set of distinct inflammatory events can induce long-term modifications of the microglial innate immune response through the induction of epigenetic changes in the enhancer landscape, which in turn shaped pathology of cerebral β -amyloidosis. With the identification of innate immune memory in microglia induced by preceding peripheral immune stimulation, we suggest a new strategy to alter the microglial immune response, which should be considered in future studies examining the contribution of the innate immune system on neurological diseases.

3.6 References

- Abbott, N.J. (2004). Evidence for bulk flow of brain interstitial fluid: significance for physiology and pathology. *Neurochem. Int.* 45, 545–552.
- Ajami, B., Bennett, J.L., Krieger, C., McNagny, K.M., and Rossi, F.M.V. (2011). Infiltrating monocytes trigger EAE progression, but do not contribute to the resident microglia pool. *Nature Neuroscience* 14, 1142–1149.
- Ajami, B., Bennett, J.L., Krieger, C., Tetzlaff, W., and Rossi, F.M.V. (2007). Local self-renewal can sustain CNS microglia maintenance and function throughout adult life. *Nature Neuroscience* 10, 1538–1543.
- Akakura, S., Singh, S., Spataro, M., Akakura, R., Kim, J.-I., Albert, M.L., and Birge, R.B. (2004). The opsonin MFG-E8 is a ligand for the α v β 5 integrin and triggers DOCK180-dependent Rac1 activation for the phagocytosis of apoptotic cells. *Exp. Cell Res.* 292, 403–416.
- Albert, M.L., Kim, J.I., and Birge, R.B. (2000). α v β 5 integrin recruits the CrkII-Dock180-rac1 complex for phagocytosis of apoptotic cells. *Nat. Cell Biol.* 2, 899–905.
- Alberts, B., Johnson, A., Lewis, J., Raff, M., and Roberts, K. (2002). Innate immunity.
- Alzforum (2017a). Mutations Search | ALZFORUM. <http://www.alzforum.org/mutationssearchgenesBDdiseasesBDkeywords-Entrykeywordsresults> 1–10.
- Alzforum (2017b). Mutations Search | ALZFORUM. <http://www.alzforum.org/mutationssearchgenesBDgenesBDdiseasesBDkeywords-Entrykeywordsresults> 1–39.
- Alzheimer, A. (1906). Über einen eigenartigen schweren Erkrankungsprozess der Hirnrinde. *Neurologisches Centralblatt* 25, 1134–2311.
- Alzheimer, A. (1907). Über eine eigenartige Erkrankung der Hirnrinde. *Allgemeine Zeitschrift für Psychiatrie* 64, 146–148.
- Askew, K., Li, K., Olmos-Alonso, A., Garcia-Moreno, F., Liang, Y., Richardson, P., Tipton, T., Chapman, M.A., Riecken, K., Beccari, S., et al. (2017). Coupled Proliferation and Apoptosis Maintain the Rapid Turnover of Microglia in the Adult Brain. *Cell Rep* 18, 391–405.
- Auffray, C., Sieweke, M.H., and Geissmann, F. (2009). Blood monocytes: development, heterogeneity, and relationship with dendritic cells. *Annu. Rev. Immunol.* 27, 669–692.
- Axelsson, R., Røyttä, M., Sourander, P., Akesson, H.O., and Andersen, O. (1984). Hereditary diffuse leucoencephalopathy with spheroids. *Acta Psychiatr Scand Suppl* 314, 1–65.
- Barozzi, I., Simonatto, M., Bonifacio, S., Yang, L., Rohs, R., Ghisletti, S., and Natoli, G. (2014). Coregulation of transcription factor binding and nucleosome occupancy through DNA features of mammalian enhancers. *Mol. Cell* 54, 844–857.
- Bell, R.D., and Zlokovic, B.V. (2009). Neurovascular mechanisms and blood-brain barrier disorder in Alzheimer's disease. *Acta Neuropathol* 118, 103–113.
- Bell, R.D., Sagare, A.P., Friedman, A.E., Bedi, G.S., Holtzman, D.M., Deane, R., and Zlokovic, B.V. (2006). Transport Pathways for Clearance of Human Alzheimer's Amyloid β -Peptide and Apolipoproteins E and J in the Mouse Central Nervous System. *Journal of Cerebral Blood Flow & Metabolism* 27, 909–918.
- Ben-Zvi, A., Lacoste, B., Kur, E., Andreone, B.J., Mayshar, Y., Yan, H., and Gu, C. (2014). Mfsd2a is critical for the formation and function of the blood-brain barrier. *Nature* 509, 507–511.

Benn, C.S., Netea, M.G., Selin, L.K., and Aaby, P. (2013). A small jab - a big effect: nonspecific immunomodulation by vaccines. *Trends in Immunology* *34*, 431–439.

Berg, Vom, J., Prokop, S., Miller, K.R., Obst, J., Kälin, R.E., Lopategui-Cabezas, I., Wegner, A., Mair, F., Schipke, C.G., Peters, O., et al. (2012). Inhibition of IL-12/IL-23 signaling reduces Alzheimer's disease-like pathology and cognitive decline. *Nat Med* *18*, 1812–1819.

Betmouni, S., Perry, V.H., and Gordon, J.L. (1996). Evidence for an early inflammatory response in the central nervous system of mice with scrapie. *Neuroscience* *74*, 1–5.

Beyreuther, K., and Masters, C.L. (1991). Amyloid precursor protein (APP) and beta A4 amyloid in the etiology of Alzheimer's disease: precursor-product relationships in the derangement of neuronal function. *Brain Pathol.* *1*, 241–251.

Bénil, P., Letouzé, E., Rak, M., Aubry, L., Burnichon, N., Favier, J., Gimenez-Roqueplo, A.-P., and Rustin, P. (2014). Unsuspected task for an old team: Succinate, fumarate and other Krebs cycle acids in metabolic remodeling. *Biochimica Et Biophysica Acta (BBA) - Bioenergetics* *1837*, 1330–1337.

Biber, K., Möller, T., Boddeke, E., and Prinz, M. (2016). Central nervous system myeloid cells as drug targets: current status and translational challenges. *Nat Rev Drug Discov* *15*, 110–124.

Blacker, D., Haines, J.L., Rodes, L., Terwedow, H., Go, R.C., Harrell, L.E., Perry, R.T., Bassett, S.S., Chase, G., Meyers, D., et al. (1997). ApoE-4 and age at onset of Alzheimer's disease: the NIMH genetics initiative. *Neurology* *48*, 139–147.

Blessed, G., Tomlinson, B.E., and Roth, M. (1968). The association between quantitative measures of dementia and of senile change in the cerebral grey matter of elderly subjects. *Br J Psychiatry* *114*, 797–811.

Boddaert, J., Kinugawa, K., Lambert, J.-C., Boukhtouche, F., Zoll, J., Merval, R., Blanc-Brude, O., Mann, D., Berr, C., Vilar, J., et al. (2010). Evidence of a Role for Lactadherin in Alzheimer's Disease. *The American Journal of Pathology* *170*, 921–929.

Bogdan, C., Paik, J., Vodovotz, Y., and Nathan, C. (1992). Contrasting mechanisms for suppression of macrophage cytokine release by transforming growth factor-beta and interleukin-10. *Journal of Biological Chemistry* *267*, 23301–23308.

Bohlen, C.J., Bennett, F.C., Tucker, A.F., Collins, H.Y., Mulinyawe, S.B., and Barres, B.A. (2017). Diverse Requirements for Microglial Survival, Specification, and Function Revealed by Defined-Medium Cultures. *Neuron* *94*, 759–773.e8.

Bolmont, T., Haiss, F., Eicke, D., Radde, R., Mathis, C.A., Klunk, W.E., Kohsaka, S., Jucker, M., and Calhoun, M.E. (2008). Dynamics of the Microglial/Amyloid Interaction Indicate a Role in Plaque Maintenance. *Journal of Neuroscience* *28*, 4283–4292.

Borenstein, A.R., Copenhaver, C.I., and Mortimer, J.A. (2006). Early-life risk factors for Alzheimer disease. *Alzheimer Dis Assoc Disord* *20*, 63–72.

Bouchon, A., Hernández-Munain, C., Cella, M., and Colonna, M. (2001). A DAP12-mediated pathway regulates expression of CC chemokine receptor 7 and maturation of human dendritic cells. *J Exp Med* *194*, 1111–1122.

Brosnan, C.F., Bornstein, M.B., and Bloom, B.R. (1981). The effects of macrophage depletion on the clinical and pathologic expression of experimental allergic encephalomyelitis. *The Journal of Immunology* *126*, 614–620.

Brydon, L., Harrison, N.A., Walker, C., Steptoe, A., and Critchley, H.D. (2008). Peripheral inflammation is associated with altered substantia nigra activity and psychomotor slowing in humans. *Biol. Psychiatry* *63*, 1022–1029.

Butovsky, O., Jedrychowski, M.P., Moore, C.S., Cialic, R., Lanser, A.J., Gabriely, G., Koeglsperger, T., Dake, B., Wu, P.M., Doykan, C.E., et al. (2014). Identification of a unique TGF- β -dependent molecular and functional signature in microglia. *Nature Neuroscience* 17, 131–143.

C A Janeway, J. (1989). Approaching the Asymptote? Evolution and Revolution in Immunology. *Cold Spring Harb Symp Quant Biol* 54, 1–13.

Carare, R.O., Bernardes Silva, M., Newman, T.A., Page, A.M., Nicoll, J.A.R., Perry, V.H., and Weller, R.O. (2008). Solutes, but not cells, drain from the brain parenchyma along basement membranes of capillaries and arteries: significance for cerebral amyloid angiopathy and neuroimmunology. *Neuropathol Appl Neurobiol* 34, 131–144.

Caron, E., Self, A.J., and Hall, A. (2000). The GTPase Rap1 controls functional activation of macrophage integrin α M β 2 by LPS and other inflammatory mediators. *Current Biology* 10, 974–978.

Castellano, J.M., Kim, J., Stewart, F.R., Jiang, H., DeMattos, R.B., Patterson, B.W., Fagan, A.M., Morris, J.C., Mawuenyega, K.G., Cruchaga, C., et al. (2011). Human apoE isoforms differentially regulate brain amyloid- β peptide clearance. *Sci Transl Med* 3, 89ra57–89ra57.

Cella, M., Buonsanti, C., Strader, C., Kondo, T., Salmaggi, A., and Colonna, M. (2003). Impaired differentiation of osteoclasts in TREM-2-deficient individuals. *J Exp Med* 198, 645–651.

Cheng, G., Huang, C., Deng, H., and Wang, H. (2012). Diabetes as a risk factor for dementia and mild cognitive impairment: a meta-analysis of longitudinal studies. *Intern Med J* 42, 484–491.

Cheng, S.-C., Quintin, J., Cramer, R.A., Shepardson, K.M., Saeed, S., Kumar, V., Giamarellos-Bourboulis, E.J., Martens, J.H.A., Rao, N.A., Aghajanirofeh, A., et al. (2014). mTOR- and HIF-1 α -mediated aerobic glycolysis as metabolic basis for trained immunity. *Science* 345, 1250684–1250684.

Chibnik, L.B., Shulman, J.M., Leurgans, S.E., Schneider, J.A., Wilson, R.S., Tran, D., Aubin, C., Buchman, A.S., Heward, C.B., Myers, A.J., et al. (2011). CR1 is associated with amyloid plaque burden and age-related cognitive decline. *Ann. Neurol.* 69, 560–569.

Chudakov, D.M., Matz, M.V., Lukyanov, S., and Lukyanov, K.A. (2010). Fluorescent proteins and their applications in imaging living cells and tissues. *Physiol. Rev.* 90, 1103–1163.

Chung, H. (1999). Uptake, Degradation, and Release of Fibrillar and Soluble Forms of Alzheimer's Amyloid beta -Peptide by Microglial Cells. *Journal of Biological Chemistry* 274, 32301–32308.

Chung, H., Brazil, M.I., Irizarry, M.C., Hyman, B.T., and Maxfield, F.R. (2001). Uptake of fibrillar beta-amyloid by microglia isolated from MSR-A (type I and type II) knockout mice. *NeuroReport* 12, 1151–1154.

Citron, M., Oltsdorf, T., Haass, C., McConlogue, L., Hung, A.Y., Seubert, P., Vigo-Pelfrey, C., Lieberburg, I., and Selkoe, D.J. (1992). Mutation of the beta-amyloid precursor protein in familial Alzheimer's disease increases beta-protein production. *Nature* 360, 672–674.

Combrinck, M.I., Perry, V.H., and Cunningham, C. (2002). Peripheral infection evokes exaggerated sickness behaviour in pre-clinical murine prion disease. *Neuroscience* 112, 7–11.

Coraci, I.S., Husemann, J., Berman, J.W., Hulette, C., Dufour, J.H., Campanella, G.K., Luster, A.D., Silverstein, S.C., and Khoury, E.J. (2002). CD36, a class B scavenger receptor, is expressed on microglia in Alzheimer's disease brains and can mediate production of reactive oxygen species in response to beta-amyloid fibrils. *The American Journal of Pathology* 160, 101–112.

Corder, E.H., Saunders, A.M., Risch, N.J., Strittmatter, W.J., Schmechel, D.E., Gaskell, P.C., Rimmler, J.B., Locke, P.A., Conneally, P.M., and Schmechel, K.E. (1994). Protective effect of apolipoprotein E type 2 allele for late onset Alzheimer disease. *Nat Genet* 7, 180–184.

Corder, E.H., Saunders, A.M., Strittmatter, W.J., Schmechel, D.E., Gaskell, P.C., Small, G.W., Roses, A.D., Haines, J.L., and Pericak-Vance, M.A. (1993). Gene dose of apolipoprotein E type 4 allele and the risk of Alzheimer's disease in late onset families. *Science* 261, 921–923.

Cramer, T., Yamanishi, Y., Clausen, B.E., Förster, I., Pawlinski, R., Mackman, N., Haase, V.H., Jaenisch, R., Corr, M., Nizet, V., et al. (2003). HIF-1alpha is essential for myeloid cell-mediated inflammation. *Cell* 112, 645–657.

Creyghton, M.P., Cheng, A.W., Welstead, G.G., Kooistra, T., Carey, B.W., Steine, E.J., Hanna, J., Lodato, M.A., Frampton, G.M., Sharp, P.A., et al. (2010). Histone H3K27ac separates active from poised enhancers and predicts developmental state. *Proc. Natl. Acad. Sci. U.S.a.* 107, 21931–21936.

Cribbs, D.H., Berchtold, N.C., Perreau, V., Coleman, P.D., Rogers, J., Tenner, A.J., and Cotman, C.W. (2012). Extensive innate immune gene activation accompanies brain aging, increasing vulnerability to cognitive decline and neurodegeneration: a microarray study. *Journal of Neuroinflammation* 9, 179.

Cunningham, C., Boche, D., and Perry, V.H. (2002). Transforming growth factor beta1, the dominant cytokine in murine prion disease: influence on inflammatory cytokine synthesis and alteration of vascular extracellular matrix. *Neuropathol Appl Neurobiol* 28, 107–119.

Cunningham, C., Wilcockson, D.C., Campion, S., Lunnon, K., and Perry, V.H. (2005). Central and Systemic Endotoxin Challenges Exacerbate the Local Inflammatory Response and Increase Neuronal Death during Chronic Neurodegeneration. *Journal of Neuroscience* 25, 9275–9284.

Dagher, N.N., Najafi, A.R., Kayala, K.M.N., Elmore, M.R.P., White, T.E., Medeiros, R., West, B.L., and Green, K.N. (2015). Colony-stimulating factor 1 receptor inhibition prevents microglial plaque association and improves cognition in 3xTg-AD mice. *Journal of Neuroinflammation* 12, 139.

Dantzer, R. (2001). Cytokine-induced sickness behavior: mechanisms and implications. *Ann. N. Y. Acad. Sci.* 933, 222–234.

Davies, R. Gill Livingston: transforming dementia prevention and care. TheLancet.com

De Strooper, B., Saffig, P., Craessaerts, K., Vanderstichele, H., Guhde, G., Annaert, W., Figura, Von, K., and Van Leuven, F. (1998). Deficiency of presenilin-1 inhibits the normal cleavage of amyloid precursor protein. *Nature* 391, 387–390.

De Strooper, B., and Karran, E. (2016). The Cellular Phase of Alzheimer's Disease. *Cell* 164, 603–615.

Deane, R., Bell, R.D., Sagare, A., and Zlokovic, B.V. (2009). Clearance of Amyloid-β Peptide Across the Blood-Brain Barrier: Implication for Therapies in Alzheimer's Disease. *CNS Neurol Disord Drug Targets* 8, 16–30.

Deane, R., Sagare, A., Hamm, K., Parisi, M., Lane, S., Finn, M.B., Holtzman, D.M., and Zlokovic, B.V. (2008). apoE isoform-specific disruption of amyloid beta peptide clearance from mouse brain. *J. Clin. Invest.* 118, 4002–4013.

Deane, R., Wu, Z., Sagare, A., Davis, J., Yan, Du, S., Hamm, K., Xu, F., Parisi, M., LaRue, B., Hu, H.W., et al. (2004). LRP/amyloid beta-peptide interaction mediates differential brain efflux of Abeta isoforms. *Neuron* 43, 333–344.

DeMattos, R.B., Cirrito, J.R., Parsadanian, M., May, P.C., O'Dell, M.A., Taylor, J.W., Harmony, J.A.K., Aronow, B.J., Bales, K.R., Paul, S.M., et al. (2004). ApoE and clusterin cooperatively suppress Abeta levels and deposition: evidence that ApoE regulates extracellular Abeta metabolism in vivo. *Neuron* 41, 193–202.

- Depino, A.M., Earl, C., Kaczmarczyk, E., Ferrari, C., Besedovsky, H., Del Rey, A., Pitossi, F.J., and Oertel, W.H. (2003). Microglial activation with atypical proinflammatory cytokine expression in a rat model of Parkinson's disease. *Eur. J. Neurosci.* *18*, 2731–2742.
- Derecki, N.C., Cronk, J.C., Lu, Z., Xu, E., Abbott, S.B.G., Guyenet, P.G., and Kipnis, J. (2012). Wild-type microglia arrest pathology in a mouse model of Rett syndrome. *Nature* *484*, 105–109.
- Di Luzio, N.R., and Williams, D.L. (1978). Protective effect of glucan against systemic *Staphylococcus aureus* septicemia in normal and leukemic mice. *Infect. Immun.* *20*, 804–810.
- Dighe, A.S., Campbell, D., Hsieh, C.S., Clarke, S., Greaves, D.R., Gordon, S., Murphy, K.M., and Schreiber, R.D. (1995). Tissue-specific targeting of cytokine unresponsiveness in transgenic mice. *Immunity* *3*, 657–666.
- Dogan, R.-N.E., Elhofy, A., and Karpus, W.J. (2008). Production of CCL2 by central nervous system cells regulates development of murine experimental autoimmune encephalomyelitis through the recruitment of TNF- and iNOS-expressing macrophages and myeloid dendritic cells. *The Journal of Immunology* *180*, 7376–7384.
- Donohoe, D.R., and Bultman, S.J. (2012). Metaboloepigenetics: interrelationships between energy metabolism and epigenetic control of gene expression. *J. Cell. Physiol.* *227*, 3169–3177.
- Dunn, N., Mullee, M., Perry, V.H., and Holmes, C. (2005). Association between dementia and infectious disease: evidence from a case-control study. *Alzheimer Dis Assoc Disord* *19*, 91–94.
- Durrant, W.E., and Dong, X. (2004). Systemic acquired resistance. *Annu Rev Phytopathol* *42*, 185–209.
- Dyrks, T., Weidemann, A., Multhaup, G., Salbaum, J.M., Lemaire, H.G., Kang, J., Müller-Hill, B., Masters, C.L., and Beyreuther, K. (1988). Identification, transmembrane orientation and biogenesis of the amyloid A4 precursor of Alzheimer's disease. *Embo J.* *7*, 949–957.
- Eli Lilly Press Release (2016). Eli Lilly and Company announces top-line results on solanezumab phase 3 clinical trials in patients with Alzheimer's disease.
- Elmore, M.R.P., Najafi, A.R., Koike, M.A., Dagher, N.N., Spangenberg, E.E., Rice, R.A., Kitazawa, M., Matusow, B., Nguyen, H., West, B.L., et al. (2014). Colony-Stimulating Factor 1 Receptor Signaling Is Necessary for Microglia Viability, Unmasking a Microglia Progenitor Cell in the Adult Brain. *Neuron* *82*, 380–397.
- Escott-Price, V., Sims, R., Bannister, C., Harold, D., Vronskaya, M., Majounie, E., Badarinarayan, N., GERAD/PERADES, IGAP consortia, Morgan, K., et al. (2015). Common polygenic variation enhances risk prediction for Alzheimer's disease. *Brain* *138*, 3673–3684.
- Feil, S., Valtcheva, N., and Feil, R. (2009). Inducible Cre mice. *Methods Mol. Biol.* *530*, 343–363.
- Fiala, M., Zhang, L., Gan, X., Sherry, B., Taub, D., Graves, M.C., Hama, S., Way, D., Weinand, M., Witte, M., et al. (1998). Amyloid-beta induces chemokine secretion and monocyte migration across a human blood-brain barrier model. *Mol Med* *4*, 480–489.
- Fleischhacker, W.W., Buchgeher, A., and Schubert, H. (1986). Memantine in the treatment of senile dementia of the Alzheimer type. *Prog. Neuropsychopharmacol. Biol. Psychiatry* *10*, 87–93.
- Fonseca, M.I., Chu, S., Pierce, A.L., Brubaker, W.D., Hauhart, R.E., Mastroeni, D., Clarke, E.V., Rogers, J., Atkinson, J.P., and Tenner, A.J. (2016). Analysis of the Putative Role of CR1 in Alzheimer's Disease: Genetic Association, Expression and Function. *PLoS ONE* *11*, e0149792.
- Foster, S.L., Hargreaves, D.C., and Medzhitov, R. (2007). Gene-specific control of inflammation by TLR-induced chromatin modifications. *Nature* *447*, 972–978.

- Frank, S., Burbach, G.J., Bonin, M., Walter, M., Streit, W., Bechmann, I., and Deller, T. (2008). TREM2 is upregulated in amyloid plaque-associated microglia in aged APP23 transgenic mice. *Glia* *56*, 1438–1447.
- Fricker, M., Neher, J.J., Zhao, J.-W., Théry, C., Tolkovsky, A.M., and Brown, G.C. (2012). MFG-E8 mediates primary phagocytosis of viable neurons during neuroinflammation. *J. Neurosci.* *32*, 2657–2666.
- Fu, H., Liu, B., Frost, J.L., Hong, S., Jin, M., Ostaszewski, B., Shankar, G.M., Costantino, I.M., Carroll, M.C., Mayadas, T.N., et al. (2012). Complement component C3 and complement receptor type 3 contribute to the phagocytosis and clearance of fibrillar A β by microglia. *Glia* *60*, 993–1003.
- Fuller, A.D., and Van Eldik, L.J. (2008). MFG-E8 regulates microglial phagocytosis of apoptotic neurons. *J Neuroimmune Pharmacol* *3*, 246–256.
- Füger, P., Hefendehl, J.K., Veeraraghavalu, K., Wendeln, A.-C., Schlosser, C., Obermüller, U., Wegenast-Braun, B.M., Neher, J.J., Martus, P., Kohsaka, S., et al. (2017). Microglia turnover with aging and in an Alzheimer's model via long-term in vivo single-cell imaging. *Nature Neuroscience* *138*, 3.
- Ganeshan, K., and Chawla, A. (2014). Metabolic regulation of immune responses. *Annu. Rev. Immunol.* *32*, 609–634.
- Gazzar, El, M., Yoza, B.K., Chen, X., Garcia, B.A., Young, N.L., and McCall, C.E. (2009). Chromatin-specific remodeling by HMGB1 and linker histone H1 silences proinflammatory genes during endotoxin tolerance. *Mol. Cell. Biol.* *29*, 1959–1971.
- Geissmann, F., Jung, S., and Littman, D.R. (2003). Blood monocytes consist of two principal subsets with distinct migratory properties. *Immunity* *19*, 71–82.
- Geissmann, F., Manz, M.G., Jung, S., Sieweke, M.H., Merad, M., and Ley, K. (2010). Development of monocytes, macrophages, and dendritic cells. *Science* *327*, 656–661.
- Ghebranious, N., Ivacic, L., Mallum, J., and Dokken, C. (2005). Detection of ApoE E2, E3 and E4 alleles using MALDI-TOF mass spectrometry and the homogeneous mass-extend technology. *Nucleic Acids Res.* *33*, e149–e149.
- Ghisletti, S., Barozzi, I., Mietton, F., Polletti, S., De Santa, F., Venturini, E., Gregory, L., Lonie, L., Chew, A., Wei, C.-L., et al. (2010). Identification and characterization of enhancers controlling the inflammatory gene expression program in macrophages. *Immunity* *32*, 317–328.
- Ginhoux, F., Greter, M., Leboeuf, M., Nandi, S., See, P., Gokhan, S., Mehler, M.F., Conway, S.J., Ng, L.G., Stanley, E.R., et al. (2010). Fate Mapping Analysis Reveals That Adult Microglia Derive from Primitive Macrophages. *Science* *330*, 841–845.
- Ginhoux, F., and Jung, S. (2014). Monocytes and macrophages: developmental pathways and tissue homeostasis. *Nat. Rev. Immunol.* *14*, 392–404.
- Gjoneska, E., Pfenning, A.R., Mathys, H., Quon, G., Kundaje, A., Tsai, L.-H., and Kellis, M. (2015). Conserved epigenomic signals in mice and humans reveal immune basis of Alzheimer's disease. *Nature* *518*, 365–369.
- Glennner, G.G., and Wong, C.W. (1984a). Alzheimer's disease: initial report of the purification and characterization of a novel cerebrovascular amyloid protein. *Biochemical and Biophysical Research Communications* *120*, 885–890.
- Glennner, G.G., and Wong, C.W. (1984b). Alzheimer's disease and Down's syndrome: sharing of a unique cerebrovascular amyloid fibril protein. *Biochemical and Biophysical Research Communications* *122*, 1131–1135.

Goate, A., Chartier-Harlin, M.C., Mullan, M., Brown, J., Crawford, F., Fidani, L., Giuffra, L., Haynes, A., Irving, N., and James, L. (1991). Segregation of a missense mutation in the amyloid precursor protein gene with familial Alzheimer's disease. *Nature* *349*, 704–706.

Godbout, J.P., Chen, J., Abraham, J., Richwine, A.F., Berg, B.M., Kelley, K.W., and Johnson, R.W. (2005). Exaggerated neuroinflammation and sickness behavior in aged mice following activation of the peripheral innate immune system. *FASEB J.* *19*, 1329–1331.

Goldgaber, D., Lerman, M.I., McBride, O.W., Saffiotti, U., and Gajdusek, D.C. (1987). Characterization and chromosomal localization of a cDNA encoding brain amyloid of Alzheimer's disease. *Science* *235*, 877–880.

Goldmann, T., Wieghofer, P., Müller, P.F., Wolf, Y., Varol, D., Yona, S., Brendecke, S.M., Kierdorf, K., Staszewski, O., Datta, M., et al. (2013). A new type of microglia gene targeting shows TAK1 to be pivotal in CNS autoimmune inflammation. *Nature Neuroscience* *16*, 1618–1626.

Gorevic, P.D., Goñi, F., Pons-Estel, B., Alvarez, F., Peress, N.S., and Frangione, B. (1986). Isolation and partial characterization of neurofibrillary tangles and amyloid plaque core in Alzheimer's disease: immunohistological studies. *J. Neuropathol. Exp. Neurol.* *45*, 647–664.

Gosselin, D., Link, V.M., Romanoski, C.E., Fonseca, G.J., Eichenfield, D.Z., Spann, N.J., Stender, J.D., Chun, H.B., Garner, H., Geissmann, F., et al. (2014). Environment drives selection and function of enhancers controlling tissue-specific macrophage identities. *Cell* *159*, 1327–1340.

Gosselin, D., Skola, D., Coufal, N.G., Holtman, I.R., Schlachetzki, J.C.M., Sajti, E., Jaeger, B.N., O'Connor, C., Fitzpatrick, C., Pasillas, M.P., et al. (2017). An environment-dependent transcriptional network specifies human microglia identity. *Science* *356*, eaal3222.

Grathwohl, S.A., Kälin, R.E., Bolmont, T., Prokop, S., Winkelmann, G., Kaeser, S.A., Odenthal, J., Radde, R., Eldh, T., Gandy, S., et al. (2009). Formation and maintenance of Alzheimer's disease beta-amyloid plaques in the absence of microglia. *Nature Neuroscience* *12*, 1361–1363.

Greter, M., Lelios, I., Pelczar, P., Hoeffel, G., Price, J., Leboeuf, M., Kündig, T.M., Frei, K., Ginhoux, F., Merad, M., et al. (2012). Stroma-derived interleukin-34 controls the development and maintenance of langerhans cells and the maintenance of microglia. *Immunity* *37*, 1050–1060.

Guerreiro, R., Wojtas, A., Bras, J., Carrasquillo, M., Rogaeve, E., Majounie, E., Cruchaga, C., Sassi, C., Kauwe, J.S.K., Younkin, S., et al. (2013). TREM2 variants in Alzheimer's disease. *N Engl J Med* *368*, 117–127.

Gut, P., and Verdin, E. (2013). The nexus of chromatin regulation and intermediary metabolism. *Nature* *502*, 489–498.

Haass, C., Lemere, C.A., Capell, A., Citron, M., Seubert, P., Schenk, D., Lannfelt, L., and Selkoe, D.J. (1995). The Swedish mutation causes early-onset Alzheimer's disease by β -secretase cleavage within the secretory pathway. *Nat Med* *1*, 1291–1296.

Hagan, N., and Ben-Zvi, A. (2015). The molecular, cellular, and morphological components of blood-brain barrier development during embryogenesis. *Semin. Cell Dev. Biol.* *38*, 7–15.

Hamerman, J.A., Jarjoura, J.R., Humphrey, M.B., Nakamura, M.C., Seaman, W.E., and Lanier, L.L. (2006). Cutting edge: inhibition of TLR and FcR responses in macrophages by triggering receptor expressed on myeloid cells (TREM)-2 and DAP12. *The Journal of Immunology* *177*, 2051–2055.

Hanayama, R., Tanaka, M., Miwa, K., Shinohara, A., Iwamatsu, A., and Nagata, S. (2002). Identification of a factor that links apoptotic cells to phagocytes. *Nature* *417*, 182–187.

- Hanayama, R., Tanaka, M., Miyasaka, K., Aozasa, K., Koike, M., Uchiyama, Y., and Nagata, S. (2004). Autoimmune disease and impaired uptake of apoptotic cells in MFG-E8-deficient mice. *Science* *304*, 1147–1150.
- Hardy, J.A., and Higgins, G.A. (1992). Alzheimer's disease: the amyloid cascade hypothesis. *Science* *256*, 184–185.
- Hardy, J.A., and Allsop, D. (1991). Amyloid deposition as the central event in the aetiology of Alzheimer's disease. *Trends Pharmacol. Sci.* *12*, 383–388.
- Harman, D. (2006). Alzheimer's disease pathogenesis: role of aging. *Ann. N. Y. Acad. Sci.* *1067*, 454–460.
- Harold, D., Abraham, R., Hollingworth, P., Sims, R., Gerrish, A., Hamshere, M.L., Pahwa, J.S., Moskvin, V., Dowzell, K., Williams, A., et al. (2009). Genome-wide association study identifies variants at *CLU* and *PICALM* associated with Alzheimer's disease. *Nat Genet* *41*, 1088–1093.
- Harrison, N.A., Brydon, L., Walker, C., Gray, M.A., Steptoe, A., and Critchley, H.D. (2009). Inflammation causes mood changes through alterations in subgenual cingulate activity and mesolimbic connectivity. *Biol. Psychiatry* *66*, 407–414.
- Hart, B.L. (1988). Biological basis of the behavior of sick animals. *Neurosci Biobehav Rev* *12*, 123–137.
- Hashimoto, D., Chow, A., Noizat, C., Teo, P., Beasley, M.B., Leboeuf, M., Becker, C.D., See, P., Price, J., Lucas, D., et al. (2013). Tissue-resident macrophages self-maintain locally throughout adult life with minimal contribution from circulating monocytes. *Immunity* *38*, 792–804.
- Hawkes, C.A., Härtig, W., Kacza, J., Schliebs, R., Weller, R.O., Nicoll, J.A., and Carare, R.O. (2011). Perivascular drainage of solutes is impaired in the ageing mouse brain and in the presence of cerebral amyloid angiopathy. *Acta Neuropathol* *121*, 431–443.
- Hawkes, C.A., Jayakody, N., Johnston, D.A., Bechmann, I., and Carare, R.O. (2014). Failure of Perivascular Drainage of β -amyloid in Cerebral Amyloid Angiopathy. *Brain Pathology* *24*, 396–403.
- Hayashi, S., and McMahon, A.P. (2002). Efficient recombination in diverse tissues by a tamoxifen-inducible form of Cre: a tool for temporally regulated gene activation/inactivation in the mouse. *Dev. Biol.* *244*, 305–318.
- Häggqvist, B., Näslund, J., Sletten, K., Westermark, G.T., Mucchiano, G., Tjerneberg, L.O., Nordstedt, C., Engström, U., and Westermark, P. (1999). Medin: an integral fragment of aortic smooth muscle cell-produced lactadherin forms the most common human amyloid. *Proceedings of the National Academy of Sciences* *96*, 8669–8674.
- Heinz, S., Benner, C., Spann, N., Bertolino, E., Lin, Y.C., Laslo, P., Cheng, J.X., Murre, C., Singh, H., and Glass, C.K. (2010). Simple combinations of lineage-determining transcription factors prime cis-regulatory elements required for macrophage and B cell identities. *Mol. Cell* *38*, 576–589.
- Heneka, M.T., Carson, M.J., Khoury, E.J., Landreth, G.E., Brosseron, F., Feinstein, D.L., Jacobs, A.H., Wyss-Coray, T., Vitorica, J., Ransohoff, R.M., et al. (2015a). Neuroinflammation in Alzheimer's disease. *Lancet Neurology* *14*, 388–405.
- Heneka, M.T., Golenbock, D.T., and Latz, E. (2015b). Innate immunity in Alzheimer's disease. *Nature Publishing Group* *16*, 229–236.
- Heneka, M.T., Kummer, M.P., Stutz, A., Delekate, A., Schwartz, S., Vieira-Saecker, A., Griep, A., Axt, D., Remus, A., Tzeng, T.-C., et al. (2013). nature11729. *Nature* *493*, 674–678.

- Heppner, F.L., Greter, M., Marino, D., Falsig, J., Raivich, G., Hövelmeyer, N., Waisman, A., Rüllicke, T., Prinz, M., Priller, J., et al. (2005). Experimental autoimmune encephalomyelitis repressed by microglial paralysis. *Nat Med* *11*, 146–152.
- Hickman, S.E., and Khoury, E.I., J. (2014). TREM2 and the neuroimmunology of Alzheimer's disease. *Biochem. Pharmacol.* *88*, 495–498.
- Hickman, S.E., Allison, E.K., and Khoury, E.I., J. (2008). Microglial Dysfunction and Defective β -Amyloid Clearance Pathways in Aging Alzheimer's Disease Mice. *Journal of Neuroscience* *2012*, 8354–8360.
- Hickman, S.E., Kingery, N.D., Ohsumi, T.K., Borowsky, M.L., Wang, L.-C., Means, T.K., and Khoury, E.I., J. (2013). The microglial sensome revealed by direct RNA sequencing. *Nature Neuroscience* *16*, 1896–1905.
- Hodges, J.R. (2006). Alzheimer's centennial legacy: origins, landmarks and the current status of knowledge concerning cognitive aspects.
- Hoeffel, G., and Ginhoux, F. (2015). Ontogeny of Tissue-Resident Macrophages. *Front Immunol* *6*, 486.
- Hollingworth, P., Harold, D., Sims, R., Gerrish, A., Lambert, J.-C., Carrasquillo, M.M., Abraham, R., Hamshere, M.L., Pahwa, J.S., Moskvin, V., et al. (2011). Common variants at ABCA7, MS4A6A/MS4A4E, EPHA1, CD33 and CD2AP are associated with Alzheimer's disease. *Nat Genet* *43*, 429–435.
- Holmes, C., Cunningham, C., Zotova, E., Culliford, D., and Perry, V.H. (2011). Proinflammatory cytokines, sickness behavior, and Alzheimer disease. *Neurology* *77*, 212–218.
- Holmes, C., Cunningham, C., Zotova, E., Woolford, J., Dean, C., Kerr, S., Culliford, D., and Perry, V.H. (2009). Systemic inflammation and disease progression in Alzheimer disease. *Neurology* *73*, 768–774.
- Holtman, I.R., Raj, D.D., Miller, J.A., Schaafsma, W., Yin, Z., Brouwer, N., Wes, P.D., Möller, T., Orre, M., Kamphuis, W., et al. (2015). Induction of a common microglia gene expression signature by aging and neurodegenerative conditions: a co-expression meta-analysis. *Acta Neuropathol Commun* *3*, 31.
- Holtzman, D.M., Morris, J.C., and Goate, A.M. (2011). Alzheimer's disease: the challenge of the second century. *Sci Transl Med* *3*, 77sr1–77sr1.
- Huitinga, I., Van Rooijen, N., De Groot, C.J., Uitdehaag, B.M., and Dijkstra, C.D. (1990). Suppression of experimental allergic encephalomyelitis in Lewis rats after elimination of macrophages. *J Exp Med* *172*, 1025–1033.
- Humphrey, M.B., Daws, M.R., Spusta, S.C., Niemi, E.C., Torchia, J.A., Lanier, L.L., Seaman, W.E., and Nakamura, M.C. (2006). TREM2, a DAP12-associated receptor, regulates osteoclast differentiation and function. *J. Bone Miner. Res.* *21*, 237–245.
- Ifrim, D.C., Quintin, J., Joosten, L.A.B., Jacobs, C., Jansen, T., Jacobs, L., Gow, N.A.R., Williams, D.L., van der Meer, J.W.M., and Netea, M.G. (2014). Trained immunity or tolerance: opposing functional programs induced in human monocytes after engagement of various pattern recognition receptors. *Clin. Vaccine Immunol.* *21*, 534–545.
- Iliff, J.J., Wang, M., Liao, Y., Plogg, B.A., Peng, W., Gundersen, G.A., Benveniste, H., Vates, G.E., Deane, R., Goldman, S.A., et al. (2012). A paravascular pathway facilitates CSF flow through the brain parenchyma and the clearance of interstitial solutes, including amyloid β . *Sci Transl Med* *4*, 147ra111–147ra111.
- Ivashkiv, L.B. (2013). Epigenetic regulation of macrophage polarization and function. *Trends in Immunology* *34*, 216–223.

Izikson, L., Klein, R.S., Charo, I.F., Weiner, H.L., and Luster, A.D. (2000). Resistance to experimental autoimmune encephalomyelitis in mice lacking the CC chemokine receptor (CCR)2. *J Exp Med* 192, 1075–1080.

Janeway, C., Travers, P., Walport, M., and Shlomchik, M.J. (2001). *Immunobiology 5: the immune system in health and disease* (New York, Garland Pub.).

Jarrett, J.T., Berger, E.P., and Lansbury, P.T. (1993). The carboxy terminus of the beta amyloid protein is critical for the seeding of amyloid formation: implications for the pathogenesis of Alzheimer's disease. *Biochemistry* 32, 4693–4697.

Jay, T.R., Hirsch, A.M., Broihier, M.L., Miller, C.M., Neilson, L.E., Ransohoff, R.M., Lamb, B.T., and Landreth, G.E. (2017). Disease Progression-Dependent Effects of TREM2 Deficiency in a Mouse Model of Alzheimer's Disease. *J. Neurosci.* 37, 637–647.

Jay, T.R., Miller, C.M., Cheng, P.J., Graham, L.C., Bemiller, S., Broihier, M.L., Xu, G., Margevicius, D., Karlo, J.C., Sousa, G.L., et al. (2015). TREM2 deficiency eliminates TREM2+ inflammatory macrophages and ameliorates pathology in Alzheimer's disease mouse models. *Journal of Experimental Medicine* 212, 287–295.

Jha, A.K., Huang, S.C.-C., Sergushichev, A., Lampropoulou, V., Ivanova, Y., Loginicheva, E., Chmielewski, K., Stewart, K.M., Ashall, J., Everts, B., et al. (2015). Network integration of parallel metabolic and transcriptional data reveals metabolic modules that regulate macrophage polarization. *Immunity* 42, 419–430.

Jonsson, T., Stefansson, H., Steinberg, S., Jonsdottir, I., Jonsson, P.V., Snaedal, J., Björnsson, S., Huttenlocher, J., Levey, A.I., Lah, J.J., et al. (2013). Variant of TREM2 associated with the risk of Alzheimer's disease. *N Engl J Med* 368, 107–116.

Jorm, A.F. (1986). Effects of cholinergic enhancement therapies on memory function in Alzheimer's disease: a meta-analysis of the literature. *Aust N Z J Psychiatry* 20, 237–240.

Jung, S., Aliberti, J., Graemmel, P., Sunshine, M.J., Kreutzberg, G.W., Sher, A., and Littman, D.R. (2000). Analysis of fractalkine receptor CX(3)CR1 function by targeted deletion and green fluorescent protein reporter gene insertion. *Mol. Cell. Biol.* 20, 4106–4114.

Kachroo, A., and Robin, G.P. (2013). Systemic signaling during plant defense. *Curr. Opin. Plant Biol.* 16, 527–533.

Kaikkonen, M.U., Spann, N.J., Heinz, S., Romanoski, C.E., Allison, K.A., Stender, J.D., Chun, H.B., Tough, D.F., Prinjha, R.K., Benner, C., et al. (2013). Remodeling of the enhancer landscape during macrophage activation is coupled to enhancer transcription. *Mol. Cell* 51, 310–325.

Kamer, A.R., Craig, R.G., Dasanayake, A.P., Brys, M., Glodzik-Sobanska, L., and de Leon, M.J. (2008). Inflammation and Alzheimer's disease: possible role of periodontal diseases. *Alzheimers Dement* 4, 242–250.

Kang, J., and Müller-Hill, B. (1990). Differential splicing of Alzheimer's disease amyloid A4 precursor RNA in rat tissues: PreA4(695) mRNA is predominantly produced in rat and human brain. *Biochemical and Biophysical Research Communications* 166, 1192–1200.

Kang, J., Lemaire, H.G., Unterbeck, A., Salbaum, J.M., Masters, C.L., Grzeschik, K.H., Multhaup, G., Beyreuther, K., and Müller-Hill, B. (1987). The precursor of Alzheimer's disease amyloid A4 protein resembles a cell-surface receptor. *Nature* 325, 733–736.

Kannan, V., Brouwer, N., Hanisch, U.-K., Regen, T., Eggen, B.J.L., and Boddeke, H.W.G.M. (2013). Histone deacetylase inhibitors suppress immune activation in primary mouse microglia. *J. Neurosci. Res.* 91, 1133–1142.

- Katzman, R. (1976). The Prevalence and Malignancy of Alzheimer Disease: A Major Killer. *Arch Neurol* *33*, 217–218.
- Kawabe, K., Takano, K., Moriyama, M., and Nakamura, Y. (2018). Microglia Endocytose Amyloid β Through the Binding of Transglutaminase 2 and Milk Fat Globule EGF Factor 8 Protein. *Neurochem. Res.* *43*, 32–40.
- Kent, S., Bluthé, R.-M., Kelley, K.W., and Dantzer, R. (1992). Sickness behavior as a new target for drug development. *Trends Pharmacol. Sci.* *13*, 24–28.
- Keren-Shaul, H., Spinrad, A., Weiner, A., Matcovitch-Natan, O., Dvir-Szternfeld, R., Ulland, T.K., David, E., Baruch, K., Lara-Astaiso, D., Toth, B., et al. (2017). A Unique Microglia Type Associated with Restricting Development of Alzheimer's Disease. *Cell* *169*, 1276–1290.e17.
- Kettenmann, H., Kirchhoff, F., and Verkhratsky, A. (2013). Microglia: new roles for the synaptic stripper. *Neuron* *77*, 10–18.
- Khoury, El, J.B., Moore, K.J., Means, T.K., Leung, J., Terada, K., Toft, M., Freeman, M.W., and Luster, A.D. (2003). CD36 Mediates the Innate Host Response to β -Amyloid. *J Exp Med* *197*, 1657–1666.
- Khoury, El, J., Toft, M., Hickman, S.E., Means, T.K., Terada, K., Geula, C., and Luster, A.D. (2007). *Ccr2* deficiency impairs microglial accumulation and accelerates progression of Alzheimer-like disease. *Nat Med* *13*, 432–438.
- Kim, J., Basak, J.M., and Holtzman, D.M. (2009). The role of apolipoprotein E in Alzheimer's disease. *Neuron* *63*, 287–303.
- Kleinnijenhuis, J., Quintin, J., Preijers, F., Joosten, L.A.B., Ifrim, D.C., Saeed, S., Jacobs, C., van Loenhout, J., de Jong, D., Stunnenberg, H.G., et al. (2012). Bacille Calmette-Guerin induces NOD2-dependent nonspecific protection from reinfection via epigenetic reprogramming of monocytes. *Proc. Natl. Acad. Sci. U.S.A.* *109*, 17537–17542.
- Konsman, J.P., Parnet, P., and Dantzer, R. (2002). Cytokine-induced sickness behaviour: mechanisms and implications. *Trends Neurosci.* *25*, 154–159.
- Kosik, K.S., Joachim, C.L., and Selkoe, D.J. (1986). Microtubule-associated protein tau (τ) is a major antigenic component of paired helical filaments in Alzheimer disease. *Proceedings of the National Academy of Sciences* *83*, 4044–4048.
- Koso, H., Tshako, A., Lai, C.-Y., Baba, Y., Otsu, M., Ueno, K., Nagasaki, M., Suzuki, Y., and Watanabe, S. (2016). Conditional rod photoreceptor ablation reveals *Sall1* as a microglial marker and regulator of microglial morphology in the retina. *Glia* *64*, 2005–2024.
- Krabbe, G., Halle, A., Matyash, V., Rinnenthal, J.L., Eom, G.D., Bernhardt, U., Miller, K.R., Prokop, S., Kettenmann, H., and Heppner, F.L. (2013). Functional Impairment of Microglia Coincides with Beta-Amyloid Deposition in Mice with Alzheimer-Like Pathology. *PLoS ONE* *8*, e60921.
- Kraepelin, E. (1910). *Das senile und präsenile Irresein (Psychiatrie: Ein Lehrbuch für Studierende und Ärzte)*.
- Krahenbuhl, J.L., Sharma, S.D., Ferraresi, R.W., and Remington, J.S. (1981). Effects of muramyl dipeptide treatment on resistance to infection with *Toxoplasma gondii* in mice. *Infect. Immun.* *31*, 716–722.
- Krych-Goldberg, M., and Atkinson, J.P. (2001). Structure-function relationships of complement receptor type 1. *Immunol. Rev.* *180*, 112–122.

- Kurtz, J., and Franz, K. (2003). Innate defence: evidence for memory in invertebrate immunity. *Nature* *425*, 37–38.
- Kyrkanides, S., Tallents, R.H., Miller, J.-N.H., Olschowka, M.E., Johnson, R., Yang, M., Olschowka, J.A., Brouxhon, S.M., and O'Banion, M.K. (2011). Osteoarthritis accelerates and exacerbates Alzheimer's disease pathology in mice. *Journal of Neuroinflammation* *8*, 112.
- Lambert, J.-C., Grenier-Boley, B., Chouraki, V., Heath, S., Zelenika, D., Fiévet, N., Hannequin, D., Pasquier, F., Hanon, O., Brice, A., et al. (2010). Implication of the immune system in Alzheimer's disease: evidence from genome-wide pathway analysis. *J. Alzheimers Dis.* *20*, 1107–1118.
- Lambert, J.-C., Heath, S., Even, G., Campion, D., Sleegers, K., Hiltunen, M., Combarros, O., Zelenika, D., Bullido, M.J., Tavernier, B., et al. (2009). Genome-wide association study identifies variants at *CLU* and *CR1* associated with Alzheimer's disease. *Nat Genet* *41*, 1094–1099.
- Lambert, J.-C., Ibrahim-Verbaas, C.A., Harold, D., Naj, A.C., Sims, R., Bellenguez, C., Jun, G., DeStefano, A.L., Bis, J.C., Beecham, G.W., et al. (2013). Meta-analysis of 74,046 individuals identifies 11 new susceptibility loci for Alzheimer's disease. *Nat Genet* *45*, 1452–1458.
- Larsson, A., Malmström, S., and Westermark, P. (2011). Signs of cross-seeding: aortic medin amyloid as a trigger for protein AA deposition. *Amyloid* *18*, 229–234.
- Lavin, Y., Winter, D., Blecher-Gonen, R., David, E., Keren-Shaul, H., Merad, M., Jung, S., and Amit, I. (2014). Tissue-Resident Macrophage Enhancer Landscapes Are Shaped by the Local Microenvironment. *Cell* *159*, 1312–1326.
- Lawson, L.J., Perry, V.H., and Gordon, S. (1992). Turnover of resident microglia in the normal adult mouse brain. *Neuroscience* *48*, 405–415.
- Lawson, L.J., Perry, V.H., Dri, P., and Gordon, S. (1990). Heterogeneity in the distribution and morphology of microglia in the normal adult mouse brain. *Neuroscience* *39*, 151–170.
- Lee, J., Chan, S.L., and Mattson, M.P. (2002). Adverse effect of a presenilin-1 mutation in microglia results in enhanced nitric oxide and inflammatory cytokine responses to immune challenge in the brain. *Neuromolecular Med.* *2*, 29–45.
- Lefrère, J.J., Mariotti, M., Ferrer-Le-Coeur, F., Rouger, P., Noël, B., and Bosser, C. (1990). PCR testing in HIV-1 seronegative haemophilia. *Lancet* *336*, 1386.
- Leibson, C.L., Rocca, W.A., Hanson, V.A., Cha, R., Kokmen, E., O'Brien, P.C., and Palumbo, P.J. (1997). The risk of dementia among persons with diabetes mellitus: a population-based cohort study. *Ann. N. Y. Acad. Sci.* *826*, 422–427.
- Li, E., Noda, M., Doi, Y., Parajuli, B., Kawanokuchi, J., Sonobe, Y., Takeuchi, H., Mizuno, T., and Suzumura, A. (2012). The neuroprotective effects of milk fat globule-EGF factor 8 against oligomeric amyloid β toxicity. *Journal of Neuroinflammation* *9*, 148.
- Liu, Y., Walter, S., Stagi, M., Cherny, D., Letiembre, M., Schulz-Schaeffer, W., Heine, H., Penke, B., Neumann, H., and Fassbender, K. (2005). LPS receptor (CD14): a receptor for phagocytosis of Alzheimer's amyloid peptide. *Brain* *128*, 1778–1789.
- Lucin, K.M., and Wyss-Coray, T. (2009). Immune activation in brain aging and neurodegeneration: too much or too little? *Neuron* *64*, 110–122.
- Ma, Q., Ineichen, B.V., Detmar, M., and Proulx, S.T. (2017). Outflow of cerebrospinal fluid is predominantly through lymphatic vessels and is reduced in aged mice. *Nature Communications* *8*, 1434.

- Mahley, R.W. (1988). Apolipoprotein E: cholesterol transport protein with expanding role in cell biology. *Science* *240*, 622–630.
- Mandrekar, S., Jiang, Q., Lee, C.Y.D., Koenigsknecht-Talboo, J., Holtzman, D.M., and Landreth, G.E. (2009). Microglia Mediate the Clearance of Soluble A β through Fluid Phase Macropinocytosis. *Journal of Neuroscience* *29*, 4252–4262.
- Masters, C.L., Multhaup, G., Simms, G., Pottgiesser, J., Martins, R.N., and Beyreuther, K. (1985a). Neuronal origin of a cerebral amyloid: neurofibrillary tangles of Alzheimer's disease contain the same protein as the amyloid of plaque cores and blood vessels. *Embo J.* *4*, 2757–2763.
- Masters, C.L., Simms, G., Weinman, N.A., Multhaup, G., McDonald, B.L., and Beyreuther, K. (1985b). Amyloid plaque core protein in Alzheimer disease and Down syndrome. *Proceedings of the National Academy of Sciences* *82*, 4245–4249.
- Maurer, K., Volk, S., and Gerbaldo, H. (1997). Auguste D and Alzheimer's disease.
- Mawuenyega, K.G., Sigurdson, W., Ovod, V., Munsell, L., Kasten, T., Morris, J.C., Yarasheski, K.E., and Bateman, R.J. (2010). Decreased clearance of CNS beta-amyloid in Alzheimer's disease. *Science* *330*, 1774–1774.
- Mazaheri, F., Snaidero, N., Kleinberger, G., Madore, C., Daria, A., Werner, G., Krasemann, S., Capell, A., Trümbach, D., Wurst, W., et al. (2017). TREM2 deficiency impairs chemotaxis and microglial responses to neuronal injury. *EMBO Rep* *18*, 1186–1198.
- McGleenon, B.M., Dynan, K.B., and Passmore, A.P. (1999). Acetylcholinesterase inhibitors in Alzheimer's disease. *Br J Clin Pharmacol* *48*, 471–480.
- Medvedev, A.E., Kopydlowski, K.M., and Vogel, S.N. (2000). Inhibition of lipopolysaccharide-induced signal transduction in endotoxin-tolerized mouse macrophages: dysregulation of cytokine, chemokine, and toll-like receptor 2 and 4 gene expression. *The Journal of Immunology* *164*, 5564–5574.
- Mehta, N.N., McGillicuddy, F.C., Anderson, P.D., Hinkle, C.C., Shah, R., Pruscino, L., Tabita-Martinez, J., Sellers, K.F., Rickels, M.R., and Reilly, M.P. (2010). Experimental endotoxemia induces adipose inflammation and insulin resistance in humans. *Diabetes* *59*, 172–181.
- Melchior, B., Garcia, A.E., Hsiung, B.-K., Lo, K.M., Doose, J.M., Thrash, J.C., Stalder, A.K., Staufienbiel, M., Neumann, H., and Carson, M.J. (2010). Dual induction of TREM2 and tolerance-related transcript, *Tmem176b*, in amyloid transgenic mice: implications for vaccine-based therapies for Alzheimer's disease. *ASN Neuro* *2*, e00037.
- Meyer-Luehmann, M., and Prinz, M. (2015). Myeloid cells in Alzheimer's disease: culprits, victims or innocent bystanders? *Trends Neurosci.* *38*, 659–668.
- Mildner, A., Mack, M., Schmidt, H., Brück, W., Djukic, M., Zabel, M.D., Hille, A., Priller, J., and Prinz, M. (2009). CCR2+Ly-6Chi monocytes are crucial for the effector phase of autoimmunity in the central nervous system. *Brain* *132*, 2487–2500.
- Mildner, A., Schlevogt, B., Kierdorf, K., Böttcher, C., Erny, D., Kummer, M.P., Quinn, M., Brück, W., Bechmann, I., Heneka, M.T., et al. (2011). Distinct and Non-Redundant Roles of Microglia and Myeloid Subsets in Mouse Models of Alzheimer's Disease. *Journal of Neuroscience* *31*, 11159–11171.
- Mildner, A., Schmidt, H., Nitsche, M., Merkler, D., Hanisch, U.-K., Mack, M., Heikenwalder, M., Brück, W., Priller, J., and Prinz, M. (2007). Microglia in the adult brain arise from Ly-6ChiCCR2+ monocytes only under defined host conditions. *Nature Neuroscience* *10*, 1544–1553.

- Mills, E.L., Kelly, B., Logan, A., Costa, A.S.H., Varma, M., Bryant, C.E., Tourlomousis, P., Däbritz, J.H.M., Gottlieb, E., Latorre, I., et al. (2016). Succinate Dehydrogenase Supports Metabolic Repurposing of Mitochondria to Drive Inflammatory Macrophages. *Cell* *167*, 457–470.e13.
- Miners, J.S., Baig, S., Palmer, J., Palmer, L.E., Kehoe, P.G., and Love, S. (2008). Abeta-degrading enzymes in Alzheimer's disease. *Brain Pathol.* *18*, 240–252.
- Minogue, A.M., Jones, R.S., Kelly, R.J., McDonald, C.L., Connor, T.J., and Lynch, M.A. (2014). Age-associated dysregulation of microglial activation is coupled with enhanced blood-brain barrier permeability and pathology in APP/PS1 mice. *Neurobiology of Aging* *35*, 1442–1452.
- Mogi, M., Harada, M., Kondo, T., Riederer, P., Inagaki, H., Minami, M., and Nagatsu, T. (1994). Interleukin-1 beta, interleukin-6, epidermal growth factor and transforming growth factor-alpha are elevated in the brain from parkinsonian patients. *Neurosci. Lett.* *180*, 147–150.
- Morimoto, K., Horio, J., Satoh, H., Sue, L., Beach, T., Arita, S., Tooyama, I., and Konishi, Y. (2011). Expression profiles of cytokines in the brains of Alzheimer's disease (AD) patients compared to the brains of non-demented patients with and without increasing AD pathology. *J. Alzheimers Dis.* *25*, 59–76.
- Mullan, M., Crawford, F., Axelman, K., Houlden, H., Lilius, L., Winblad, B., and Lannfelt, L. (1992). A pathogenic mutation for probable Alzheimer's disease in the APP gene at the N-terminus of beta-amyloid. *Nat Genet* *1*, 345–347.
- Muñoz, N., Van Maele, L., Marqués, J.M., Rial, A., Sirard, J.-C., and Chabalgoity, J.A. (2010). Mucosal administration of flagellin protects mice from *Streptococcus pneumoniae* lung infection. *Infect. Immun.* *78*, 4226–4233.
- Naert, G., and Rivest, S. (2011). CC chemokine receptor 2 deficiency aggravates cognitive impairments and amyloid pathology in a transgenic mouse model of Alzheimer's disease. *J. Neurosci.* *31*, 6208–6220.
- Naert, G., and Rivest, S. (2013). A deficiency in CCR2+ monocytes: the hidden side of Alzheimer's disease. *J Mol Cell Biol* *5*, 284–293.
- Naik, S., Larsen, S.B., Gomez, N.C., Alaverdyan, K., Sendoel, A., Yuan, S., Polak, L., Kulukian, A., Chai, S., and Fuchs, E. (2017). Inflammatory memory sensitizes skin epithelial stem cells to tissue damage. *Nature* *550*, 475–480.
- Naj, A.C., Jun, G., Beecham, G.W., Wang, L.-S., Vardarajan, B.N., Buross, J., Gallins, P.J., Buxbaum, J.D., Jarvik, G.P., Crane, P.K., et al. (2011). Common variants at MS4A4/MS4A6E, CD2AP, CD33 and EPHA1 are associated with late-onset Alzheimer's disease. *Nat Genet* *43*, 436–441.
- Netea, M.G., Joosten, L.A.B., Latz, E., Mills, K.H.G., Natoli, G., Stunnenberg, H.G., O'Neill, L.A.J., and Xavier, R.J. (2016). Trained immunity: A program of innate immune memory in health and disease. *Science* *352*, aaf1098–aaf1098.
- Netea, M.G., Quintin, J., and van der Meer, J.W.M. (2011). Trained immunity: a memory for innate host defense. *Cell Host Microbe* *9*, 355–361.
- Norden, D.M., and Godbout, J.P. (2013). Review: Microglia of the aged brain: primed to be activated and resistant to regulation. *Neuropathol Appl Neurobiol* *39*, 19–34.
- Obermeier, B., Daneman, R., and Ransohoff, R.M. (2013). Development, maintenance and disruption of the blood-brain barrier. *Nat Med* *19*, 1584–1596.
- Oshima, K., Aoki, N., Kato, T., Kitajima, K., and MATSUDA, T. (2002). Secretion of a peripheral membrane protein, MFG-E8, as a complex with membrane vesicles. *Eur J Biochem* *269*, 1209–1218.

- Ostuni, R., Piccolo, V., Barozzi, I., Polletti, S., Termanini, A., Bonifacio, S., Curina, A., Prosperini, E., Ghisletti, S., and Natoli, G. (2013). Latent enhancers activated by stimulation in differentiated cells. *Cell* *152*, 157–171.
- Otero, K., Shinohara, M., Zhao, H., Cella, M., Gilfillan, S., Colucci, A., Faccio, R., Ross, F.P., Teitelbaum, S.L., Takayanagi, H., et al. (2012). TREM2 and β -catenin regulate bone homeostasis by controlling the rate of osteoclastogenesis. *J. Immunol.* *188*, 2612–2621.
- Paloneva, J., Mandelin, J., Kiialainen, A., Bohling, T., Prudlo, J., Hakola, P., Haltia, M., Kontinen, Y.T., and Peltonen, L. (2003). DAP12/TREM2 deficiency results in impaired osteoclast differentiation and osteoporotic features. *J Exp Med* *198*, 669–675.
- Paolicelli, R.C., Bolasco, G., Pagani, F., Maggi, L., Scianni, M., Panzanelli, P., Giustetto, M., Ferreira, T.A., Guiducci, E., Dumas, L., et al. (2011). Synaptic pruning by microglia is necessary for normal brain development. *Science* *333*, 1456–1458.
- Paresce, D.M., Ghosh, R.N., and Maxfield, F.R. (1996). Microglial cells internalize aggregates of the Alzheimer's disease amyloid beta-protein via a scavenger receptor. *Neuron* *17*, 553–565.
- Parkhurst, C.N., Yang, G., Ninan, I., Savas, J.N., Yates, J.R., Lafaille, J.J., Hempstead, B.L., Littman, D.R., and Gan, W.-B. (2013). Microglia promote learning-dependent synapse formation through brain-derived neurotrophic factor. *Cell* *155*, 1596–1609.
- Passlick, B., Flieger, D., and Ziegler-Heitbrock, H.W. (1989). Identification and characterization of a novel monocyte subpopulation in human peripheral blood. *Blood* *74*, 2527–2534.
- Patel, A.A., Zhang, Y., Fullerton, J.N., Boelen, L., Rongvaux, A., Maini, A.A., Bigley, V., Flavell, R.A., Gilroy, D.W., Asquith, B., et al. (2017). The fate and lifespan of human monocyte subsets in steady state and systemic inflammation. *Journal of Experimental Medicine* *214*, 1913–1923.
- Patel, S., and Player, M.R. (2009). Colony-stimulating factor-1 receptor inhibitors for the treatment of cancer and inflammatory disease. *Curr Top Med Chem* *9*, 599–610.
- Pedersen, N.L., Gatz, M., Berg, S., and Johansson, B. (2004). How heritable is Alzheimer's disease late in life? Findings from Swedish twins. *Ann. Neurol.* *55*, 180–185.
- Peng, Q., Malhotra, S., Torchia, J.A., Kerr, W.G., Coggeshall, K.M., and Humphrey, M.B. (2010). TREM2- and DAP12-dependent activation of PI3K requires DAP10 and is inhibited by SHIP1. *Sci Signal* *3*, ra38.
- Perry, V.H., and Holmes, C. (2014). Microglial priming in neurodegenerative disease. *Nat Rev Neurol* *10*, 217–224.
- Perry, V.H., Cunningham, C., and Boche, D. (2002). Atypical inflammation in the central nervous system in prion disease. *Curr. Opin. Neurol.* *15*, 349–354.
- Perry, V.H., Cunningham, C., and Holmes, C. (2007). Systemic infections and inflammation affect chronic neurodegeneration. *Nat. Rev. Immunol.* *7*, 161–167.
- Pimentel-Coelho, P.M., and Rivest, S. (2012). The early contribution of cerebrovascular factors to the pathogenesis of Alzheimer's disease. *Eur. J. Neurosci.* *35*, 1917–1937.
- Prince, M., Wimo, A., Guerchet, M., Ali, G.-C., Wu, Y.-T., and Prina, M. (2015). World Alzheimer Report 2015, The Global Impact of Dementia: An analysis of prevalence, incidence, cost and trends. 1–87.
- Prinz, M., and Priller, J. (2014). Microglia and brain macrophages in the molecular age: from origin to neuropsychiatric disease. *Nat Rev Neurosci* *15*, 300–312.

Prokop, S., Miller, K.R., Drost, N., Handrick, S., Mathur, V., Luo, J., Wegner, A., Wyss-Coray, T., and Heppner, F.L. (2015). Impact of peripheral myeloid cells on amyloid- β pathology in Alzheimer's disease-like mice. *J Exp Med* 212, jem.20150479–jem.20151818.

Rada-Iglesias, A., Bajpai, R., Swigut, T., Brugmann, S.A., Flynn, R.A., and Wysocka, J. (2011). A unique chromatin signature uncovers early developmental enhancers in humans. *Nature* 470, 279–283.

Radde, R., Bolmont, T., Kaeser, S.A., Coomaraswamy, J., Lindau, D., Stoltze, L., Calhoun, M.E., Jäggi, F., Wolburg, H., Gengler, S., et al. (2006). A β 42-driven cerebral amyloidosis in transgenic mice reveals early and robust pathology. *EMBO Rep* 7, 940–946.

Rademakers, R., Baker, M., Nicholson, A.M., Rutherford, N.J., Finch, N., Soto-Ortolaza, A., Lash, J., Wider, C., Wojtas, A., DeJesus-Hernandez, M., et al. (2011). Mutations in the colony stimulating factor 1 receptor (CSF1R) gene cause hereditary diffuse leukoencephalopathy with spheroids. *Nat Genet* 44, 200–205.

Raj, D.D.A., Jaarsma, D., Holtman, I.R., Olah, M., Ferreira, F.M., Schaafsma, W., Brouwer, N., Meijer, M.M., de Waard, M.C., van der Pluijm, I., et al. (2014). Priming of microglia in a DNA-repair deficient model of accelerated aging. *Neurobiology of Aging* 35, 2147–2160.

Ramirez-Carrozzi, V.R., Braas, D., Bhatt, D.M., Cheng, C.S., Hong, C., Doty, K.R., Black, J.C., Hoffmann, A., Carey, M., and Smale, S.T. (2009). A Unifying Model for the Selective Regulation of Inducible Transcription by CpG Islands and Nucleosome Remodeling. *Cell* 138, 114–128.

Ramirez-Carrozzi, V.R., Nazarian, A.A., Li, C.C., Gore, S.L., Sridharan, R., Imbalzano, A.N., and Smale, S.T. (2006). Selective and antagonistic functions of SWI/SNF and Mi-2 β nucleosome remodeling complexes during an inflammatory response. *Genes Dev.* 20, 282–296.

Ransohoff, R.M., and Khoury, El, J. (2015). Microglia in Health and Disease. *Cold Spring Harb Perspect Biol* 8, a020560.

Ransohoff, R.M., and Perry, V.H. (2009). Microglial physiology: unique stimuli, specialized responses. *Annu. Rev. Immunol.* 27, 119–145.

Reed-Geaghan, E.G., Savage, J.C., Hise, A.G., and Landreth, G.E. (2009). CD14 and toll-like receptors 2 and 4 are required for fibrillar A β -stimulated microglial activation. *J. Neurosci.* 29, 11982–11992.

Research, A.R.J.O.N., 1995 Alzheimer's disease as a model of molecular gerontology.

Rezaie, P., and Hanisch, U.-K. (2014). Historical Context. In *Autoimmune Disease and Impaired Uptake of Apoptotic Cells in MFG-E8-Deficient Mice*, (New York, NY: Springer, New York, NY), pp. 7–46.

Réu, P., Khosravi, A., Bernard, S., Mold, J.E., Salehpour, M., Alkass, K., Perl, S., Tisdale, J., Possnert, G., Druid, H., et al. (2017). The Lifespan and Turnover of Microglia in the Human Brain. *Cell Rep* 20, 779–784.

Richard, K., Pierce, S.K., and Song, W. (2008). The agonists of TLR4 and 9 are sufficient to activate memory B cells to differentiate into plasma cells in vitro but not in vivo. *J. Immunol.* 181, 1746–1752.

Rivest, S. (2009). Regulation of innate immune responses in the brain. *Nat. Rev. Immunol.* 9, 429–439.

Robakis, N.K., Ramakrishna, N., Wolfe, G., and Wisniewski, H.M. (1987). Molecular cloning and characterization of a cDNA encoding the cerebrovascular and the neuritic plaque amyloid peptides. *Proceedings of the National Academy of Sciences* 84, 4190–4194.

Rogers, J., Li, R., Mastroeni, D., Grover, A., Leonard, B., Ahern, G., Cao, P., Kolody, H., Vedders, L., Kolb, W.P., et al. (2006). Peripheral clearance of amyloid beta peptide by complement C3-dependent adherence to erythrocytes. *Neurobiology of Aging* 27, 1733–1739.

Rohan de Silva, H.A., Jen, A., Wickenden, C., Jen, L.S., Wilkinson, S.L., and Patel, A.J. (1997). Cell-specific expression of beta-amyloid precursor protein isoform mRNAs and proteins in neurons and astrocytes. *Brain Res. Mol. Brain Res.* 47, 147–156.

Rojas-Gutierrez, E., Muñoz-Arenas, G., Treviño, S., Espinosa, B., Chavez, R., Rojas, K., Flores, G., Díaz, A., and Guevara, J. (2017). Alzheimer's disease and metabolic syndrome: A link from oxidative stress and inflammation to neurodegeneration. *Synapse* 71, e21990.

Roth, M., Tomlinson, B.E., and Blessed, G. (1966). Correlation between scores for dementia and counts of “senile plaques” in cerebral grey matter of elderly subjects. *Nature* 209, 109–110.

Saederup, N., Cardona, A.E., Croft, K., Mizutani, M., Cotleur, A.C., Tsou, C.-L., Ransohoff, R.M., and Charo, I.F. (2010). Selective Chemokine Receptor Usage by Central Nervous System Myeloid Cells in CCR2-Red Fluorescent Protein Knock-In Mice. *PLoS ONE* 5, e13693.

Saeed, S., Quintin, J., Kerstens, H.H.D., Rao, N.A., Aghajani-refah, A., Matarese, F., Cheng, S.-C., Ratter, J., Berentsen, K., van der Ent, M.A., et al. (2014). Epigenetic programming of monocyte-to-macrophage differentiation and trained innate immunity. *Science* 345, 1251086–1251086.

Saido, T., and Leissring, M.A. (2012). Proteolytic degradation of amyloid β -protein. *Cold Spring Harbor Perspectives in Medicine* 2, a006379–a006379.

Sastre, M., Dewachter, I., Landreth, G.E., Willson, T.M., Klockgether, T., van Leuven, F., and Heneka, M.T. (2003). Nonsteroidal anti-inflammatory drugs and peroxisome proliferator-activated receptor-gamma agonists modulate immunostimulated processing of amyloid precursor protein through regulation of beta-secretase. *J. Neurosci.* 23, 9796–9804.

Sato, S., Sanjo, H., Takeda, K., Ninomiya-Tsuji, J., Yamamoto, M., Kawai, T., Matsumoto, K., Takeuchi, O., and Akira, S. (2005). Essential function for the kinase TAK1 in innate and adaptive immune responses. *Nat. Immunol.* 6, 1087–1095.

Saunders, A.M., Strittmatter, W.J., Schmechel, D., George-Hyslop, P.H., Pericak-Vance, M.A., Joo, S.H., Rosi, B.L., Gusella, J.F., Crapper-MacLachlan, D.R., and Alberts, M.J. (1993). Association of apolipoprotein E allele epsilon 4 with late-onset familial and sporadic Alzheimer's disease. *Neurology* 43, 1467–1472.

Schafer, D.P., Lehrman, E.K., Kautzman, A.G., Koyama, R., Mardinly, A.R., Yamasaki, R., Ransohoff, R.M., Greenberg, M.E., Barres, B.A., and Stevens, B. (2012). Microglia sculpt postnatal neural circuits in an activity and complement-dependent manner. *Neuron* 74, 691–705.

Selkoe, D.J. (1991). The molecular pathology of Alzheimer's disease. *Neuron* 6, 487–498.

Selkoe, D.J. (2001). Alzheimer's disease: genes, proteins, and therapy. *Physiol. Rev.* 81, 741–766.

Selkoe, D.J., Abraham, C.R., Podlisny, M.B., and Duffy, L.K. (1986). Isolation of low-molecular-weight proteins from amyloid plaque fibers in Alzheimer's disease. *J Neurochem* 46, 1820–1834.

Selkoe, D.J., Podlisny, M.B., Joachim, C.L., Vickers, E.A., Lee, G., Fritz, L.C., and Oltersdorf, T. (1988). Beta-amyloid precursor protein of Alzheimer disease occurs as 110- to 135-kilodalton membrane-associated proteins in neural and nonneural tissues. *Proceedings of the National Academy of Sciences* 85, 7341–7345.

Seubert, P., Oltersdorf, T., Lee, M.G., Barbour, R., Blomquist, C., Davis, D.L., Bryant, K., Fritz, L.C., Galasko, D., and Thal, L.J. (1993). Secretion of beta-amyloid precursor protein cleaved at the amino terminus of the beta-amyloid peptide. *Nature* 361, 260–263.

- Shakespeare, M.R., Halili, M.A., Irvine, K.M., Fairlie, D.P., and Sweet, M.J. (2011). Histone deacetylases as regulators of inflammation and immunity. *Trends in Immunology* *32*, 335–343.
- Shen, J., and Kelleher, R.J. (2007). The presenilin hypothesis of Alzheimer's disease: evidence for a loss-of-function pathogenic mechanism. *Proceedings of the National Academy of Sciences* *104*, 403–409.
- Sherrington, R., Rogaev, E.I., Liang, Y., Rogaeva, E.A., Levesque, G., Ikeda, M., Chi, H., Lin, C., Li, G., Holman, K., et al. (1995). Cloning of a gene bearing missense mutations in early-onset familial Alzheimer's disease. *Nature* *375*, 754–760.
- Shibata, M., Yamada, S., Kumar, S.R., Calero, M., Bading, J., Frangione, B., Holtzman, D.M., Miller, C.A., Strickland, D.K., Ghiso, J., et al. (2000). Clearance of Alzheimer's amyloid- β 1-40 peptide from brain by LDL receptor-related protein-1 at the blood-brain barrier. *J. Clin. Invest.* *106*, 1489–1499.
- Silverberg, G.D., Mayo, M., Saul, T., Rubenstein, E., and McGuire, D. (2003). Alzheimer's disease, normal-pressure hydrocephalus, and senescent changes in CSF circulatory physiology: a hypothesis. *The Lancet Neurology* *2*, 506–511.
- Silvestre, J.-S., Théry, C., Hamard, G., Boddaert, J., Aguilar, B., Delcayre, A., Houbron, C., Tamarat, R., Blanc-Brude, O., Heeneman, S., et al. (2005). Lactadherin promotes VEGF-dependent neovascularization. *Nat Med* *11*, 499–506.
- Simard, A.R., Soulet, D., Gowing, G., Julien, J.-P., and Rivest, S. (2006). Bone marrow-derived microglia play a critical role in restricting senile plaque formation in Alzheimer's disease. *Neuron* *49*, 489–502.
- Sly, L.M., Krzesicki, R.F., Brashler, J.R., Buhl, A.E., McKinley, D.D., Carter, D.B., and Chin, J.E. (2001). Endogenous brain cytokine mRNA and inflammatory responses to lipopolysaccharide are elevated in the Tg2576 transgenic mouse model of Alzheimer's disease. *Brain Res. Bull.* *56*, 581–588.
- Smale, S.T., and Natoli, G. (2014). Transcriptional Control of Inflammatory Responses. *Cold Spring Harb Perspect Biol* *6*, a016261–a016261.
- Smale, S.T., Tarakhovsky, A., and Natoli, G. (2014). Chromatin contributions to the regulation of innate immunity. *Annu. Rev. Immunol.* *32*, 489–511.
- Smits, H.A., Rijmsmus, A., van Loon, J.H., Wat, J.W.Y., Verhoef, J., Boven, L.A., and Nottet, H.S.L.M. (2002). Amyloid- β -induced chemokine production in primary human macrophages and astrocytes. *Journal of Neuroimmunology* *127*, 160–168.
- Song, W., Hooli, B., Mullin, K., Jin, S.C., Cella, M., Ulland, T.K., Wang, Y., Tanzi, R.E., and Colonna, M. (2017). Alzheimer's disease-associated TREM2 variants exhibit either decreased or increased ligand-dependent activation. *Alzheimers Dement* *13*, 381–387.
- Spangenberg, E.E., Lee, R.J., Najafi, A.R., Rice, R.A., Elmore, M.R.P., Blurton-Jones, M., West, B.L., and Green, K.N. (2016). Eliminating microglia in Alzheimer's mice prevents neuronal loss without modulating amyloid- β pathology. *Brain* *139*, 1265–1281.
- Sparks Stein, P., Steffen, M.J., Smith, C., Jicha, G., Ebersole, J.L., Abner, E., and Dawson, D. (2012). Serum antibodies to periodontal pathogens are a risk factor for Alzheimer's disease. *Alzheimers Dement* *8*, 196–203.
- Spittau, B., Rilka, J., Steinfath, E., Zöller, T., and Kriegelstein, K. (2014). TGF β 1 increases microglia-mediated engulfment of apoptotic cells via upregulation of the milk fat globule-EGF factor 8. *Glia* n/a–n/a.

Stalder, A.K., Ermini, F., Bondolfi, L., Krenger, W., Burbach, G.J., Deller, T., Coomaraswamy, J., Staufenbiel, M., Landmann, R., and Jucker, M. (2005). Invasion of hematopoietic cells into the brain of amyloid precursor protein transgenic mice. *J. Neurosci.* *25*, 11125–11132.

Stamatovic, S.M., Shakui, P., Keep, R.F., Moore, B.B., Kunkel, S.L., van Rooijen, N., and Andjelkovic, A.V. (2005). Monocyte Chemoattractant Protein-1 Regulation of Blood–Brain Barrier Permeability. *Journal of Cerebral Blood Flow & Metabolism* *25*, 593–606.

Stewart, C.R., Stuart, L.M., Wilkinson, K., van Gils, J.M., Deng, J., Halle, A., Rayner, K.J., Boyer, L., Zhong, R., Frazier, W.A., et al. (2010). CD36 ligands promote sterile inflammation through assembly of a Toll-like receptor 4 and 6 heterodimer. *Nature Publishing Group* *11*, 155–161.

Storck, S.E., Meister, S., Nahrath, J., Meißner, J.N., Schubert, N., Di Spiezio, A., Baches, S., Vandenbroucke, R.E., Bouter, Y., Prikulis, I., et al. (2016). Endothelial LRP1 transports amyloid- β 1–42 across the blood-brain barrier. *The Journal of Clinical Investigation* *126*, 123–136.

Stubbs, J.D., Lekutis, C., Singer, K.L., Bui, A., Yuzuki, D., Srinivasan, U., and Parry, G. (1990). cDNA cloning of a mouse mammary epithelial cell surface protein reveals the existence of epidermal growth factor-like domains linked to factor VIII-like sequences. *Proceedings of the National Academy of Sciences* *87*, 8417–8421.

Sturchler-Pierrat, C., Abramowski, D., Duke, M., Wiederhold, K.H., Mistl, C., Rothacher, S., Ledermann, B., Bürki, K., Frey, P., Paganetti, P.A., et al. (1997). Two amyloid precursor protein transgenic mouse models with Alzheimer disease-like pathology. *Proceedings of the National Academy of Sciences* *94*, 13287–13292.

Szaruga, M., Munteanu, B., Lismont, S., Veugelen, S., Horr , K., Mercken, M., Saido, T.C., Ryan, N.S., De Vos, T., Savvides, S.N., et al. (2017). Alzheimer's-Causing Mutations Shift A β Length by Destabilizing γ -Secretase-A β n Interactions. *Cell* *170*, 443–456.e14.

Tahara, K., Kim, H.-D., Jin, J.-J., Maxwell, J.A., Li, L., and Fukuchi, K.-I. (2006). Role of toll-like receptor signalling in A β uptake and clearance. *Brain* *129*, 3006–3019.

Takahashi, K., Rochford, C.D.P., and Neumann, H. (2005). Clearance of apoptotic neurons without inflammation by microglial triggering receptor expressed on myeloid cells-2. *J Exp Med* *201*, 647–657.

Takami, M., Nagashima, Y., Sano, Y., Ishihara, S., Morishima-Kawashima, M., Funamoto, S., and Ihara, Y. (2009). γ -Secretase: successive tripeptide and tetrapeptide release from the transmembrane domain of beta-carboxyl terminal fragment. *J. Neurosci.* *29*, 13042–13052.

Tannahill, G.M., Curtis, A.M., Adamik, J., Palsson-McDermott, E.M., McGettrick, A.F., Goel, G., Frezza, C., Bernard, N.J., Kelly, B., Foley, N.H., et al. (2013). Succinate is an inflammatory signal that induces IL-1 β through HIF-1 α . *Nature* *496*, 238–242.

Tanzi, R.E., Gusella, J.F., Watkins, P.C., Bruns, G.A., St George-Hyslop, P., Van Keuren, M.L., Patterson, D., Pagan, S., Kurnit, D.M., and Neve, R.L. (1987). Amyloid beta protein gene: cDNA, mRNA distribution, and genetic linkage near the Alzheimer locus. *Science* *235*, 880–884.

Tarasoff-Conway, J.M., Carare, R.O., Osorio, R.S., Glodzik, L., Butler, T., Fieremans, E., Axel, L., Rusinek, H., Nicholson, C., Zlokovic, B.V., et al. (2015). Clearance systems in the brain-implications for Alzheimer disease. *Nat Rev Neurol* *11*, 457–470.

Tay, T.L., Mai, D., Dautzenberg, J., Fern ndez-Klett, F., Lin, G., Sagar, Datta, M., Drougard, A., Stempf, T., Ardura-Fabregat, A., et al. (2017). A new fate mapping system reveals context-dependent random or clonal expansion of microglia. *Nature Neuroscience* *20*, 793–803.

Terawaki, H., Yokoyama, K., Yamada, Y., Maruyama, Y., Iida, R., Hanaoka, K., Yamamoto, H., Obata, T., and Hosoya, T. (2010). Low-grade endotoxemia contributes to chronic inflammation in

hemodialysis patients: examination with a novel lipopolysaccharide detection method. *Ther Apher Dial* 14, 477–482.

Town, T., Laouar, Y., Pittenger, C., Mori, T., Szekely, C.A., Tan, J., Duman, R.S., and Flavell, R.A. (2008). Blocking TGF-beta-Smad2/3 innate immune signaling mitigates Alzheimer-like pathology. *Nat Med* 14, 681–687.

Tremblay, M.-È., Lowery, R.L., and Majewska, A.K. (2010). Microglial interactions with synapses are modulated by visual experience. *PLoS Biol.* 8, e1000527.

Tribouley, J., Tribouley-Duret, J., and Appriou, M. (1978). [Effect of Bacillus Callmette Guerin (BCG) on the receptivity of nude mice to *Schistosoma mansoni*]. *C. R. Seances Soc. Biol. Fil.* 172, 902–904.

Turnbull, I.R., Gilfillan, S., Cella, M., Aoshi, T., Miller, M., Piccio, L., Hernandez, M., and Colonna, M. (2006). Cutting edge: TREM-2 attenuates macrophage activation. *The Journal of Immunology* 177, 3520–3524.

Ulland, T.K., Song, W.M., Huang, S.C.-C., Ulrich, J.D., Sergushichev, A., Beatty, W.L., Loboda, A.A., Zhou, Y., Cairns, N.J., Kambal, A., et al. (2017). TREM2 Maintains Microglial Metabolic Fitness in Alzheimer's Disease. *Cell* 170, 649–663.e13.

Ulrich, J.D., Finn, M.B., Wang, Y., Shen, A., Mahan, T.E., Jiang, H., Stewart, F.R., Piccio, L., Colonna, M., and Holtzman, D.M. (2014). Altered microglial response to A β plaques in APPPS1-21 mice heterozygous for TREM2. *Molecular Neurodegeneration* 9, 1–9.

Ulrich, J.D., Ulland, T.K., Colonna, M., and Holtzman, D.M. (2017). Elucidating the Role of TREM2 in Alzheimer's Disease. *Neuron* 94, 237–248.

van 't Wout, J.W., Poell, R., and van Furth, R. (1992). The role of BCG/PPD-activated macrophages in resistance against systemic candidiasis in mice. *Scand. J. Immunol.* 36, 713–719.

van Beek, J., Elward, K., and Gasque, P. (2003). Activation of complement in the central nervous system: roles in neurodegeneration and neuroprotection. *Ann. N. Y. Acad. Sci.* 992, 56–71.

van der Poll, T., and Opal, S.M. (2008). Host-pathogen interactions in sepsis. *Lancet Infect Dis* 8, 32–43.

van Marum, R.J. (2009). Update on the use of memantine in Alzheimer's disease. *Neuropsychiatr Dis Treat* 5, 237–247.

Varvel, N.H., Grathwohl, S.A., Baumann, F., Liebig, C., Bosch, A., Brawek, B., Thal, D.R., Charo, I.F., Heppner, F.L., Aguzzi, A., et al. (2012). Microglial repopulation model reveals a robust homeostatic process for replacing CNS myeloid cells. *Proceedings of the National Academy of Sciences* 109, 18150–18155.

Varvel, N.H., Grathwohl, S.A., Degenhardt, K., Resch, C., Bosch, A., Jucker, M., and Neher, J.J. (2015). Replacement of brain-resident myeloid cells does not alter cerebral amyloid- β deposition in mouse models of Alzheimer's disease. *J Exp Med* 212, 1803–1809.

Vergheze, P.B., Castellano, J.M., Garai, K., Wang, Y., Jiang, H., Shah, A., Bu, G., Frieden, C., and Holtzman, D.M. (2013). ApoE influences amyloid- β (A β) clearance despite minimal apoE/A β association in physiological conditions. *Proc. Natl. Acad. Sci. U.S.A.* 110, E1807–E1816.

Vukic, V., Callaghan, D., Walker, D., Lue, L.F., Liu, Q.Y., Couraud, P.-O., Romero, I.A., Weksler, B., Stanimirovic, D.B., and Zhang, W. (2009). Expression of inflammatory genes induced by beta-amyloid peptides in human brain endothelial cells and in Alzheimer's brain is mediated by the JNK-AP1 signaling pathway. *Neurobiology of Disease* 34, 95–106.

- Walker, D.G., Yasuhara, O., Patston, P.A., McGeer, E.G., and McGeer, P.L. (1995). Complement C1 inhibitor is produced by brain tissue and is cleaved in Alzheimer disease. *Brain Res.* *675*, 75–82.
- Walker, K.A., Hoogeveen, R.C., Folsom, A.R., Ballantyne, C.M., Knopman, D.S., Windham, B.G., Jack, C.R., and Gottesman, R.F. (2017). Midlife systemic inflammatory markers are associated with late-life brain volume: The ARIC study. *Neurology* *89*, 2262–2270.
- Walsh, D.T., Betmouni, S., and Perry, V.H. (2001). Absence of detectable IL-1beta production in murine prion disease: a model of chronic neurodegeneration. *J. Neuropathol. Exp. Neurol.* *60*, 173–182.
- Wang, C., Yu, J.-T., Miao, D., Wu, Z.-C., Tan, M.-S., and Tan, L. (2014). Targeting the mTOR signaling network for Alzheimer's disease therapy. *Mol Neurobiol* *49*, 120–135.
- Wang, P. (2014). MFG-E8 and Inflammation.
- Wang, Y., Cella, M., Mallinson, K., Ulrich, J.D., Young, K.L., Robinette, M.L., Gilfillan, S., Krishnan, G.M., Sudhakar, S., Zinselmeyer, B.H., et al. (2015). TREM2 lipid sensing sustains the microglial response in an Alzheimer's disease model. *Cell* *160*, 1061–1071.
- Wang, Y., Szretter, K.J., Vermi, W., Gilfillan, S., Rossini, C., Cella, M., Barrow, A.D., Diamond, M.S., and Colonna, M. (2012). IL-34 is a tissue-restricted ligand of CSF1R required for the development of Langerhans cells and microglia. *Nat. Immunol.* *13*, 753–760.
- Wang, Y., Ulland, T.K., Ulrich, J.D., Song, W., Tzaferis, J.A., Hole, J.T., Yuan, P., Mahan, T.E., Shi, Y., Gilfillan, S., et al. (2016). TREM2-mediated early microglial response limits diffusion and toxicity of amyloid plaques. *Journal of Experimental Medicine* *213*, 667–675.
- Weggen, S., and Beher, D. (2012). Molecular consequences of amyloid precursor protein and presenilin mutations causing autosomal-dominant Alzheimer's disease. *Alzheimers Res Ther* *4*, 9.
- Weidemann, A., König, G., Bunke, D., Fischer, P., Salbaum, J.M., Masters, C.L., and Beyreuther, K. (1989). Identification, biogenesis, and localization of precursors of Alzheimer's disease A4 amyloid protein. *Cell* *57*, 115–126.
- Weller, R.O., Subash, M., Preston, S.D., Mazanti, I., and Carare, R.O. (2008). Perivascular drainage of amyloid-beta peptides from the brain and its failure in cerebral amyloid angiopathy and Alzheimer's disease. *Brain Pathol.* *18*, 253–266.
- Wendeln, A.-C., Degenhardt, K., Kaurani, L., Gertig, M., Ulas, T., Jain, G., Wagner, J., Häslér, L.M., Wild, K., Skodras, A., et al. Innate immune memory in the brain shapes neurological disease hallmarks. accepted in *Nature* 23.02.2018.
- Wider, C., Van Gerpen, J.A., DeArmond, S., Shuster, E.A., Dickson, D.W., and Wszolek, Z.K. (2009). Leukoencephalopathy with spheroids (HDLS) and pigmentary leukodystrophy (POLD): a single entity? *Neurology* *72*, 1953–1959.
- Wieghofer, P., Knobeloch, K.-P., and Prinz, M. (2015). Genetic targeting of microglia. *Glia* *63*, 1–22.
- Wiesner, P., Choi, S.-H., Almazan, F., Benner, C., Huang, W., Diehl, C.J., Gonen, A., Butler, S., Witztum, J.L., Glass, C.K., et al. (2010). Low doses of lipopolysaccharide and minimally oxidized low-density lipoprotein cooperatively activate macrophages via nuclear factor kappa B and activator protein-1: possible mechanism for acceleration of atherosclerosis by subclinical endotoxemia. *Circulation Research* *107*, 56–65.
- Wimo, A., Guerchet, M., Ali, G.-C., Wu, Y.-T., Prina, A.M., Winblad, B., Jönsson, L., Liu, Z., and Prince, M. (2017). The worldwide costs of dementia 2015 and comparisons with 2010. *Alzheimers Dement* *13*, 1–7.

Wolfe, M.S., Xia, W., Ostaszewski, B.L., Diehl, T.S., Kimberly, W.T., and Selkoe, D.J. (1999). Two transmembrane aspartates in presenilin-1 required for presenilin endoproteolysis and gamma-secretase activity. *Nature* *398*, 513–517.

Wu, K., Byers, D.E., Jin, X., Agapov, E., Alexander-Brett, J., Patel, A.C., Cella, M., Gilfilan, S., Colonna, M., Kober, D.L., et al. (2015). TREM-2 promotes macrophage survival and lung disease after respiratory viral infection. *Journal of Experimental Medicine* *212*, 681–697.

Yamamoto, M., Kiyota, T., Horiba, M., Buescher, J.L., Walsh, S.M., Gendelman, H.E., and Ikezu, T. (2007). Interferon-gamma and tumor necrosis factor-alpha regulate amyloid-beta plaque deposition and beta-secretase expression in Swedish mutant APP transgenic mice. *The American Journal of Pathology* *170*, 680–692.

Ye, S.M., and Johnson, R.W. (1999). Increased interleukin-6 expression by microglia from brain of aged mice. *Journal of Neuroimmunology* *93*, 139–148.

Ye, S.M., and Johnson, R.W. (2001). An age-related decline in interleukin-10 may contribute to the increased expression of interleukin-6 in brain of aged mice. *Neuroimmunomodulation* *9*, 183–192.

Yona, S., Kim, K.-W., Wolf, Y., Mildner, A., Varol, D., Breker, M., Strauss-Ayali, D., Viukov, S., Guilliams, M., Misharin, A., et al. (2013). Fate mapping reveals origins and dynamics of monocytes and tissue macrophages under homeostasis. *Immunity* *38*, 79–91.

Yoshida, K., Maekawa, T., Zhu, Y., Renard-Guillet, C., Chatton, B., Inoue, K., Uchiyama, T., Ishibashi, K.-I., Yamada, T., Ohno, N., et al. (2015). The transcription factor ATF7 mediates lipopolysaccharide-induced epigenetic changes in macrophages involved in innate immunological memory. *Nature Publishing Group* *16*, 1034–1043.

Yuan, P., Condello, C., Keene, C.D., Wang, Y., Bird, T.D., Paul, S.M., Luo, W., Colonna, M., Baddeley, D., and Grutzendler, J. (2016). TREM2 Haplodeficiency in Mice and Humans Impairs the Microglia Barrier Function Leading to Decreased Amyloid Compaction and Severe Axonal Dystrophy. *Neuron* *90*, 724–739.

Zhang, B., Chassaing, B., Shi, Z., Uchiyama, R., Zhang, Z., Denning, T.L., Crawford, S.E., Puijssers, A.J., Iskarpatyoti, J.A., Estes, M.K., et al. (2014). Viral infection. Prevention and cure of rotavirus infection via TLR5/NLRC4-mediated production of IL-22 and IL-18. *Science* *346*, 861–865.

Zhang, Q., Yu, J.-T., Zhu, Q.-X., Zhang, W., Wu, Z.-C., Miao, D., and Tan, L. (2010). Complement receptor 1 polymorphisms and risk of late-onset Alzheimer's disease. *Brain Res.* *1348*, 216–221.

Zhang, Y.-W., Thompson, R., Zhang, H., and Xu, H. (2011). APP processing in Alzheimer's disease. *Mol Brain* *4*, 3.

Zhao, R., Hu, W., Tsai, J., Li, W., and Gan, W.-B. (2017). Microglia limit the expansion of β -amyloid plaques in a mouse model of Alzheimer's disease. *Molecular Neurodegeneration* *12*, 47.

4. Publications

4.1 Description of personal contribution

A *Replacement of brain-resident myeloid cells does not alter cerebral amyloid- β deposition in mouse models of Alzheimer's disease*

Nicholas H. Varvel*, Stefan A. Grathwohl*, Karoline Degenhardt, Claudia Resch, Andrea Bosch, Mathias Jucker and Jonas J. Neher

Personal contribution: establishment of immunofluorescence staining protocol for TREM2 and confocal imaging (together with J.J.N; Fig 2)

Others: N.H.V., S.A.G., M.J., J.J.N. designed research; N.H.V., S.A.G. and J.J.N. performed microglia replacement experiments, A.B. and C.R. performed immunohistochemical staining and stereological analyses, J.J.N. analyzed data, N.H.V., S.A.G. and J.J.N. wrote the paper.

*These authors contributed equally to this paper.

B *Innate immune memory in the brain shapes neurological disease hallmarks*

Ann-Christin Wendeln*, Karoline Degenhardt*, Lalit Kaurani, Michael Gertig, Thomas Ulas, Gaurav Jain, Jessica Wagner, Lisa M. Häsler, Katleen Wild, Angelos Skodras, Thomas Blank, Ori Staszewski, Moumita Datta, Tonatiuh Pena Centeno, Vincenzo Capece, Md. Rezaul Islam, Cemil Kerimoglu, Matthias Staufenbiel, Joachim L. Schultze, Marc Beyer, Marco Prinz, Mathias Jucker, André Fischer and Jonas J. Neher

Personal contribution: intraperitoneal injections of LPS in WT and APP23 mice and subsequent preparation of the first batch of animals (included in Fig. 1, Fig. 2); immunostaining for A β and determination of plaque load of batch 1 (included in Fig. 2); immunostaining for Iba1 and PU.1 and stereological analyses of plaque-associated microglia (Fig. 2); biochemical sample preparation for ELISA (Fig. 2) and Western Blotting (Extended Fig. 3), establishment of microglia isolation protocol for FAC sorting (Extended Fig. 6); microglial FAC sorting for ChIP-Seq (together with A.C.W; Fig. 4); data analysis and editing of the manuscript (together with all authors).

Others: J.W., P.R., L.M.H., K.W., A.S., T.B., O.S., M.D. and J.J.N performed further *in vivo* experiments; M.G., L.K., G.J., T.P., V.C., A.F., M.B., T.U., J.L.S. and J.J.N. performed ChIP-Seq and RNA sequencing experiments and data analysis; J.J.N. conceived and

coordinated the study together with M.J., A.F., M.P., M.B., J.L.S. and M.S.; J.J.N. wrote the manuscript.

*These authors contributed equally to this paper.

C *Lack of MFG-E8 reduces pathology in mouse models of cerebral β -amyloidosis*

Karoline Degenhardt*, Jessica Wagner*, Konstantina Kapolou, Domenico Del Turco, Thomas Deller, Mathias Jucker, Jonas J. Neher

Personal contribution: experimental design of the study together with J.J.N.; maintenance and preparation of the APPPS1 x *Mfge8* and APP23 x *Mfge8* mouse lines; histological staining for GFAP (Fig. 1), MFG-E8 (Fig. 1, 3), A β (Fig. 3, 6), PU.1 and Iba1 (Fig. 4); determination of A β load, plaque number and microglia number (together with J.W., Fig. 4, 6, Supplement Fig. 2, 3); biochemical analysis (together with J.W.) for A β , APP, CTF- β and MFG-E8 with Western Blot and ELISA (Fig. 2, 6, Supplement Fig. 2); microglia isolation via FAC sorting for cytokine determination (together with J.W., Fig. 4); Methoxy-X04 injections for *in vivo* phagocytosis experiments with subsequent microglia analysis (together with J.W. Fig. 5); data analysis (together with J.W.); image acquisition; manuscript preparation and figure preparation.

Others: K.K. helped with histology and biochemical analyses; D.D.T and T.D. performed electron microscopy; M.J. and J.J.N. helped with experimental design and edited the manuscript.

*These authors contributed equally to this paper.

Replacement of brain-resident myeloid-cells does not alter cerebral amyloid- β deposition in mouse models of Alzheimer's disease

Nicholas H. Varvel*, Stefan A. Grathwohl*, Karoline Degenhardt, Claudia Resch, Andrea Bosch, Mathias Jucker and Jonas J. Neher

Published in:

The Journal of Experimental Medicine 2015 Vol. 212, No. 11, 1803-1809

Replacement of brain-resident myeloid cells does not alter cerebral amyloid- β deposition in mouse models of Alzheimer's disease

Nicholas H. Varvel,^{1,2*} Stefan A. Grathwohl,^{1*} Karoline Degenhardt,^{1,2} Claudia Resch,^{1,2} Andrea Bosch,^{1,2} Mathias Jucker,^{1,2} and Jonas J. Neher^{1,2}

¹Department of Cellular Neurology, Hertie Institute for Clinical Brain Research, University of Tübingen, 72076 Tübingen, Germany

²German Center for Neurodegenerative Diseases (DZNE), 72076 Tübingen, Germany

Immune cells of myeloid lineage are encountered in the Alzheimer's disease (AD) brain, where they cluster around amyloid- β plaques. However, assigning functional roles to myeloid cell subtypes has been problematic, and the potential for peripheral myeloid cells to alleviate AD pathology remains unclear. Therefore, we asked whether replacement of brain-resident myeloid cells with peripheral monocytes alters amyloid deposition in two mouse models of cerebral β -amyloidosis (APP23 and APPS1). Interestingly, early after repopulation, infiltrating monocytes neither clustered around plaques nor showed Trem2 expression. However, with increasing time in the brain, infiltrating monocytes became plaque associated and also Trem2 positive. Strikingly, however, monocyte repopulation for up to 6 mo did not modify amyloid load in either model, independent of the stage of pathology at the time of repopulation. Our results argue against a long-term role of peripheral monocytes that is sufficiently distinct from microglial function to modify cerebral β -amyloidosis. Therefore, myeloid replacement by itself is not likely to be effective as a therapeutic approach for AD.

CORRESPONDENCE

Jonas J. Neher:
jonas.neher@uni-tuebingen.de

Abbreviations used: A β , amyloid- β ; AD, Alzheimer's disease; GCV, ganciclovir; icv, intra-cerebroventricular; TK, CD11b-HSVTK.

Alzheimer's disease (AD) is a common dementing disorder characterized by deposition of the amyloid- β (A β) peptide, neurofibrillary tangles, and neuron loss (Holtzman et al., 2011). These pathological alterations are accompanied by a robust neuroinflammatory response, and innate immune myeloid cells are invariably found in close proximity to A β plaques within the AD brain (Prinz et al., 2011; Wyss-Coray and Rogers, 2012; Heneka et al., 2015). Notably, recent genome-wide association studies implicate variants of immune-related genes as risk factors for late-onset AD. These genes are expressed by myeloid cells within the brain and include, for example, *CD33*, *CR1*, and *Trem2* (Guerreiro et al., 2013; Lambert et al., 2013). This indicates an important role for myeloid cells in AD pathogenesis.

Microglia, the brain's resident macrophages, are a myeloid population that is developmentally and functionally distinct from circulating monocytes (Lavin et al., 2014; Hoeffel et al., 2015). Importantly, numerous studies have provided evidence that peripheral myeloid cells

can infiltrate brain tissue and mitigate A β deposition (Simard et al., 2006; El Khoury et al., 2007; Town et al., 2008; Lebson et al., 2010). Furthermore, recent data indicate that infiltrating monocytes rather than resident microglia express Trem2 (Jay et al., 2015), which would further substantiate a significant role of peripheral myeloid cells in AD pathogenesis. However, distinguishing myeloid cell populations (resident vs. infiltrating) is difficult because of shared expression of marker proteins and experimental confounds associated with whole-body irradiation and bone marrow grafts, in particular blood-brain barrier permeability after irradiation (Ajami et al., 2007; Mildner et al., 2011). Thus, assessing the contribution of specific myeloid cell subtypes to AD pathology has been exceedingly difficult.

Furthermore, the accurate characterization of myeloid subtype functions in AD is particularly important in light of recent evidence suggesting

*N.H. Varvel and S.A. Grathwohl contributed equally to this paper.

© 2015 Varvel et al. This article is distributed under the terms of an Attribution-Noncommercial-Share Alike-No Mirror Sites license for the first six months after the publication date (see <http://www.rupress.org/terms>). After six months it is available under a Creative Commons License (Attribution-Noncommercial-Share Alike 3.0 Unported license, as described at <http://creativecommons.org/licenses/by-nc-sa/3.0/>).

JEM

that microglial dysfunction, as part of the normal aging process or as the result of pathological changes, may be a driver of AD pathology (Streit et al., 2009; Krabbe et al., 2013; Hefendehl et al., 2014). If so, the replacement of brain-resident myeloid cells with peripheral monocytes could be of therapeutic value for the treatment of AD, as indicated for other neurological disorders (Cartier et al., 2009; Derecki et al., 2012).

In this study, we therefore used our recently described central nervous system myeloid cell repopulation model (Varvel et al., 2012) to examine whether infiltrating peripheral monocytes could attenuate cerebral A β pathology. As expected, peripheral monocytes rapidly replaced brain-resident myeloid cells after ablation. Although infiltrating monocytes were initially distinct from brain-resident myeloid cells, over time they adopted features similar to the myeloid cells present before repopulation, such as morphology, plaque association, and Trem2 expression. Furthermore, long-term myeloid replacement did not alter A β deposition, arguing that under these conditions invading monocytes do not perform a long-term function in mitigating A β pathology that is distinct from microglia. Thus, myeloid replacement by itself is not a likely therapeutic approach for AD.

RESULTS AND DISCUSSION

A β deposition is not altered by myeloid cell repopulation in depositing APPPS1 mice

To investigate the effects of replacing brain-resident myeloid cells with peripheral monocytes during cerebral β -amyloidosis, we crossed APPPS1 mice, which develop first amyloid deposits at 6–8 wk of age (Radde et al., 2006), with the CD11b-HSVTK (TK) line (Heppner et al., 2005). TK mice express herpes simplex thymidine kinase in myeloid cells, which allows for myeloid cell ablation through a 2-wk intracerebroventricular (icv) ganciclovir (GCV) administration in wild-type as well as APPPS1 mice (Grathwohl et al., 2009; Varvel et al., 2012). Importantly, we have previously shown that upon discontinuation of GCV administration, peripheral monocytes repopulate the entire brain within 2 wk (either using eGFP bone marrow reconstitution or an irradiation-independent model, i.e., animals expressing red fluorescent protein under the inflammatory monocyte-specific chemokine receptor-2 promoter; Varvel et al., 2012).

3-mo-old depositing APPPS1/TK animals were subjected to 2 wk of icv GCV treatment. Histological examination of brain tissue from APPPS1/TK animals was then performed 2 wk later. As expected, APPPS1/TK⁻ mice displayed congophilic A β deposits throughout the neocortex, and Iba1-positive myeloid cells were tightly clustered around these plaques (Fig. 1 a). In contrast, Iba1-positive cells in the repopulated APPPS1/TK⁺ mice did not closely surround congophilic plaques, although some processes extending from the myeloid cells appeared to be in contact with the deposits. In addition, the morphology of the Iba1-positive cells in repopulated APPPS1/TK⁺ mice was remarkably homogeneous throughout the cortex, with cells displaying shorter, asymmetrically oriented processes and enlarged cell bodies compared

with Iba1-positive cells in APPPS1/TK⁻ animals, regardless of their position in relation to individual A β plaques (Fig. 1 a). Quantitative stereological analysis further demonstrated that $\sim 2.0 \times 10^6$ Iba1-positive cells engrafted during the 2 wk after termination of GCV treatment, approximately double the number of microglia in the APPPS1/TK⁻ controls (Fig. 1 c). Notably, at this early time point after repopulation, no change in congophilic amyloid or total A β load was detectable (Fig. 1 b).

To determine whether the continued presence of brain-engrafted monocytes would alter their responses to A β plaques and/or modify A β deposition, APPPS1/TK mice were analyzed 12 wk after GCV treatment. Again, in APPPS1/TK⁻ animals, Iba1-positive cells clustered tightly around A β deposits. Interestingly, some clustering of the engrafted myeloid cells was also observed in the APPPS1/TK⁺ animals at this later time point (Fig. 1 a), and brain sections showed $\sim 1.8 \times 10^6$ Iba1-positive cells in the monocyte-repopulated APPPS1/TK⁺ mice and $\sim 1.5 \times 10^6$ Iba1-positive cells in the age-matched controls (Fig. 1 c), consistent with our previous work (Varvel et al., 2012). Despite similar numbers of myeloid cells and visible responses of invading monocytes to amyloid deposits, no change in congophilic plaques or total A β deposits was observed at this later time point (Fig. 1 b). Furthermore, amyloid-associated dystrophic neuritic structures persisted in the myeloid cell-repopulated APPPS1/TK⁺ mice (Fig. 1 d).

A β deposition is not altered by myeloid cell repopulation in depositing APP23 mice

It is possible that amyloid deposition was not altered in the APPPS1 mice because of the early and rapid nature of cerebral β -amyloidosis in this model. Therefore, we crossed TK mice to a second APP transgenic mouse model, APP23, which develops cerebral β -amyloidosis at 6–8 mo of age and shows more slowly progressing A β deposition in both dense cored and diffuse plaques (Sturchler-Pierrat et al., 1997).

9-mo-old APP23/TK animals were treated with GCV for 2 wk, and the mice were sacrificed 6 mo later. Histological examination of APP23/TK⁻ control mice revealed the presence of dense core, congophilic amyloid deposits tightly surrounded by Iba1-positive myeloid cells. Strikingly, in repopulated APP23/TK⁺ mice Iba1-positive cells also showed noticeable clustering around congophilic deposits (Fig. 1 e), although their cell bodies remained further detached from plaques than observed in TK⁻ animals, reminiscent of results from the APPPS1 model (Fig. 1 a). Also, infiltrating monocytes remained morphologically distinct from brain-resident myeloid cells, with larger cell bodies and shorter processes (Fig. 1 e). Of note, stereological analysis revealed similar numbers of Iba1-positive cells in APP23/TK⁻ ($\sim 1.3 \times 10^6$) and APP23/TK⁺ ($\sim 1.2 \times 10^6$) animals (Fig. 1 g).

Despite comparable numbers of Iba1-positive cells and clustering of the invading peripheral myeloid cells around congophilic plaques in APP23/TK⁻ and APP23/TK⁺ animals, no changes in congophilic amyloid or total A β load was detectable (Fig. 1 f). Furthermore, dystrophic neuritic structures

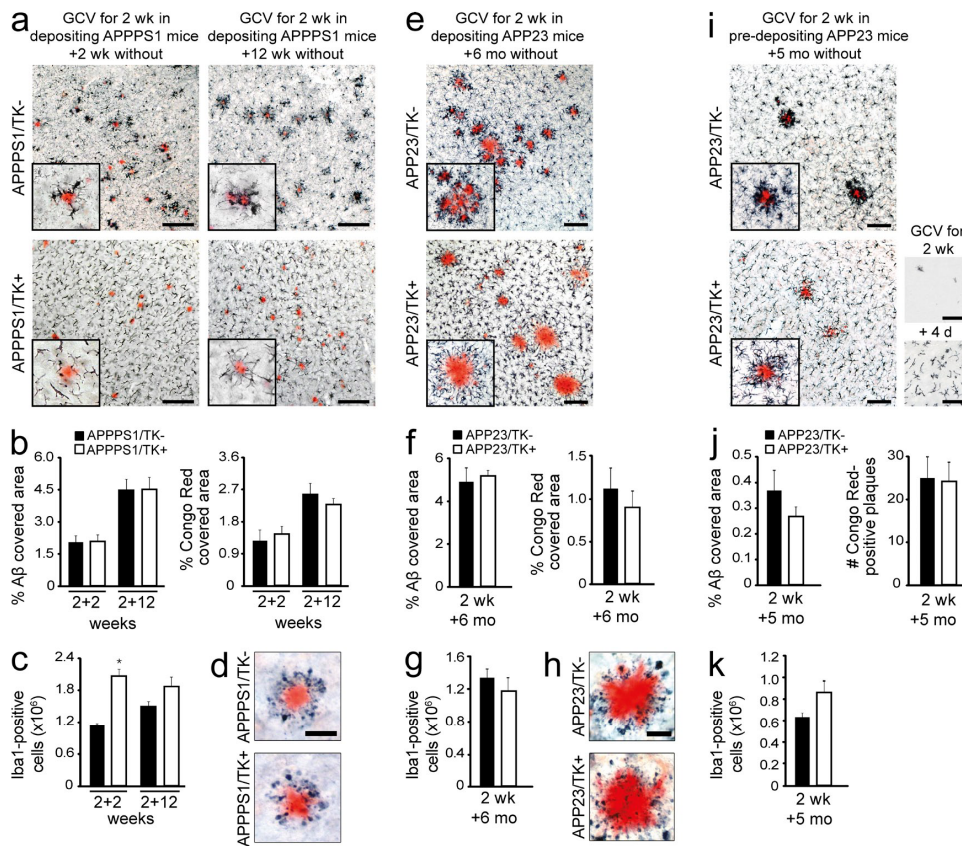


Figure 1. Long-term myeloid cell replacement does not alter Aβ deposition. Analysis of the effects of myeloid cell replacement in two APP transgenic mouse models, APPPS1 and APP23. (a) Brain-resident myeloid cells were ablated in 3-mo-old, depositing APPPS1 mice, which then remained untreated for 2 or 12 wk. Immunostaining shows Iba1-positive myeloid cells and amyloid plaques (Congo red) in APPPS1/TK⁻ mice (top) and APPPS1/TK⁺ mice (bottom). (b) Stereological quantification of congophilic deposits (Congo red staining) and total Aβ load (anti-Aβ staining) at 2 or 12 wk after GCV treatment in APPPS1/TK⁻ mice compared with repopulated APPPS1/TK⁺ animals. (c) Stereological analysis of total Iba1⁺ cells in APPPS1/TK⁺ compared with APPPS1/TK⁻ mice (ANOVA: transgene × time point interaction, $F(3,25) = 6.417$, $P < 0.001$; Tukey's HSD post hoc: *, $P < 0.05$). (d) Amyloid-associated neuritic dystrophy in APPPS1/TK⁺ and APPPS1/TK⁻ mice (Congo red and APP staining). (e) 9-mo-old, depositing APP23/TK mice received GCV treatment and then remained untreated for 6 mo. Immunostaining shows Iba1-positive myeloid cells and amyloid plaques (Congo red). (f) Stereological quantification of congophilic deposits and total Aβ load. (g) Stereological analysis of cortical Iba1-positive cells in APP23/TK⁻ compared with APP23/TK⁺ mice. (h) Amyloid-associated neuritic dystrophy in APP23/TK⁺ and APP23/TK⁻ mice (Congo red and APP staining). (i) APP23/TK mice at 5 mo of age, i.e., before onset of plaque deposition, received GCV treatment and then remained untreated for 5 mo. Immunostaining shows Iba1-positive myeloid cells and amyloid plaques (Congo red). (bottom right, top picture) Iba1 staining after initial depletion; (bottom picture) myeloid cell morphology upon invasion. (a, e, and i) Insets show higher-magnification images. (j) Stereological quantification of total Aβ load and total number of congophilic deposits in APP23 animals. (k) Quantitative stereological analysis of Iba1-positive cells in APP23/TK⁺ and APP23/TK⁻ animals. Bars: (a, e, and i) 100 μm; (d and h) 50 μm. Data were pooled from at least two independent experiments. Analyses were performed in a–d for APPPS1/TK⁻: $n = 7/8$ males and APPPS1/TK⁺: $n = 6/5$ males for the 2+2/2+12 wk time points, respectively; in e–h for APP23/TK⁺: $n = 4$ females, 3 males and APP23/TK⁻: $n = 4$ females, 2 males; and i–k for APP23/TK⁺: $n = 4$ males and APP23/TK⁻: $n = 7$ males. Immunostainings were independently replicated at least two times. Data are presented as mean ± SEM.

persisted in the myeloid cell-repopulated mice 6 mo after termination of GCV treatment in the APP23/TK⁺ mice (Fig. 1 j). This suggests that over the 6-mo incubation period infiltrating monocytes do not perform a function that is distinct from microglia during cerebral β-amyloidosis. Rather, with increasing time in the brain the infiltrating cells appear to become more similar to microglia, as indicated by comparable cell numbers

being present in the brain (Fig. 1 g), as well as their association with amyloid plaques (Fig. 1 e).

Aβ deposition is not altered by myeloid cell repopulation in predepositing APP23 mice

To examine the possibility that myeloid cell replacement might be beneficial before the onset of Aβ deposition rather than

JEM

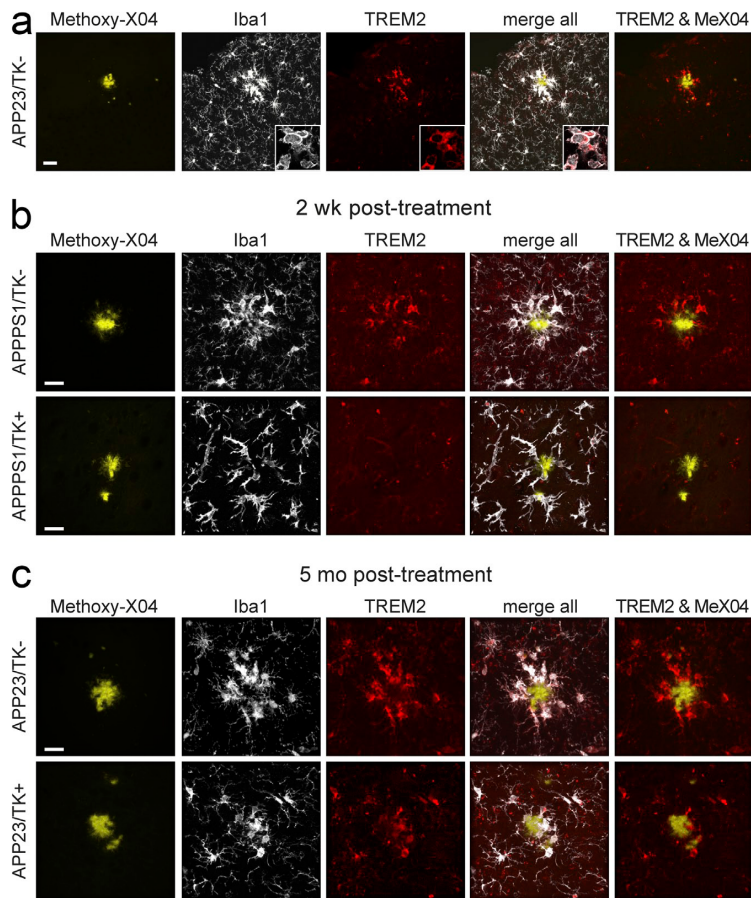


Figure 2. Trem2 expression in myeloid cells occurs with plaque association. (a) Trem2 expression is observed in myeloid cells (Iba1 positive) associated with plaques (stained with Methoxy-X04) in APP23 (shown) and APPPS1 mice (not depicted). Images are maximum projections of confocal z-stacks (insets show representative high-magnification images of a single confocal plane in plaque-associated cells). (b) Maximum projection of confocal z-stack in 4-mo-old APPPS1/TK⁻ animals shows Iba1-positive cells expressing Trem2 in APPPS1/TK⁻ animals, whereas nonplaque-associated infiltrating monocytes do not express Trem2 in APPPS1/TK⁺ mice. (c) APP23/TK⁻ as well as APP23/TK⁺ animals repopulated before A β deposition show plaque-associated myeloid cells positive for Trem2 at the age of 10 mo. Bars: (a) 30 μ m; (b and c) 20 μ m. Immunostaining was performed for $n \geq 4$ randomly chosen animals and replicated three times.

during established cerebral β -amyloidosis, we also repopulated predepositing APP23/TK⁺ mice at 5 mo of age. We performed this experiment only in male mice because of a later onset of A β deposition compared with females (Sturchler-Pierrat et al., 1997), yielding a larger time window for repopulation in the absence of A β deposition. We confirmed that with the same GCV administration protocol, efficient microglial ablation and brain repopulation could also be achieved in APP23 mice (Fig. 1 i). Histological analysis was performed at 10 mo of age, i.e., at early stages of plaque deposition.

Strikingly, in APP23/TK⁺ animals repopulated before the onset of A β deposition, Iba1-positive cells clustered strongly around plaques, reminiscent of myeloid cells in APP23/TK⁻ animals. Also, in plaque-free areas Iba1-positive cells in APP23/TK⁺ animals appeared morphologically more similar to microglia, showing smaller cell bodies and a more ramified appearance than in the other repopulated groups (Fig. 1 i). Despite these similarities, no alteration of congophilic or total A β plaque load was observed (Fig. 1 j). Of note, the number of

Iba1-positive cells was not significantly different in APP23/TK⁻ versus APP23/TK⁺ animals (Fig. 1 k).

TREM2 expression occurs in peripheral monocytes only after plaque association

It has recently been reported that reduced numbers of plaque-associated microglia are encountered in APP transgenic mouse models either haploinsufficient or deficient in *Trem2* (Ulrich et al., 2014; Jay et al., 2015; Wang et al., 2015). Therefore, we analyzed whether the differences in plaque association observed in our repopulated versus nonrepopulated groups could be related to Trem2 expression. In TK⁻ animals, plaque-associated Iba1-positive cells were Trem2 immunoreactive (Fig. 2 a), in line with the findings by Jay et al. (2015). Surprisingly, early after repopulation, when infiltrating monocytes did not cluster around plaques, these cells showed no detectable Trem2 expression in APPPS1 mice (Fig. 2 b; APPPS1/TK⁺ group 2 wk after GCV treatment discontinuation is shown). However, in long-term repopulated animals

where plaque association was evident, Iba1-positive cells clustering around amyloid deposits also showed Trem2 expression (Fig. 2 c; the APP23/TK⁺ group repopulated at the age of 5 mo, which displayed the most pronounced plaque association, is shown). Our current data do not allow for a conclusion regarding the origin of myeloid cells (brain resident or peripheral) in control TK⁻ mice, wherein the brain-resident myeloid cells have not been ablated; nevertheless, they indicate that Trem2 expression is induced in myeloid cells in response to the local plaque environment rather than as a result of macrophage origin.

In summary, our data suggest that in our experimental models monocytes do not perform a long-term function in the brain that is sufficiently distinct from the role of microglia to modify cerebral β -amyloidosis. These data are in line with our previous work (Varvel et al., 2012), where we reported nearly complete functional overlap between resident microglia and long-term engrafted peripheral monocytes in the measures examined, including parenchymal coverage and responses to purinergic agonists. Furthermore, monocytes invading the brain quickly down-regulated monocyte-specific markers such as, e.g., CCR2 (Varvel et al., 2012). Accordingly, it was recently shown that upon transplantation into different tissues (such as lung, spleen, and liver), bone marrow-derived macrophages show molecular reprogramming to match the resident macrophage population (Lavin et al., 2014). Thus, our work may indicate that also in the brain, the tissue environment dominates over myeloid cell origin, although more work will be needed to definitively prove this point.

A recent study used a CSF1-receptor inhibitor to deplete resident microglia and found that, in contrast to the HSVTK model, myeloid repopulation occurred from a brain-resident microglial progenitor (Elmore et al., 2014). This raises the possibility that in our long-term repopulation experiments, some peripherally derived myeloid cells may, over time, be replaced by endogenous microglial precursors. Additionally, it is possible that some of the repopulating myeloid cells may originate from the proliferation of small numbers of surviving microglia. However, the engrafted myeloid cells in our model showed clear morphological differences throughout the entire period of our experiments, whereas in the study by Elmore et al. (2014), the repopulating cells showed a ramified morphology indistinguishable from microglia. Therefore, the majority of brain-resident myeloid cells after GCV-induced microglial ablation are likely to be derived from peripheral monocytes. Strong support for this interpretation also comes from the study by Prokop et al. in this issue, where heterochronic parabiosis experiments clearly demonstrate that the repopulating cells are peripherally derived.

Our data presented here show that even during brain disease, i.e., cerebral β -amyloidosis, engrafted monocytes adopt features (such as cellular ramification, plaque association, and Trem2 expression) of brain-resident myeloid cells (be it microglia or long-term engrafted peripheral monocytes) and do not modify A β deposition. Therefore, myeloid replacement by itself is not a likely therapeutic

option for AD or other chronic neurodegenerative diseases that are not a direct result of genetic variants in myeloid genes.

MATERIALS AND METHODS

Animals. Female hemizygous TK mice (Heppner et al., 2005) were crossed to male hemizygous APPS1 (Radde et al., 2006) or hemizygous APP23 mice (Sturchler-Pierrat et al., 1997). APP23 mice express a transgene consisting of human APP with the KM670/671NL mutation under a Thy-1 promoter element, and APPS1 mice carry an additional mutated human presenilin 1 (PSEN1) transgene. APPS1 mice were generated on a C57BL/6 (B6) background, whereas APP23 and TK mice were originally derived on a B6D2 background and were backcrossed to B6 mice for >10 generations. Mice were kept under pathogen-free conditions, and experiments were in compliance with protocols approved by the local animal use and care authorities (Regierungspräsidium Tübingen).

icv GCV application. Approximately 40 h before surgery, osmotic pumps (model 2004, 0.25 μ l/h; Alzet) were filled with a 50 mg/ml solution of valganciclovir (F. Hoffmann-La Roche AG) diluted in PBS and primed at 37°C. Mice were anesthetized using ketamine and xylazine (100 mg/kg ketamine, 10 mg/kg xylazine), placed on a warming pad, and secured on a modified stereotaxic apparatus. The skin and the periosteum were removed and the pump reservoir was placed into a subcutaneous pocket, formed on the back of the animal. The coordinates for the cannula from bregma were +0.1 mm anteroposterior, 1.0 mm lateral, and 2.5 mm dorsoventral. The cannula (Brain Infusion kit III 1–3 mm; Alzet) was held in place by dental cement (Heraeus). After surgery, mice were treated with paracetamol (i.p. 5 mg/kg daily; Essex Pharma GmbH) for 3 d.

Removal of the osmotic pump reservoir. 2 wk after osmotic pump surgery, the animals were anesthetized using ketamine and xylazine (100 mg/kg ketamine, 10 mg/kg xylazine). A small (1 cm) incision was made in the skin between the scapulae to gain access to the subcutaneous pump reservoir and tube connecting the pump reservoir to the head cannula. The connecting tube was cut, and the pump reservoir was removed. The cannula and the attached tube were left in place, and the free end of the tube was sealed with dental cement. The incision was closed with sutures and the animal was returned to its cage. After surgery, mice were treated with acetaminophen (i.p. 5 mg/kg daily; Essex Pharma GmbH) for 3 d.

Histology. After transcardial perfusion, brains were removed and the hemisphere contralateral to the implanted cannula was fresh frozen for biochemical analysis. The hemisphere that received cannula insertion was fixed in 4% PFA for 24 h, followed by cryoprotection in 30% sucrose in PBS. Brains were subsequently frozen in 2-methylbutane and coronally sectioned at 40 μ m using a freezing-sliding microtome. Immunohistochemical stainings were performed using the VECTASTAIN Elite ABC kits (Vector Laboratories). The following primary antibodies were used: rabbit polyclonal antibody to ionized calcium binding adapter molecule 1 (Iba1; Wako Pure Chemical Industries), rabbit polyclonal antibody to human A β (CN3), and rabbit polyclonal antibody 5313 to the N terminus of APP (as a marker of dystrophic neurites; provided by C. Haass, Ludwig Maximilians University Munich, Munich, Germany). All antibodies were used at a dilution of 1:2,000. Congo red staining was performed according to standard laboratory procedures. Images were acquired on an Axioplan 2 microscope with AxioCam MRm, using a 20 \times /0.5 air objective and AxioVision 4.7 software (all from Carl Zeiss).

For immunofluorescence staining, sections were prepared as in the previous paragraph, blocked for 1 h with 5% goat serum, and incubated overnight, at 4°C, with antibodies against rabbit anti-Iba1 (1:2,000; Wako Pure Chemical Industries) and sheep anti-TREM2 (1:100; R&D Systems). Please note that this antibody was established by Jay et al. (2015) to be specific for murine Trem2 (as indicated by lack of staining in Trem2^{-/-} animals). Primary antibody incubation was followed by extensive washing and incubation with anti-sheep-Alexa Fluor 546 and anti-rabbit-Alexa Fluor 647 secondary

JEM

antibodies (Jackson ImmunoResearch Laboratories, Inc.). Plaques were then counterstained with Methoxy-X04 (4% vol of 10 mg/ml Methoxy-X04 in dimethyl sulfoxide and 7.7% vol Cremophor EL in PBS) and sections washed extensively. Images were acquired with an LSM 510 META (Axiovert 200M) confocal microscope using a 63 \times oil objective (1.4 NA) and LSM software 4.2 (all from Carl Zeiss). Laser lines 405, 543, and 633 were used to sequentially excite the fluorophores, and z-stacks of 17- μ m thickness were acquired (1- μ m intervals). Maximum-intensity projections were created using IMARIS 7.7.2 software (Bitmap).

Stereological assessment of amyloid load and Iba1 cell number. Numbers of Iba1-positive cells and A β load were assessed on random sets of every 12th systematically sampled 40- μ m-thick sections through the neocortex typically yielding 8–10 sections/mouse. Analysis was performed with the aid of the Stereo Investigator software (Stereo Investigator 6; MBF Bioscience) and a motorized x-y-z stage coupled to a video microscopy system (Microfire color microscope camera; Optronics). For Iba1 quantification, the optical fractionator technique was used with three-dimensional dissectors (area 495 \times 495 μ m², height 15 μ m, guard height 2 μ m, counting frame 50 \times 50 μ m²). Iba1-positive cells with complete soma within the disector volume were counted (Grathwohl et al., 2009; Varvel et al., 2012). Congophilic amyloid and A β load was analyzed using the area fraction technique (Bondolfi et al., 2002).

Statistical analysis. Statistical analysis was performed using JMP 7.1 software. The results are expressed as mean values \pm SEM. Student's *t* test was used for comparison of two groups, and two-way ANOVA was used for comparison of multiple groups followed by Tukey's HSD post hoc analysis.

We thank Dr. Adriano Aguzzi (University of Zurich, Zurich, Switzerland) for kindly providing the HSVTK mouse line and J. Odenthal for experimental help and advice.

This work was supported by the Alzheimer's Association (N.H. Varvel), The Alexander von Humboldt Foundation (N.H. Varvel), and a Roman Herzog Postdoctoral Fellowship of the Hertie Foundation (J.J. Neher).

The authors declare no competing financial interests.

Submitted: 16 March 2015

Accepted: 11 September 2015

REFERENCES

- Ajami, B., J.L. Bennett, C. Krieger, W. Tetzlaff, and F.M.V. Rossi. 2007. Local self-renewal can sustain CNS microglia maintenance and function throughout adult life. *Nat. Neurosci.* 10:1538–1543. <http://dx.doi.org/10.1038/nn2014>
- Bondolfi, L., M. Calhoun, F. Ermini, H.G. Kuhn, K.-H. Wiederhold, L. Walker, M. Staufenbiel, and M. Jucker. 2002. Amyloid-associated neuron loss and gliogenesis in the neocortex of amyloid precursor protein transgenic mice. *J. Neurosci.* 22:515–522.
- Cartier, N., S. Hacein-Bey-Abina, C.C. Bartholomae, G. Veres, M. Schmidt, I. Kutschera, M. Vidaud, U. Abel, L. Dal-Cortivo, L. Caccavelli, et al. 2009. Hematopoietic stem cell gene therapy with a lentiviral vector in X-linked adrenoleukodystrophy. *Science*. 326:818–823. <http://dx.doi.org/10.1126/science.1171242>
- Derecki, N.C., J.C. Cronk, Z. Lu, E. Xu, S.B.G. Abbott, P.G. Guyenet, and J. Kipnis. 2012. Wild-type microglia arrest pathology in a mouse model of Rett syndrome. *Nature*. 484:105–109. <http://dx.doi.org/10.1038/nature10907>
- El Khoury, J., M. Tof, S.E. Hickman, T.K. Means, K. Terada, C. Geula, and A.D. Luster. 2007. Ccr2 deficiency impairs microglial accumulation and accelerates progression of Alzheimer-like disease. *Nat. Med.* 13:432–438. <http://dx.doi.org/10.1038/nm1555>
- Elmore, M.R., A.R. Najafi, M.A. Koike, N.N. Dagher, E.B. Spangenberg, R.A. Rice, M. Kitazawa, B. Matusow, H. Nguyen, B.L. West, and K.N. Green. 2014. Colony-stimulating factor 1 receptor signaling is necessary for microglia viability, unmasking a microglia progenitor cell in the adult brain. *Neuron*. 82:380–397. <http://dx.doi.org/10.1016/j.neuron.2014.02.040>
- Grathwohl, S.A., R.E. Kälin, T. Bolmont, S. Prokop, G. Winkelmann, S.A. Kaeser, J. Odenthal, R. Radde, T. Eldh, S. Gandy, et al. 2009. Formation and maintenance of Alzheimer's disease β -amyloid plaques in the absence of microglia. *Nat. Neurosci.* 12:1361–1363. <http://dx.doi.org/10.1038/nn.2432>
- Guerreiro, R., A. Wojtas, J. Bras, M. Carrasquillo, E. Rogava, E. Majounie, C. Cruchaga, C. Sassi, J.S.K. Kauwe, S. Younkin, et al. Alzheimer Genetic Analysis Group. 2013. TREM2 variants in Alzheimer's disease. *N. Engl. J. Med.* 368:117–127. <http://dx.doi.org/10.1056/NEJMoa1211851>
- Hefendehl, J.K., J.J. Neher, R.B. Sühs, S. Kohsaka, A. Skodras, and M. Jucker. 2014. Homeostatic and injury-induced microglia behavior in the aging brain. *Aging Cell*. 13:60–69. <http://dx.doi.org/10.1111/acel.12149>
- Heneka, M.T., D.T. Golenbock, and E. Latz. 2015. Innate immunity in Alzheimer's disease. *Nat. Immunol.* 16:229–236. <http://dx.doi.org/10.1038/ni.3102>
- Heppner, F.L., M. Greter, D. Marino, J. Falsig, G. Raivich, N. Hövelmeyer, A. Waisman, T. Rüllicke, M. Prinz, J. Priller, et al. 2005. Experimental autoimmune encephalomyelitis repressed by microglial paralysis. *Nat. Med.* 11:146–152. <http://dx.doi.org/10.1038/nm1177>
- Hoefel, G., J. Chen, Y. Lavin, D. Low, F.F. Almeida, P. See, A.E. Beaudin, J. Lum, I. Low, E.C. Forsberg, et al. 2015. C-Myb⁺ erythro-myeloid progenitor-derived fetal monocytes give rise to adult tissue-resident macrophages. *Immunity*. 42:665–678.
- Holtzman, D.M., J.C. Morris, and A.M. Goate. 2011. Alzheimer's disease: the challenge of the second century. *Sci. Transl. Med.* 3:77sr1. <http://dx.doi.org/10.1126/scitranslmed.3002369>
- Jay, T.R., C.M. Miller, P.J. Cheng, L.C. Graham, S. Bemiller, M.L. Broihier, G. Xu, D. Margevicius, J.C. Karlo, G.L. Sousa, et al. 2015. TREM2 deficiency eliminates TREM2⁺ inflammatory macrophages and ameliorates pathology in Alzheimer's disease mouse models. *J. Exp. Med.* 212:287–295. <http://dx.doi.org/10.1084/jem.20142322>
- Krabbe, G., A. Halle, V. Matyash, J.L. Rinnenthal, G.D. Eom, U. Bernhardt, K.R. Miller, S. Prokop, H. Kettenmann, and F.L. Heppner. 2013. Functional impairment of microglia coincides with Beta-amyloid deposition in mice with Alzheimer-like pathology. *PLoS ONE*. 8:e60921. <http://dx.doi.org/10.1371/journal.pone.0060921>
- Lambert, J.-C., C.A. Ibrahim-Verbaas, D. Harold, A.C. Naj, R. Sims, C. Bellenguez, A.L. DeStafano, J.C. Bis, G.W. Beecham, B. Grenier-Boley, et al. Cohorts for Heart and Aging Research in Genomic Epidemiology. 2013. Meta-analysis of 74,046 individuals identifies 11 new susceptibility loci for Alzheimer's disease. *Nat. Genet.* 45:1452–1458. <http://dx.doi.org/10.1038/ng.2802>
- Lavin, Y., D. Winter, R. Blecher-Gonen, E. David, H. Keren-Shaul, M. Merad, S. Jung, and I. Amit. 2014. Tissue-resident macrophage enhancer landscapes are shaped by the local microenvironment. *Cell*. 159:1312–1326. <http://dx.doi.org/10.1016/j.cell.2014.11.018>
- Lebson, L., K. Nash, S. Kamath, D. Herber, N. Carty, D.C. Lee, Q. Li, K. Szekeres, U. Jinwal, J. Koren, et al. 2010. Trafficking CD11b-positive blood cells deliver therapeutic genes to the brain of amyloid-depositing transgenic mice. *J. Neurosci.* 30:9651–9658. <http://dx.doi.org/10.1523/JNEUROSCI.0329-10.2010>
- Mildner, A., B. Schlevogt, K. Kierdorf, C. Böttcher, D. Erny, M.P. Kummer, M. Quinn, W. Brück, I. Bechmann, M.T. Heneka, et al. 2011. Distinct and non-redundant roles of microglia and myeloid subsets in mouse models of Alzheimer's disease. *J. Neurosci.* 31:11159–11171. <http://dx.doi.org/10.1523/JNEUROSCI.6209-10.2011>
- Prinz, M., J. Priller, S.S. Sisodia, and R.M. Ransohoff. 2011. Heterogeneity of CNS myeloid cells and their roles in neurodegeneration. *Nat. Neurosci.* 14:1227–1235. <http://dx.doi.org/10.1038/nn.2923>
- Prokop, S., K.R. Miller, N. Drost, S. Handrick, V. Mathur, J. Luo, A. Wegner, T. Wyss-Coray, and F.L. Heppner. 2015. Impact of peripheral myeloid cells on amyloid- β pathology in Alzheimer's disease-like mice. *J. Exp. Med.* 212. <http://dx.doi.org/10.1084/jem.20150479>
- Radde, R., T. Bolmont, S.A. Kaeser, J. Coomaraswamy, D. Lindau, L. Stoltze, M.E. Calhoun, F. Jäggi, H. Wolburg, S. Gengler, et al. 2006. A β 42-driven cerebral amyloidosis in transgenic mice reveals early and robust pathology. *EMBO Rep.* 7:940–946. <http://dx.doi.org/10.1038/sj.embor.7400784>
- Simard, A.R., D. Soulet, G. Gowing, J.-P. Julien, and S. Rivest. 2006. Bone marrow-derived microglia play a critical role in restricting senile plaque

Brief Definitive Report

- formation in Alzheimer's disease. *Neuron*. 49:489–502. <http://dx.doi.org/10.1016/j.neuron.2006.01.022>
- Streit, W.J., H. Braak, Q.-S. Xue, and I. Bechmann. 2009. Dystrophic (senescent) rather than activated microglial cells are associated with tau pathology and likely precede neurodegeneration in Alzheimer's disease. *Acta Neuropathol.* 118:475–485. <http://dx.doi.org/10.1007/s00401-009-0556-6>
- Sturchler-Pierrat, C., D. Abramowski, M. Duke, K.H. Wiederhold, C. Mistl, S. Rothacher, B. Ledermann, K. Bürki, P. Frey, P.A. Paganetti, et al. 1997. Two amyloid precursor protein transgenic mouse models with Alzheimer disease-like pathology. *Proc. Natl. Acad. Sci. USA*. 94:13287–13292. <http://dx.doi.org/10.1073/pnas.94.24.13287>
- Town, T., Y. Laouar, C. Pittenger, T. Mori, C.A. Szekeley, J. Tan, R.S. Duman, and R.A. Flavell. 2008. Blocking TGF- β -Smad2/3 innate immune signaling mitigates Alzheimer-like pathology. *Nat. Med.* 14:681–687. <http://dx.doi.org/10.1038/nm1781>
- Ulrich, J.D., M.B. Finn, Y. Wang, A. Shen, T.E. Mahan, H. Jiang, F.R. Stewart, L. Piccio, M. Colonna, and D.M. Holtzman. 2014. Altered microglial response to A β plaques in APPPS1-21 mice heterozygous for TREM2. *Mol. Neurodegener.* 9:20. <http://dx.doi.org/10.1186/1750-1326-9-20>
- Varvel, N.H., S.A. Grathwohl, F. Baumann, C. Liebig, A. Bosch, B. Brawek, D.R. Thal, I.F. Charo, F.L. Heppner, A. Aguzzi, et al. 2012. Microglial repopulation model reveals a robust homeostatic process for replacing CNS myeloid cells. *Proc. Natl. Acad. Sci. USA*. 109:18150–18155. <http://dx.doi.org/10.1073/pnas.1210150109>
- Wang, Y., M. Cella, K. Mallinson, J.D. Ulrich, K.L. Young, M.L. Robinette, S. Giffillan, G.M. Krishnan, S. Sudhakar, B.H. Zinselmeyer, et al. 2015. TREM2 lipid sensing sustains the microglial response in an Alzheimer's disease model. *Cell*. 160:1061–1071. <http://dx.doi.org/10.1016/j.cell.2015.01.049>
- Wyss-Coray, T., and J. Rogers. 2012. Inflammation in Alzheimer disease—a brief review of the basic science and clinical literature. *Cold Spring Harb. Perspect. Med.* 2:a006346. <http://dx.doi.org/10.1101/cshperspect.a006346>

Innate immune memory in the brain shapes neurological disease hallmarks

Ann-Christin Wendeln*, Karoline Degenhardt*, Lalit Kaurani, Michael Gertig, Thomas Ulas, Gaurav Jain, Jessica Wagner, Lisa M. Häsler, Katleen Wild, Angelos Skodras, Thomas Blank, Ori Staszewski, Moumita Datta, Tonatiuh Pena, Vincenzo Capece, Md. Rezaul Islam, Cemil Kerimoglu, Matthias Staufenbiel, Joachmin L. Schultze, Marc Beyer, Marco Prinz, Mathias Jucker, André Fischer and Jonas J. Neher

Accepted in Nature 23.02.2018

Innate immune memory in the brain shapes neurological disease hallmarks

Ann-Christin Wendeln^{1,2,3*}, Karoline Degenhardt^{1,2,3*}, Lalit Kaurani^{4,5}, Michael Gertig^{4,5}, Thomas Ulas⁶, Gaurav Jain^{4,5}, Jessica Wagner^{1,2,3}, Lisa M. Häslér^{1,2}, Katleen Wild^{1,2}, Angelos Skodras^{1,2}, Thomas Blank⁸, Ori Staszewski⁸, Moumita Datta⁸, Tonatiuh Pena Centeno⁵, Vincenzo Capece⁵, Md. Rezaul Islam⁵, Cemil Kerimoglu⁵, Matthias Staufenbiel^{1,2}, Joachim L. Schultze^{6,7}, Marc Beyer⁹, Marco Prinz^{8,10}, Mathias Jucker^{1,2}, André Fischer^{4,5} and Jonas J. Neher^{1,2#}

¹German Center for Neurodegenerative Diseases (DZNE), Otfried-Müller-Str. 23, 72076 Tübingen, Germany

²Department of Cellular Neurology, Hertie Institute for Clinical Brain Research, University of Tübingen, Tübingen, Germany

³Graduate School of Cellular and Molecular Neuroscience, University of Tübingen, Tübingen, Germany

⁴Department of Psychiatry and Psychotherapy, University Medical Center Göttingen, Grisebachstr. 5, 37077 Göttingen, Germany

⁵Department for Systems Medicine and Epigenetics in Neurodegenerative Diseases, German Center for Neurodegenerative Diseases (DZNE) Göttingen, Von-Siebold-Str. 3a, D-37075 Göttingen

⁶Genomics and Immunoregulation, LIMES-Institute, University of Bonn, 53115, Bonn, Germany

⁷Platform for Single Cell Genomics and Epigenomics at the University of Bonn and the German Center for Neurodegenerative Diseases, Bonn, Germany

⁸Institute of Neuropathology, Faculty of Medicine, University of Freiburg, Freiburg, Germany

⁹Molecular Immunology in Neurodegeneration, German Center for Neurodegenerative Diseases (DZNE), Bonn, Germany

¹⁰BIOSS Centre for Biological Signalling Studies, University of Freiburg, Freiburg, Germany

* *contributed equally*

corresponding author

Abstract

'Innate immune memory' is a vital mechanism of myeloid cell plasticity that occurs in response to environmental stimuli and alters subsequent immune responses. Two types of immunological imprinting can be distinguished, *training* and *tolerance*, which are epigenetically mediated and enhance or suppress subsequent inflammation, respectively. Whether immune memory occurs in tissue-resident macrophages *in vivo* and how it may affect pathology remains largely unknown. Here we demonstrate that peripherally applied inflammatory stimuli induce acute immune training and tolerance in the brain and lead to differential epigenetic reprogramming of brain-resident macrophages, microglia, that persists for at least six months. Strikingly, in a mouse model of Alzheimer's pathology, immune training exacerbates cerebral β -amyloidosis while tolerance alleviates it; similarly, peripheral immune stimulation modifies pathological features after stroke. Our results identify immune memory in the brain as an important modifier of neuropathology.

Main text

Contrary to the long-held assumption that immunological memory exists only in cells of the adaptive immune system, recent evidence indicates that myeloid cells also display memory effects^{1,2}. For example, certain immune stimuli ‘train’ blood monocytes to generate enhanced immune responses to subsequent immune insults^{3,4}. In contrast, other stimuli induce immune tolerance, i.e. suppression of inflammatory responses to subsequent stimuli^{3,5}. Innate immune memory lasts for several days *in vitro* and for up to three months in circulating monocytes *in vivo* and is mediated by epigenetic reprogramming in cultured cells, with chromatin changes also apparent *in vivo*^{3,6,7}. However, whether immune memory occurs in long-lived tissue-resident macrophages and whether it alters tissue-specific pathology remains unknown.

Microglia, the brain-resident macrophages, were recently shown to be very long-lived cells^{8,9}. This makes them particularly interesting for studying immune memory, as virtually permanent modification of their molecular profile appears possible. As microglia are also known to significantly affect many neurological diseases¹⁰⁻¹², we investigated whether immune memory occurs in microglia *in vivo* and how it affects neuropathology.

Acute immune memory in the brain

It is well-established that inflammation in the periphery can prompt immune responses in the brain¹³. To evaluate whether immune memory is inducible in the brain by peripheral stimulation, mice received daily intraperitoneal injections of low-dose lipopolysaccharides (LPS) on four consecutive days, leading to mild sickness behaviour and temporary weight loss (Fig.1a and Extended Data Fig.1a). Three hours after application, the first LPS injection (1xLPS) led to a pronounced increase of blood cytokine levels, but only modest increases in brain cytokines. Upon the second injection (2xLPS), the blood levels of the pro-inflammatory cytokines IL-1 β , TNF- α , IL-6, IL-12 and IFN- γ were diminished compared to 1xLPS while IL-10 release occurred at similar levels, indicating peripheral immune tolerance. In sharp contrast, brain cytokines were dramatically increased with 2xLPS injections, indicating a brain-specific training effect induced by the first LPS stimulus (Figs.1b/c and Extended Data Fig.2). Accordingly, a conspicuous morphological change in microglia occurred after 2xLPS, while activated (GFAP+) astrocytes only increased after 3xLPS (Extended Data Figs.1b-d). Importantly, 4xLPS virtually abolished TNF- α , IL-1 β and IL-6 release in the brain while IL-10 remained elevated, indicating immune tolerance.

Next, we examined the contribution of microglia to immune memory in the brain using inducible CX3CR1-CreER (Cre) mice crossed with mouse lines carrying loxP-flanked genes, where tamoxifen-induced Cre expression results in persistent recombination in long-lived microglia but not in short-lived myeloid cells, including blood monocytes¹⁴. We induced microglial knockout of either 'transforming growth factor- β -activated kinase 1' (*Tak1*), which results in inhibition of NF- κ B, JNK and ERK1/2 pathways¹⁴, or histone deacetylases-1 and -2 (*Hdac1/2*), two major regulators of epigenetic reprogramming and macrophage inflammatory responses^{15,16}. As expected, tamoxifen-induced knockout of either *Tak1* or *Hdac1/2* did not alter the peripheral inflammatory response. Furthermore, brain cytokine levels were indistinguishable after 1xLPS, but the training effect following 2xLPS injections was virtually abolished in Cre+ animals. Notably, the cytokines showing the most pronounced training and tolerance effects (IL-1 β , TNF- α , IL-6) were also most affected by microglial gene knockout (Figs.1b/c and Extended Data Fig.2), indicating that immune memory in the brain is predominantly microglia-mediated. Moreover, after 1xLPS, Cre+ and Cre- mice showed indistinguishable weight loss (Extended Data Fig.1a) and sickness behaviour (not shown); however, in animals with microglial *Tak1* knockout, sickness behaviour after 2xLPS was noticeably alleviated (Supplementary Movie 1).

After intraperitoneal injections, LPS was found in the blood but not in the brain, indicating that neither significant entry of LPS into the brain nor opening of the blood-brain barrier occurred, corresponding with previous reports¹⁷. The latter was confirmed by the absence of blood iron in the brain parenchyma. Also, using 'type 2 CC chemokine receptor' (CCR2) reporter mice¹⁸, no extravasation of circulating monocytes was found (Extended Data Figs.1e-g), confirming that immune memory was mediated by brain-resident macrophages alone.

Immune memory shapes neuropathology

Next, we analysed whether the training- and tolerance-inducing stimuli 1xLPS and 4xLPS, respectively, could lead to long-term alterations of brain immune responses and thereby modify disease pathogenesis. APP23 mice are a model of Alzheimer's disease (AD) pathology, where plaques of insoluble amyloid- β develop from 6 months of age. Amyloid plaques lead to activation of microglia¹⁹, thereby providing a stimulus that should reveal microglial immune memory. We injected 3-month-old APP23 mice with 1x/4xLPS, then analysed pathology 6 months later (Fig.2a). Strikingly, 1xLPS significantly increased while 4xLPS significantly decreased both plaque load and total amyloid-

β levels compared to control animals (Fig.2b), with plaque-associated neuritic damage correlating directly with plaque size in all treatment groups (Extended Data Figs.3a-c). Also, the protein levels of amyloid- β precursor protein (APP) and its cleavage products were indistinguishable amongst groups, indicating equivalent amyloid- β generation (Extended Data Fig.3d). Furthermore, neither the total number of microglia nor the number of microglia clustering around plaques was altered by LPS treatments (Fig.2c), while the number of activated (GFAP+) astrocytes decreased slightly both with 1x and 4xLPS treatment (Extended Data Fig.3e). However, the brain levels of IL-1 β , IL-6 and IL-12 were reduced in 4xLPS-treated APP animals, while in 1xLPS-treated APP mice IL-10 was reduced. In contrast, brain cytokine levels were not altered in wildtype littermate controls and baseline blood cytokine levels were unchanged in wildtype and APP animals. Furthermore, an additional LPS injection at 9 months of age caused indistinguishable peripheral cytokine responses (Fig.2d and Extended Data Figs.4a-c). Thus, peripheral immune stimuli cause long-term alterations in the brain immune response and differentially affect AD pathology.

To test for immune memory effects in a second disease model, we injected wildtype animals with 1x/4xLPS and induced focal brain ischemia one month later. One day post-ischemia, neuronal damage and microglial numbers were indistinguishable amongst treatment groups (Fig.3a), indicating that the initial ischemic insult was unaffected by 1x/4xLPS. However, the acute inflammatory response, which is driven by brain-resident cells early after ischemia¹², differed, showing increased levels of IL-1 β in 1xLPS- and decreased levels in 4xLPS-treated animals. In contrast, the release of IL-10 was significantly suppressed by 1xLPS only (Fig.3b), reminiscent of results in APP animals (Fig.2d). Other brain cytokines and blood cytokine levels were indistinguishable amongst groups (Extended Data Fig.5). Importantly, seven days after brain ischemia, the volume of neuronal damage and microglial activation was strongly reduced by 4xLPS but unaffected by 1xLPS (Figs.3c/d). These results confirm long-term modulation of brain immune responses and suggest persistent modification of stroke pathology following a tolerizing but not a training stimulus, possibly due to the severity of the insult preventing its further exacerbation through amplification of the immune response.

Microglial molecular profiles

In vitro, immune memory in macrophages results from epigenetically-mediated alterations in the enhancer repertoire, leading to transcriptional changes^{3,20,21}. Since our data indicated that acute immune memory in the brain is mediated predominantly by microglia, we isolated microglia by cell

sorting (Extended Data Fig.6) from 9-month-old animals stimulated with 1x/4xLPS at 3 months of age and performed chromatin immunoprecipitation for mono-methylation at lysine 4 of histone 3 (H3K4me1) and acetylation at lysine 27 of histone 3 (H3K27ac), which define active enhancers^{20,21}. Thus, we identified 20,241 putative active enhancers across all conditions.

First, we focussed on H3K4me1 marks, which should mark all enhancers activated in response to the first and/or second immune stimulus (as enhancers may lose H3K27ac after cessation of inflammation but retain H3K4me1 marks)^{20,21}. Strikingly, H3K4me1 levels differed significantly between control and LPS treatment groups both in wildtype and APP animals but also between 1x- and 4xLPS-treated mice (Extended Data Fig.7b; Supplementary Table1). For example, enhancers with increased H3K4me1 levels in microglia from 1xLPS versus 4xLPS wildtype animals showed enrichment for the 'thyroid hormone signalling pathway', including a putative enhancer for hypoxia inducible factor-1 α (HIF-1 α). Similarly, enhancers with higher H3K4me1 levels in 1xLPS versus 4xLPS-treated APP mice were enriched for the 'HIF-1 signalling pathway'. On the other hand, 4xLPS-treated APP animals showed increased H3K4me1 levels in putative enhancers related to phagocytic function (Fig.4a). Importantly, no pathway enrichment was found when comparing H3K4me1 levels in microglia from APP and wildtype controls (Fig.4a), indicating that H3K4me1 levels were altered predominantly in response to LPS stimulation.

Next, we analysed enhancer activation by determining differential regulation of H3K27ac levels. In line with the requirement of an acute stimulus for H3K27ac deposition²⁰, differential enhancer activation was more pronounced in APP animals (where amyloid plaques activate microglia) than in wildtype groups (190 \pm 18 in APP, 69 \pm 5 in wildtype groups; Extended Data Fig.7e; Supplementary Table2). For example, differentially regulated H3K27ac levels in microglia from 1xLPS-treated versus control APP animals were enriched for the 'HIF-1 signalling pathway', with enhancer regions also being enriched for HIF-1 α binding motifs (Fig.4b and Extended Data Fig.8), in line with changes in H3K4me1 levels (Fig.4a) and the reported key role of HIF-1 α in trained immunity and macrophage inflammatory responses^{4,22}.

Active enhancers in microglia from 4xLPS-treated versus control APP animals only showed enrichment for the 'Rap1 signalling pathway', a pathway implicated in phagocytosis of opsonized targets^{23,24}, again matching changes in H3K4me1 levels (Figs.4a/b). Strikingly, the comparison of microglia from APP animals that received the training- (1xLPS) and tolerance-inducing (4xLPS) stimuli, showed no pathway enrichment for active enhancers in 4xLPS-treated animals while

enhancers in 1xLPS-treated animals were enriched for a large number of inflammation-related pathways, highlighting the differential effects of the two immune memory states. Finally, the comparison of microglia from vehicle-treated wildtype and APP animals demonstrated a small number of differentially activated enhancers with enrichment for the 'thyroid hormone signalling pathway' (including a putative active enhancer for *Hif1a*) as well as the 'mTOR signalling pathway' (Fig.4b), indicating that microglia are also epigenetically reprogrammed in response to brain pathology alone.

We next examined microglial mRNA levels under the same conditions to determine whether epigenetic alterations were reflected in gene expression levels (Supplementary Table3). First, we determined the concordance between 772 enhancers with significantly increased/decreased H3K27ac levels (Supplementary Table2) and the direction of change in the expression of their nearest gene. Indeed, there was a significant (albeit modest) concordance between alterations in H3K27ac levels and gene expression (median concordance of pairwise comparisons =58%, P=0.03). This suggested that gene expression is directly affected by the microglial active enhancer repertoire. Accordingly, weighted gene correlation network analysis (WGCNA²⁵) revealed striking parallels to epigenetic changes (Figs.5a-c and Supplementary Table4). For example, the red module (MEred) contained the *Hif1a* gene, showed enrichment for the 'HIF-1 signalling pathway' and correlated strongly with the 1xLPS-treated APP group. Furthermore, gene expression in MEred was significantly upregulated in APP versus wildtype control animals and further increased by 1xLPS but downregulated by 4xLPS treatment.

HIF-1 α activation in inflammatory-stimulated macrophages can occur downstream of mitochondrial hyperpolarization; enhanced HIF-1 α signalling in turn promotes glycolysis, measurable as lactate release²⁶. Accordingly, the green module (MEgreen), which correlated positively with control and 1xLPS-treated APP groups but negatively with control and 4xLPS-treated wildtype groups, was found to be enriched in genes of the 'glycolysis' pathway. Microglial gene expression in MEgreen was upregulated in APP versus wildtype control animals and again further increased in APP animals by 1xLPS but decreased by 4xLPS treatment. Therefore, we analysed mitochondrial membrane potential and lactate release in microglia. Strikingly, microglia from 1xLPS-treated APP animals showed strongly increased mitochondrial membrane potential, which correlated positively with the release of lactate (Fig.5d), functionally corroborating the epigenetic and transcriptional alterations in trained microglia. Additionally, immunostaining confirmed higher protein levels of HIF-1 α in plaque-associated microglia, which were further increased in 1xLPS-treated APP animals (Figs.5e/f). Thus, HIF-1 α

signalling and a metabolic switch to glycolysis are activated in response to cerebral β -amyloid deposition, and are enhanced by immune training but reduced by immune tolerance in microglia.

In contrast to MEred/green, MEgrey correlated positively with the control wildtype but negatively with control and 1xLPS-treated APP groups. Compared to wildtype controls, microglial gene expression in MEgrey was downregulated in APP control animals and further decreased by 1xLPS stimulation, but showed unchanged levels in 4xLPS-treated APP animals (Figs.5a-c). Importantly, MEgrey was enriched for phagocytosis-related pathways, including the 'Rap1 signalling pathway' (Figs.5a-c), again reflecting epigenetic changes (Fig.4). We therefore tested whether phagocytosis of A β was enhanced in 4xLPS-treated APP animals. Indeed, microglial A β content was increased ~1.75-fold in 4xLPS-treated compared to APP control animals (Fig.5g), providing further functional validation of the microglial enhancer repertoire and gene expression profiles.

Recent data indicate that context-specific microglial phenotypes exist, e.g. 'disease-associated microglia' (DAM²⁷) and the 'microglial neurodegenerative phenotype' (MGnD²⁸). Interestingly, the brown module (MEbrown), which was significantly upregulated by both LPS treatments in wildtype as well as in all APP groups, contained a number of homeostatic microglial genes (e.g. *Hexb*, *Cx3cr1*, *Csf1r*) but also all of the 'stage 1 DAM' core-genes except *ApoE*, as well as 4 of 12 'stage 2' core-genes²⁷ (Fig.5c). Of note, the gene encoding ApoE, which may be crucial for promoting a detrimental microglial phenotype^{28,29} was found in the same module as *Hif1a* (MEred). MEred also contained other genes genetically linked to AD risk, namely *Cd33* and *Inpp5d*³⁰, suggesting that HIF-1 α may also be a detrimental modulator of AD pathology.

The epigenetic landscape of microglia has only been described under homeostatic conditions³¹⁻³³. Our data now demonstrate epigenetic modifications in microglia in response to peripheral immune stimulation but also as a result of cerebral β -amyloidosis, including activation of the HIF-1 α and mTOR pathways, and leading to transcriptional and functional alterations. While the global epigenetic and transcriptional changes were relatively modest, they were likely driven by a small number of microglia that received the required secondary immune stimulation, as evidenced for example by increased levels of HIF-1 α in plaque-associated microglia (Fig.5). mTOR activation is a well-known event in early AD³⁴ and was recently shown in microglia, where it activated HIF-1 α and glycolysis to sustain microglial energy demand in AD models³⁵. Our data now indicate that mTOR activation may be mediated by epigenetic microglial reprogramming in response to cerebral β -amyloidosis and that HIF-

1 α signalling downstream of mTOR could be a detrimental event, because augmentation or suppression of HIF-1 α signalling occurred concomitantly with aggravated or alleviated A β deposition, respectively.

We here provide evidence of both immune training and tolerance in microglia and demonstrate their impact on neuropathology for the first time. While we cannot completely exclude that other cell-types contribute to immune memory and modulation of pathology in the brain, microglial-specific gene knockout of *Tak1* or *Hdac1/2* virtually abolished immune training (Fig.1), indicating that microglia are likely the major effectors of immune memory. Importantly, in our experiments, immune memory effects mostly became apparent following a secondary inflammatory stimulus, corroborating the concept of innate immune memory^{1,3}. However, while in the periphery training may be beneficial due to enhanced pathogen elimination^{7,36,37}, and tolerance may be detrimental due to higher rates of infection resulting from immune suppression⁵, we found that training promotes while tolerance alleviates neuropathology. This is consistent with the beneficial effects of preventing microglial pro-inflammatory responses in models of AD pathology and stroke^{12,38} and the worsening of cerebral β -amyloidosis in response to pro-inflammatory peripheral stimuli in animal models³⁹. Similarly, immune training has recently been described in epithelial stem cells, where it promotes wound healing but may also underlie autoimmune disorders⁴⁰. Thus, immune memory in the brain could conceivably affect the severity of any neurological disease that presents with an inflammatory component, but this will need to be studied for each individual condition.

Our data provide proof-of-principle for innate immune memory in microglia, and while our different LPS injection paradigms may not necessarily model physiological stimuli, we found that individual cytokines applied peripherally may also elicit immune memory effects in the brain (Extended Data Fig.9). These results suggest that a wide variety of immune challenges may induce microglial immune memory and provide a possible mechanism for LPS-induced immune memory in the brain. It will be crucial to determine which other stimuli may lead to long-term modulation of microglial responses and thereby contribute to the severity of many neurological diseases.

References

1. Netea, M. G., Latz, E., Mills, K. H. G. & O'Neill, L. A. J. Innate immune memory: a paradigm shift in understanding host defense. *Nature Immunology* 16, 675–679 (2015).

2. Netea, M. G. et al. Trained immunity: A program of innate immune memory in health and disease. *Science* 352, aaf1098 (2016).
3. Saeed, S. et al. Epigenetic programming of monocyte-to-macrophage differentiation and trained innate immunity. *Science* 345, 1251086 (2014).
4. Cheng, S. C. et al. mTOR- and HIF-1 -mediated aerobic glycolysis as metabolic basis for trained immunity. *Science* 345, 1250684–1250684 (2014).
5. Biswas, S. K. & Lopez-Collazo, E. Endotoxin tolerance: new mechanisms, molecules and clinical significance. *Trends in Immunology* 30, 475–487 (2009).
6. Novakovic, B. et al. β -Glucan Reverses the Epigenetic State of LPS- Induced Immunological Tolerance. *Cell* 167, 1354–1368.e14 (2016).
7. Kleinnijenhuis, J. et al. Bacille Calmette-Guerin induces NOD2-dependent nonspecific protection from reinfection via epigenetic reprogramming of monocytes. *Proceedings of the National Academy of Sciences of the United States of America* 109, 17537–17542 (2012).
8. Tay, T. L. et al. A new fate mapping system reveals context-dependent random or clonal expansion of microglia. *Nature Neuroscience* (2017). doi:10.1038/nn.4547
9. Fügen, P. et al. Microglia turnover with aging and in an Alzheimer's model via long-term in vivo single-cell imaging. *Nature Neuroscience* 20, 1371–1376 (2017).
10. Prinz, M. & Priller, J. Microglia and brain macrophages in the molecular age: from origin to neuropsychiatric disease. *Nat Rev Neurosci* 15, 300–312 (2014).
11. Heneka, M. T., Kummer, M. P. & Latz, E. Innate immune activation in neurodegenerative disease. *Nat Rev Immunol* 14, 463–477 (2014).
12. Iadecola, C. & Anrather, J. The immunology of stroke: from mechanisms to translation. *Nature Medicine* 17, 796–808 (2011).
13. Perry, V. H., Cunningham, C. & Holmes, C. Systemic infections and inflammation affect chronic neurodegeneration. *Nat Rev Immunol* 7, 161–167 (2007).
14. Goldmann, T. et al. A new type of microglia gene targeting shows TAK1 to be pivotal in CNS autoimmune inflammation. *Nature Neuroscience* 16, 1618–1626 (2013).
15. Jacob, C. et al. HDAC1 and HDAC2 control the transcriptional program of myelination and the survival of Schwann cells. *Nature Neuroscience* 14, 429–436 (2011).
16. Datta M, et al. HDAC1/2 are required for microglia identity during development, homeostasis and neurodegeneration in a context-dependent manner, *Immunity* 2018 (in press).
17. Banks, W. A. & Robinson, S. M. Minimal penetration of lipopolysaccharide across the murine blood-brain barrier. *Brain, Behavior, and Immunity* 24, 102–109 (2010).
18. Saederup, N. et al. Selective chemokine receptor usage by central nervous system myeloid cells in CCR2-red fluorescent protein knock-in mice. *PLoS ONE* 5, e13693 (2010).
19. Sturchler-Pierrat, C. et al. Two amyloid precursor protein transgenic mouse models with Alzheimer disease-like pathology. *Proceedings of the National Academy of Sciences of the United States of America* 94, 13287–13292 (1997).
20. Ostuni, R. et al. Latent Enhancers Activated by Stimulation in Differentiated Cells. *Cell* 152, 157–171 (2013).

21. Kaikkonen, M. U. et al. Remodeling of the Enhancer Landscape during Macrophage Activation Is Coupled to Enhancer Transcription. *Molecular Cell* 51, 310–325 (2013).
22. Cramer, T. et al. HIF-1alpha is essential for myeloid cell-mediated inflammation. *Cell* 112, 645–657 (2003).
23. Caron, E., Self, A. J. & Hall, A. The GTPase Rap1 controls functional activation of macrophage integrin alphaMbeta2 by LPS and other inflammatory mediators. *Curr. Biol.* 10, 974–978 (2000).
24. Li, Y. et al. Rap1a null mice have altered myeloid cell functions suggesting distinct roles for the closely related Rap1a and 1b proteins. *J. Immunol.* 179, 8322–8331 (2007).
25. Langfelder, P. & Horvath, S. WGCNA: an R package for weighted correlation network analysis. *BMC Bioinformatics* 9, 559 (2008).
26. Mills, E. L. et al. Succinate Dehydrogenase Supports Metabolic Repurposing of Mitochondria to Drive Inflammatory Macrophages. *Cell* 167, 457–461.e14 (2016).
27. Keren-Shaul, H. et al. A Unique Microglia Type Associated with Restricting Development of Alzheimer's Disease. *Cell* 1–33 (2017). doi:10.1016/j.cell.2017.05.018
28. Krasemann, S. et al. The TREM2-APOE Pathway Drives the Transcriptional Phenotype of Dysfunctional Microglia in Neurodegenerative Diseases. *Immunity* 47, 566–581.e9 (2017).
29. Shi, Y. et al. ApoE4 markedly exacerbates tau-mediated neurodegeneration in a mouse model of tauopathy. *Nature* 1–20 (2017). doi:10.1038/nature24016
30. Lambert, J. C. et al. Meta-analysis of 74,046 individuals identifies 11 new susceptibility loci for Alzheimer's disease. *Nature Genetics* 45, 1452–1458 (2013).
31. Gosselin, D. et al. Environment drives selection and function of enhancers controlling tissue-specific macrophage identities. *Cell* 159, 1327–1340 (2014).
32. Lavin, Y. et al. Tissue-resident macrophage enhancer landscapes are shaped by the local microenvironment. *Cell* 159, 1312–1326 (2014).
33. Gosselin, D. et al. An environment-dependent transcriptional network specifies human microglia identity. *Science* 1617, eaal3222 (2017).
34. Wang, C. et al. Targeting the mTOR signaling network for Alzheimer's disease therapy. *Mol. Neurobiol.* 49, 120–135 (2014).
35. Ulland, T. K. et al. TREM2 Maintains Microglial Metabolic Fitness in Alzheimer's Disease. *Cell* 170, 649–656.e13 (2017).
36. Kaufmann, E. et al. BCG Educates Hematopoietic Stem Cells to Generate Protective Innate Immunity against Tuberculosis. *Cell* 172, 176–190.e19 (2018).
37. Arts, R. J. W. et al. BCG Vaccination Protects against Experimental Viral Infection in Humans through the Induction of Cytokines Associated with Trained Immunity. *Cell Host Microbe* 23, 89–100.e5 (2018).
38. Heneka, M. T., Golenbock, D. T. & Latz, E. Innate immunity in Alzheimer's disease. *Nature Immunology* 16, 229–236 (2015).
39. O'Banion, M. K. Does peripheral inflammation contribute to Alzheimer disease? Evidence from animal models. *Neurology* 83, 480–481 (2014).
40. Naik, S. et al. Inflammatory memory sensitizes skin epithelial stem cells to tissue damage. *Nature* 550, 475–480 (2017).

41. Liu, F., Yuan, R., Benashski, S. E. & McCullough, L. D. Changes in experimental stroke outcome across the life span. *Journal of Cerebral Blood Flow & Metabolism* 29, 792–802 (2009).
42. Sturchler-Pierrat, C. & Staufenbiel, M. Pathogenic mechanisms of Alzheimer's disease analyzed in the APP23 transgenic mouse model. *Annals of the New York Academy of Sciences* 920, 134–139 (2000).
43. Neher, J. J. et al. Phagocytosis executes delayed neuronal death after focal brain ischemia. *Proceedings of the National Academy of Sciences* 110, E4098–107 (2013).
44. Hefendehl, J. K. et al. Repeatable target localization for long-term in vivo imaging of mice with 2-photon microscopy. *Journal of Neuroscience Methods* 205, 357–363 (2012).
45. Eisele, Y. S. et al. Peripherally Applied A β -Containing Inoculates Induce Cerebral β -Amyloidosis. *Science* 330, 980–982 (2010).
46. Varvel, N. H. et al. Replacement of brain-resident myeloid cells does not alter cerebral amyloid- β deposition in mouse models of Alzheimer's disease. *Journal of Experimental Medicine* 212, 1803–1809 (2015).
47. Rottenberg, H. & Wu, S. Quantitative assay by flow cytometry of the mitochondrial membrane potential in intact cells. *Biochim. Biophys. Acta* 1404, 393–404 (1998).
48. Picelli, S. et al. Full-length RNA-seq from single cells using Smart-seq2. *Nature Protocols* 9, 171–181 (2014).
49. Leek, J. T., Johnson, W. E., Parker, H. S., Jaffe, A. E. & Storey, J. D. The sva package for removing batch effects and other unwanted variation in high-throughput experiments. *Bioinformatics* 28, 882–883 (2012).
50. Ritchie, M. E. et al. limma powers differential expression analyses for RNA-sequencing and microarray studies. *Nucleic Acids Res* 43, e47 (2015).
51. Halder, R. et al. DNA methylation changes in plasticity genes accompany the formation and maintenance of memory. *Nature Neuroscience* 19, 102–110 (2016).
52. Quinlan, A. R. BEDTools: The Swiss-Army Tool for Genome Feature Analysis. *Curr Protoc Bioinformatics* 47, 11.12.1–34 (2014).

Acknowledgements

We thank Richard Ransohoff (Boston) and Patrick Matthias (FMI, Basel) for providing CCR2-RFP and Hdac1/2 fl/fl mice, respectively; Patrizia Rizzu (DZNE Tuebingen) for experimental advice, Lary Walker (Emory University) for manuscript comments and Donna Bryce (Univ. Tuebingen) for statistical advice. This study was supported by a PhD fellowship of the Studienstiftung des Deutschen Volkes (A.C.W.), a Roman Herzog Fellowship of the Hertie Foundation (J.J.N.), and grants from the network 'Neuroinflammation in Neurodegeneration' (State of Baden-Wuerttemberg, Germany; M.J. and M.P.), the Sobek-Stiftung (M.P.), the DFG (SFB992, Reinhart-Koselleck-Grant to M.P., SFB704 to J.L.S.), the European Research Council (A.F.) the Fortüne Program (Med. Faculty, Univ. Tuebingen; 2075-1-0; J.J.N.), the Fritz Thyssen Foundation (Cologne, Germany; J.J.N.) and the Paul G. Allen Family Foundation (Seattle, USA; J.J.N.). M.B. and J.L.S. are members of the Excellence Cluster ImmunoSensation.

Author Contributions:

K.D., A.C.W., J.W., P.R., L.M.H., K.W., A.S., T.B., O.S., M.D., J.J.N. performed microglial isolation, *in vivo* and *ex vivo* experiments and histological/biochemical analyses. M.G., L.K., G.J., T.P., V.C., R.I., C.K., A.F., M.B., T.U., J.L.S. and J.J.N. performed ChIP-Seq/RNA-Seq analyses. J.J.N. conceived the study and coordinated the experiments together with M.J., A.F., M.P., M.B., J.L.S. and M.S.; J.J.N. wrote the manuscript, with contributions from all authors.

Author Information:

The authors have no competing financial interests.

Correspondence and requests for materials should be addressed to jonas.neher@dzne.de

Materials and Methods

Animals

For all experiments, 3 month-old hemizygous APP23 transgenic (C57BL/6J-Tg(Thy1-APP_{K670N;M671L})23), APP23 transgene-negative littermates or C57BL/6J (wildtype) mice (Jackson Laboratory) were used.

For experiments analysing immune responses after acute LPS and cytokine stimulation (see below), both male and female mice were used. For microglia-specific gene knockouts, CX3CR1-CreER animals were crossed with *Tak1* fl/fl animals and Cre recombinase expression was induced by subcutaneous tamoxifen injections as previously described¹⁴. Similarly, microglial-specific knockout of *Hdac1/2* was achieved after crossing CX3CR1-CreER animals with a *Hdac1/2* fl/fl line¹⁵. Both *Tak1* fl/fl and *Hdac1/2* fl/fl were injected at 2-3 months of age and were incubated for four weeks without further treatment. Tamoxifen-injected CX3CR1-Cre negative littermates were used as controls (because responses in CX3CR1-Cre negative animals were indistinguishable in *Hdac1/2* fl/fl and *Tak1* fl/fl lines, pooled data are shown in Fig. 1).

As there is a significant gender effect on the pathology of both brain ischemia and cerebral β -amyloidosis,^{41,42} only female mice were used for the analyses of brain pathology. APP23 mice express a transgene consisting of human amyloid- β precursor protein (APP) with the KM670/671NL mutation under the Thy-1 promoter, and have been backcrossed with C57BL/6J mice for >20 generations. Female mice develop cerebral β -amyloid lesions in the neocortex around 6 months of age¹⁹.

Animals were maintained under specific pathogen-free conditions. All experiments were performed in accordance with the veterinary office regulations of Baden-Württemberg (Germany) and were approved by the Ethical Commission for animal experimentation of Tübingen and Freiburg, Germany.

Peripheral immune stimulation

3-month-old mice were randomly assigned to treatment groups and were injected intraperitoneally (i.p.) with bacterial lipopolysaccharides (LPS from *Salmonella enterica* serotype typhimurium, Sigma) at a daily dose of 500 μ g/kg bodyweight. Animals received either four LPS injections on four consecutive days (4xLPS), a single LPS injection followed by three vehicle injections on the following three days (1xLPS) or four vehicle injections (PBS). Acute stimulation showed indistinguishable cytokine responses in wildtype and APP23 transgenic animals; Figure 1 shows the pooled data from

both genotypes (see Extended Data Fig. 2 for data separated by genotype). Furthermore, as cytokine responses were indistinguishable in animals treated with 1/2/3/4xPBS, pooled data from all time points are shown.

For peripheral cytokine treatments, recombinant murine cytokines (TNF- α , IL-10; PeproTech) were aliquoted as by the manufacturer's instructions and stored at -80°C until use. To determine whether a long-term change in the brain's immune response (training or tolerance) occurred after peripheral cytokine injection, mice were treated on four consecutive days with 0.1 μ g/g bodyweight IL-10 or once with 0.1/0.2 μ g/g bodyweight TNF- α . Control mice received four vehicle injections (PBS). Four weeks later, cytokine- and control-treated mice received LPS (1 μ g/g bodyweight) or PBS, and were prepared 3 hours after the injection.

At the specified time-points, animals were deeply anaesthetised using sedaxylan/ketamine (64 mg/kg//472 mg/kg), blood was collected from the right ventricle of the heart and animals were transcardially perfused with ice-cold PBS through the left ventricle. The brain was removed and sagittally separated into the two hemispheres, which were either fixed in 4% paraformaldehyde (PFA) or fresh-frozen on dry ice. Fresh-frozen hemispheres were homogenised using a Precellys[®] lysing kit and machine at 10 or 20% (w/v) in homogenisation buffer (50 mM Tris pH 8, 150 mM NaCl, 5 mM EDTA) containing phosphatase and protease inhibitors (Pierce). Fixed hemispheres were kept in 4% PFA for 24h, followed by cryoprotection in 30% sucrose in PBS, subsequently frozen in 2-methylbutane and coronally sectioned at 25 μ m using a freezing-sliding microtome (Leica).

Focal brain ischemia

For the induction of a focal cortical stroke, we modified existing models of endothelin-1 (ET-1)-induced brain ischemia⁴³ to avoid traumatic injury to the brain. Under anaesthesia and analgesia (Fentanyl, Midazolam, Medetomidin: 0.05//5//0.5 mg/kg bodyweight), 3-month-old animals were fixed in a stereotactic frame and a circular piece of skull was removed (5 mm diameter, centred on Bregma; as described in⁴⁴). The dura mater was carefully removed with the help of a microhook (Fine Science Tools) and 5 μ l of ET-1 (Bachem; 64 μ M) in Hanks Buffered Salt Solution (Invitrogen) or vehicle solution was topically applied to the cortex and incubated for 10 min. The craniotomy was then covered with a 5 mm glass coverslip, which was fixed in place with dental cement (Hybond), the skin was sutured, then the mice received antidote (Flumazenil, Atipamezol: 0.5//2.5mg/kg bodyweight) and were health-monitored. Control mice underwent the same surgical procedure with application of

vehicle solution to the cortex. After 4 weeks, animals were deeply anesthetized and prepared as described above.

Western Blotting analysis

For Western Blotting, total brain homogenates were sonicated 3x5 seconds (LabSonic, B. Braun Biotech), protein levels of the brain homogenates were quantified with a microplate bicinchoninic acid (BCA) assay (Pierce) and adjusted accordingly. Samples were then analysed on NuPage Bis-Tris gels (Invitrogen) using standard procedures. Proteins were transferred to nitrocellulose membranes, blocking was performed with 5% milk in PBS containing 0.05% Tween (PBST) for 1h and blots were incubated with mouse anti-A β (6E10; 1:1000, Covance) in PBST overnight at 4°C. Membranes were then probed with the secondary HRP-labelled antibodies (1:20,000, Jackson ImmunoLaboratories). Protein bands were detected using chemiluminescent peroxidase substrate (ECL prime, GE Healthcare). Densitometric values of the protein band intensities were analysed with the software package Aida v.4.27 and normalised to GAPDH intensities.

Immunostaining

Immunohistochemical staining was performed on free-floating sections using either Vectastain Elite ABC kits (Vector laboratories) or fluorescent secondary antibodies (Jackson Immunolaboratories). Unless otherwise noted, brain sections were blocked for 1h with 5% normal serum of the secondary antibody species, followed by primary antibody incubation overnight at 4°C. Primary antibodies used were: rabbit anti-Pu.1 (1:1000, Cell Signalling), rabbit anti-Iba1 (1:1,000; Wako; catalogue no. 019-19741), rabbit anti-GFAP (1:500, Biozol; catalogue no. Z0334), rabbit anti-A β (CN3; 1:2,000⁴⁵), mouse anti-HIF-1 α (1:500; Novus Biologicals, catalogue no. NB100-105, clone H1alpha67), rat anti-CD11b (1:2000; Millipore, catalogue no. MAB1387Z), rabbit anti-APP (antibody 5313 to the ectodomain of APP, 1:750; kind gift of Prof. Christian Haas, Munich). Sections were then washed and incubated with secondary antibodies. Cresylviolet and Congo Red staining was conducted according to standard procedures. Fluorescent plaque staining was achieved using Methoxy-X04 (4% vol of 10 mg/ml methoxy-X04 in DMSO, and 7.7% vol CremophorEL in 88.3% vol PBS) for 20 min, RT.

Images were acquired on an Axioplan 2 microscope with Axioplan MRm and AxioVision 4.7 software (Carl Zeiss). Fluorescent images were acquired using a LSM 510 META (Axiovert 200M) confocal microscope with an oil immersion 63X/1.4NA objective and LSM software 4.2 (Carl Zeiss), using

sequential excitation of fluorophores. Maximum-intensity projections were generated using IMARIS 8.3.1 software (Bitmap).

For quantitative comparisons, sections from all groups were stained in parallel and analysed with the same microscope settings by an observer blinded to the treatment groups. To quantify the intensity of total microglial HIF-1 α staining, high-resolution bright field images were acquired using fixed camera exposure time and lamp intensity and subsequently analysed with Fiji software. Colour channels were split and a fixed intensity threshold was applied to the red channel. On each image, the thresholded area over the total image area was calculated. Area fractions were measured on images of at least 9 plaques and 15 plaque-free regions per animal. To exclude an influence of plaque-size on microglial HIF-1 α levels, plaques of similar size were selected for analysis of HIF-1 α levels in the different treatment groups (average plaque size: PBS i.p.: 1.73 \pm 0.15, 1xLPS i.p.: 1.84 \pm 0.19, 4xLPS i.p. 2.27 \pm 0.39% Congo red area fraction).

For nuclear HIF-1 α staining, a modified staining protocol was used. Briefly, sections were blocked with mouse Ig blocking reagent (Vector laboratories) for 1h, RT, followed by blocking with normal donkey serum for 1h, RT. Sections were then incubated overnight with mouse anti-HIF1 α (clone mgc3, 1:50; Thermo Fisher Scientific, catalogue no. MA1-516) and rabbit anti-Pu.1 (1:250; New England Biolabs, catalogue no. 2258S. Clone 9G7), 4°C. To quantify the intensity of nuclear HIF-1 α staining, z-stacks from 3 plaques and plaque-free regions per animal were acquired with the same microscope settings and subsequently analysed with IMARIS 8.3.1 software. Using the surfaces tool, a mask based on microglial nuclei was created using staining for Pu.1. A filter for area was applied to exclude background staining. The created surface was used to mask the HIF-1 α channel. The mean masked HIF-1 α intensity was then determined.

To quantify neuronal dystrophy, fluorescent images from 5-10 plaques per animal were acquired with the same microscope settings and subsequently analysed with Fiji software. Maximum intensity projections were generated to choose the region of interest consisting of APP-staining and the plaque. Fluorescence channels were split and intensity thresholds were applied to each channel. For every plaque, the thresholded area within the region of interest was calculated as a measure of plaque size and dystrophic area.

Stereological and morphological quantification

Stereological quantification was performed by a blinded observer on random sets of every 12th systematically sampled 25 µm thick sections throughout the neocortex. Analysis was conducted using the Stereologer software (Stereo Investigator 6; MBF Bioscience) and a motorized x-y-z stage coupled to a video microscopy system (Optronics). For quantification of total Pu.1- and GFAP-positive cells, the optical fractionator technique was used with three-dimensional dissectors as previously described⁴⁶. For the quantification of plaque-associated cells, plaques were identified based on Congo Red staining and cells in their immediate vicinity were counted. Plaque load was determined by analysing the cortical area covered by Congo Red and/or anti-Aβ staining using the area fraction fractionator technique⁴⁶. The volume of neuronal damage and microglial activation after brain ischemia was determined using the Cavalieri estimator technique.

For analysing microglial morphology, three images from three non-consecutive brain sections per animal were acquired from Iba-1 immunostained sections using identical camera acquisition settings, at 20X/0.5NA magnification. In order to perform the filament tracing in IMARIS (v.8.3.1), images were pre-processed in Fiji to optimise their contrast for reconstruction. The image background was subtracted using the in-built Fiji plugin to obtain an evenly distributed intensity and enhance contrast to the cells; subsequently the images were sharpened and their intensity was adjusted to the respective minimum and maximum histogram values. Filaments were then traced in IMARIS using the in-built Autopath algorithm. Reconstruction parameters were kept constant among all images; each cell was reconstructed as a 'filament' element in IMARIS, associated with a total length and volume.

ELISA

For quantification of Aβ by ELISA (Meso Scale Discovery) in brain homogenates or by SIMOA (Single Molecule Array, Quanterix) in isolated microglial cells, samples were pre-treated with formic acid (Sigma-Aldrich, final concentration: 70% vol/vol), sonicated for 35 seconds on ice, and centrifuged at 25,000g for 1 hour at 4°C. Neutralization buffer (1 M Tris base, 0.5 M Na₂HPO₄, 0.05% NaN₃ (wt/vol)) was then added at a 1:20 ratio. Aβ was measured by an observer blinded to the treatment groups using human (6E10) Aβ triplex assay (Meso Scale Discovery, MSD) in brain homogenates or Simoa Human Abeta 42 2.0 Kit (Quanterix) in isolated microglia according to the manufacturer's instructions. Soluble APPβ containing the Swedish mutations (as present in the APP23 transgene) was measured using the sw soluble APPβkit (Mesoscale Discovery) following the manufacturer's instructions after extraction with 1% Triton-X 100 and ultracentrifugation for 1h, 135,000g, 4 °C.

For cytokine measurements, brain homogenates were centrifuged at 25,000g for 30 minutes at 4°C. Supernatants were analysed using the mouse pro-inflammatory panel 1 V-plex plate (Mesoscale Discovery) according to the manufacturer's instructions. To determine blood cytokines, serum was obtained by coagulation of whole blood in Vacuettes (Greiner Bio-One) for 10 min, RT, and centrifugation for 10 min, 2,000g. Serum samples were diluted 1:2 before measurements. The investigator was blinded to the treatment groups.

Measurements were performed on a Mesoscale Sector Imager 6000 or a Simoa HD-1 Analyzer. For analyses of brain homogenates, protein levels were normalised against total protein amount as measured by BCA protein assay (Pierce).

To determine levels of LPS in blood and brain homogenates, the Limulus Amebocyte Lysate assay was used according to the manufacturer's instructions (Pierce LAL Chromogenic Endotoxin Quantitation Kit). Standards were prepared either in serum or brain homogenate from non-injected control animals. Serum samples were diluted 1:100 and brain homogenates 1:5 to eliminate matrix effects.

Isolation of microglia and fluorescence-activated cell sorting (FACS) analysis

Fluorescence-activated cell sorting of microglia was performed based on CD11b^{high} and CD45^{low} as previously described⁹ (see also Extended Data Fig.6).

Assessment of microglial mitochondrial membrane potential and lactate release

To assess the microglial mitochondrial membrane potential, 10k microglia were sorted into 70 µl PBS. Cells were incubated at 37°C with 3,3'-Dihexyloxacarbocyanine Iodide, DiOC₆(3) (Thermo Fisher Scientific) at a final concentration of 0.2 nM for 20 minutes. At this concentration, mitochondrial dye accumulation is largely dependent on the mitochondrial membrane potential, with only minor contributions of the plasma membrane potential⁴⁷. After incubation, the cell suspension was diluted with ice-cold PBS and DiOC₆(3) fluorescence was immediately acquired with a Sony SH800 instrument.

For the assessment of microglial lactate release, 50k microglia from the same animals as used for DiOC₆(3) staining were plated in 96-well plates with 125 µl of macrophage serum-free medium (Thermo Fisher Scientific) and incubated for 24h at 37°C, 5% CO₂. Lactate concentration in the media was determined using a Lactate Assay Kit (BioVision) following the manufacturer's instructions and

was correlated to DiOC₆(3) fluorescence values from cells of the same animal using IBM SPSS Statistics 22 software.

RNA-sequencing

For RNA sequencing, 10k microglia were directly sorted into RNase-free PCR strips containing 30 μ l of H₂O with 0.2% Triton-X and 0.8 U/ μ l RNase inhibitor (Clontech) and samples were immediately frozen on dry ice. RNA was isolated using NucleoSpin RNA XS kit (Macherey-Nagel) according to the manufacturer's instructions. 3 ng total RNA was used as input material for cDNA synthesis. cDNA synthesis and enrichment was performed following the Smart-seq2 v4 protocol as described by the manufacturer (Clontech). Sequencing Libraries were prepared with 1 ng of cDNA using the Nextera XT library preparation kit (Illumina) as described⁴⁸. Multiplexing of samples was achieved using three different index-primers in each lane. For sequencing, samples from each group (APP and WT) were pooled to rule out amplification and sequencing biases. Libraries were quality-controlled and quantified using a Qubit 2.0 Fluorometer (Life Technologies) and Agilent 2100 Bioanalyzer (Agilent Technologies). Final library concentration of 2 nM was used for sequencing. Sequencing was performed using a 50 bp single read setup on the Illumina HiSeq 2000 platform.

Base calling from raw images and file conversion to fastq files were achieved by Illumina standard pipeline scripts (bcl2fastq v.2.18.0). Quality control was then performed using FASTQC (v.2.18.0) program (<http://www.bioinformatics.babraham.ac.uk/projects/fastqc/>), eliminating one sample which had less than 20 million reads. Reads were trimmed off for sequencing adaptor and were mapped to mouse reference transcriptome (mm10) using STAR aligner 2.5.2b with non-default parameters. Unique read counts were obtained for each sample using HOMER v.4.8 software (<http://homer.salk.edu/homer/>) and 'maketagdirectory -tbp 1' command, followed by 'analyzeRepeats.pl rna mm10 -count exons -noadj -condenseGenes'. Raw read counts were imported into R (v.3.2) and normalized using the Bioconductor (v.3.2) DESeq2 package (v.1.10.1) using default parameter. After normalization, all transcripts having a maximum overall group mean lower than 10 were removed. Unwanted or hidden sources of variation, such as batch and preparation date, were removed using the sva package⁴⁹. The normalized rlog transformed expression values were adjusted according to the surrogate variables identified by sva using the function removeBatchEffect from the limma package⁵⁰. To determine gene clusters associated with wildtype or APP23 animals following i.p. injections of 1x or 4xLPS at 3 months of age, we then used the 13,627 present genes and applied the

R implementation of the Weighted Gene Correlation Network Analysis (WGCNA). We then performed WGCNA clustering using the '1-TOMsimilarityFromExpr' function with the network type "signed hybrid", a power parameter of 7 (as established by scale free topology network criteria), and a minimum module size of 50 dissecting the data into 10 modules. Finally, pathway enrichment analysis of genes within modules was performed using the 'findmotifs.pl' function of HOMER. Correction for multiple comparisons for KEGG pathway analyses was performed using the STATS package of R and applying Benjamini-Hochberg correction. To focus on the most important molecular pathways, only pathways with $\log P \leq -3$ and at least 5 genes were considered.

Chromatin Immunoprecipitation, library preparation and analysis

For microglia isolation for chromatin purification, 1 mM sodium butyrate, an inhibitor of histone deacetylases³¹, was added to the dissection medium and FACS buffers. After staining, microglia were fixed in 1% PFA for 10 minutes at room temperature, followed by addition of glycine (final concentration: 125 mM) for 5 minutes and washing in HBSS. Microglia were then sorted into homogenisation buffer (0.32 M sucrose, 5 mM CaCl_2 , 5 mM MgAc_2 , 50 mM HEPES, 0.1 mM EDTA, 1 mM DTT, 0.1% vol/vol Triton-X-100) and centrifuged at 950 g for 5 minutes at 4 °C. The pellet was resuspended in 100 μl Nelson buffer (50 mM Tris, 150 mM NaCl, 20 mM EDTA, 1% vol/vol Triton-X-100, 0.5% vol/vol NP-40) and frozen on dry ice.

ChIP-sequencing was performed as previously described⁵¹, with slight modifications. In brief, two biological replicates were analysed for each condition and targeted histone modification. Cell lysates from 8-10 mice were pooled giving a total cell number of approximately 0.8-1 million cells per replicate. The cross-linked chromatin was sheared for 3x7 cycles (30 sec. On/Off) in a BioruptorPlus (Diagenode) to achieve an average fragment size of 350 bps. Proper shearing and chromatin concentration was validated by DNA isolation and quantification using a small amount of each sample individually. Samples were split in half and 1 μg of ChIP-grade antibody (H3K4me1: Abcam ab8895 or H3K27ac: Abcam ab4729) was added and incubated overnight at 4°C. From each sample, 1% of the total volume was taken as input control prior to antibody binding. Immunoprecipitation was performed by incubating samples with 30 μl BSA-blocked protein A magnetic beads (Dynabeads, Invitrogen) for 1h at 4°C. After purifying the precipitated chromatin and isolating the DNA, DNA libraries were generated using the Next Ultra DNA Library Prep Kit for Illumina and the Q5 polymerase (New England Biolabs). Multiplexing of samples was done using 6 different index-primers from the Library

Prep Kit. For each replicate, samples from each condition (genotype and treatment) were pooled to rule out amplification and sequencing biases within the final data. Input samples were pooled and processed accordingly. The ideal number of amplification cycles was estimated via RealTime PCR to avoid over-amplification. Accordingly, samples were amplified for 13-15 cycles and the DNA was isolated afterwards. Individual libraries were pooled whereby each pool represented one whole batch of samples for each condition and targeted histone modification and was set to a final DNA concentration of 2 nM before sequencing (50 bp) on a HiSeq 2000 (Illumina) according to the manufacturer's instructions.

Base calling from raw images and file conversion to fastq files was achieved by standard Illumina pipeline scripts. Sequencing reads were then mapped to mouse reference genome (mm10) using rna-STAR aligner v2.3.0 with non-default parameters. Data were further processed using HOMER software (<http://homer.salk.edu/homer/>), following two recently published analyses on microglial epigenetic profiles^{31,32}. Tag directories were created from bam files using 'makeTagDirectory' for individual samples and inputs, and peak calling was performed using 'findpeaks -style histone' with 4-fold enrichment over background and input, a Poisson p-value of 0.0001, and a peak width of 500 bp for H3K4me1 and 250 bp for H3K27ac. Peaks common to both replicates were determined using 'mergepeaks' (-prefix) function. To focus analysis on enhancers, peaks within ± 2.5 kb of known TSS were filtered out. Union peak files for H3K4me1 and H3K27ac marks were then created for group-wise comparisons using 'mergepeaks' function. Active enhancers, i.e. genomic regions containing both H3K4me1 and H3K27ac peaks, were identified using the 'window' function of bedtools2 [52], requiring peaks of both marks to be located within a genomic region of 4 kb. Union peak files of active enhancers were then used for comparisons amongst groups for both H3K4me1 and H3K27ac marks using the 'getDifferentialPeaks' function (using a fold-change cut-off of 1.5 and a cumulative Poisson p-value of 0.0001). Finally, differential peaks were annotated using the 'annotatepeaks.pl' function, including gene ontology analysis. Correction for multiple comparisons for KEGG pathway analyses was performed using the STATS package of R and applying Benjamini-Hochberg correction. To focus on the most important molecular pathways, only pathways with $\log P \leq -3$ and at least three genes were considered.

For the generation of UCSC browser files, the 'makeUCSCfile' function was used, including normalisation to respective input and library size, with a resolution of 10 bp. Files for heatmaps of 24

kb genomic regions and with a resolution of 250 bp were generated using the 'annotatePeaks.pl' function; clustering was then performed using Gene Cluster 3.0 and visualised using JavaTreeView. To identify transcription factors involved in the differential activation of enhancers, the 'findMotifsGenome.pl' command was used to analyse a region of 500 bp around enhancer peaks (-size 500), as this resulted in more robust identification of motifs for known microglial lineage-determining transcription factors when determining motifs of all identified microglial enhancers (Extended Data Fig.8). For all active enhancers, motif analysis was performed using the union H3K27ac peak file and standard background (i.e. random genomic sequence created by HOMER). In the case of pairwise comparisons amongst conditions, the first condition's specific H3K27ac peak file was used as input and the second condition's peak file as background. Because motif enrichment was often relatively low, we focussed on the most relevant results by determining transcription factor (families), whose motifs occurred at least twice in 'known' and 'de-novo' motifs.

Comparison between enhancer activation and gene expression

From our 14 pairwise comparisons (Fig.4, Extended Data Fig.7 and Supplementary Table 2), we analysed 772 differentially activated enhancers and compared increased/decreased H3K27ac levels with the direction of change in the expression of the nearest gene (difference in z-scores between the groups used for pairwise comparisons). The 14 concordance values were then statistically compared to chance level (50%) using a two-tailed Wilcoxon signed rank test.

Statistics and Reproducibility

Statistical analyses were performed using IBM SPSS Statistics 22 or Prism 5 software. Data were assessed for normal distribution (Shapiro-Wilk test) and statistical outliers using the 'explore' function. If the normality criterion was met, data were analysed using a one-way ANOVA (for experiments on single genotypes), followed by pairwise comparison (if $P < 0.05$) with post-hoc Tukey correction (for samples with non-significant homogeneity of variance Levene's test) or Dunnett test (if homogeneity of variances not given). For comparisons across treatments and genotypes (e.g. cytokine analyses in Fig.2), a two-way ANOVA was performed, followed by posthoc testing with Tukey correction for significant main effects ($P < 0.05$). As the cytokine data for acute LPS stimulation (Fig.1) showed inequality of variance as well as skewedness, a non-parametric independent-samples median test was performed followed by pairwise comparison with correction for multiple comparison.

All experiments were performed at least twice and in independent batches of animals for key findings (figures show the pooled data). Due to batch-related variation in some dependent variables, 'batch' was added as a random variable to analyses where a significant batch effect was observed. For data sets with small sample size (e.g. Western Blotting analyses), the Kruskal-Wallis test was performed, followed by pairwise comparisons if $P < 0.05$. In the figure legends 'n' denotes the number of animals per treatment group. Minimum sample sizes were determined a priori using power analyses or as dictated by the methodology (e.g. ChIP-Seq).

Raw and processed data are provided in the Gene Expression Omnibus (accession number GSE82170; subseries GSE82168 for ChIP-Seq and GSE104630 for RNA-Seq datasets). Other data that support the findings of this study are available from the corresponding author upon reasonable request.

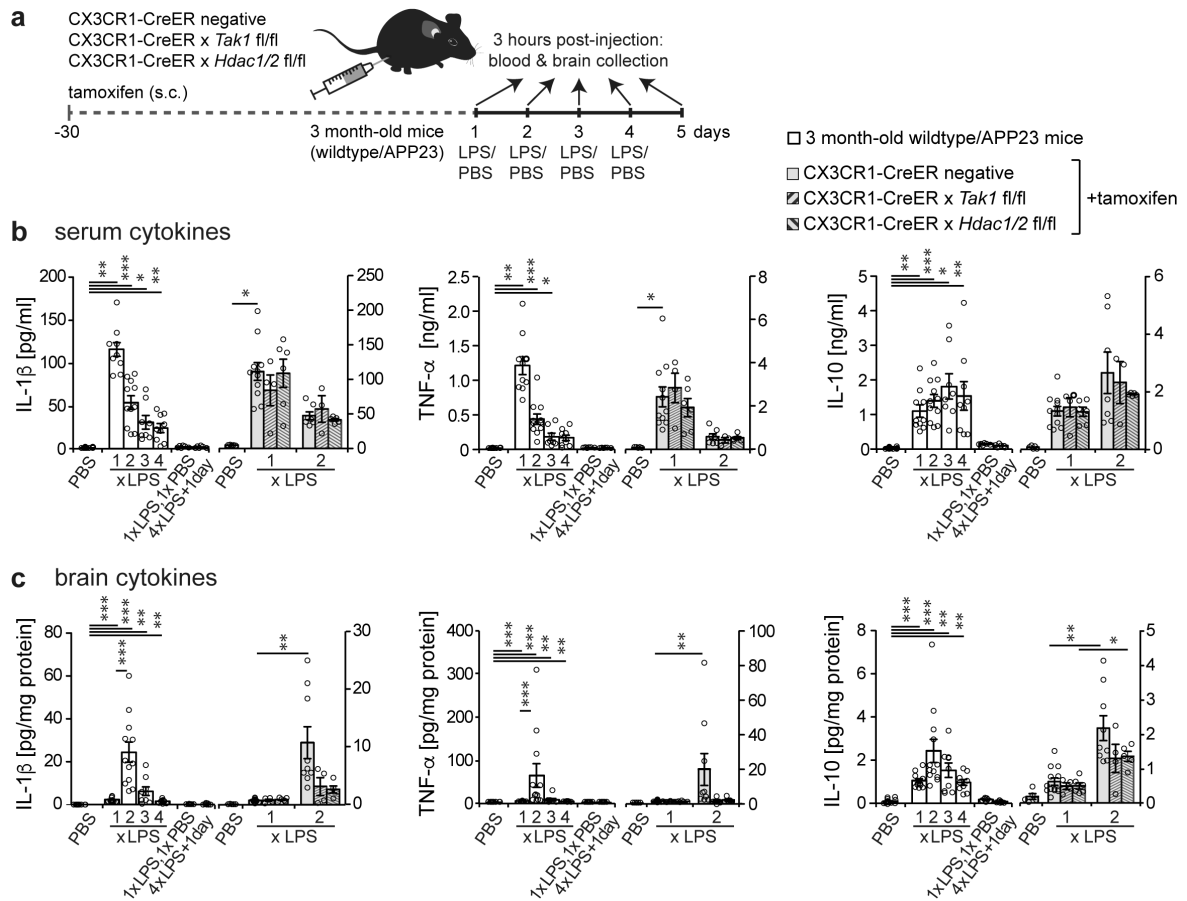


Figure 1: Peripheral immune stimulation evokes immune memory in microglia.

a, Experimental approach. **b**, *White bars*: Peripheral cytokine levels in wildtype/APP23 animals following lipopolysaccharide (LPS) injections. Note that tolerance is induced with repeated injections. **c**, Brain cytokine levels: 2xLPS amplifies IL-1 β /TNF- α release, demonstrating immune training; tolerance occurs with 3x/4xLPS. Cytokines return to baseline within 24h (1xLPS,1xPBS/4xLPS+1day). *Grey bars*: Microglia-specific knockout of *Tak1* or *Hdac1/2* selectively prevents immune training in the brain. In (b/c) n=16,11,12,9,9,7,7 | 5,13,4,6,9,4,5 from left to right. */**/*** P <0.05/0.01/0.001 for independent-samples median test with correction for multiple comparisons. Data are means \pm s.e.m.

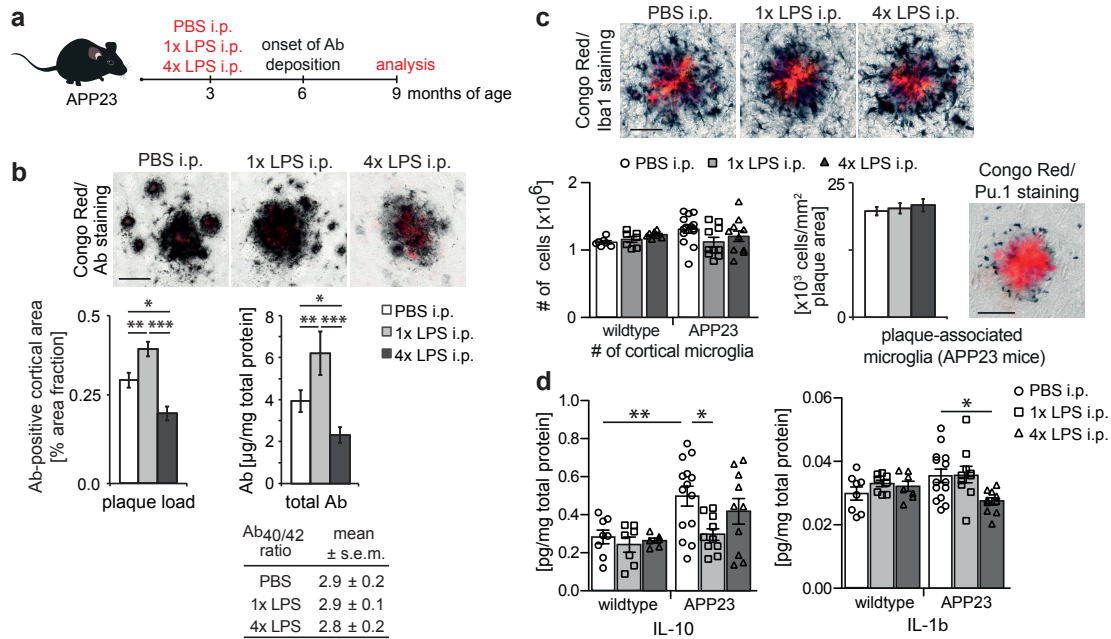


Figure 2: Cerebral β -amyloidosis is altered after peripheral immune stimulation. **a**, Experimental design. **b**, Analysis of cortical amyloid- β plaque load ($n=22,10,10$ animals) and protein levels ($n=14,10,10$ animals). **c**, Analysis of total cortical and plaque-associated microglia ($n=7,7,7,14,10,10$ animals) and **d**, cytokine levels of IL-10 and IL-1 β in wildtype and APP23 mice ($n=8,8,7$ and $n=14,10,10$ animals). Scale bar: 50 μ m. ******/*******/******** $P < 0.05/0.01/0.001$ for one-way (b) and two-way ANOVA (c/d) with Tukey correction. Data are means \pm s.e.m.

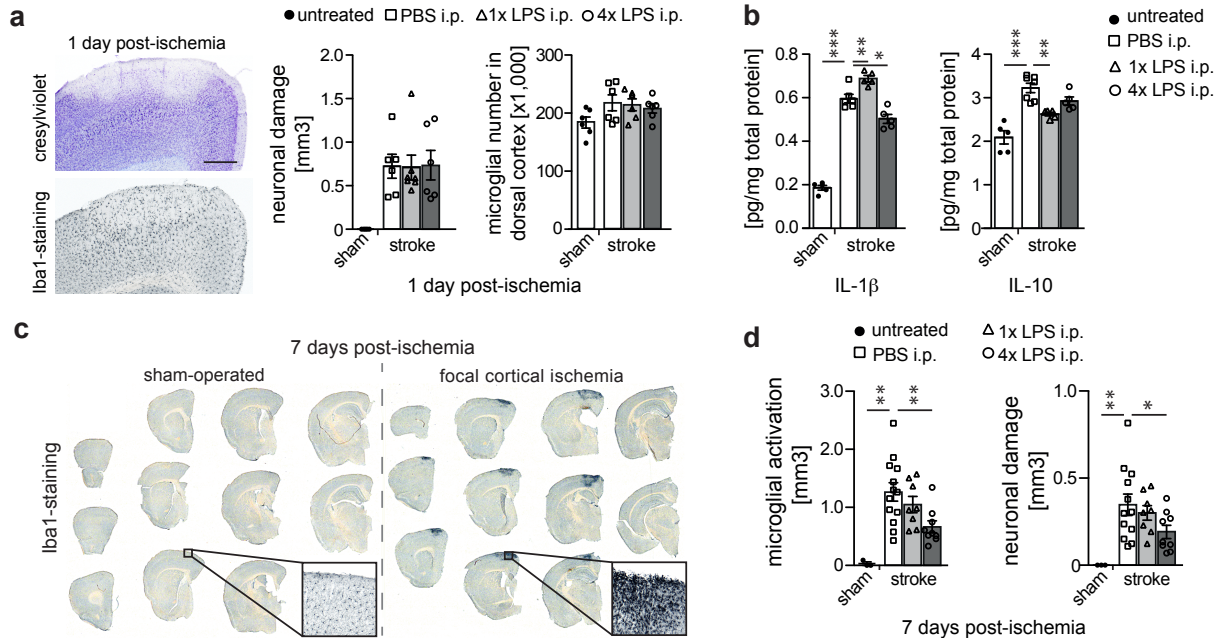


Figure 3: Stroke pathology is altered after peripheral immune stimulation. Pathological features of brain ischemia induced one month after intraperitoneal injection with 1x or 4xLPS. **a**, Neuronal damage (cresylviolet, $n=6,6,6,7,6$ animals), microglial numbers (Iba1-positive, $n=6,6,6$ animals) and **b**, cytokine profiles one day post-ischemia ($n=5,7,5,5$ animals). **c**, Overview of microglial activation in the infarct and **d**, quantification of neuronal damage and microglial activation seven days post-ischemia ($n=3,13,8,9$ animals). Scale bar: 500 μ m. ******/*******/******** $P < 0.05/0.01/0.001$ for one-way ANOVA with Tukey correction. Data are means \pm s.e.m.

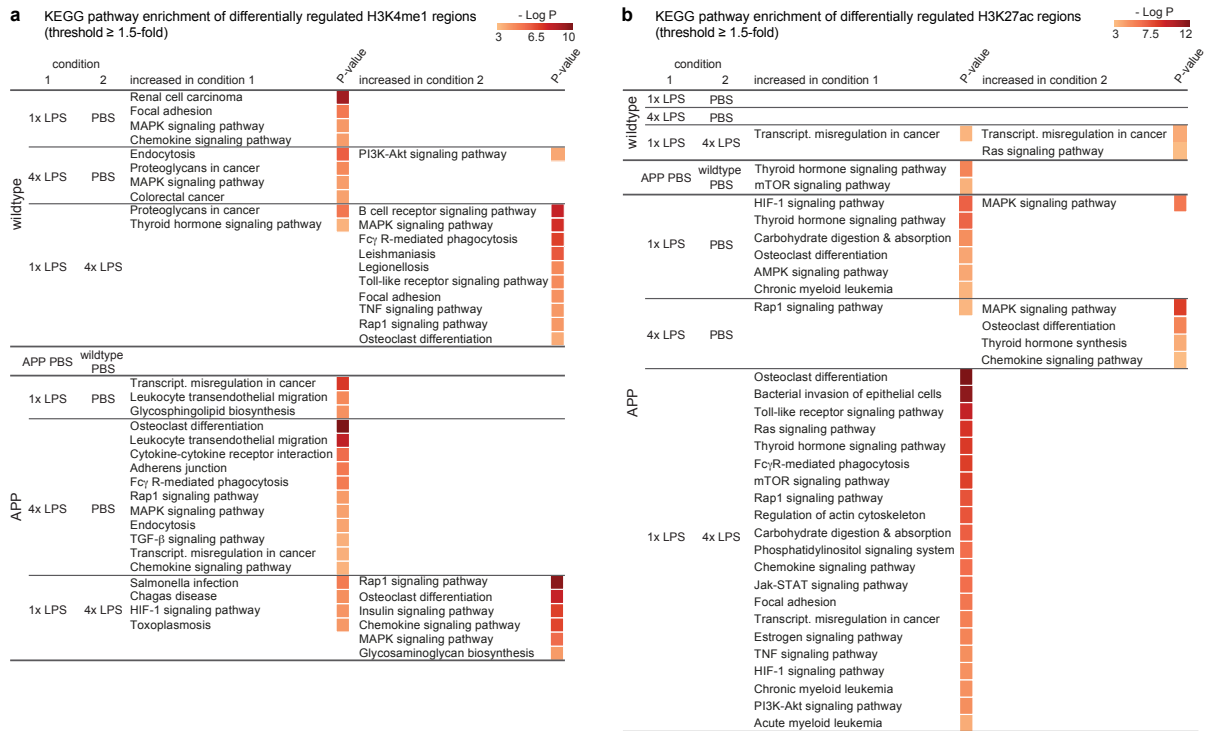


Figure 4: The microglial enhancer repertoire 6 months after immune stimulation. Pathway enrichment of enhancers (with Benjamini-Hochberg correction) with differentially regulated H3K4me1 (a) and H3K27ac (b) levels (based on nearest gene; cumulative Poisson P-value <0.0001). n=2 replicates (8-10 animals/replicate).

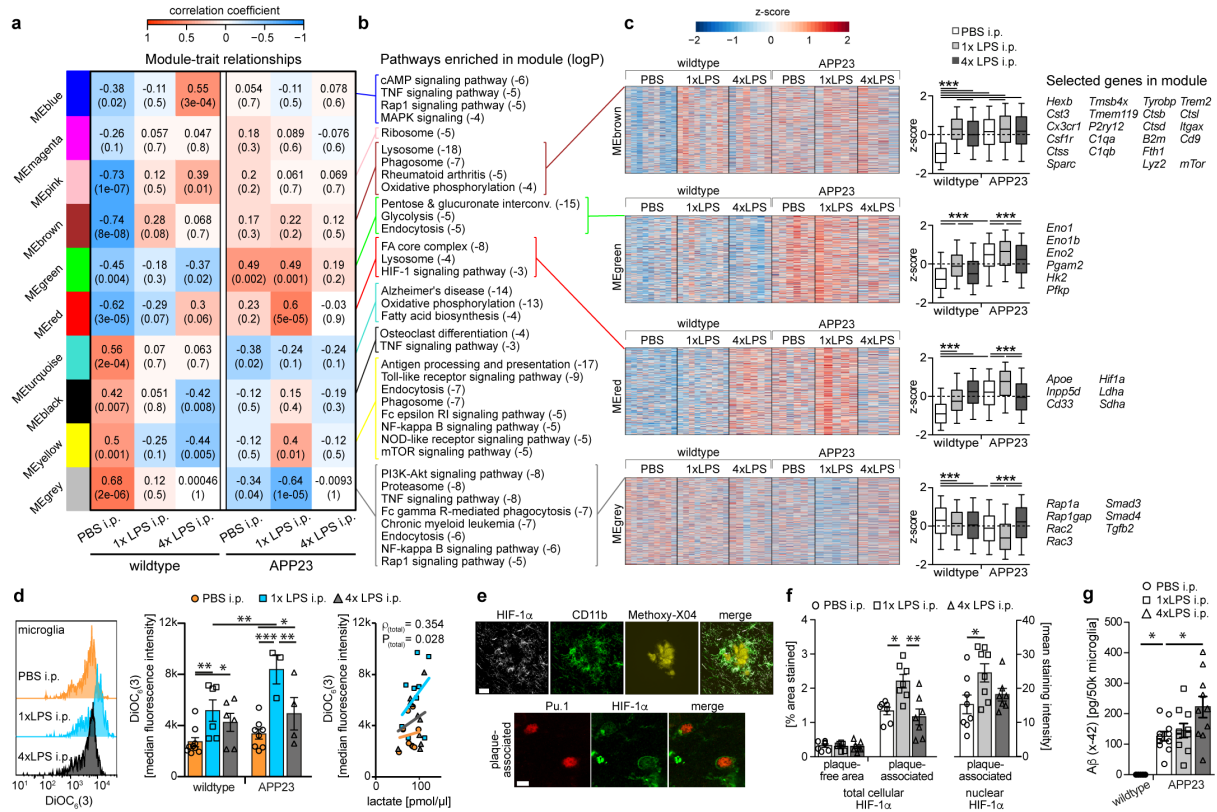
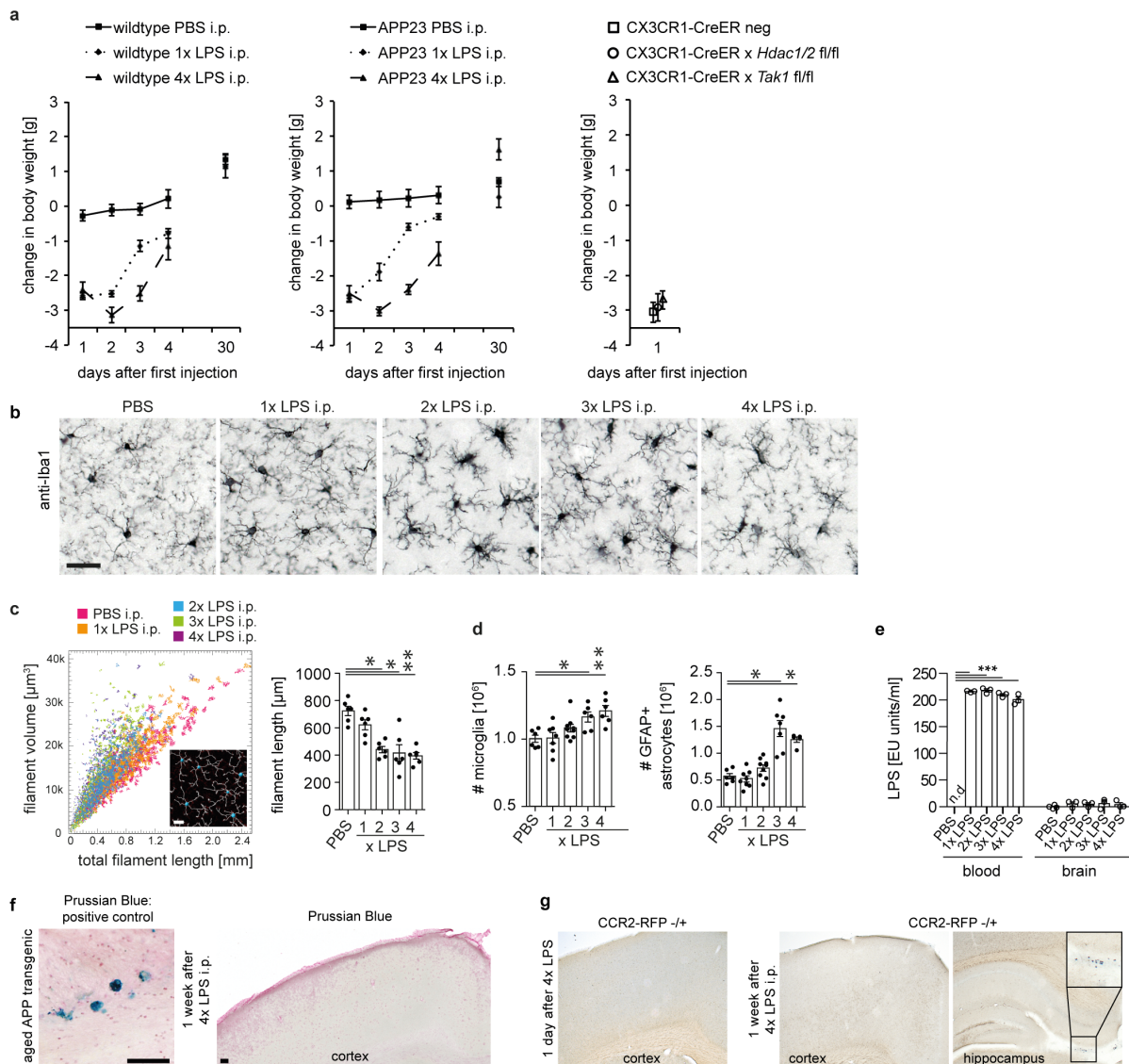
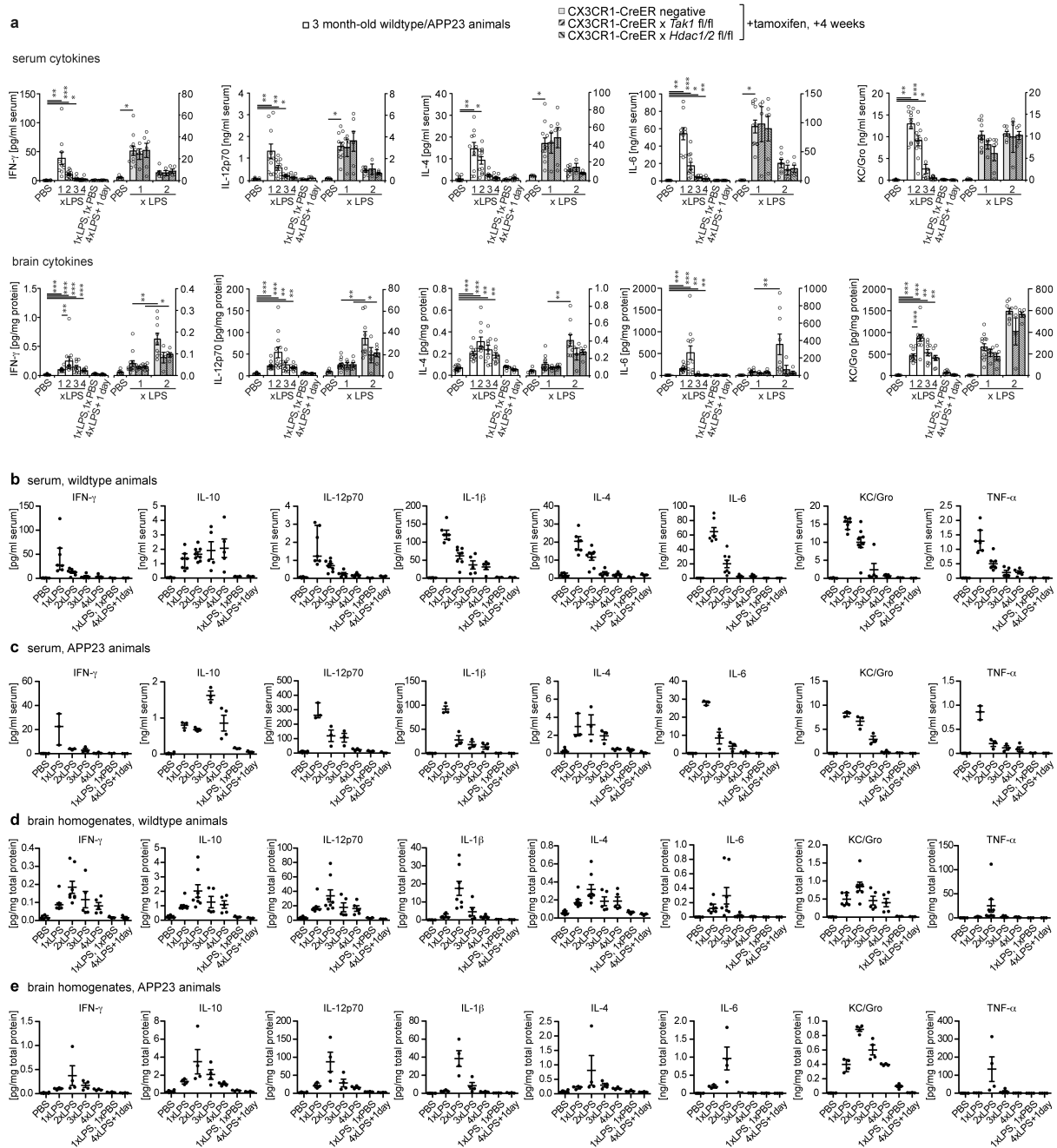


Figure 5: Microglial gene expression and function 6 months after immune stimulation.
a, Weighted gene correlation network analysis (top: correlation coefficient; bottom: P-value; n=9,9,6,6,5,4 animals). **b**, Selected KEGG pathways enriched in modules. **c**, Heatmaps of genes within modules, z-scores (boxplot whiskers: 5-95th percentile; n=1601,990,949,3543 genes in modules) and selected genes. **d**, Microglial mitochondrial membrane potential (left/middle; n=9,6,6,8,3,4 animals) and Pearson's correlation with lactate release (right; n=11,10,10 animals). **e**, Staining for *top*: HIF-1 α , microglia (CD11b) and amyloid plaques (Methoxy-X04) and *bottom*: HIF-1 α and microglial nuclei (Pu.1; single confocal plane) in brain sections from 9-month-old animals. Scale bars: 20/5 μ m (top/bottom). **f**, Total cellular (n=7,7,7 animals) and nuclear (n=8,8,7 animals) HIF-1 α staining intensity. **g**, Microglial A β content (n=5,11,10,10 animals). */**/** P<0.05/0.01/0.001 for one-way ANOVA with Tukey correction. Data are means \pm s.e.m.



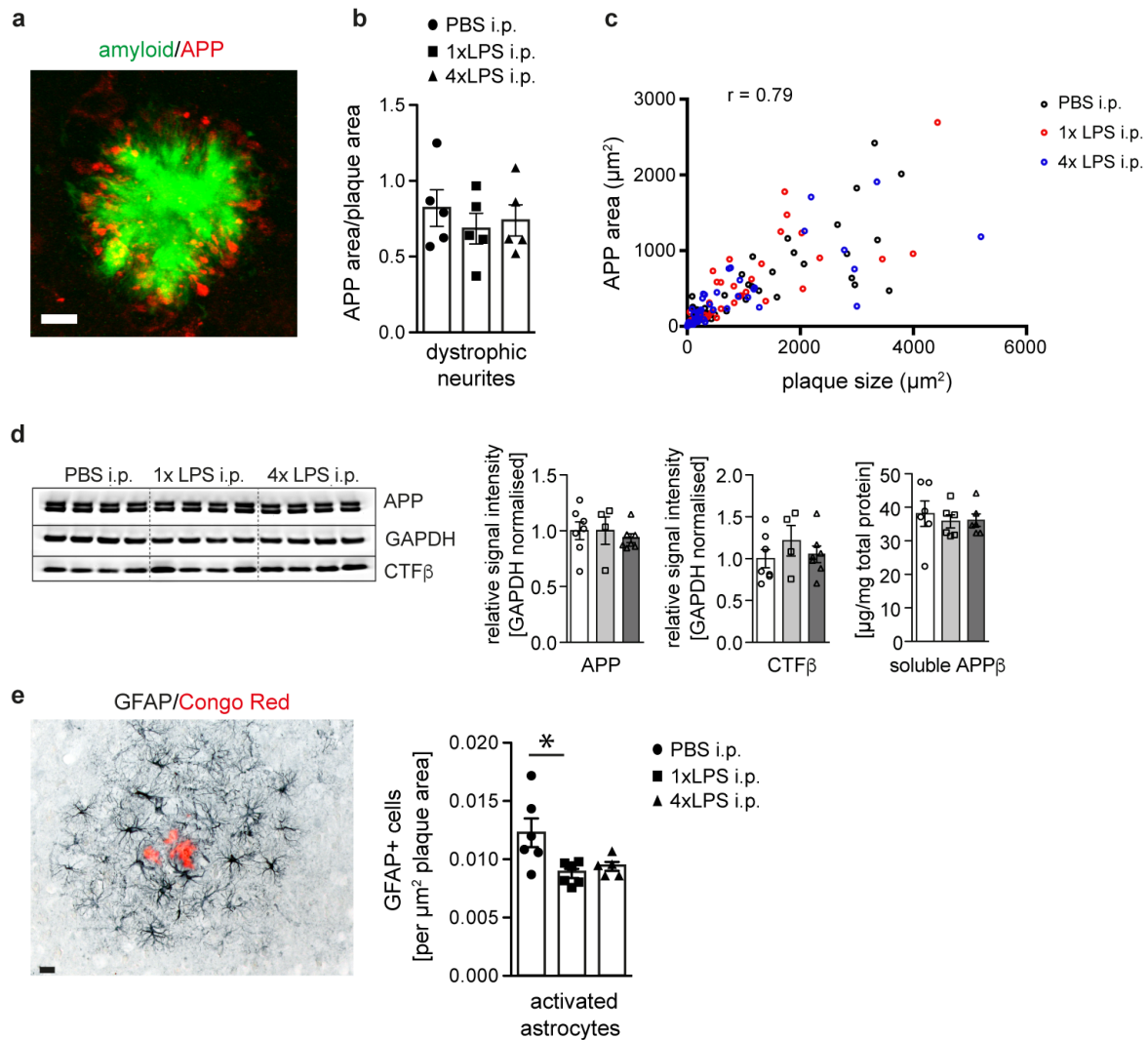
Extended Data Figure 1: Acute responses to LPS injections.

a, Weight changes after injection of lipopolysaccharides (LPS) (wildtype animals: n=11,11,11,11,4 for PBS, n=9,9,9,8,7 for 1xLPS, n=10,10,10,10,7 for 4xLPS; APP animals: n=14,14,14,14,7 for PBS, n=8,8,8,5,5 for 1xLPS; n=10,10,10,10,10 for 4xLPS; Cre animals n=5,5,4). **b/c**, Morphological changes in microglia (n=6,6,6,6 animals). Scale bar: 50 μ m. **d**, Numbers of microglia and activated (GFAP⁺) astrocytes (microglia n=6,7,8,6,6 animals, astrocytes n=6,8,9,7,5 animals). **e**, Blood and brain levels of LPS after daily injections with 500 μ g/kg bodyweight (n=4,3,3,3,3 animals). **f**, Assessment of iron entry from the blood (detected by Prussian Blue staining) shows positive staining in an aged (>25 months) APP transgenic animal, but not after repeated intraperitoneal LPS injections (n=3 mice analysed). **g**, In mice expressing red fluorescent protein (RFP) under the 'type 2 CC chemokine receptor' (*Ccr2*) promoter, no entry of CCR2-expressing blood monocytes is detected after repeated LPS injection (staining for RFP; insert shows RFP-positive monocytes in the choroid plexus; n=3 mice analysed). Scale bar: 100 μ m. Data are means \pm s.e.m. */**/** P < 0.05/0.01/0.001 for one-way ANOVA with Tukey correction.



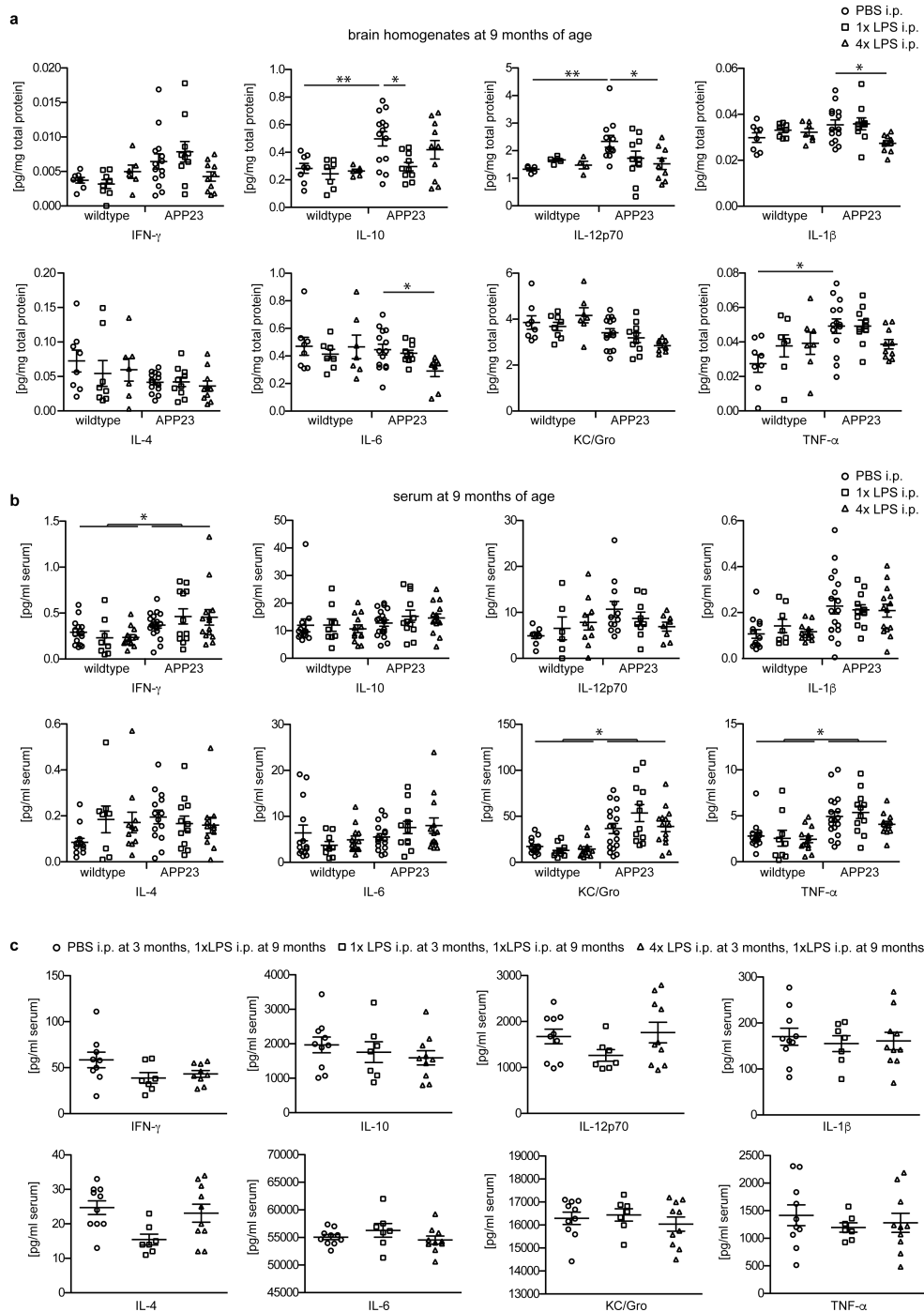
Extended Data Figure 2: Cytokine response after acute LPS injections.

a, Additional cytokines (cp. Fig.1) analysed in the serum (top) and brain (bottom) 3h after each daily intraperitoneal lipopolysaccharide (LPS) injection on four consecutive days in 3-month-old mice (control animals received PBS injections; n=16,11,12,9,9,7 | 5,13,4,6,9,4,5 mice for groups from left to right). **b/c**, Cytokine response in the blood only in wildtype (b, n=6,7,8,5,5,3,3 animals) or APP23 (c, n=10,3,3,3,4,3,3 animals) mice. **d/e**, Cytokine response in the brain only in wildtype (d, n=6,7,8,5,5,3,3 animals) or APP23 (e, n=10,4,4,4,4,4,4 animals) mice. Data are means± s.e.m. */**/** *P*<0.05/0.01/ 0.001 for independent-samples median test with correction for multiple comparisons.



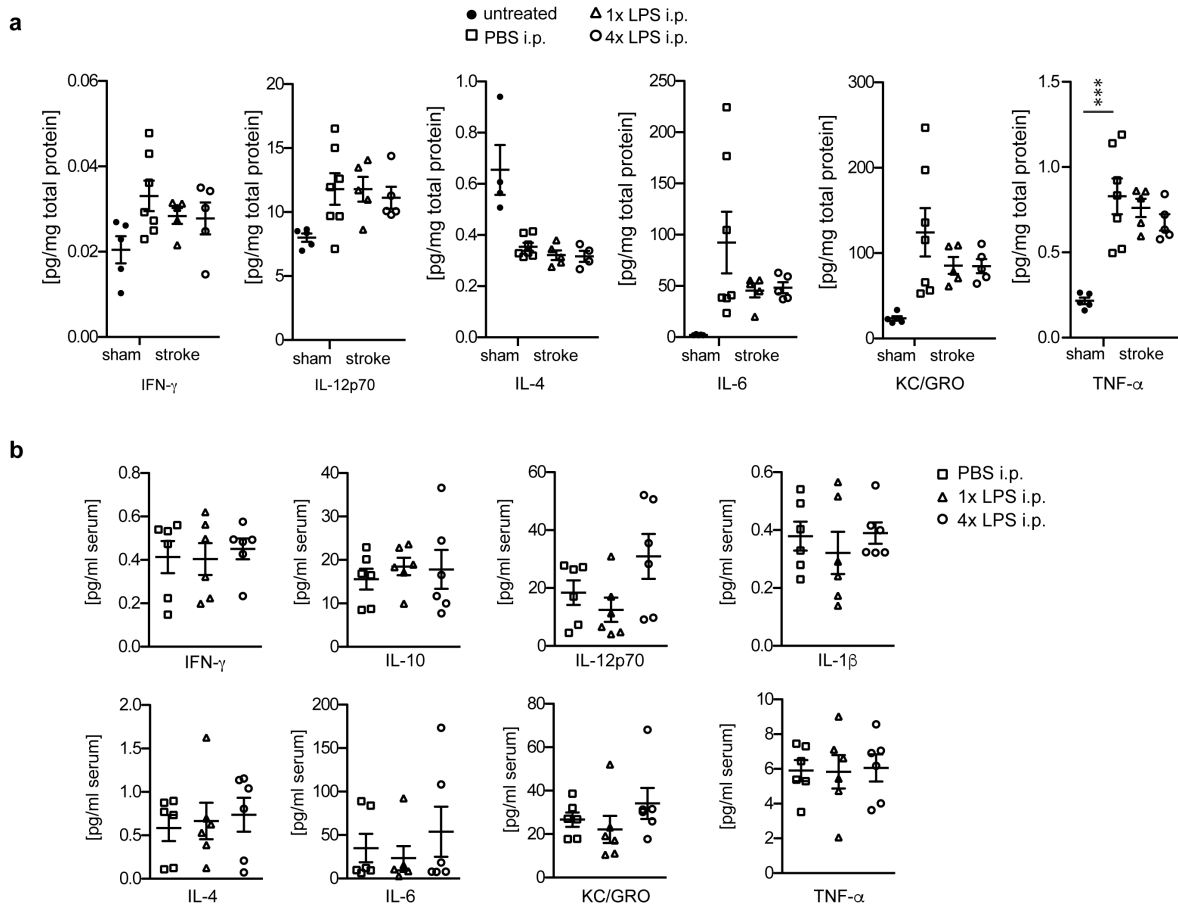
Extended Data Figure 3: APP levels and processing, neuritic dystrophy and astrocyte activation in 9-month-old APP23 animals.

a/b, Micrograph of fluorescent staining for amyloid plaque (Methoxy-X04; green) and amyloid precursor protein (APP; red) shows neuritic dystrophy surrounding the amyloid deposit, which is unchanged by LPS treatments (b; $n=5,5,5$ animals). **c**, Overall Pearson's correlation of plaque size with neuritic dystrophy ('APP area'; $n=49,39,42$ plaques for PBS/1xLPS/4xLPS groups). **d**, Western Blotting analysis (for gel source data, see Supplementary Figure 1) of brain homogenates for amyloid precursor protein (APP) and C-terminal fragment- β (CTF β ; $n=7,4,7$ animals), and soluble APP β ELISA ($n=6,6,6$ animals). **e**, Micrograph of activated astrocytes (glial fibrillar acidic protein: GFAP) surrounding an amyloid plaque (Congo Red) and quantification of the number of plaque-associated GFAP-positive astrocytes ($n=6,6,5$ animals). Scale bar: 10 μm in (a), 20 μm in (e). Data are means \pm s.e.m. * $P < 0.05$ for one-way ANOVA with Tukey correction.



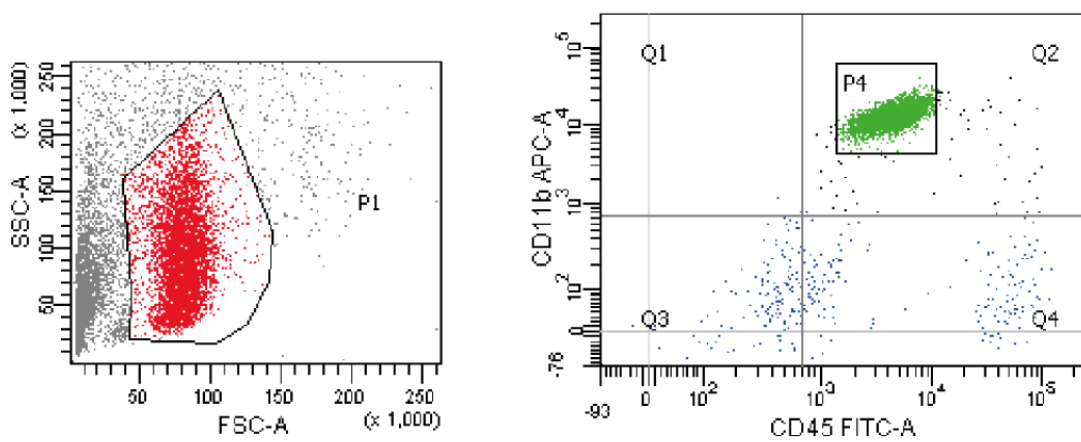
Extended Data Figure 4: Cytokine levels in 9-month-old animals

a, Cytokine measurements in brain homogenates of 9-month-old wildtype (n=8,8,7 animals) and APP23 (n=14,10,10 animals) mice treated i.p. with 1x or 4xLPS at 3 months of age. **b**, Cytokine measurements in the serum of 9-month-old wildtype (WT; n=14,9,13 animals) and APP23 (APP; n=18,12,14 animals) mice after i.p. stimulation with 1x or 4xLPS at 3 months of age. **c**, Cytokine measurements in the serum of wildtype animals stimulated i.p. with 1x or 4xLPS at 3 months of age and re-stimulated with an additional LPS injection (500 µg/kg) at 9 months of age (n=10,7,10 animals). Data are means±s.e.m. */** $P < 0.05/0.01$ for two-way ANOVA with Tukey correction. In (b) a significant main effect for genotype is indicated by bars spanning all conditions of the same genotype.



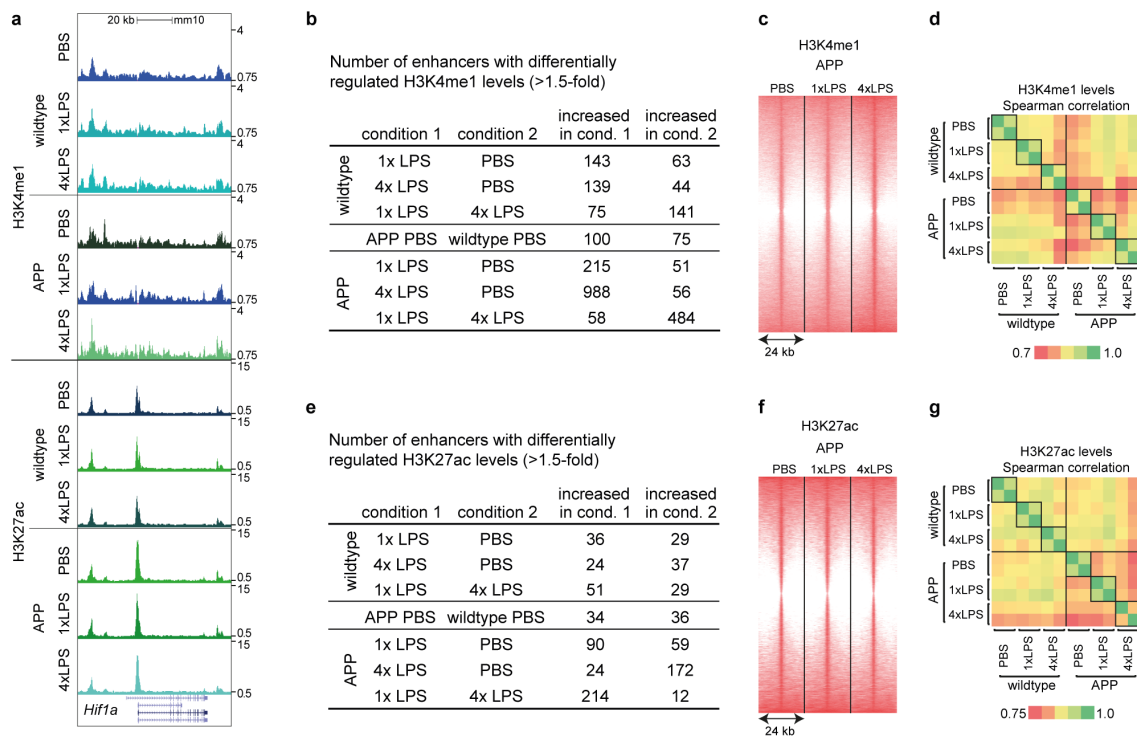
Extended Data Figure 5: Cytokine levels after brain ischemia and in blood of 4-month-old animals.

Three-month-old animals were i.p. injected with 1x or 4xLPS and incubated for 4 weeks before receiving a stroke. **a**, Cytokine measurements in brain homogenates 24h after stroke (n=5,7,5 animals). **b**, Cytokine measurements in the serum (n=6,6,6 animals). Data are means \pm s.e.m. *** P<0.001 for one-way ANOVA with Tukey correction.



Extended Data Figure 6: Microglial sorting strategy.

Microglia were sorted as CD11b^{high} and CD45^{low} cells (population P4) from 9-month-old APP23 animals or wildtype littermates following i.p. injections of 1x or 4xLPS at 3 months of age.



Extended Data Figure 7: Analysis of microglial enhancers.

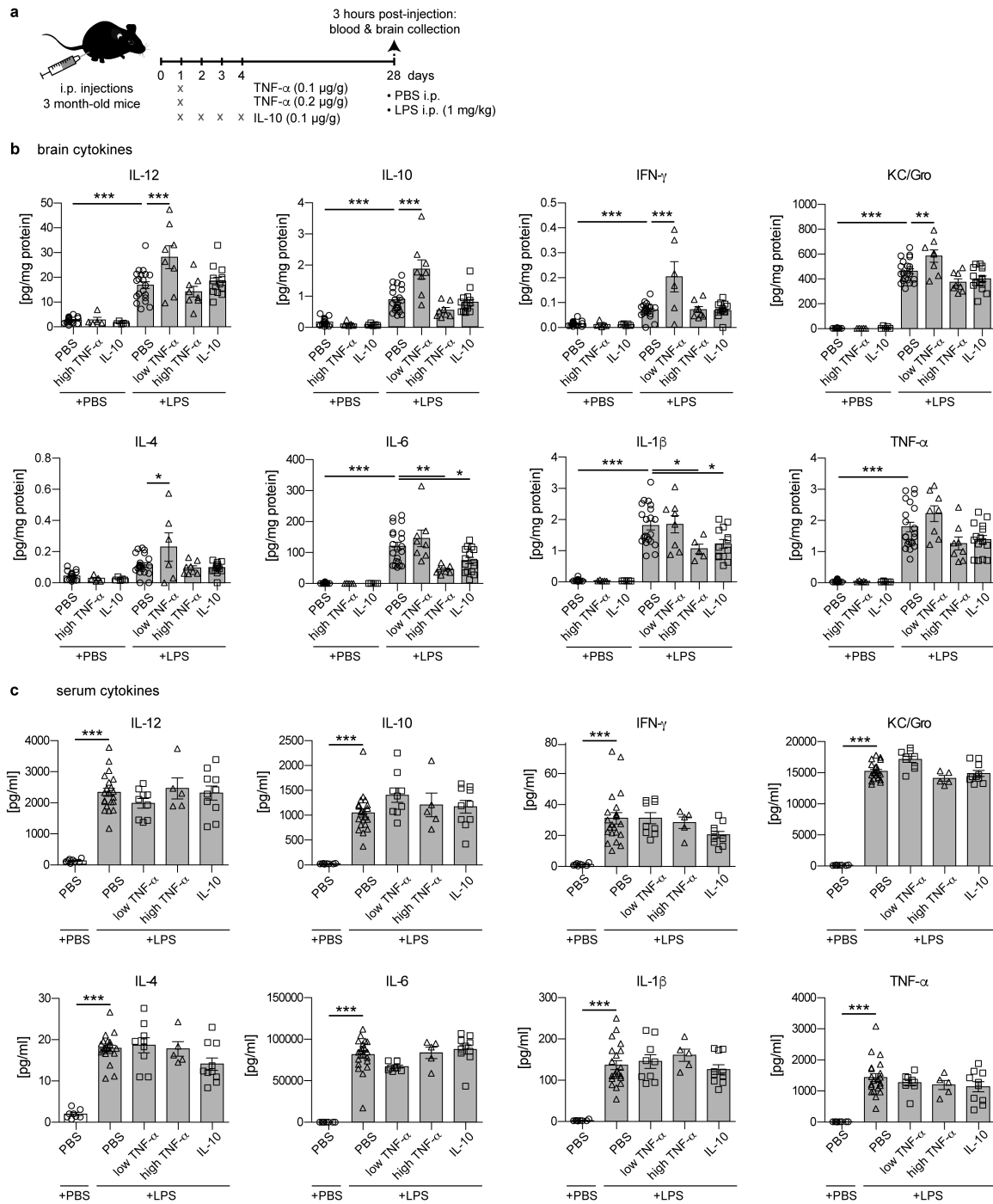
Microglial enhancers were analysed in 9-month-old wildtype and APP23 (APP) mice treated intraperitoneally with 1x or 4xLPS at 3 months of age. **a**, Exemplary UCSC browser images of genomic region around the *Hif1a* gene (normalised to input and library dimension). **b**, Numbers of regions with differentially regulated H3K4me1 levels. **c**, Heatmaps of H3K4me1 regions (centred on H3K27ac peaks). **d**, Pairwise correlations between the two replicates of H3K4me1 read densities in differentially regulated regions. **e-g**, Analyses of H3K27ac levels analogous to (b-d) for H3K4me1. n=2 replicates (8-10 animals/replicate); differential enhancers showed a cumulative Poisson P-value <0.0001; Benjamini-Hochberg correction was applied for pathway enrichment.

| a | | motifs enriched in all active enhancers (random background): | | | | Known motifs | | % Sequences with Motif | | De novo motifs | | | |
|---|--|--|---------|---------|------------|--------------|---------|------------------------|------------|----------------|---------|---------|------------|
| | | Best Match | P-value | Targets | Background | Best Match | P-value | Targets | Background | Best Match | P-value | Targets | Background |
| | | PU.1(ETS) | 1e-624 | 26.58% | 12.58% | Sfp1 | 1e-946 | 39.65% | 19.51% | | | | |
| | | ELF5(ETS) | 1e-549 | 32.44% | 17.80% | PU.1:IRF8 | 1e-101 | 48.30% | 40.82% | | | | |
| | | SpiB(ETS) | 1e-511 | 14.65% | 5.42% | Mef2a | 1e-91 | 10.79% | 6.90% | | | | |
| | | ETS1(ETS) | 1e-492 | 39.47% | 24.34% | RUNX2 | 1e-78 | 41.54% | 35.16% | | | | |
| | | ETV1(ETS) | 1e-471 | 47.55% | 31.83% | Foxo1 | 1e-70 | 29.13% | 23.68% | | | | |

| b | | comparison known and de novo motifs enriched in enhancers of condition 1 | | | | | | known and de novo motifs enriched in enhancers of condition 2 | | | | | |
|--------------|-----------------|--|------------|---------|------------------------|---------|----------------|---|---------|------------------------|------------|--|--|
| condition 1 | condition 2 | Motif | Best match | P-value | % Sequences with Motif | | Motif | Best match | P-value | % Sequences with Motif | | | |
| | | | | Targets | Background | Targets | Background | | | Targets | Background | | |
| APP PBS | wildtype PBS | AGATCAAAAG | TCF3 | 1e-06 | 6.80% | 5.86% | TGTCAG | TGIF2 | 1e-14 | 69.21% | 65.97% | | |
| | | AGCTTTGAAC | TCF3 | 1e-36 | 0.58% | 0.10% | GTGCA | TGIF1 | 1e-08 | 66.14% | 63.66% | | |
| | | ATCACCCCAE | SREBP1a | 1e-03 | 4.69% | 4.16% | AACCCCTCTCA | TGIF2 | 1e-40 | 0.30% | 0.01% | | |
| | | CACACGGATGA | SREBP1a | 1e-34 | 0.33% | 0.04% | GTTCCGAGAT | IRF4 | 1e-50 | 0.50% | 0.04% | | |
| | | AGTGAACCC | IRF4 | 1e-03 | 11.90% | 10.96% | ATGAACTGC | IRF4 | 1e-23 | 0.26% | 0.03% | | |
| | | GAAAAATTTC | IRF4 | 1e-25 | 0.27% | 0.04% | TGCTCTCTT | Smad2/3 | 1e-29 | 1.03% | 0.32% | | |
| | | XGLAAAAATAG | Mef2c | 1e-03 | 12.17% | 11.31% | TCAGACATCCA | Smad3 | 1e-26 | 0.28% | 0.03% | | |
| | | TGTATGTATG | Mef2b | 1e-57 | 0.53% | 0.05% | CGAGACAA | Smad2 | 1e-19 | 1.77% | 0.92% | | |
| | | | | | | | CTATCCGCTCTT | ATF1 | 1e-26 | 0.28% | 0.03% | | |
| | | | | | | | AGGAAATAT | ATF1 | 1e-25 | 0.27% | 0.03% | | |
| APP 1xLPS | APP 4xLPS | ATTGSCAAG | CEBPb | 1e-08 | 13.68% | 12.23% | AGAGCAAGTG | PU.1(ETS) | 1e-10 | 24.57% | 22.45% | | |
| | | GTGTGCGAA | CEBPb | 1e-02 | 16.62% | 15.82% | GGAAATGAAAT | PU.1:IRF8 | 1e-04 | 8.96% | 8.11% | | |
| | | GCTTATCTC | GATA2 | 1e-06 | 15.98% | 14.62% | GGAAATGAAAT | PU.1:IRF | 1e-03 | 38.94% | 37.61% | | |
| | | SAGATAAGG | GATA1 | 1e-05 | 14.26% | 13.10% | GTGCTGCTC | PU.1(ETS) | 1e-17 | 0.37% | 0.10% | | |
| | | AGATAAAG | GATA4 | 1e-04 | 24.00% | 22.65% | GCTGATCAGCA | MafK | 1e-04 | 7.18% | 6.42% | | |
| | | GCATAAAG | GATA3 | 1e-04 | 34.99% | 33.52% | GGATCAGCAATL | MafF | 1e-02 | 6.29% | 5.77% | | |
| | | GCCTATCAGCA | GATA4 | 1e-43 | 0.32% | 0.03% | TGCTGACTCA | MafA | 1e-02 | 22.71% | 21.88% | | |
| | | ATACCTGC | HIF-1b | 1e-05 | 22.67% | 21.23% | TTGTAATAAAA | MafB | 1e-52 | 0.30% | 0.02% | | |
| | | TACCTGC | HIF-1a | 1e-02 | 4.20% | 3.77% | GTGTGCTGAGAT | MafA | 1e-31 | 0.26% | 0.03% | | |
| | | GTACGTAC | HIF-1a | 1e-24 | 0.69% | 0.23% | AGTGAACCA | IRF4 | 1e-03 | 11.89% | 11.04% | | |
| APP 1xLPS | APP 4xLPS | GCCTGTA | ARNT:HIF1A | 1e-17 | 0.27% | 0.06% | CCAGAACCTT | IRF4 | 1e-45 | 0.27% | 0.02% | | |
| | | CCCTGAGCA | AP-2gamma | 1e-04 | 22.16% | 20.85% | TGTCAG | TGIF2 | 1e-02 | 67.78% | 66.88% | | |
| | | ATSCCTGAGCC | AP-2alpha | 1e-03 | 16.77% | 15.77% | GTGCA | TGIF1 | 1e-02 | 64.71% | 63.81% | | |
| | | GCCTTA | MYB | 1e-04 | 39.46% | 38.06% | GGGGGAGC | E2F | 1e-02 | 6.96% | 6.39% | | |
| | | ATATTAACIG | MYB | 1e-53 | 0.56% | 0.07% | GGGGGAG | E2F | 1e-02 | 1.93% | 1.65% | | |
| | | AGATCAAGTGG | MYB | 1e-53 | 0.30% | 0.01% | GGATCAAG | c-Jun | 1e-02 | 6.18% | 5.71% | | |
| | | GGGGAATCT | TEAD4 | 1e-04 | 18.79% | 17.65% | ATGACCTCAAG | JunD | 1e-02 | 1.85% | 1.59% | | |
| | | CGGACATTC | TEAD4 | 1e-58 | 0.40% | 0.03% | | | | | | | |
| | | AGTCAAAAG | TCFL2 | 1e-03 | 2.39% | 1.98% | | | | | | | |
| | | GACTAGAAAG | TCFL2 | 1e-41 | 0.44% | 0.06% | | | | | | | |
| APP 1xLPS | APP PBS | GGCTGCTGC | Smad4 | 1e-02 | 42.15% | 41.21% | | | | | | | |
| | | TAGGCTCTG | Smad4 | 1e-36 | 0.54% | 0.10% | | | | | | | |
| | | ATACCTGC | HIF-1b | 1e-14 | 22.67% | 20.26% | ATGATCAAT | Atf4 | 1e-04 | 5.60% | 4.89% | | |
| | | TACGTSSE | HIF-1a | 1e-03 | 4.20% | 3.67% | GATTCCTCAG | Atf1 | 1e-47 | 0.43% | 0.04% | | |
| | | TCACATAA | HIF-1a | 1e-18 | 0.28% | 0.07% | GCTGATCAGCA | MafK | 1e-04 | 7.55% | 6.76% | | |
| | | AGTCAAGGCA | RAR:RXR | 1e-05 | 5.71% | 4.97% | TGCTGACTCA | MafA | 1e-03 | 23.32% | 22.13% | | |
| | | AGTCAAGGCA | RAR:RXR | 1e-04 | 3.02% | 2.51% | GGATCAGCAATL | MafF | 1e-02 | 6.49% | 5.92% | | |
| | | SAGATAAAG | GATA4 | 1e-04 | 24.00% | 22.76% | AGAGCAAGTG | PU.1(ETS) | 1e-02 | 23.81% | 22.80% | | |
| | | GCCTTATCTC | GATA2 | 1e-03 | 15.98% | 15.04% | GGAAATGAAAT | PU.1:IRF8 | 1e-02 | 8.85% | 8.27% | | |
| | | AGATAAAG | GATA3 | 1e-03 | 34.99% | 33.77% | GGAAATGAAAT | PU.1:IRF | 1e-02 | 39.43% | 38.50% | | |
| APP 4xLPS | APP PBS | SAGATAAAG | GATA1 | 1e-02 | 14.26% | 13.45% | GGGGGAGATGATCT | GATA3 | 1e-02 | 2.99% | 2.67% | | |
| | | ATATCATCTCC | MYC | 1e-59 | 0.35% | 0.01% | GCATAGCTAAG | GATA1 | 1e-51 | 0.40% | 0.02% | | |
| | | CCGATGTG | MYC | 1e-33 | 1.28% | 0.50% | TATCTCAA | GATA3 | 1e-17 | 1.95% | 1.12% | | |
| | | GCTCATGGG | MYC | 1e-29 | 0.27% | 0.04% | | | | | | | |
| | | AAAGSGAAATG | SpiB | 1e-15 | 13.15% | 11.19% | CCCTGAGCA | AP-2gamma | 1e-06 | 22.50% | 20.82% | | |
| | | CCCTCTCTCTT | SpiB | 1e-29 | 0.31% | 0.04% | ATGATCAAT | AP-2alpha | 1e-05 | 17.06% | 15.76% | | |
| | | ATGATCAAG | ATF3 | 1e-04 | 15.98% | 14.83% | GACCAAI | Atf4 | 1e-17 | 0.34% | 0.08% | | |
| | | GGTCAAGTCA | ATF7 | 1e-02 | 9.72% | 9.05% | XGLAAAAATAG | Mef2c | 1e-05 | 12.17% | 11.05% | | |
| | | GTGACCTCA | ATF1 | 1e-02 | 13.83% | 13.05% | CGAAAAATAG | Mef2a | 1e-02 | 10.90% | 10.14% | | |
| | | ATGACGCTAAG | JunD | 1e-04 | 1.85% | 1.47% | AGATCAAAAG | Tcf4 | 1e-04 | 11.57% | 10.53% | | |
| APP 4xLPS | APP PBS | ATGACGCTAAG | c-Jun | 1e-02 | 6.39% | 5.92% | TCAGAGGCA | Tcf4 | 1e-61 | 0.45% | 0.03% | | |
| | | GGCTGCAAG | MEIS1 | 1e-02 | 42.34% | 41.46% | AGCTTTGAAC | Tcf3 | 1e-37 | 0.76% | 0.17% | | |
| | | TGACAGCAACC | MEIS1 | 1e-43 | 0.34% | 0.04% | ATTSCAAG | CEBPb | 1e-03 | 13.80% | 12.81% | | |
| | | | | | | | ATACCGA | CEBPg | 1e-13 | 0.16% | 0.02% | | |
| | | | | | | | GCCTTA | Myb | 1e-02 | 39.82% | 38.67% | | |
| | | | | | | | GCAGTCAGAG | Myb | 1e-68 | 0.39% | 0.01% | | |
| | | | | | | | ALLTGTATCTC | Gata5 | 1e-97 | 0.51% | 0.02% | | |
| | | | | | | | CTTATCCTGATA | Gata6 | 1e-45 | 0.36% | 0.02% | | |
| | | | | | | | CATAGTCT | Smad3 | 1e-27 | 6.22% | 4.28% | | |
| | | | | | | | GCTCTCAG | Smad2 | 1e-16 | 2.08% | 1.25% | | |

Extended Data Figure 8: Transcription factor motif analysis of active enhancer regions.

Motif analysis was performed for selected conditions to identify transcription factors involved in the differential activation of enhancers (using putative enhancer regions present in both replicates within 500 bp around enhancer peaks). **a**, For all active enhancers, motif analysis was performed using the union H3K27ac peak file and standard background (random genomic sequence). **b**, Pairwise comparisons between conditions, using the first condition's H3K27ac peak file as input and the second condition's peak file as background. As motif enrichment was often relatively low, the analysis was focussed on transcription factor (families), whose motifs occurred at least twice in 'known' (black) and 'de-novo' motifs (blue). Motifs are identified by HOMER software using hypergeometric testing (no adjustment for multiple comparisons was made).



Extended Data Figure 9: Peripherally applied cytokines induce immune memory in the brain.

a, Experimental design. **b**, Cytokine responses in the brain, four weeks after peripheral cytokine application ($n=17,5,5,21,8,8,15$ animals). Note that TNF- α dose-dependently enhances (low dose) or decreases (high dose) certain cytokines. Similar to high dose TNF- α , certain cytokines are also reduced by peripheral application of IL-10 four weeks earlier. **c**, Cytokine responses in the periphery are unaffected ($n=8,21,9,5,10$ animals). Data are means \pm s.e.m. */**/** $P<0.05/0.01/0.001$ for one-way ANOVA with Tukey correction.

**Lack of MFG-E8 reduces pathology in mouse models of cerebral
 β -amyloidosis**

Karoline Degenhardt*, Jessica Wagner*, Konstantina Kapolou, Domenico Del Turco,
Thomas Deller, Mathias Jucker, Jonas J. Neher

Manuscript in preparation

Lack of MFG-E8 reduces pathology in mouse models of cerebral β -amyloidosis

Karoline Degenhardt^{1,2,3*}, Jessica Wagner^{1,2,3*}, Konstantina Kapolou³, Domenico Del Turco⁴,
Thomas Deller⁴, Mathias Jucker^{1,2}, Jonas J. Neher^{1,2}

¹Department of Cellular Neurology, Hertie-Institute for Clinical Brain Research, University of Tübingen, D-72076 Tübingen, Germany. ²German Center for Neurodegenerative Diseases (DZNE), Tübingen, D-72076 Tübingen, Germany. ³Graduate School of Cellular and Molecular Neuroscience, University of Tübingen, D-72074 Tübingen, Germany. ⁴Institute of Clinical Neuroanatomy, J.W. Goethe-University, Theodor-Stern-Kai 7, D-60590 Frankfurt/Main, Germany.

Acknowledgement: We would like to thank Andrea Bosch, Ulrike Obermüller, Lisa Häsler and Marius Lambert for experimental help. This work was funded by grants from the “Deutsche Forschungsgemeinschaft” (DFG) (NE 1951/2-1).

* These authors contributed equally to this work.

Correspondence: Jonas Neher, E-Mail: Jonas.neher@dzne.de

Abstract

The phagocytic removal of amyloid- β (A β) in Alzheimer's disease (AD) may be able to combat disease progression and is therefore of therapeutic interest. Previously, it was suggested that the protein milk fat globule-EGF factor 8 (MFG-E8) may play a role in the removal of A β via microglia-mediated phagocytosis. Moreover, altered MFG-E8 levels in the brain of AD patients suggest a function of MFG-E8 in the pathology of AD. Here, we report that genetic deletion of MFG-E8 in APP transgenic (tg) mice results in significantly reduced A β levels and plaque load at early stages of cerebral β -amyloidosis, but does not induce alterations in the microglial phagocytosis of A β nor in inflammatory cytokine production. However, immunostaining for MFG-E8 in the brain of APP tg mice showed very strong co-localization with A β plaques and MFG-E8 levels increased both with age and the extent of cerebral β -amyloidosis. Furthermore, electron microscopy confirmed localization of MFG-E8-immunoreactivity to A β fibrils. These data argue against a beneficial effect of MFG-E8 on A β pathology through facilitating the removal of A β , but suggest a microglia-independent interaction between MFG-E8 and A β that accelerates A β plaque formation. Preventing this detrimental interaction between MFG-E8 and A β may therefore provide a novel opportunity for therapeutic interference with A β deposition.

Introduction

The aggregation and deposition of the amyloid- β (A β) peptide in the brain can be a result of increased production and/or impaired clearance. For the rare forms of familial Alzheimer's disease (FAD), it is well known that genetic alterations in the *APP* or *PSEN1/2* genes result in an overproduction of A β ¹⁻⁵. In contrast, for sporadic late-onset AD (LOAD), which accounts for >99 percent of all AD cases⁵, a variety of risk factors such as obesity or type 2 diabetes have been reported^{6,7}. In addition, recent genome-wide association studies (GWAS) have revealed several new susceptibility genes that are associated with innate immunity and inflammation suggesting an immune system dysfunction in LOAD⁸⁻¹⁰. In the brain, microglia are the main immune effector cells; however, for many of the identified risk loci, the exact role in the microglia-mediated immune response is still a matter of debate. Therefore, studies that aim to understand the overall contribution of the innate immune response to the pathogenesis of AD are of great importance to therapeutically target such risk factors.

Our study focused on milk-fat globule-EGF factor 8 (MFG-E8, also known as lactadherin), a bivalent-binding, secretory glycoprotein known for its role in promoting the phagocytic removal of apoptotic neurons in the injured brain¹¹. Moreover, MFG-E8 was previously reported to directly bind A β and initiate its phagocytosis by microglia¹². In particular, genetic deletion of MFG-E8 was shown to decrease phagocytosis of A β by peritoneal macrophages¹². Furthermore, in human post-mortem AD brains, MFG-E8 staining was found to be reduced in areas enriched in A β plaques, suggesting that A β favors accumulation in areas with reduced MFG-E8 production or that MFG-E8 is removed after binding to A β . However, the exact mechanism how MFG-E8 modifies the pathogenesis of AD remains to be elucidated.

To study the *in vivo* contribution of MFG-E8 to A β pathology, we generated two transgenic mouse models of cerebral β -amyloidosis, APPPS1 and APP23, which were deficient for MFG-E8, and analyzed pathological hallmarks. Here we demonstrate that lack of MFG-E8 has no significant effects on the microglia-mediated immune response to cerebral β -amyloidosis, including the phagocytosis of A β . However, contrary to the hypothesis that MFG-E8 may be beneficial for AD pathology, the deficiency of MFG-E8 in mouse models of AD pathology significantly reduced cortical A β plaque burden at early stages of A β deposition. Thus, our results indicate a critical role for MFG-E8 in the initial process of A β aggregation and suggest MFG-E8 as a potential candidate for therapeutic intervention of A β aggregation.

Material and Methods

Mice

APPPS1 (C57BL/6J- Tg(Thy1-APP_{K670N/M671L}) and Thy1-PS1_{L166P}) and APP23 mice (C57BL/6J-Tg(Thy1-APP_{K670N;M671L}) that have been backcrossed with C57BL/6J mice for >20 generations were bred in-house (APP tg mice)^{13,14}. *Mfge8*^{-/-} mice (B6.129P2 Mfge8Gt(KST227)Byg) were obtained from Clotilde Théry, PhD (INSERM U932, Institut Curie, France)¹⁵. Hemizygous APP tg mice were crossed with *Mfge8*^{-/-} mice. The resulting APP tg x *Mfge8*^{+/-} males were crossed with *Mfge8*^{+/-} females to obtain APP tg and non-tg *Mfge8*^{+/+} and *Mfge8*^{-/-} animals.

The mice were maintained under specific pathogen-free conditions. All experiments were performed in accordance with the veterinary office regulations of Baden-Württemberg (Germany) and were approved by the Ethical Commission for animal experimentation of Tübingen, Germany.

Tissue collection

For brain preparation, mice were deeply anesthetized using sedaxylan/ketamine (64 mg/kg//472 mg/kg) and killed by transcardial perfusion with phosphate-buffered saline (PBS). Brains were removed and hemispheres were separated. One half was freshly frozen on dry ice for biochemical analyses, whereas the other half was stored for 24 h in 4 % paraformaldehyde (PFA) in PBS and was then transferred to 30 % sucrose for another 48 h. PFA-fixed hemispheres were frozen in 2-methyl-butane and coronal sections of 25 µm thickness were cut with a freezing sliding microtome (Leica). Cut sections were stored at -20°C in cryoprotectant medium.

Microglia isolation

APPPS1 x *Mfge8*^{+/+} and APPPS1 x *Mfge8*^{-/-} mice were deeply anesthetized and perfused as described. The cerebellum and brain stem were removed from the brain and discarded. The rest of the brain was finely minced in ice-cold Hanks Buffered Salt Solution (HBSS) containing 15 mM HEPES, 0.54 % D-Glucose and 0.1 % DNase weight/volume (w/v). Minced tissue was sequentially homogenized in Dounce and Potter homogenizers to achieve a homogeneous solution. Homogenates were filtered through a 70 µm cell strainer and centrifuged at 300 g for 10 min at 4°C. The resulting pellet was resuspended in 70 % isotonic Percoll solution, overlaid with 37 % and 30 % isotonic Percoll layers and centrifuged for 30 min, 800 g, 4°C. Cells were recovered from the 70/37 % interphase and washed in fluorescence-activated cell sorting

(FACS) buffer (PBS, 2 % fetal calf serum, 10 mM EDTA). Washed cells were resuspended and blocked with Fc block (BD Bioscience) for 10 minutes on ice, followed by staining for 15 min at 4°C with CD11b-APC (1:200, BioLegend) and CD45-Alexa700 (1:200, Sony). CD11b^{high}/CD45^{low} microglia were sorted on a Sony SH800 flow cytometer and collected in FACS buffer containing 25 mM HEPES. Cells were pelleted at 800 g for 7 min and, supernatant was discarded and cells were resuspended in lysis buffer (50 mM Tris pH8, 150 mM NaCl, 5 mM EDTA, phosphatase and protease inhibitors and 1 % Triton X-100) and snap frozen on dry ice.

***In vivo* phagocytosis assay**

Prior to microglia isolation (24 h), 2-and 4-month-old APPPS1 x *Mfge8*^{+/+} and APPPS1 x *Mfge8*^{-/-} mice received an intraperitoneal injection of the amyloid dye Methoxy-X04 (stock: 4 % vol of 10 mg/ml Methoxy-X04 in DMSO, 7.7 % vol CremophoreEL in 88.3 % vol PBS; 17.5 µl/g bodyweight). Microglia were isolated as described above and the proportion of Methoxy-X04-positive microglia was determined by flow cytometry with a MACSQuant[®] Analyzer (Miltenyi Biotec). Microglia from 2-month-old mice were additionally stained with Methoxy-X04 for 15 min (1:250). Background signals of Methoxy-X04 were eliminated after signal subtraction of the analyzed microglia fraction from APPPS1 non-tg mice. Signals of APPPS1 x *Mfge8*^{-/-} were normalized to the APPPS1 x *Mfge8*^{+/+} group of each experiment. The Methoxy-X04-positive fraction of APPPS1 x *Mfge8*^{+/+} was normalized to the mean of the entire experimental group.

Immunostaining

Immunostainings were performed on free-floating sections either using Vectastain Elite ABC kits (Vector laboratories) or fluorescent secondary antibodies. For immunohistochemical (IHC) detection, sections were quenched 30 min with H₂O₂ (0.3 %) prior blocking with the respective antiserum for 1 h. The following primary antibodies were applied over night at 4°C: rabbit anti-Iba1 (WAKO; 1:1,000), rabbit anti-PU.1 (Cell Signaling, 1:1,000 for IHC, 1:250 for immunofluorescence staining (IF)), rat-anti CD68 (AbD Serotec, 1:1,000), goat anti-MFG-E8 (R&D; 1:1,000) and rabbit anti-Aβ (in-house CN6; 1:1,000). Congo-red staining was conducted in accordance to standard protocols. Images were acquired on an Axioplan 2 microscope with Axioplan MRm and AxioVision 4.7 software (Carl Zeiss).

For immunofluorescent staining, sections were incubated with the respective fluorophore-conjugated IgG secondary antibodies (Invitrogen, 1:250). For plaque labeling, Methoxy-X04

staining was applied for 15 min (1:10) on brain sections. For staining of the arteries, sections were incubated 1-2 min with Alexa Fluor 633 hydrazide (1:1,000) as previously described¹⁶. Fluorescent images were acquired using a LSM 510 META (Axiovert 200M) confocal microscope with an oil immersion 63X/1.4NA objective and LSM software 4.2 (Carl Zeiss), using sequential excitation of fluorophores.

For CD68 quantification, z-stacks of three plaques per section (3 sections/animal) stained in parallel were acquired. Methoxy-X04-positive plaques were randomly and blinded chosen. PU.1 staining was used to confirm that CD68 was expressed by microglia. Analysis of signal intensity of CD68 around plaques was performed using ImageJ. Quantification of co-localization of CD68 and Methoxy-X04, as well as reconstruction of 3D images were done with Imaris 8.3.1.

Western Blotting

Fresh frozen hemispheres were homogenized using a Precellys[®] lysing kit at 10 % (w/v) in Tris-HCl buffer (50 mM Tris pH 8, 150 mM NaCl, 5 mM EDTA) containing phosphatase and protease inhibitors (Pierce) and sonicated 3x5 seconds (LabSonic, B. Braun Biotech International GmbH, 0.5 mm diameter sonotrode, cycle 1, amplitude 80).

Total protein of the brain homogenates was quantified with a microplate bicinchoninic acid (BCA) assay (Pierce Biotechnology) and adjusted to 10-15 µg for Western Blot analysis.

For APP, CTF-β and Aβ analysis, samples were diluted in NuPAGE[®] LDS sample buffer (Thermo fisher Scientific Inc.) containing 5 % β-mercaptoethanol, heated at 70°C and run on NuPage Bis-Tris mini gels (Invitrogen). For MFG-E8 levels, samples were treated with urea (final concentration 6 M), diluted in sample buffer (10 % glycerol, 2 % SDS, 2 % β-mercaptoethanol, 0.1 M Tris-HCl pH 8.6) and loaded on a Tris-Tricine 10-20 % gradient gel (Invitrogen). After electrophoresis, gels were transferred to a nitrocellulose membrane in a semi-dry blotting system. Transfer was confirmed by Ponceau-S staining and the membrane was boiled for 5 min in PBS. Blocking was performed with 5 % milk (APP, CTF-β, Aβ) or 5 % donkey serum (MFG-E8) in PBS-T for 1 h. Subsequently, membranes were incubated over night at 4°C with either mouse anti-Aβ (6E10, 1:1,000, Covance Research Products), anti-CTF-β (1:2,000, Sigma-Aldrich) or goat anti-MFG-E8 (R&D, 1:1,000) diluted in PBS-T. Membranes were then probed with the respective secondary horseradish peroxidase (HRP)-labelled antibodies (1:20,000, Jackson ImmunoLaboratories). Protein bands were detected using a chemiluminescent peroxidase substrate (ECL prime, GE Healthcare). Images of the blots were recorded using an ECL imager (Stella 3200, Raytest). Densitometric values of the

protein band intensities were analyzed with the software package Aida (or ImageJ for MFG-E8) and normalized to GAPDH.

ELISA

For quantification of A β by ELISA (Meso Scale Discovery) in brain homogenates or by SIMOA (single Molecule Array, Quanterix) in isolated microglial cells (50 000 cells/sample), samples were pre-treated with formic acid (Sigma-Aldrich, final concentration: 70 % vol/vol), sonicated for 30 seconds on ice, and centrifuged at 25,000 g for 1 hour at 4°C. Supernatants were equilibrated in neutralization buffer (1 M Tris base, 0.5 M Na₂HPO₄, 0.05 % NaN₃ (w/v)). A β was measured by a commercial human (6E10) A β triplex assay (Meso Scale Discovery, MSD) in brain homogenates or with the SIMOA Human A β 42 2.0 Kit (Quanterix) in isolated microglia according to the manufacturer's instructions. Samples and calibrators were measured as duplicates. Brain A β levels were normalized against total protein amount as measured by BCA protein assay.

For microglial cytokine measurements, cells were diluted in 50 μ l Tris-HCl buffer containing 1 % Triton X-100 and phosphatase inhibitor (50 mM Tris pH8, 150 mM NaCl, 5 mM EDTA). Cytokines were recorded in single measurements using the mouse pro-inflammatory panel 1 V-plex plate (MSD).

Electron microscopy

Two-month-old APPPS1 x *Mfge8*^{+/+} and APPPS1 x *Mfge8*^{-/-} mice were deeply anesthetized using sedaxylan/ketamine (64 mg/kg//472 mg/kg) and killed by transcardial perfusion with a fixative containing 4 % PFA, 0.1 % glutardialdehyde in sodium cacodylate buffer (0.2 M, pH 7.4). The brain was removed and post-fixed in 4 % PFA in PBS. Brains were cut with a vibratome (50 μ m) and washed in PBS. Sections were stained according to standard 3,3' diaminobenzidine (DAB) staining protocols. Sections were osmicated (0.5 % OsO₄ in PBS), dehydrated (70 % ethanol containing 1% uranyl acetate) and embedded between liquid release-coated slides. Selected sections were re-embedded in blocks and ultrathin sections were collected and examined using a Zeiss electron microscope (Zeiss EM 900).

Stereology and plaque number analysis

Stereological analysis was performed by a blinded observer on sets of every 36th systematically sampled 25 μ m thick brain section throughout the neocortex using a microscope (Axioskop, Zeiss, Germany) equipped with a motorized x-y-z-stage coupled to a video-microscopy system (Microfire, Optronics, California, USA). Analysis was conducted using the Stereologer

software (Stereo Investigator 6; MBF Bioscience). For the determination of the number of microglia per brain, Iba1-positive cells were determined with the optical fractionator technique with three dimensional dissectors as previously described¹⁷. For the assessment of plaque associated PU.1-positive cells the diameter of the Congo red-positive plaques was determined and only microglia in the two-fold vicinity of the size of the plaque diameter were counted. Plaque load was determined based on Congo red and anti-A β staining using the area fraction fractionator technique¹⁸.

For the analysis of the plaque number, mosaics of the same brain sections as sampled for plaque load were acquired on an Axioplan 2 microscope with Axioplan MRm and AxioVision 4.7 software (Carl Zeiss). Plaque number was determined with Fiji software. On each brain section, the cortical region was selected and a manually set intensity threshold was applied to identify plaques. In the APPPS1 mice, plaques were grouped as < 25 μm^2 (very small), 25-100 μm^2 (small), 100-300 μm^2 (medium), 300-600 μm^2 (large) and > 600 μm^2 (very large). In APP23 mice, size groups were the following 10-25 μm^2 (very small), 25-100 μm^2 (small), 100-1000 μm^2 (medium) and > 1000 μm^2 (large).

Statistics

All values reported are mean \pm s.e.m. and a p-value < 0.05 was considered as significant. Test for Gaussian distribution of the data was performed with D'Agostino-Pearson normality test. If the normality criterion was met, statistical significance of pairwise comparisons of experimental groups was tested with Student's t-test. Data that did not meet normality criterion were analyzed using non-parametric Mann-Whitney-U test. For analysis of more than two groups Kruskal-Wallis test was performed, if $p < 0.05$ Dunn's post hoc test was conducted. For comparisons of different plaque sizes multiple t-tests corrected for multiple comparisons, (Holm-Sidak) were performed. All analyses were done with Prism 6.0 software.

Results

MFG-E8 is produced by glial cells and can be found in the cerebral vasculature

Macrophages in a variety of tissues have been shown to express and secrete MFG-E8¹⁹⁻²¹. In the brain, RNA sequencing of different central nervous system (CNS)-derived cells demonstrated that MFG-E8 is expressed by the resident glia cells, especially by astrocytes, but to a lesser degree also by microglia²². Accordingly, immuno-staining after stroke demonstrated that MFG-E8 co-localizes with astrocytes and microglia²³. By co-staining of MFG-E8 and glial

fibrillary acidic protein (GFAP; a marker for astrocytes) in brain sections from wildtype mice, we could confirm high protein levels of MFG-E8 in astrocytes (Fig. 1A). Moreover, cerebral arteries visualized with an artery-specific dye, Alexa Fluor 633 hydrazide¹⁶, which binds to elastin fibers, were positive for MFG-E8 (Fig. 1B) indicating its occurrence in vascular cells and around vascular structures as previously described²⁴. To confirm staining specificity, we used genetically modified mice, in which the genetic insertion of a transmembrane domain fused to the β -galactosidase reporter protein (TM- β -geo) into the C2 domain of the *Mfge8* gene results in the retention of the resulting MFG-E8- β -galactosidase fusion protein within the cell (Fig. 1C)²⁴. Retention within the cell leads to a rapid degradation and, therefore, to a loss of MFG-E8 function. Accordingly, in mice homozygous for the inserted TM- β -geo construct (hereafter referred to as *Mfge8*^{-/-}), only intracellular, punctate MFG-E8 staining was observed confirming the specificity of the MFG-E8 signal (Fig. 1B).

To evaluate the role of MFG-E8 in the pathology of AD *in vivo*, we bred two mouse models of cerebral β -amyloidosis with *Mfge8*^{-/-} mice, namely the APPPS1 mouse line that co-expresses mutated human *APP* and *PSEN1* genes leading to rapid onset of β -cerebral amyloidosis at six to eight weeks¹³ and the APP23 mouse line that overexpresses mutant human *APP* leading to a disease onset of around six to seven months of age¹⁴. Western Blotting of primary microglia isolated from APPPS1 x *Mfge8*^{-/-} and APPPS1 x *Mfge8*^{+/+} mice, showed the presence of the two described different isoforms of the MFG-E8 protein only in APPPS1 x *Mfge8*^{+/+} microglia, which validates the specificity of MFG-E8 deficiency in the crossed APPPS1 mice and further confirms MFG-E8 expression in microglia (Fig. 1D)²⁵.

MFG-E8 levels increase with A β pathology

To determine whether the levels of MFG-E8 change with ageing and/or cerebral β -amyloidosis, we analyzed the protein levels of MFG-E8 across different ages and at different stages of cerebral β -amyloidosis. In particular, we compared MFG-E8 levels of the shorter but more abundant isoform in brain homogenates of young (3-4 months) and aged (20 months) wildtype, APPPS1 and APP23 mice by Western Blotting (Fig. 2A). In accordance with published findings¹¹, MFG-E8 expression in the brain increased more than threefold in wildtype mice with age (Fig. 2A/B). However, in contrast to previous studies indicating that MFG-E8 levels decrease in a mouse model of AD pathology and in human AD brain tissue^{11,12}, we found that cerebral β -amyloidosis induced a significant increase in MFG-E8 levels both in APPPS1 and APP23 lines (Fig. 2A/B). Strikingly, a strong increase in MFG-E8 levels coincided with the onset of A β deposition. Thus, APPPS1 mice with an onset of plaque deposition at six to eight

weeks had 2.5-fold higher MFG-E8 levels at young age compared to wildtype mice. In contrast, APP23 mice, which only start to deposit plaques around six to seven months of age, showed no consistent increase in MFG-E8 levels in the young age group (Fig. 2A). However, at 20 months of age, when A β levels in APP23 mice are the highest, MFG-E8 was also drastically elevated and even exceeded MFG-E8 levels in APPPS1 mice (Fig. 2A/B).

The effects of ageing and AD disease progression on MFG-E8 levels were further studied in additional age groups of APP23 mice. Similarly, the results showed a steady increase in MFG-E8 concentration that mirrored the rise in A β (Fig. 2C/D). In particular, the robust increase of MFG-E8 between 12 and 20 months of age is also reflected by A β levels in the brain of APP23 mice (Fig. 2C).

MFG-E8 co-localizes with A β deposits in APP transgenic mice

To determine the origin of the sudden increase in MFG-E8 protein levels in parallel with the onset of A β plaque pathology in APP transgenic (tg) mice, we stained brain sections of APPPS1 and APP23 mice with an antibody directed against MFG-E8. In both mouse models, MFG-E8 was not only present in astrocytes but also co-localized strongly with Congo red-positive amyloid plaques. Of note, the absence of MFG-E8 immunoreactivity on plaques, but the presence of the intracellular punctate MFG-E8 signal in APPPS1 x *Mfge8*^{-/-} mice confirmed the specificity of the detected signal (Fig. 3A). Since no cellular marker, such as Iba1 or GFAP to visualize microglia or astrocytes respectively, showed co-localization with the plaque-associated MFG-E8 signal (data not shown), the secreted, soluble form of MFG-E8 seems to strongly associate with amyloid plaques.

Immunofluorescent co-staining of MFG-E8 with A β and subsequent 3D-reconstruction revealed that MFG-E8 was found throughout the entire amyloid plaque and partially co-localized with A β (Fig. 3B). In addition, immuno-electron microscopy of amyloid plaques from APPPS1 x *Mfge8*^{+/+} and APPPS1 x *Mfge8*^{-/-} mice stained for MFG-E8 confirmed the association of secreted MFG-E8 with A β fibrils (Fig. 3C). Notably, electron microscopy analysis also suggested the presence of less fibrillar material in amyloid plaques of APPPS1 x *Mfge8*^{-/-} mice, indicating that the lack of MFG-E8 influences amyloid aggregation.

The microglial immune response is unaffected in APPPS1 x *Mfge8*^{-/-} mice

MFG-E8 may have an immuno-protective function in AD as it has been reported to play a role in macrophage-mediated phagocytosis of A β ¹². Thus, we investigated whether the absence of the MFG-E8 protein in APPPS1 tg mice would lead to alterations in the microglial immune

response during the pathogenesis of cerebral β -amyloidosis. Therefore, we analyzed microglia in two- and four-month-old mice reflecting either an early disease state or a robust amyloid pathology in the brain. To determine if lack of MFG-E8 affects cortical microglia number, we immuno-stained brain sections for the myeloid transcription factor PU.1 and stereologically quantified the number of PU.1-positive cells in the cortex of APPPS1 x *Mfge8*^{+/+} mice compared to APPPS1 x *Mfge8*^{-/-} mice. Although we observed the expected increase in microglia with cerebral A β deposition from two to four months of age, no differences in the microglial cell number between the age-matched APPPS1 x *Mfge8*^{-/-} and APPPS1 x *Mfge8*^{+/+} animals were noticeable (Fig. 4A). Also, the number of plaque-associated microglia was indistinguishable in APPPS1 x *Mfge8*^{-/-} mice compared to APPPS1 x *Mfge8*^{+/+} mice (Fig. 4B,C), suggesting that MFG-E8 is not required for the induction of microgliosis found around A β depositions.

We next examined whether microglial cytokine production in APPPS1 mice is affected by the lack of MFG-E8. For that purpose, we used fluorescence-activated cell sorting (FACS) to isolate microglia from APPPS1 x *Mfge8*^{+/+} and APPPS1 x *Mfge8*^{-/-} mice, which were identified as the CD11b^{high}, CD45^{low} cell population. We then determined microglial cytokine levels by enzyme linked immunosorbent assay (ELISA). At two months of age the microglial production of pro- and anti-inflammatory cytokines was comparable between the genotypes (Fig. 4D). However, at four months of age we noticed a general trend towards reduced cytokine levels in APPPS1 x *Mfge8*^{-/-} microglia, with the release of the pro-inflammatory cytokine TNF- α being significantly reduced by 51 ± 19 percent in APPPS1 x *Mfge8*^{-/-} mice ($P < 0.05$; Fig. 4E).

Suppression of inflammation has been shown to increase phagocytosis of A β ²⁶, therefore we analyzed the phagocytic capacity of microglia *in vivo* using intraperitoneal administration of the amyloid-staining dye Methoxy-X04 in APPPS1 x *Mfge8*^{+/+} and APPPS1 x *Mfge8*^{-/-} animals. Microglial cells were isolated, identified by flow cytometry and analyzed for their Methoxy-X04 signal intensity (Fig. 5A). In accordance with the cytokine levels, the uptake of Methoxy-X04-labeled A β , was unaffected at two months of age, but unexpectedly also at four months of age (Fig. 5B). Interestingly, the direct determination of A β ₄₂ levels from isolated microglia by ELISA showed a trend towards less A β ₄₂ in APPPS1 x *Mfge8*^{-/-} at two and also four months of age, but did not reach statistical significance (Fig. 5C).

Since A β visualization with Methoxy-X04 and also ELISA measurements cannot necessarily distinguish between bound, already engulfed or degraded A β , we determined whether lack of MFG-E8 influences the intracellular degradation process of A β . To this end, we additionally analyzed phagocytic activity of plaque-associated microglia by performing triple-staining for CD68 (a marker for phagolysosomes), PU.1 and Methoxy-X04 in brain

sections of APPPS1 x *Mfge8*^{+/+} and APPPS1 x *Mfge8*^{-/-} mice (Supplementary fig. 1A). We then quantified immunofluorescence intensity of CD68 levels in plaque-associated microglia in three-dimensional reconstructed z-stack images taken by confocal microscopy. However, intensity analysis of plaque-associated CD68-immunoreactivity in microglia revealed similar levels between genotypes (Supplementary fig. 1B).

Lack of MFG-E8 reduces pathology of cerebral β -amyloidosis in mice

Given the strong co-localization of MFG-E8 with amyloid plaques and the lack of immune modulation in the absence of MFG-E8, we next investigated whether the generation or deposition of A β may be directly affected in APP transgenic mice. Strikingly, A β ₄₀₊₄₂ levels declined by 38 \pm 12 percent ($P < 0.01$) in two-month-old APPPS1 x *Mfge8*^{-/-} mice in formic acid-extracted (Fig. 6A) and by 43 \pm 14 percent ($P < 0.01$) in SDS-soluble fractions of brain homogenates (Fig. 6B, E). Of note, these reductions in A β levels occurred while amyloid precursor protein (APP) and its processing product C-terminal fragment- β (CTF- β) levels were unaffected (Fig. 6C, D), indicating that changes in A β were not a result of altered APP production or cleavage.

To determine whether the decrease in A β levels results in reduced plaque deposition, we immuno-stained brain sections of APPPS1 x *Mfge8*^{+/+} and APPPS1 x *Mfge8*^{-/-} mice for A β and Congo red. In line with the reduction in A β levels measured by ELISA, stereological quantification of the area covered by A β plaques in the cortical region of APPPS1 x *Mfge8*^{-/-} mice revealed a 39 \pm 9 percent reduced plaque load compared to APPPS1 x *Mfge8*^{+/+} mice ($P < 0.001$; Fig. 6F/G).

We confirmed these results by crossing *Mfge8*^{-/-} mice to the APP23 mouse line, which has a slower disease onset with initial plaques occurring at six to seven months of age¹⁴. A β levels in the resulting APP23 x *Mfge8*^{-/-} mouse line were analyzed at nine months of age, a time point reflecting approximately the same time span between the first appearance of cortical A β plaques and analysis as performed in the APPPS1 mouse line. In accordance with the results from the APPPS1 x *Mfge8*^{-/-} mouse line, APP23 x *Mfge8*^{-/-} mice had reduced A β levels as well as less A β plaque deposition compared to aged-matched APP23 x *Mfge8*^{+/+} mice (Supplementary fig. 2A-D). Again, APP processing was unaffected (Supplementary fig. 2C/D).

Interestingly, when we analyzed plaque deposition in mice at a more advanced disease state of four months (APPPS1 x *Mfge8*^{-/-}) or 12 months of age (APP23 x *Mfge8*^{-/-}), differences in plaque load and A β levels were no longer apparent (Supplementary Fig. 2A, B), arguing for an early role of MFG-E8 in promoting amyloid plaque deposition.

We next quantified the number cortical plaques and grouped them into different size categories to determine whether MFG-E8 had an influence on the generation of new plaques or plaque growth. We observed a significant increase in small plaques in two- and four-month-old APPPS1 x *Mfge8*^{+/+} mice (Fig. 6H, Supplementary fig. 3C). However, when we did the same analysis in male 12-month-old APP23 mice, the absolute plaque number in the different size groups was indistinguishable between *Mfge8*^{+/+} and *Mfge8*^{-/-} genotypes (Supplementary Fig. 3D). These observations suggest that the initial reduction in A β plaque load resulting from the lack of MFG-E8 may have been caused by a delay in the early formation of insoluble A β aggregates.

Discussion

Two studies have previously investigated the possible contribution of MFG-E8 to AD pathology and concluded that MFG-E8 can directly interact with A β and facilitate its phagocytosis by macrophages^{11,12}. This suggested that increasing the levels of MFG-E8 may be a valuable tool for the clearance of A β . However, our findings provide evidence for a detrimental role of MFG-E8 in the pathology of cerebral β -amyloidosis, as we show that the absence of MFG-E8 in mouse models of AD pathology reduces A β plaque load.

MFG-E8 was initially identified as a secreted bridging protein that mediates phosphatidylserine-dependent phagocytosis in many different tissues by binding to both apoptotic cells and macrophages. In brain tissue, several transcriptome-based studies on cells of the CNS identified astrocytes as the main source of MFG-E8^{22,27}. We confirmed those findings by immunofluorescent staining of mouse brain sections with MFG-E8 and GFAP that showed strong co-localization throughout most of the cell (Fig. 1A). Interestingly, microglia, which are the key players for phagocytosis in the brain, were reported to express only minor amounts of MFG-E8²². Nevertheless, we detected the two existing isoforms for MFG-E8 in primary isolated microglia by Western Blotting and a recent proteomics analysis in a different mouse model of AD pathology also found that microglial MFG-E8 levels increased with progressing pathology²⁸.

Apart from MFG-E8-mediated engulfment of apoptotic neurons, it has been reported that released MFG-E8 can bind to A β and facilitate its removal by peripheral macrophages¹², which raises the question about its contribution to the pathogenesis of AD. To address this issue, we analyzed both the inflammatory immune response and A β pathology in two mouse models for cerebral β -amyloidosis, APPPS1 and APP23, which were deficient for functional MFG-E8.

To our surprise, we found that the lack of MFG-E8 reduced A β plaque burden in brains of the APPPS1 and APP23 mice at early disease stages with only minor alterations in the immune response, including negligible changes in A β phagocytosis by microglia. These findings deviate from the previously held assumption that MFG-E8 enhances phagocytic removal of A β and thereby alleviates neuropathology¹². In fact, at the time point when plaque load was reduced in APPPS1 x *Mfge8*^{-/-} mice, no alterations in the immune response as determined by microglial number, cytokine levels or A β phagocytosis, were observed.

In particular, the unaltered phagocytic uptake of A β by microglia in APPPS1 x *Mfge8*^{-/-} mice was not expected but, to our knowledge, this is the first *in vivo* study that analyzed the capability of microglia to phagocytose A β in APP transgenic mice deficient for MFG-E8. Therefore, it cannot be ruled out that the relatively slow but inexorable A β accumulation *in vivo* affects the microglial phagocytic function differently than the rapid addition of high concentrations of fibrillar A β to cultured microglia used for the reported *in vitro* studies¹². Additionally, MFG-E8 may have a different affinity to *in vivo* formed A β fibrils compared to recombinant A β preparations that were applied to cultivated microglia.

Since our results point towards a role of MFG-E8 in the A β aggregation process rather than A β clearance, we examined whether MFG-E8 affects the production of A β . Although we observed the same trend of reduction in SDS-soluble A β levels in APPPS1 x *Mfge8*^{-/-} and APP23 x *Mfge8*^{-/-} mice, both APP production and processing were unaltered by lack of MFG-E8. These findings, together with the observation that secreted MFG-E8 accumulates and co-localizes with A β depositions, indicate that MFG-E8 is involved in A β fibril formation and subsequent plaque deposition.

Similar to our findings of MFG-E8 co-localizing with A β plaques, a close association with A β has also been described for components of the classical complement activation pathway, such as C1q or C3b and C4²⁹. Moreover, *in vitro* data on A β aggregation analyzed by Thioflavin T emission showed enhanced A β fibrillation in the presence of nanomolar concentration of C1q³⁰. However contrary to the observed reduction in A β levels and plaque burden in APPPS1 x *Mfge8*^{-/-} and APP23 x *Mfge8*^{-/-} mice, lack of C1q did not affect A β levels³¹ and C3 deficiency accelerated A β deposition^{32,33}. Furthermore, absence of these complement components was reported to alter the microglial activation state³¹⁻³³, which was not detectable at time points of reduced plaque deposition in APPPS1 x *Mfge8*^{-/-} mice.

In contrast to complement factors, the depletion of receptors that are known to bind to A β such as CD14 or TLR2 induced a reduction in plaque load in APP tg mice, as reported in our study^{34,35}. But for both receptors, reduction in A β plaque load was accompanied by changes

in the microglial immune response as cytokine production or microglia number were altered as well. Thus, the underlying mechanisms that lead to the reduction of A β in APP tg x *Mfge8*^{-/-} mice appears to differ from those described for other immune-related molecules.

Interestingly, in wildtype mice, we found that brain levels of MFG-E8 increased with ageing. However, in APP23 and APPPS1 mice, an even more robust increase of MFG-E8 levels was observed that occurred simultaneously with increased levels of A β and the majority of MFG-E8 appeared to accumulate around Congo red-positive deposits. Electron microscopy of such plaques indicated that the grade of fibrillation was more pronounced in the presence of MFG-E8. These findings makes it tempting to speculate that MFG-E8 possesses characteristics that particularly promote A β aggregation. In line with this hypothesis, we counted a reduced number of small-sized cortical A β plaques in two- and four-month-old APPPS1 x *Mfge8*^{-/-} mice, but detected no difference in the number of large or medium-sized plaques suggesting that the initial plaque formation is impaired by lack of MFG-E8 but not the subsequent plaque growth.

Interestingly, in humans, MFG-E8 contains a small amyloidogenic fragment named medin that is localized within the C2 domain of the full-length protein. Several publications describe the presence of medin-amyloid in the arterial vasculature including cranial blood vessels³⁶⁻³⁸. In mice, where the *Mfge8* gene shows 64 percent sequence similarity with the human gene, medin has not yet been described. However, we found MFG-E8-positive cerebral arteries in our mice, which may indicate the presence of medin also in mice. Interestingly, a recent study showed that blood-derived A β can enter the brain and induce A β plaque pathology in wildtype mice after parabiosis with APP tg mice³⁹. Since the *Mfge8*^{-/-} mice used in our study lack the entire C2 domain that harbors the amyloidogenic medin fragment, and as the knockout of *Mfge8* in the examined APPPS1 and APP23 mice led to reduced A β levels, one could speculate about a possible cross-seeding effect of blood vessel-derived medin and A β .

During amyloid formation, the nucleation process is the rate limiting step in which medin seeds might accelerate the formation of a nucleus which in turn decreases lag time and promotes polymerization of amyloid fibrils. Accordingly, absence of medin would not only delay the nucleation process but also the initial A β deposition as reflected in a decreased plaque load in two-month-old APPPS1 x *Mfge8*^{-/-} and nine-month-old APP23 x *Mfge8*^{-/-} mice, both representing a time point of early plaque deposition. In the further course of the disease, after the first plaques are formed, the growth of fibrillar amyloid material increases exponentially and possibly overwhelms the changes in plaque load at early disease stages as we did not detect changes in A β depositions at later disease stages in four-month-old APPPS1 x *Mfge8*^{-/-} or 12-month-old APP23 x *Mfge8*^{-/-} mice.

Taken together, the data presented here extend the role of MFG-E8 in AD pathology and suggest that MFG-E8 or single fragments of the protein, such as medin, accelerate the aggregation and subsequent deposition of A β . However, further studies are necessary to precisely determine the overall contribution of MFG-E8 to A β pathology but also to identify and characterize possible fragments of MFG-E8 which might have amyloidogenic characteristics and therefore promote cerebral β -amyloidosis.

Figures

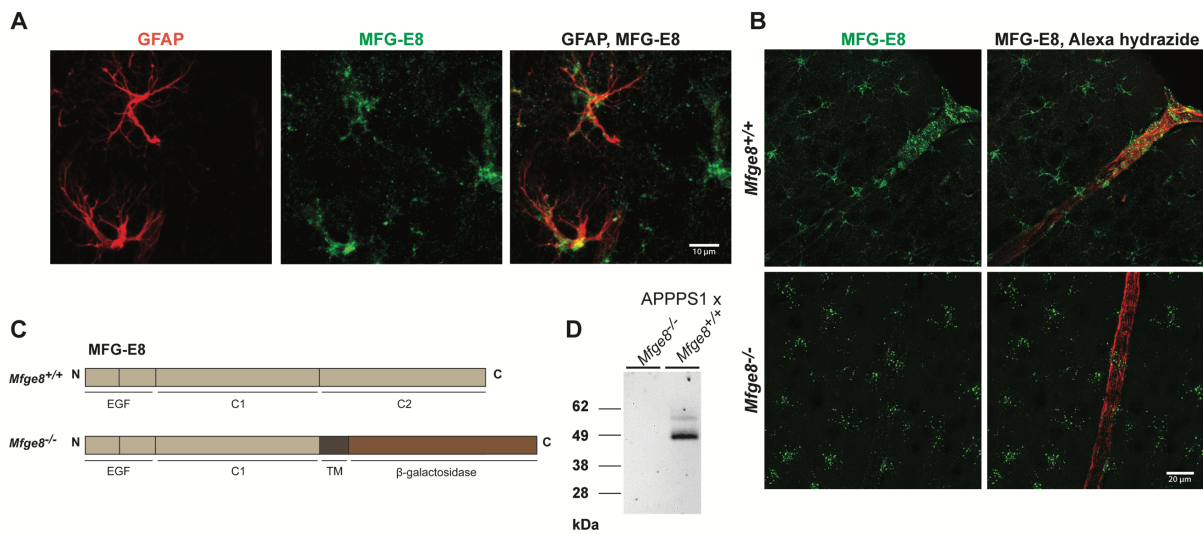


Figure 1: MFG-E8 is expressed in glia cells and cerebral blood vessels. **A**, Fluorescent staining for the astrocyte marker glial fibrillar acidic protein (GFAP) and MFG-E8 shows co-localization in cortical astrocytes of wildtype mice. **B**, MFG-E8 is present in cerebral arteries, which are visualized with the neocortical artery-specific dye Alexa Fluor 633 hydrazide. In *Mfge8*^{-/-} mice, MFG-E8 staining is intracellular due to the insertion of a transmembrane domain. **C**, Top, Schematic structure of the *Mfge8* wildtype gene. Bottom, structure of the knock-in form of truncated *Mfge8*. **D**, Western Blotting detection of the two isoforms of MFG-E8 in primary microglia isolated from APPPS1 x *Mfge8*^{+/+} and APPPS1 x *Mfge8*^{-/-} mice.

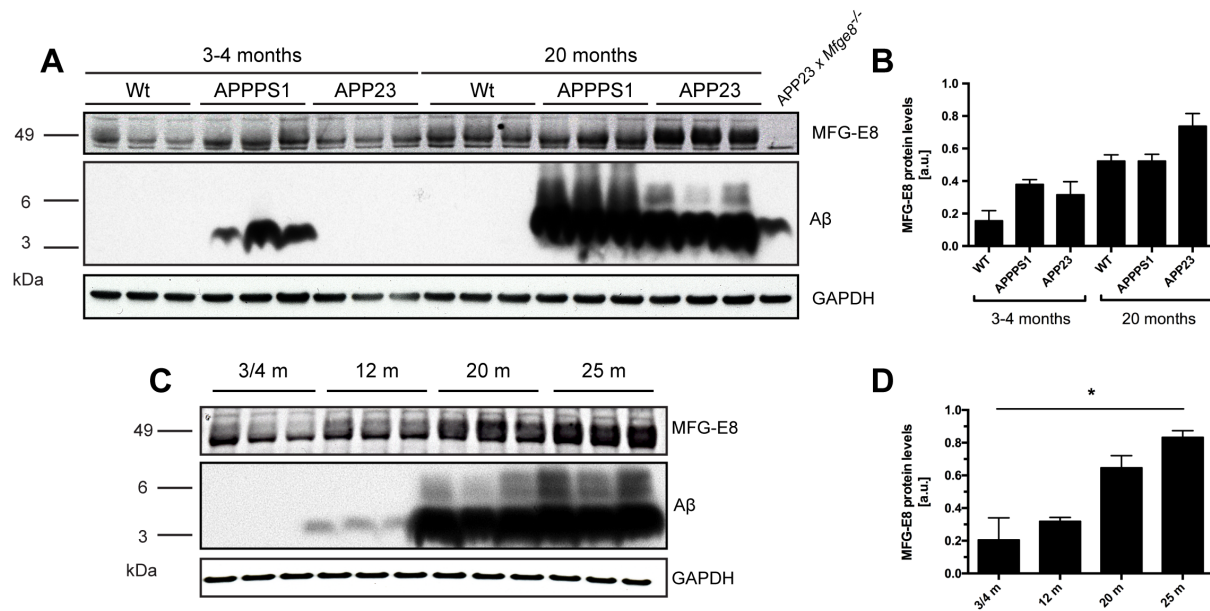


Figure 2: MFG-E8 levels increase with age and cerebral β -amyloidosis. **A**, Western Blotting analysis of MFG-E8 and A β protein levels in brain homogenates from young (3-4 months of age) and aged (20 months of age) wildtype (Wt), APPPS1, and APP23 mice. **B**, Semi-quantitative analysis of MFG-E8 levels normalized to GAPDH levels (n=3 for each group). **C**, A β pathology-dependent increase of MFG-E8 levels in APP23 mice. **D**, Semi-quantitative analysis of MFG-E8 levels normalized to GAPDH (n=3,3,3,3). * p<0.05, as determined by Dunn's multiple comparison test.

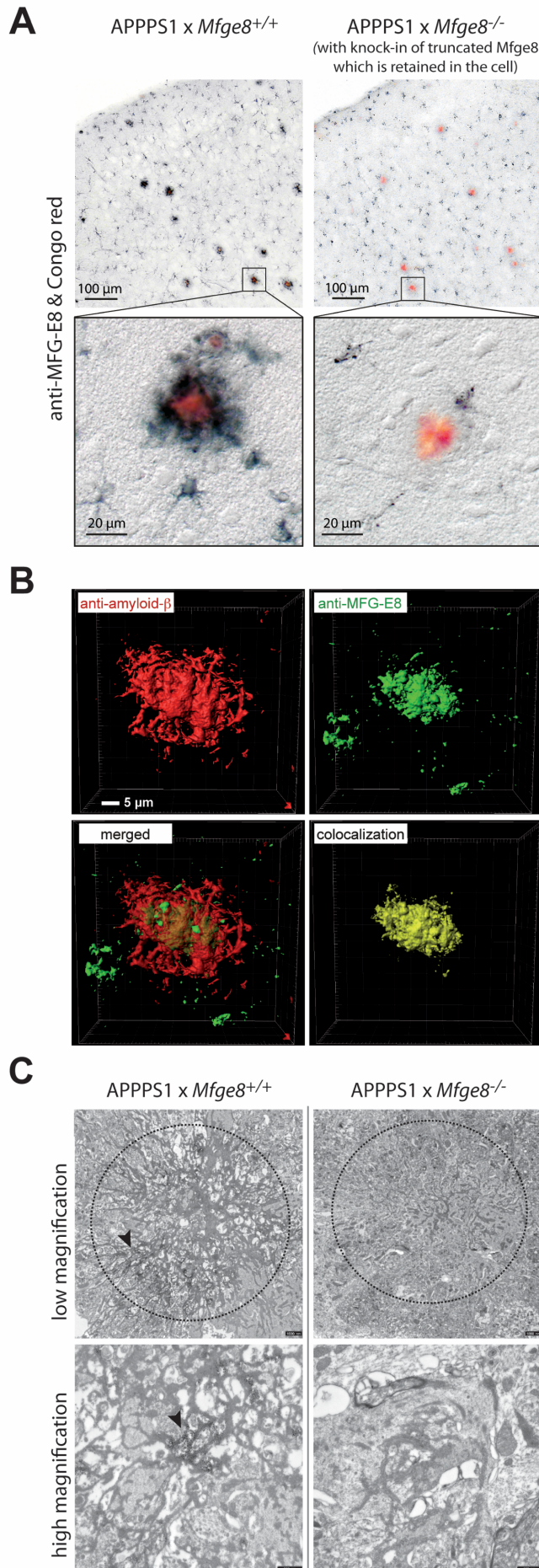


Figure 3: Co-localization of MFG-E8 with amyloid plaques in the brain of APPPS1 mice.

A, Immunohistochemical staining for MFG-E8 in APPPS1 x *Mfge8*^{+/+} and APPPS1 x *Mfge8*^{-/-} mice. Secreted MFG-E8 is closely associated with Congo red-positive amyloid plaques. **B**, 3D-reconstruction of an amyloid plaque co-stained for Aβ and MFG-E8, demonstrating their co-localization (bottom right). **C**, Electron micrographs of amyloid plaques stained for MFG-E8; arrows indicate MFG-E8 localization within the plaque structure (encircled). Please note a possible change in the plaque structure, with less pronounced fibrils in APPPS1 x *Mfge8*^{-/-} animals. Scale bar: low magnification: 1000 nm, high magnification: 500 nm.

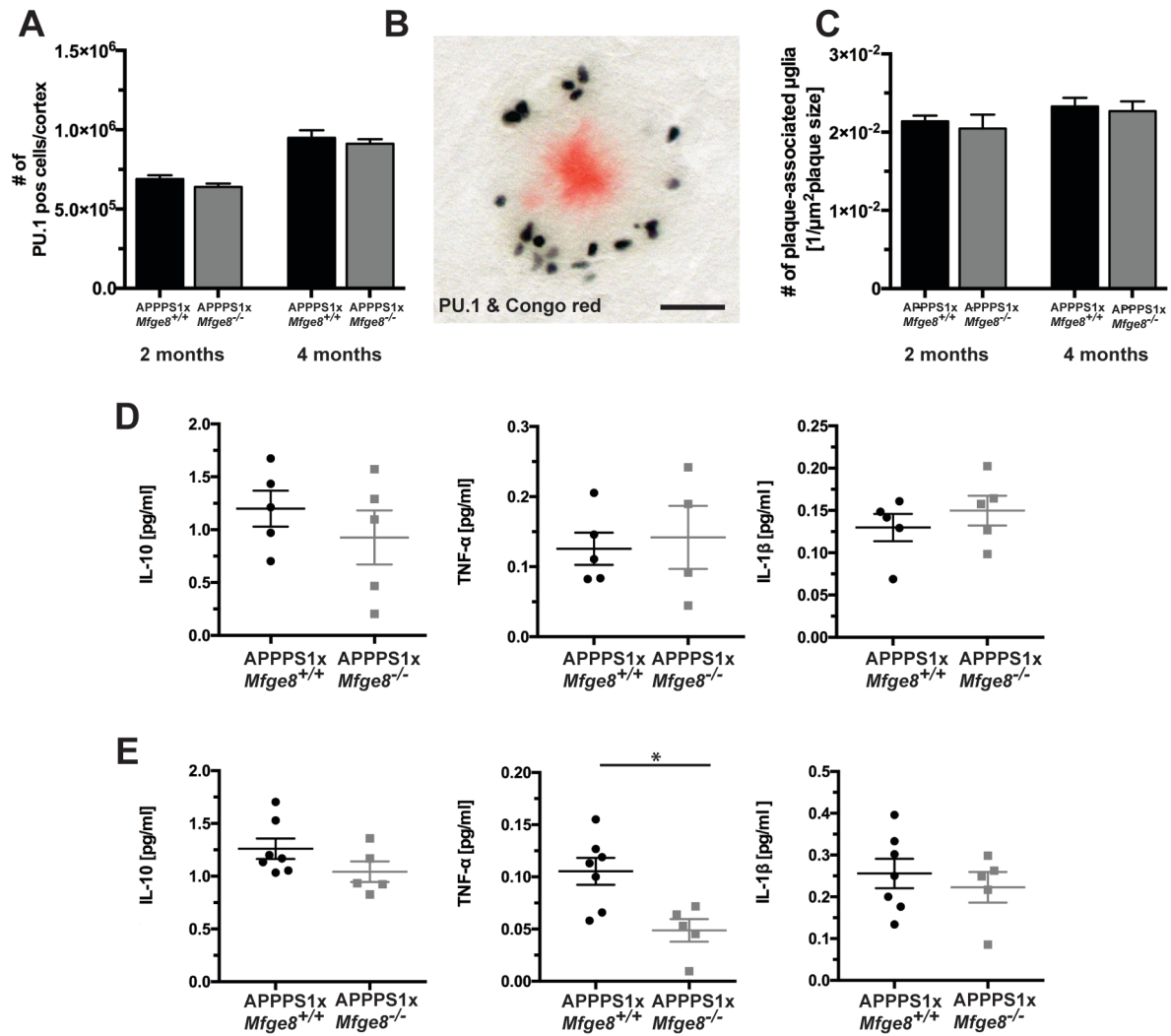


Figure 4: Microglia number and cytokine production is unaffected in APPS1 x *Mfge8*^{-/-} mice.

A, Stereological quantification of PU.1-positive cortical cells at 2 and 4 months of age in APPS1 x *Mfge8*^{+/+} and APPS1 x *Mfge8*^{-/-} mice (2 months: n=9,9; 4 months: n=6,8). **B**, Micrograph of nuclear PU.1 staining in plaque-associated microglia. Scale bar: 20 μm. **C**, Number of plaque-associated PU.1-positive cells in relation to Congo red-positive plaque area (2 months: n=9,9; 4 months: n=6,6). **D**, **E**, Cytokine measurements in primary microglia FACS isolated from APPS1 x *Mfge8*^{+/+} and APPS1 x *Mfge8*^{-/-} mice at 2 months (**D**; n=5,5) and 4 months of age (**E**; n=7,5) of age. * p < 0.05, as determined by non-parametric Mann-Whitney test.

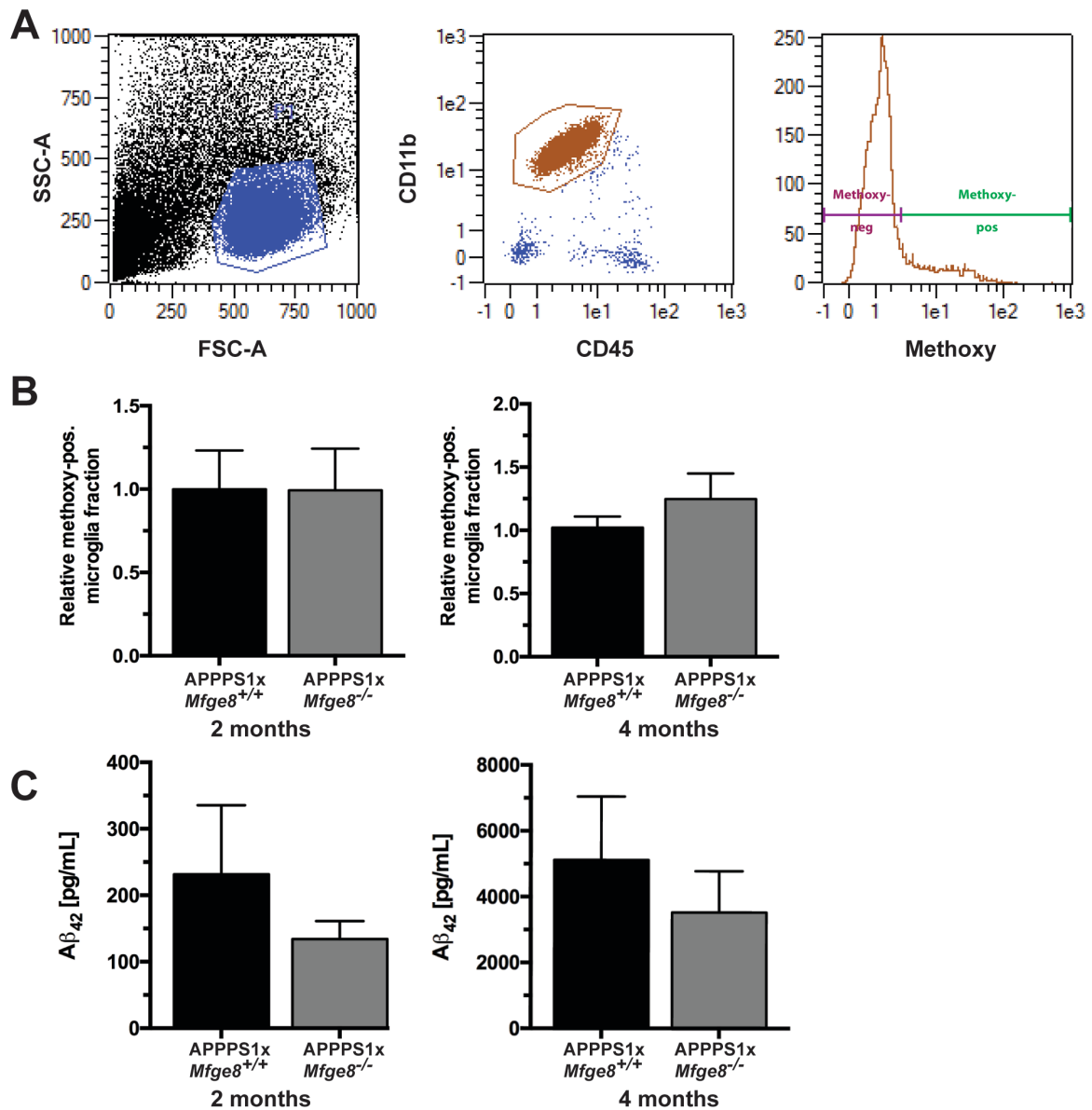


Figure 5: Microglial phagocytosis of A β is unchanged by the lack of MFG-E8. **A**, Gating strategy. Microglia were gated as CD11b^{high} and CD45^{low} and analyzed for the fraction of amyloid-containing, Methoxy-X04-positive cells (gating was established based on cells from a non-transgenic animal). **B**, Fraction of Methoxy-X04-positive microglia normalized to APPSP1 x *Mfge8*^{+/+} Methoxy-X04-positive cells at 2 (n=12,8) and 4 (n=18,15) months of age. **C**, Analysis of microglial A β ₄₂ content (n_{2months}=5,4) and (n_{4months}=4,3).

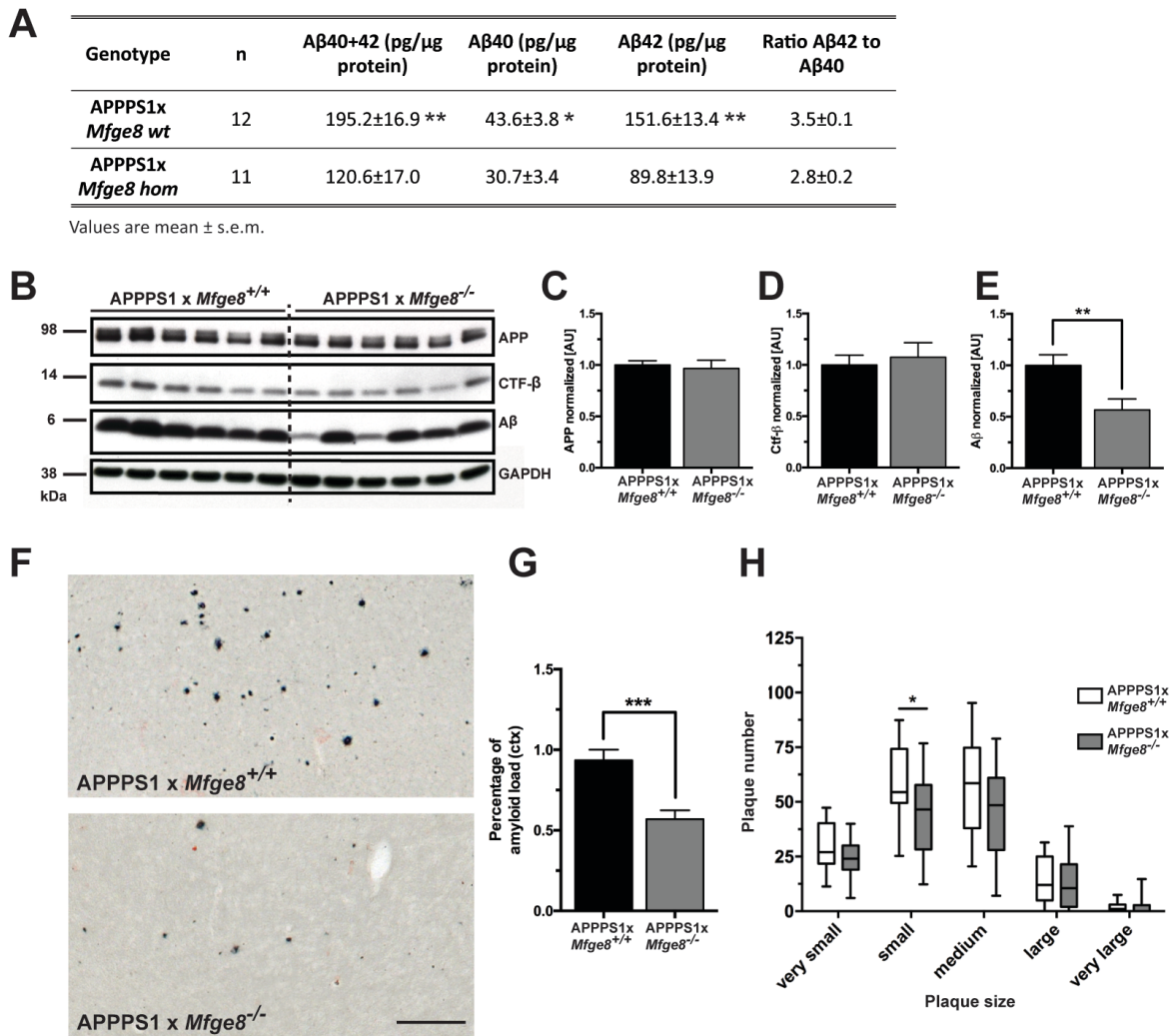
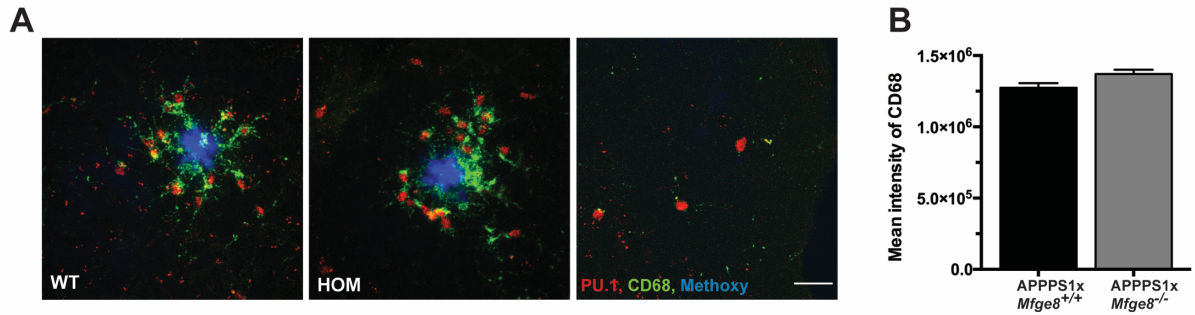
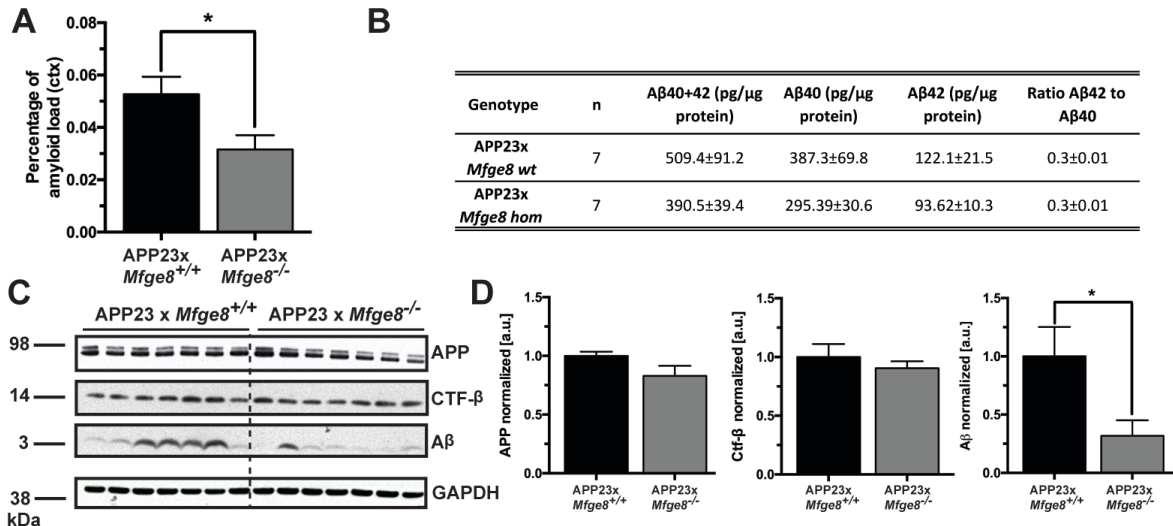


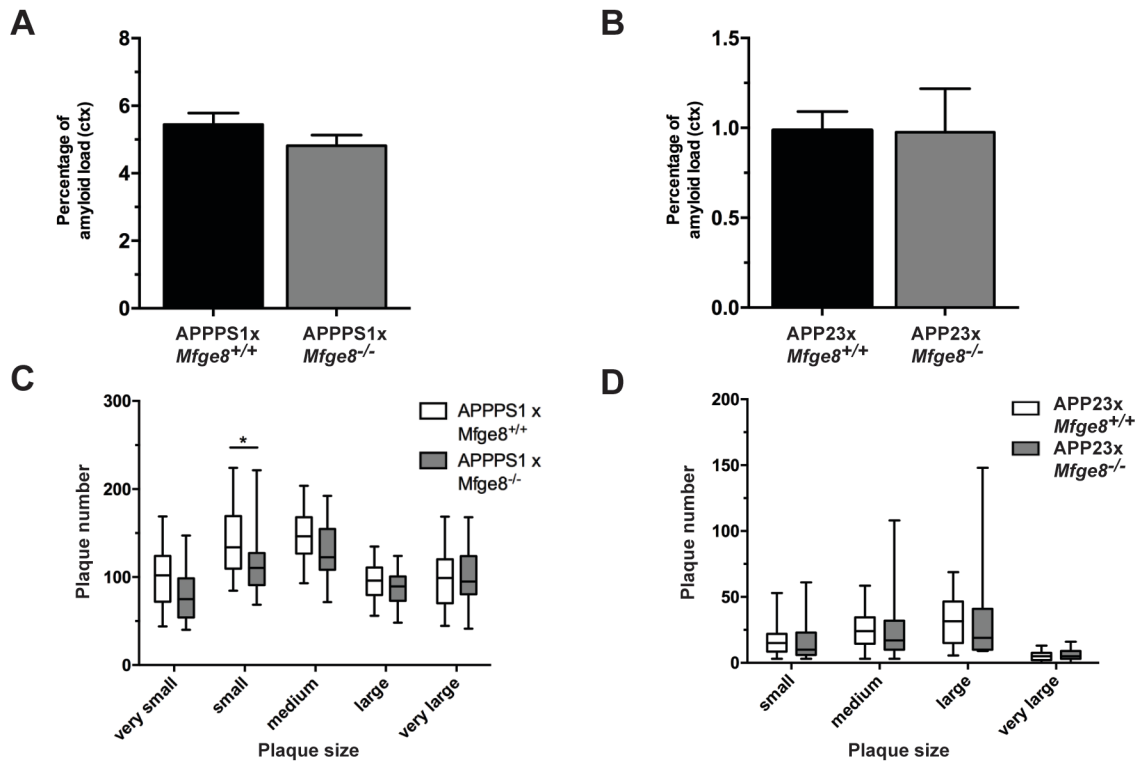
Figure 6: Genetic deletion of MFG-E8 in 2-month-old APPPS1 mice reduces A β levels and plaque load without affecting APP processing. **A**, Formic-acid extracted A β levels in brain homogenates measured by ELISA. **B**, Representative Western Blot from brain homogenates for detection of amyloid precursor protein (APP), its processing product C-terminal fragment- β (CTF- β) and A β . **C-E**, Densitometric analysis of (C) APP, (D) CTF- β and (E) A β levels normalized to GAPDH protein (n=12,12). **F**, Micrographs of cortical A β plaques. Scale bar: 50 μ m. **G**, Stereological quantification of cortical A β plaque load (n=15,15). **H**, Number of plaques grouped by size. Presented as median and 5-95 percentile (n=30,40 values per size group). Wt: APPPS1 x *Mfge8*^{+/+}, hom: APPPS1 x *Mfge8*^{-/-}. *p < 0.05, **p < 0.01, ***p < 0.001, as determined by Student's t-test (A,E,G) or multiple t-tests corrected for multiple comparisons (Holm-Sidak correction) (H). Ctx: cortex.



Supplementary figure 1: **A**, Representative staining for the lysosomal marker CD68 in plaque-associated microglia (identified with PU.1 and Methoxy-X04) in brain sections of APPPS1 x *Mfge8*^{+/+} (WT), APPPS1 x *Mfge8*^{-/-} (HOM) mice. CD68 staining was minimal in non-plaque associated microglia. **B**, Intensity quantification of the CD68 signal at 4 months of age (n=6,6).



Supplementary figure 2: MFG-E8 deficiency in male APP23 mice reduces Aβ plaque deposition. **A**, Stereological quantification of cortical Aβ plaque load at 9 months of age (n=7,7). **B**, Formic acid-extracted Aβ levels measured by ELISA. **C**, Western Blot from brain homogenates for detection of APP, CTF-β and Aβ. **D**, Densitometric analysis of APP, CTF-β and Aβ levels normalized to GAPDH expression (n=7,7). *p < 0.05, as determined by non-parametric Mann-Whitney test. Ctx: cortex.



Supplementary figure 3: MFG-E8 does not influence A β deposition and size distribution at progressing disease states. **A, B**, Stereological quantification of cerebral A β plaque load in **(A)** APPPS1 x *Mfge8*^{+/+} and APPPS1 x *Mfge8*^{-/-} mice at 4 months of age (n=15,19) and **(B)** in male APP23 x *Mfge8*^{+/+} and APP23 x *Mfge8*^{-/-} mice at 12 months of age (n=10,8). **C, D**, Number of plaques grouped by size. Presented as median and 5-95 percentile in **(C)** 4-month-old APPPS1 x *Mfge8*^{+/+} and APPPS1 x *Mfge8*^{-/-} mice (n=30,40 values per size group) and **(D)** 12-month-old APP23 x *Mfge8*^{+/+} and APP23 x *Mfge8*^{-/-} male mice (n=50,40 values per size group). *p < 0.05, as determined by multiple t-tests corrected for multiple comparisons (Holm-Sidak correction). Ctx: cortex.

References

1. Goate, A. *et al.* Segregation of a missense mutation in the amyloid precursor protein gene with familial Alzheimer's disease. *Nature* **349**, 704–706 (1991).
2. Levy-Lahad, E. *et al.* Candidate gene for the chromosome 1 familial Alzheimer's disease locus. *Science* **269**, 973–977 (1995).
3. Sherrington, R. *et al.* Cloning of a gene bearing missense mutations in early-onset familial Alzheimer's disease. *Nature* **375**, 754–760 (1995).
4. Golde, T. E., Eckman, C. B. & Younkin, S. G. Biochemical detection of Abeta isoforms: implications for pathogenesis, diagnosis, and treatment of Alzheimer's disease. *Biochim. Biophys. Acta* **1502**, 172–187 (2000).
5. Holtzman, D. M., Morris, J. C. & Goate, A. M. Alzheimer's disease: the challenge of the second century. *Sci Transl Med* **3**, 77sr1–77sr1 (2011).
6. Ott, A. *et al.* Diabetes mellitus and the risk of dementia: The Rotterdam Study. *Neurology* **53**, 1937–1942 (1999).
7. Elias, M. F., Elias, P. K., Sullivan, L. M., Wolf, P. A. & D'Agostino, R. B. Lower cognitive function in the presence of obesity and hypertension: the Framingham heart study. *Int. J. Obes. Relat. Metab. Disord.* **27**, 260–268 (2003).
8. Jones, L. *et al.* Genetic evidence implicates the immune system and cholesterol metabolism in the aetiology of Alzheimer's disease. *PLoS ONE* **5**, e13950 (2010).
9. Lambert, J.-C. *et al.* Implication of the immune system in Alzheimer's disease: evidence from genome-wide pathway analysis. *J. Alzheimers Dis.* **20**, 1107–1118 (2010).
10. Lambert, J.-C. *et al.* Meta-analysis of 74,046 individuals identifies 11 new susceptibility loci for Alzheimer's disease. *Nat Genet* **45**, 1452–1458 (2013).
11. Fuller, A. D. & Van Eldik, L. J. MFG-E8 regulates microglial phagocytosis of apoptotic neurons. *J Neuroimmune Pharmacol* **3**, 246–256 (2008).
12. Boddaert, J. *et al.* Evidence of a Role for Lactadherin in Alzheimer's Disease. *The American Journal of Pathology* **170**, 921–929 (2010).
13. Radde, R. *et al.* A β 42-driven cerebral amyloidosis in transgenic mice reveals early and robust pathology. *EMBO Rep* **7**, 940–946 (2006).
14. Sturchler-Pierrat, C. *et al.* Two amyloid precursor protein transgenic mouse models with Alzheimer disease-like pathology. *Proceedings of the National Academy of Sciences* **94**, 13287–13292 (1997).
15. Hanayama, R. *et al.* Autoimmune disease and impaired uptake of apoptotic cells in MFG-E8-deficient mice. *Science* **304**, 1147–1150 (2004).
16. Shen, Z., Lu, Z., Chhatbar, P. Y., O'Herron, P. & Kara, P. An artery-specific fluorescent dye for studying neurovascular coupling. *Nat Meth* **9**, 273–276 (2012).
17. Varvel, N. H. *et al.* Replacement of brain-resident myeloid cells does not alter cerebral amyloid- β deposition in mouse models of Alzheimer's disease. *J Exp Med* **212**, 1803–1809 (2015).
18. Bondolfi, L. *et al.* Amyloid-associated neuron loss and gliogenesis in the neocortex of amyloid precursor protein transgenic mice. *J. Neurosci.* **22**, 515–522 (2002).
19. NAKATANI, H. *et al.* Weaning-induced expression of a milk-fat globule protein, MFG-E8, in mouse mammary glands, as demonstrated by the analyses of its mRNA, protein and phosphatidylserine-binding activity. *Biochem. J.* **395**, 21–30 (2006).
20. Burgess, B. L., Abrams, T. A., Nagata, S. & Hall, M. O. MFG-E8 in the retina and retinal pigment epithelium of rat and mouse. *Mol. Vis.* **12**, 1437–1447 (2006).
21. Watanabe, T. *et al.* Production of the long and short forms of MFG-E8 by epidermal keratinocytes. *Cell Tissue Res* **321**, 185–193 (2005).

22. Zhang, Y. *et al.* Purification and Characterization of Progenitor and Mature Human Astrocytes Reveals Transcriptional and Functional Differences with Mouse. *Neuron* **89**, 37–53 (2016).
23. Neher, J. J., Emmrich, J. V. & Fricker, M. Phagocytosis executes delayed neuronal death after focal brain ischemia. in (2013). doi:10.1073/pnas.1308679110/-/DCSupplemental
24. Silvestre, J.-S. *et al.* Lactadherin promotes VEGF-dependent neovascularization. *Nat Med* **11**, 499–506 (2005).
25. Hanayama, R. *et al.* Identification of a factor that links apoptotic cells to phagocytes. *Nature* **417**, 182–187 (2002).
26. Heneka, M. T. *et al.* Locus ceruleus controls Alzheimer's disease pathology by modulating microglial functions through norepinephrine. *Proc. Natl. Acad. Sci. U.S.A.* **107**, 6058–6063 (2010).
27. Cahoy, J. D. *et al.* A Transcriptome Database for Astrocytes, Neurons, and Oligodendrocytes: A New Resource for Understanding Brain Development and Function. *Journal of Neuroscience* **28**, 264–278 (2008).
28. Boza-Serrano, A., Yang, Y., Paulus, A. & Deierborg, T. Innate immune alterations are elicited in microglial cells before plaque deposition in the Alzheimer's disease mouse model 5xFAD. *Sci Rep* **8**, 1550 (2018).
29. Eikelenboom, P. & Stam, F. C. Immunoglobulins and complement factors in senile plaques. An immunoperoxidase study. *Acta Neuropathol* **57**, 239–242 (1982).
30. Webster, S., Glabe, C. & Rogers, J. Multivalent binding of complement protein C1Q to the amyloid beta-peptide (A beta) promotes the nucleation phase of A beta aggregation. *Biochemical and Biophysical Research Communications* **217**, 869–875 (1995).
31. Fonseca, M. I., Zhou, J., Botto, M. & Tenner, A. J. Absence of C1q leads to less neuropathology in transgenic mouse models of Alzheimer's disease. *J. Neurosci.* **24**, 6457–6465 (2004).
32. Maier, M. *et al.* Complement C3 Deficiency Leads to Accelerated Amyloid Plaque Deposition and Neurodegeneration and Modulation of the Microglia/Macrophage Phenotype in Amyloid Precursor Protein Transgenic Mice. *Journal of Neuroscience* **28**, 6333–6341 (2008).
33. Shi, Q. *et al.* Complement C3 deficiency protects against neurodegeneration in aged plaque-rich APP/PS1 mice. *Sci Transl Med* **9**, eaaf6295 (2017).
34. Reed-Geaghan, E. G., Reed, Q. W., Cramer, P. E. & Landreth, G. E. Deletion of CD14 attenuates Alzheimer's disease pathology by influencing the brain's inflammatory milieu. *J. Neurosci.* **30**, 15369–15373 (2010).
35. Richard, K. L., Filali, M., Préfontaine, P. & Rivest, S. Toll-like receptor 2 acts as a natural innate immune receptor to clear amyloid beta 1-42 and delay the cognitive decline in a mouse model of Alzheimer's disease. *J. Neurosci.* **28**, 5784–5793 (2008).
36. Peng, S. *et al.* Medin and medin-amyloid in ageing inflamed and non-inflamed temporal arteries. *J. Pathol.* **196**, 91–96 (2001).
37. Häggqvist, B. *et al.* Medin: an integral fragment of aortic smooth muscle cell-produced lactadherin forms the most common human amyloid. *Proceedings of the National Academy of Sciences* **96**, 8669–8674 (1999).
38. Peng, S., Glennert, J. & Westermark, P. Medin-amyloid: A recently characterized age-associated arterial amyloid form affects mainly arteries in the upper part of the body. *Amyloid* **12**, 96–102 (2005).
39. Bu, X.-L. *et al.* Blood-derived amyloid- β protein induces Alzheimer's disease pathologies. *Nature Publishing Group* 1–9 (2017). doi:10.1038/mp.2017.204

5. Appendix

5.1 Abbreviations

| | |
|--------------|--|
| AA | Serum amyloid-A |
| ABCA7 | ATP binding cassette subfamily A member 7 |
| AD | Alzheimer's disease |
| ADAM10 | A disintegrin and metalloproteinase domain-containing protein 10 |
| AP-1 | Activator protein 1 |
| APOE | Apolipoprotein E |
| APP | Amyloid precursor protein |
| A β | Amyloid-beta |
| ATP | Adenosine triphosphate |
| BACE | Beta-secretase 1 |
| BBB | Blood-brain barrier |
| BCG | Bacillus Calmette-Guérin |
| BCSFB | Blood-cerebrospinal fluid barrier |
| BIN1 | Bridging integrator 1 |
| BM | Bone marrow |
| CAA | Cerebral amyloid angiopathy |
| C-terminal | Carboxy-terminal |
| C3 | Complement 3 |
| cAMP | Cyclic adenosine monophosphate |
| CASS4 | Cas scaffolding protein family member 4 |
| CCL2 | C-C motif chemokine ligand 2 |
| CCR2 | C-C motif chemokine receptor 2 |
| CD11b | Integrin alpha M |
| CD2AP | CD associated protein |
| CD33 | Siglec-3 |
| cDNA | complementary deoxyribonucleic acid |
| CELF1 | CUGBP Elav-like family member 1 |
| CLU | Clusterin |
| CNS | Central nervous system |
| CR1 | Complement C3b/C4b receptor 1 |
| CSF1R | Colony stimulating factor 1 receptor |
| CTF- β | C-terminal fragment beta |
| CX3CR1 | Fractalkine receptor |
| DAMP | Damage-associated molecular pattern |
| DAP | TYRO protein tyrosine kinase binding protein |
| DSG2 | Desmoglein 2 |
| EAE | Experimental autoimmune encephalomyelitis |
| EPHA1 | EPH receptor A1 |
| FAD | Familial Alzheimer's disease |
| FERMT2 | Fermitin family member 2 |

| | |
|------------------|--|
| GCV | Ganciclovir |
| GFP | Green fluorescent protein |
| GWAS | Genome-wide association studies |
| Hdac | Histone deacetylase |
| HDLS | Hereditary diffuse leukoencephalopathy with spheroids |
| Hexb | Hexosaminidase subunit beta |
| HIF-1 α | Hypoxia inducible factor 1 alpha |
| HSV | Herpes simplex virus |
| IDE | Insulin-degrading enzyme |
| IFN | Interferone |
| IL-1 β | Interleukine 1 beta |
| iNOS | inducible nitric oxide synthase |
| INPP5D | Inositol polyphosphate-5-phosphatase D |
| kDa | Kilodalton |
| LOAD | Late-onset Alzheimer's disease |
| LPS | Lipopolysaccharide |
| LRP1 | Low density lipoprotein receptor-related protein 1 |
| Ly6C | Lymphocyte antigen 6 complex |
| MAPT | Microtubule-associated protein tau |
| MCP-1 | Monocyte chemoattractant protein 1 (alias CCL2) |
| MEF2C | Myocyte enhancer factor 2C |
| MFG-E8 | Milk-fat globule-EGF factor 8 protein |
| MMP | Matrix metalloproteinase |
| MS4A | Membrane spanning 4-domains A |
| mTOR | Mechanistic target of Rapamycin |
| NAD ⁺ | Nicotinamide adenine dinucleotide |
| NF- κ B | Nuclear factor kappa B |
| NME8 | NME/NM23 family member 8 |
| P2ry12 | Purinergic receptor P2Y12 |
| PAMP | Pathogen-associated molecular pattern |
| PICALM | Phosphatidylinositol binding clathrin assembly protein |
| PLD3 | Phospholipase D family member 3 |
| PRR | Pattern recognition receptor |
| PSEN | Presenilin |
| PTK2B | Protein tyrosine kinase 2 beta |
| Rap1 | Ras-related protein 1 |
| RET | Reverse electron transport |
| RFP | Red fluorescent protein |
| RGD | Arginyl-glycyl-aspartic acid |
| RIN3 | Ras and rab interactor 3 |
| RNA | Ribonucleic acid |
| ROS | Reactive oxygen species |
| Sall1 | Spalt like transcription factor 1 |
| SAR | Systemic acquired resistance |

| | |
|---------------|--|
| SLC4A4 | Solute carrier family member 4 |
| SORL1 | Sortilin related receptor 1 |
| STAT | Signal transducer and activator of transcription |
| TAK1 | Transforming growth factor-beta-activated kinase 1 |
| TF | Transcription factor |
| Tg | Transgenic |
| TK | Thymidinkinase |
| TLR | Toll-like receptor |
| TNF- α | Tumor necrosis factor alpha |
| TREM2 | Triggering receptor expressed on myeloid cells like 2 |
| TYROBP | TYRO protein tyrosine kinase binding protein (alias DAP) |
| UNC5C | Unc-5 netrin receptor |
| VLDLR | Very-low-density-lipoprotein receptor |
| WT | Wildtype |
| ZCWPW1 | Zinc finger CW-type and PWWP domain containing 1 |

5.2 Curriculum Vitae

5.2.1 Personal Data

Name: Karoline Degenhardt

Current address: Daimlerstraße 4
72074 Tübingen
Germany

Business address: Hertie-Institute for Clinical Brain Research
Department of Cellular Neurology
Otfried-Müller-Straße 27
72076 Tübingen
Germany

Phone: +49-7071-29-87607

E-mail: karoline.degenhardt@uni-tuebingen.de

Date of Birth: 23.10.1988

Place of Birth: Berlin, Germany

Citizenship: German

5.2.2 Education and Academic Degrees

09/2013 - present Doctoral thesis at the Hertie-Institute for Clinical Brain Research,
Tübingen
Department: Cellular Biology of Neurological Diseases

Topic of the PhD thesis: “Modulation of cerebral β -amyloidosis by
myeloid cells”

10/2011 - 07/2013 Julius-Maximilians-Universität Würzburg
Master-program in Biomedical Science
Academic degree: Master of Science

Topic of the Master thesis: “Role of microglial phagocytosis
in Alzheimer`s disease”

10/2008 - 09/2011 Julius-Maximilians-Universität Würzburg
Bachelor-program in Biomedical Science
Academic degree: Bachelor of Science

Topic of the Bachelor thesis: “Analysis of platelet function in
TPCI-deficient mice”

5.3 Bibliography

Replacement of brain-resident myeloid cells does not alter cerebral amyloid- β deposition in mouse models of Alzheimer's disease

Nicholas H. Varvel*, Stefan A. Grathwohl*, Karoline Degenhardt, Claudia Resch, Andrea Bosch, Mathias Jucker and Jonas J. Neher

The Journal of Experimental Medicine 2015 Vol. 212, No. 11, 1803-1809, doi:10.1084/jem.20150478

Innate immune memory in the brain shapes neurological disease hallmarks

Ann-Christin Wendeln*, Karoline Degenhardt*, Lalit Kaurani, Michael Gertig, Thomas Ulas, Gaurav Jain, Jessica Wagner, Lisa M. Häsler, Katleen Wild, Angelos Skodras, Thomas Blank, Ori Staszewski, Moumita Datta, Tonatiuh Pena Centeno, Vincenzo Capece, Md. Rezaul Islam, Cemil Kerimoglu, Matthias Staufenbiel, Joachim L. Schultze, Marc Beyer, Marco Prinz, Mathias Jucker, André Fischer and Jonas J. Neher

Accepted in Nature 23.02.2018

Lack of MFG-E8 reduces pathology in mouse models of cerebral β -amyloidosis

Karoline Degenhardt*, Jessica Wagner*, Konstantina Kapolou, Domenico Del Turco, Thomas Deller, Mathias Jucker, Jonas J. Neher

Manuscript in preparation

5.4 Conference Proceedings

Karoline Degenhardt, Andrea Bosch, Anika Frank, Mathias Jucker and Jonas.J. Neher.

Peripheral inflammation induces long-term changes in central immunity and thereby affects secondary neuropathology. “Forschungskolloquium der Medizinischen Fakultät Tübingen”, 2014, Tübingen, Germany.

Karoline Degenhardt, Jessica Wagner, Domenico Del Turco, Hannah Davies, Ulrike

Obermueller, Jill Madine, Thomas Deller, Mathias Jucker, Jonas J. Neher. *Lack of lactadherin, the precursor of medin amyloid, reduces cerebral β -amyloidosis in mouse models of Alzheimer’s Disease.* EMBO/EMBL symposia 2017 “Mechanisms of Neurodegeneration”, Heidelberg, Germany (flash talk and poster presentation)